Evolutionary Analysis of ABCC Transporters and Characterization of Vacuolar Transport Mechanisms of the Glucosylated Phytohormone Abscisic Acid

Bo Burla

Doctoral Thesis
Faculty of Science
University of Zurich

Zürich 2012

Evolutionary Analysis of ABCC Transporters and Characterization of Vacuolar Transport Mechanisms of the Glucosylated Phytohormone Abscisic Acid

---

Dissertation

zur

Erlangung der naturwissenschaftlichen Doktorwürde

(Dr. sc. nat.)

vorgelegt der

Mathematisch-naturwissenschaftlichen Fakultät

der Universität Zürich

von

Bo Johannes Burla

von

Burg bei Murten (FR)

Promotionskomitee

Prof. Dr. Enrico Martinoia (Vorsitz und Leitung der Dissertation)

Prof. Dr. Beat Keller

Prof. Dr. Kentaro Shimizu

Zürich 2012

Table of Contents

Summary **2**

Zusammenfassung **3**

1. General Introduction **5**

1.1 Transport across biological membranes *6*

1.2 ABC proteins *9*

1.3 The plant vacuole *13*

1.4 Abscisic acid *16*

1.5 Plant ABC proteins *21*

2. Aims of the Thesis **47**

3. Chapter I: Evolution of the *ABCC* gene family **48**

3.1 Introduction *49*

3.2 Materials and Methods *50*

3.3 Results *59*

3.4 Discussion *87*

3.5 Supplementary Information *97*

4. Chapter II: Genetic and functional characterization of *AtABCC13* in *A. thaliana* **99**

4.1 Introduction *100*

4.2 Materials and Methods *102*

4.3 Results *117*

4.4 Discussion *138*

4.5 Supplementary Information *151*

5. Chapter III: Characterization of vacuolar ABA-GE uptake in *A. thaliana* **158**

5.1 Introduction *159*

5.2 Materials and Methods *162*

5.3 Results *167*

5.4 Discussion *173*

5.5 Supplementary Information *176*

6. General Conclusions **177**

6.1 Evolution of the ABCC gene family *178*

6.2 AtABCC13 - the Arabidopsis ortholog of the conserved ABCC-E clade *180*

6.3 Mechanisms of vacuolar ABA-GE uptake *182*

7. References **183**

8. Acknowledgments **201**

9. Curriculum vitae **202**

Summary

Cellular homeostasis requires a controlled exchange of molecules with the extracellular space and between subcellular compartments. ATP-binding cassette (ABC) transporters are integral components of membrane transport. They catalyze the active translocation of solutes against concentration gradients by utilizing the free energy of ATP hydrolysis. The ABCC subfamily of ABC transporters is highly conserved across eukaryotes and is known to be associated with cellular detoxification and multidrug resistance. ABCC proteins are also involved in physiological processes, such as the control of stomatal opening in plants, and the regulation of potassium channels in humans. In the first chapter of this thesis, the evolution of the *ABCC* gene subfamily across eukaryotes was analyzed. Distinct clades within the *ABCC* gene family were identified, which are shown to be either evolutionarily stable or to comprise various lineage-specific expansions. One specific clade appears to have originated during early eukaryotic evolution and is highly conserved, comprising single-copy orthologs across plant and animal species, including humans. In the second chapter, the *Arabidopsis thaliana* ortholog in this subclade, *AtABCC13,* was genetically and functionally analyzed. *AtABCC13* was found to encode for multiple transcript variants and to undergo alternative splicing. Furthermore, the results demonstrated that AtABCC13 resides on the vacuolar membrane like other *Arabidopsis thaliana* ABCCs. *AtABCC13* was found to be strongly expressed in the egg cell, chalazal seed coat, root pericycle, and in vascular tissues. An extensive screen of *AtABCC13* knockout mutants under various treatments did not reveal any mutant phenotypes. In the third chapter, the vacuolar uptake of abscisic acid glucosyl ester (ABA-GE), a catabolite of the phytohormone abscisic acid that accumulates in plant vacuoles, was studied in isolated *Arabidopsis thaliana* mesophyll vacuoles. An enzymatic method was developed to synthesize radiolabeled ABA-GE, which was required for uptake experiments. The results of the uptake experiments indicated that ABA-GE is transported by two simultaneous mechanisms: ABC transporter and proton antiport mechanisms. In summary, this thesis identifies the evolutionary relationships within the *ABCC* gene family across eukaryotes. Further, it reveals the mechanisms by which the glucosylated phytohormone ABA is sequestered into the vacuoles of *Arabidopsis thaliana*.

Zusammenfassung

Für die Funktion von Zellen ist ein kontrollierter Austausch von Substanzen sowohl mit der extrazellulären Matrix als auch zwischen intrazellulären Kompartimenten von zentraler Bedeutung. ABC (ATP-binding cassette)-Transportproteine sind integrale Bestandteile des zellulären Membrantransports. Sie verwerten die durch Hydrolyse von ATP freigesetzte Energie um Moleküle entgegen eines Konzentrationsgradienten über biologische Membranen zu transportieren. Eine Unterfamilie der ABC-Transporter, die sogenannten ABCC-Transportproteine, ist in allen eukaryotischen Lebewesen vorhanden und ist in der zellulären Entgiftung und an der Ausbildung von Medikamentenresistenzen von Pathogenen und Tumorzellen beteiligt. Des Weiteren sind ABCC-Transportproteine an spezifischen physiologischen Prozessen, wie zum Beispiel an der Regulation von Spaltöffnungsbewegungen in Pflanzen und an der Regulation spezifischer Kaliumkanäle im Menschen beteiligt.

Im ersten Projekt der vorliegenden Dissertation wurden mittels phylogenetischer Methoden die evolutionären Zusammenhänge der *ABCC*-Genfamilie in pflanzlichen und tierischen Organismen untersucht. Dabei konnte gezeigt werden, dass sich *ABCC*-Gene in unterschiedliche Gruppen einteilen lassen, die bezüglich ihres Umfangs während der Evolution entweder konserviert wurden oder sich in bestimmten Arten stark vergrössert haben. Zudem wurde eine konservierte Gruppe von *ABCC*-Gene identifiziert (*ABCC-E* Gruppe), welche früh in der Evolution der eukaryotischen Lebewesen entstanden ist. Nahezu alle Tier- und Pflanzenarten besitzen ein *ABCC*-Gen, welches dieser Gruppe zuzuordnen ist.

Im zweiten Projekt der vorliegenden Arbeit wurde das entsprechende Gen der *ABCC-E* Gruppe in der Modellpflanze *Arabidopsis thaliana* (*AtABCC13*) eingehend untersucht. Dabei wurden verschiedene Transkriptvarianten identifiziert, was auf einen möglichen regulatorischen Mechanismus mittels alternativem Splicing hinweist. Lokalisationsanalysen auf subzellulärer Ebene ergaben, dass AtABCC13, übereinstimmend mit anderen bereits beschriebenen pflanzlichen ABCC-Proteinen, in der vakuolären Membran lokalisiert ist. Auf zellulärer Ebene weisst *AtABCC13* eine

starke Expression in der Eizelle, in der chalazalen Samenschale, im Perizykel der Wurzel und in den Gefässen der Pflanze auf. Um Hinweise auf die Funktion von *AtABCC13* zu erhalten wurden zudem *AtABCC13* Insertionsmutanten unter verschiedenen Wachstumsbedingungen getestet. Jedoch konnte unter keiner dieser Bedingungen ein Unterschied zwischen Mutanten und Wildtyppflanzen festgestellt werden.

In einem dritten unabhängigen Projekt wurde der Transport des Glukoseesters der Abscisinsäure (ABA-GE) über die vakuoläre Membran der Pflanzenzelle im Hinblick auf eine mögliche Beteiligung von ABC Transportproteinen untersucht. Bei ABA-GE handelt es sich um ein inaktives Abbauprodukt des Pflanzenhormons Abscisinsäure, welches vor allem in der Vakuole gespeichert wird. Um die vakuoläre Aufnahme zu quantifizieren, wurde eine Methode entwickelt, welche die Herstellung von radioaktiv markiertem ABA-GE ermöglicht. Aufnahmeexperimente mit isolierten Vakuolen aus Arabidopsisblättern ergaben, dass sowohl ABC Transportproteine als auch durch Protonengradienten energetisierte Transporter an der ABA-GE Aufnahme beteiligt sind.

Im Rahmen dieser Dissertation konnten evolutionäre Zusammenhänge innerhalb der *ABCC*-Genfamilie aufgezeigt werden. Des Weiteren war es möglich die Mechanismen der vakuolären Aufnahme vom Glukoseester des Pflanzenhormons Abscisinsäure näher zu charakterisieren.

1. General Introduction

1.1 Transport across biological membranes

Compartmentalization is essential for biological systems. The plasma membrane defines the boundaries of a living cell and separates the highly structured and organized cellular interior from the extracellular matrix. The interior of a cell is furthermore structured into compartments by intracellular membranes. The main intracellular compartments are the nucleus, cytosol, endomembrane system, and other cell organelles such as mitochondria, chloroplasts and vacuoles. Compartmentalization allows separation and regulation of biological processes, storage of compounds, isolation of incompatible compounds, and formation of electrochemical gradients, which are used to energize biological processes.

However, cellular function does not only require compartmentalization, but also a controlled exchange of compounds between compartments. Biological membranes are lipid bilayers with integral proteins and exhibit selective permeability to different compounds. They are usually formed by two sheets of phospholipids that assemble in a tail-to-tail fashion in aqueous systems. The resulting bilayer has a hydrophobic center and hydrophilic boundaries. The hydrophobic core represents a diffusion barrier to charged and polar solutes. Moreover, bilayer membranes limit the diffusion of larger molecules and macromolecules. However, water can pass through phospholipid bilayers with a relatively high permeability. Biological membranes contain molecules that selectively modify the permeability and other properties of the bilayer. These molecules include small organic compounds such as cholesterol, but also the integral membrane proteins. Specific integral membrane proteins function in membrane transport, others function, e.g. as receptors and structural components. Membrane transport can be classified into passive and active transport (Figure 1).

Passive transport is the spontaneous movement of solutes across a membrane following a concentration and/or electrical (electrochemical) gradient. Passive transport is facilitated by uniporters, which are specific integral membrane proteins that catalyze the passive diffusion of polar, charged and large molecules across lipid bilayer membranes. These membrane proteins are classified into two groups: (i)

Facilitated transporters (also called permeases or carrier proteins). Most of these passive transporters belong to the solute carrier family (SLC) and facilitate the membrane transport of various compounds, including sugars, amino acids, nucleotides, bicarbonate and metals (Hediger et al., 2004). (ii) Membrane channels. They were originally categorized into aquaporins, ion channels, and other types of channels. Aquaporins represent the so-called water channels, but they have also been demonstrated to conduct other solutes, such as CO_2, ammonia, and other small neutral molecules (Maurel et al., 2008). Ion channels mediate the passive translocation of charged molecules along electrochemical gradients. Most ion channels are specific to one or few particular ions, e.g. calcium, sodium, potassium and chloride ions, or organic ions such as malate. The conductance of most ion channels is regulated by a process called gating. Gating can be controlled by the membrane potential (voltage-gated ion channels), by ligands (ligand-gated) or by other signals, such as the membrane tension (mechano-sensitive channels) (Ward et al., 2009). Ion channels mediate action potentials in animals and plants, and participate in selective cellular and intracellular uptake and release of ions. For instance, ion channels are involved in the regulation of stomatal opening and closing by conducting osmolytes, such as potassium, chloride, and malate (Barbier-Brygoo et al., 2011). This function is important for the controlled exchange of CO_2 and water with the atmosphere. These channels are indirectly regulated by the phytohormone abscisic acid, which will be detailed later in this introduction.

Active transport is the membrane transport of molecules against their electrochemical gradient by utilizing energy. Active transport can be divided into two types: primary and secondary active transport. Primary active transport uses the energy released by ATP hydrolysis to drive membrane transport. This transport is mediated by ATPases and ATP-binding cassette (ABC) transporters. ATPases transport protons and ions, such as sodium, potassium, calcium and chloride, and also other metal cations, including heavy metal ions (Palmgren, 2001). The ABC transporters, which mediate the transport of a multitude of compounds, are introduced in detail in Section 1.2. Secondary active transport uses the energy from an electrochemical gradient of a second solute, which

is co-transported (symport) or transported into opposite direction (antiport). In animal cells, secondary active transport in driven by sodium gradients established by the sodium pump Na^+/K^+-ATPase. In plant cells, where sodium ions are even toxic, secondary active transport is energized by proton gradients generated by proton pumps, namely the plasma membrane H^+-ATPases, the vacuolar H^+-ATPases and the vacuolar H^+-PPases (Gaxiola et al., 2007).

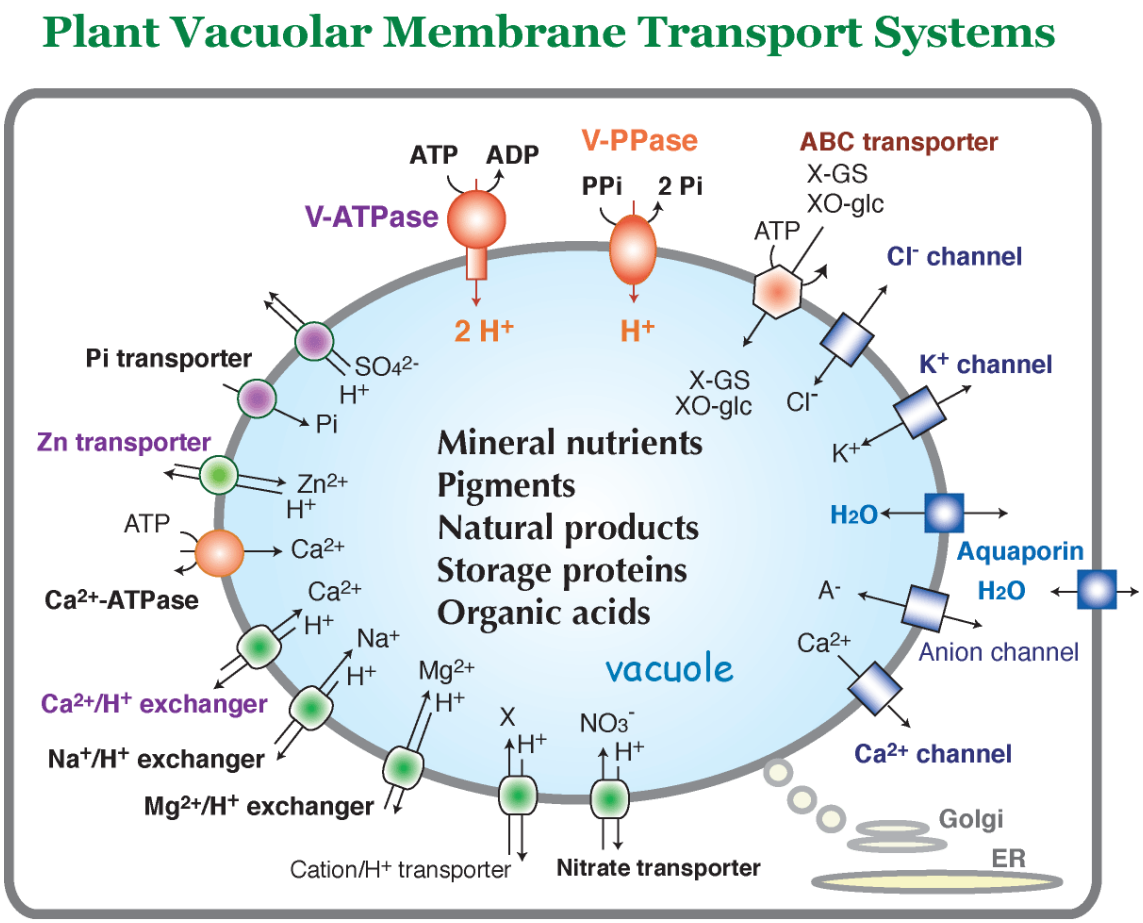

Figure 1. Plant vacuolar membrane transport systems. Channels and carrier proteins are in blue, primary active transporters are in red, secondary active transporters in green (Courtesy of Professor Masayoshi Maeshima, Nagoya University, Japan).

1.2 ABC proteins

ABC (ATP-binding cassette) transporter proteins are found in all living organisms. They function as primary active membrane transporters and are involved in a multitude of cellular processes. ABC proteins were first discovered in bacteria. First evidences for ATP-driven direct transport systems were obtained in the 1970s and the first ABC transporter was cloned from *Salmonella typhimurium* in 1982 (Higgins et al., 1982). The majority of fundamental understandings of ABC transporters came from studies of bacterial ABC transport systems (Higgins and Linton, 2003). The first cloned eukaryotic ABC transporter was the human P-glycoprotein *PGP1*, which was isolated from a multidrug-resistant cell line (Riordan et al., 1985). The name ABC (ATP-Binding Cassette) was used for the first time in 1990 to demonstrate the importance of this diverse protein family (Higgins and Linton, 2003). Interestingly, ABC transporters, i.e. the white-brown complex homolog proteins that determine the eye color of the fruit fly *Drosophila melanogaster*, played a key role in the field of genetics, long before ABC proteins were discovered (Rea et al., 2003).

Prokaryotic ABC transporters commonly mediate the uptake of nutrients such as carbohydrates and amino acids. However, eukaryotic ABC transporter function mainly as exporters, i.e. they transport solutes from the cytoplasm to the extracellular space, lysosomes and vacuoles. ABC protein-mediated transport is characterized by (i) The direct dependence on MgATP, MgGTP or MgUTP. Inorganic pyrophosphate, free or non-hydrolysable ATP are incapable to energize transportation. (ii) The insensitivity to transmembrane electrochemical potential differences. (iii) The inhibition of transport by vanadate, a phosphoryl transition-state analog that also inhibits the plasma membrane H^+-ATPase (Rea et al., 1998; Martinoia et al., 2002).

The ABC protein domains and their organization, the ABC subfamilies, and functions of ABC proteins in plants are reviewed in the article of Kang et al. (2011), of which I was a coauthor. A reprint of this article can be found in Section 1.5 of this thesis. In the next paragraph only the ABCC subfamily of ABC proteins is described in more detail.

The ABCC subfamily forms a large group of full-size eukaryotic ABC transporters within the ABC protein superfamily. Many ABCC proteins comprise an additionally transmembrane domain (TMD0) (Figure 2). In human, ABCCs with ('long' ABCCs) or without ('short' ABCCs) this domain exists (Slot et al., 2011). ABCC transporters, also named multidrug resistance-related proteins (MRPs), were originally identified in a tumor cell line that was resistant to the anticancer drug doxorubicin (Cole et al., 1992). Afterwards, human and plant ABCC proteins were identified as versatile transporters that mediate the cellular export of glutathione, glucuronate and other conjugates of organic anions, i.e. of xenotoxins and endogenous compounds (Martinoia et al., 1993; Cole and Deeley, 2006; Chen and Tiwari, 2011). Additionally, ABCC genes were also shown to confer resistance to biotic toxins, such as the resistance of insects to the Bt toxin (Gahan et al., 2010). A characteristic of many examined ABCC transporters is their substrate polyspecificity. For instance, HsABCC1 was shown to transport a multitude of structurally unrelated compounds, including folic acid, bilirubin, glutathione, sulfated bile acids, proteolysis products of beta-amyloids and conjugates of leukotriene, estradiol and aflatoxin. Moreover, HsABCC1 represents a resistance factor to distinct cytotoxic drugs, e.g. anthracyclines and vinca alkaloids (Chen and Tiwari, 2011; Krohn et al., 2011; Slot et al., 2011). Likewise, the *Arabidopsis* AtABCC2 was shown to transport phytochelatins, and conjugates of chlorophyll catabolites and xenobiotics (Lu et al., 1998; Song et al., 2010). In conclusion, most of the ABCC substrates are glutathione and glucuronate conjugates of structurally unrelated organic anions. Conjugation of oxidized lipophilic compounds including xenobiotics is a key step in the cellular detoxification process (Coleman et al., 1997). Hence, the presence of only a few polyspecific transporters allows the detoxification of a wide range of compounds. The structural and biochemical basis for the polyspecificity of ABCC transporters, which was also reported for ABCB transporters, are still not fully understood and is the subject of intensive research (Gutmann et al., 2010).

However, ABCC proteins are also implicated in processes other than cellular detoxification. In plants, the *Arabidopsis* AtABCC5 was shown to be a specific and high-affinity transporter for inositol hexaphosphate. It functions in phosphorous storage,

but is also implicated in guard cell signaling processes regulating stomatal apertures (Nagy et al., 2009). AtABCC5 represents an ABCC transporter with a very defined and narrow substrate specificity, which is in contrast to other characterized ABCC transporters that are predominantly polyspecific, e.g. the previously mentioned AtABCC2. Orthologs of AtABCC5 in rice and soybean were demonstrated to exhibit comparable functions as AtABCC5 (Shi et al., 2007; Kim et al., 2008; Zhao et al., 2008). In maize, the ABCC protein ZmMRP3 (ZmABCC3) was shown to be involved in anthocyanin transport (Goodman et al., 2004). Functions of other ABCCs in *Arabidopsis* are detailed in the review of Section 1.5.

In human, ABCCs were shown to be resistance factors of tumor cells to various drugs. However, five ABCC proteins are also associated with diseases (Chen and Tiwari, 2011). The most prominent are CFTR (ABCC7) and SUR1/2 (ABCC8/9). However, these proteins are not typical ABCC transporters. CTFR (cystic fibrosis transmembrane conductance regulator, ABCC7) is implicated in cystic fibrosis, one of the most common autosomal recessive genetic diseases. It primarily functions as an ATP-gated chloride channel in epithelial cells, controlling the fluidity of the mucus (Rowe et al., 2005). SUR1/2 (sulfonylurea receptors, ABCC8/9) are the regulatory subunits of the ATP-sensitive potassium channels (K_{ATP}) that function as metabolic sensors. SUR1/2 modulate the channel activities of the K_{ATP} pore-forming subunits, i.e. the inward-rectifying potassium channels $K_{ir}6.1$ and $K_{ir}6.2$, by sensing intracellular ATP levels. K_{ATP} channels are found in pancreatic β-cells and in muscle tissues, including the heart muscle. Mutations in SUR1/2 are implicated in diabetes, hyperinsulinism and heart diseases (Clark and Proks, 2010). In plants, there were evidences for the presence of ion channel activities and regulation mediated by ABCC proteins (Leonhardt et al., 1997; Suh et al., 2007); however, so far no specific plant ABCC was identified with such functions. The other disease-associated human ABCCs are ABCC2 and ABCC6. Mutations in *ABCC2* are associated with impaired excretion of conjugated bilirubin into the bile, causing the Dubin–Johnson syndrome (Figure 2B). ABCC2 was also shown to mediate bilirubin conjugate transport *in vitro* (Keitel et al., 2003). Various mutations in *ABCC6* were implicated with Pseudoxanthoma elasticum, a disorder affecting

connective tissues (Figure 2A). However, the endogenous substrate of ABCC6 has not been revealed so far. Interestingly, none of these mutations affect the transmembrane domain 0 (TMD0), indicating that the TMD0 is not essential for the function of ABCC6. The human *ABCC11* is a determinant for axillary odor and earwax type. Particular mutations in this *ABCC* gene result in substantially reduced axillary secretion of steroidal odorants and their precursors. In some human populations, there is a strong positive selection for dysfunctional alleles of *ABCC11*, possibly reflecting mate selection for partner with reduced body odor (Martin et al., 2009; Toyoda et al., 2009).

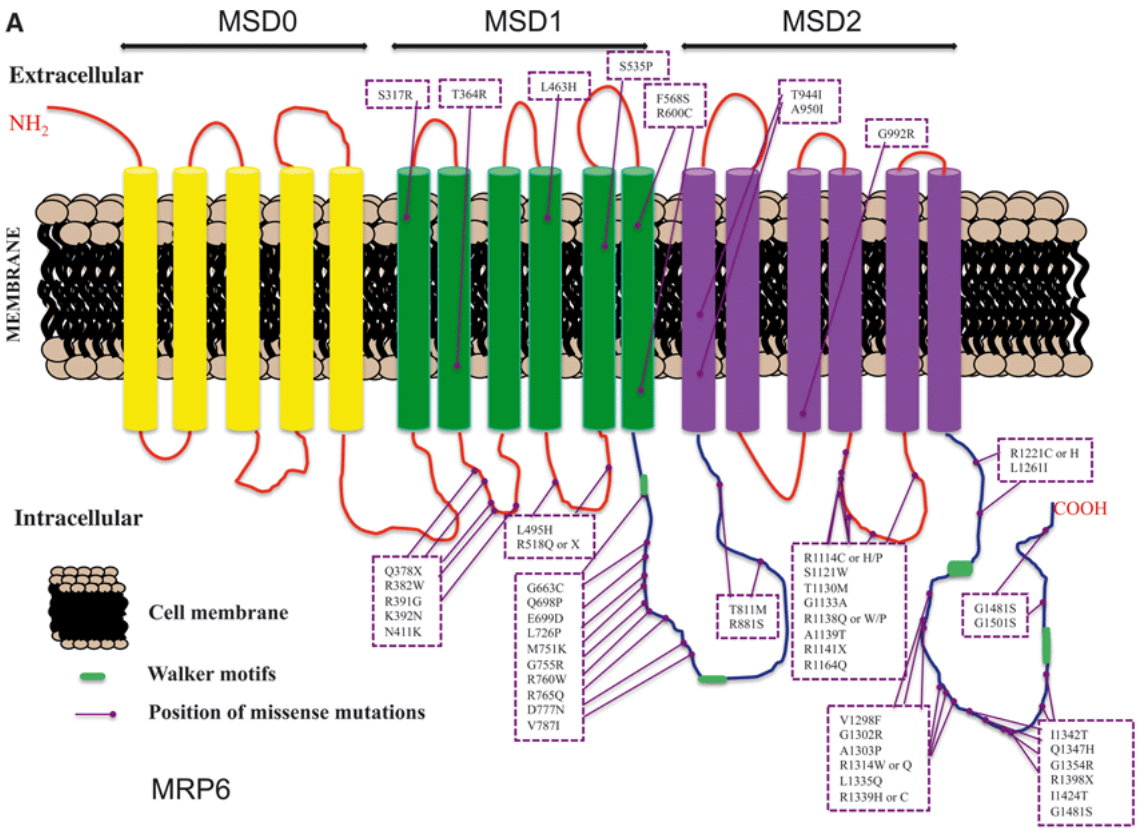

Figure 2. Membrane topology of the human ABCC6 protein with the ABCC-specific TMD0 (MSD0) domain. Distinct transmembrane domains are labeled with MSD0/1/2. Positions of disease-associated mutations are also indicated (Illustration from Chen and Tiwari, 2011).

1.3 The plant vacuole

Plant cells are characterized by the presence of large central vacuoles. Two distinct types of vacuoles exist: protein storage vacuoles (PSV) and lytic vacuoles (LV). While the storage vacuoles are mainly found in seed tissues, the lytic vacuoles represent the central vacuoles found in almost all plant cells (Herman and Larkins, 1999; Jiang et al., 2001). Plant vacuoles are multifunctional organelles that vary in their number and size, depending on the plant's developmental stage and tissue. In leaf mesophyll cells, the central vacuole comprises up to 90% of the total cell volume (Buchanan et al., 2002). Plant cellular homeostasis is based on the presence of vacuoles, which are involved in the regulation of the cytoplasmic pH, ion concentrations and cell turgor, and in lytic processes, storage of primary metabolites, and sequestration of toxic metabolites and xenobiotics.

The central vacuoles are the main storage compartments of plant cells. They contain inorganic ions, sugars, organic acids, amino acids and various other primary metabolites (Tohge et al., 2011). The vacuolar lumen has a pH of approximately 5.5. A low vacuolar pH is essential for lytic activities, and the vacuolar proton pool is involved in the regulation of the cytoplasmic pH. Moreover, the proton gradient over the vacuolar membrane (tonoplast) energizes various transport processes. The vacuole temporarily stores various physiologically relevant compounds, such as signaling molecules, e.g. Ca^{2+}, inositol hexaphosphate, and plant hormones in mostly conjugated forms, e.g. ABA, auxin, and cytokines. The release of compounds from vacuolar pools represents a quick way to increase cytosolic concentrations when *de-novo* biosynthesis is too slow or impossible (Lehmann and Glund, 1986; Buchanan et al., 2002; Nagy et al., 2009; Piotrowska and Bajguz, 2011). Vacuolar compounds are imported and exported by various tonoplast-localized transport systems, i.e. ion channels, ATPases, ABC transporters, antiporters and sympoters (Figure 1). The plant cell turgor is the result of the vacuolar water content and the counterforce from the cell wall. Solutes within the vacuole act as osmolytes that function in turgor regulation (Martinoia et al., 2007). In particular, turgor regulation is prominent in guard cells, a pair of specialized

cells forming the stomatal pores, which regulate CO_2 and water exchange with the atmosphere. In response to endogenous and environmental cues, specific channels and transporters mediate vacuolar solute movements that result in turgor changes and subsequent stomatal movements (MacRobbie, 2006; Kim et al., 2010).

Moreover, many secondary metabolites are stored in the vacuole, e.g. flavonoids, which include the anthocyanins and isoflavones. Flavonoids function e.g. as flower and seed pigments, UV protectants, antioxidants, plant-microbe symbiosis factors and antimicrobial agents (Figure 4). Furthermore, vacuolar secondary metabolites participate in the plant defense against pathogens and herbivory, and include glucosinolates, cyanogenic glycosides, phytoalexins, and defense proteins. The vacuolar compartmentalization allows the production of potentially toxic compounds by isolating them from the cytosol. Some of these toxic secondary metabolites are stored in inactive forms. They become active upon release of the vacuolar content by cell damage from infection or herbivory and subsequent action of cytosolic enzymes (Poulton, 1990; Iglesias, 2000). Vacuoles are also essential parts of the plant detoxification system. Unlike animals, plants are not able of efficiently excreting catabolites or xenobiotics. Instead, toxic compounds are removed from physiological processes by sequestration into vacuoles, where they are either degraded or accumulated. Compounds accumulated in leaf vacuoles are removed from the plant by leaf fall. Detoxification of lipophilic xenobiotics, such as herbicides, occurs via cytochrome P450 oxidation, followed by conjugation to hydrophilic moieties, e.g. glutathione, glucose, and malonate. Subsequently, these conjugates are actively transported into the vacuole, primarily by ABC transporters (Coleman et al., 1997; Frelet-Barrand et al., 2008). Heavy metals, such as arsenic, are detoxified by chelation to the metal-binding peptide phytochelatin and subsequent sequestration into vacuoles (Cobbett, 2000; Song et al., 2010; Park et al., 2011).

The plant vacuole furthermore functions as a lytic compartment, comparable to lysosomes in animal cells. The vacuolar lumen harbors various proteases, nucleases, lipases, glucosidases and other hydrolyzing enzymes that are involved in the turnover

of cellular constituents (Buchanan et al., 2002). Chlorophyll, for example, is partially degraded in the vacuole, whereby chlorophyll components, such as nitrogen are recycled (Hörtensteiner, 2006). The lytic properties of vacuoles are also important in the plant programmed cell death (PCD). Plant pathogen defense by hypersensitive response (HR) frequently triggers PCD. In vacuole-mediated PCD, the vacuolar content is released into the cytosol upon tonoplast breakup, which leads to rapid cell-death. By this means, intracellular pathogens are directly inactivated. In a different type of vacuole-mediated PCD, the vacuole fuses with the plasma membrane, thereby releasing its content into the apoplast, which consequently inactivates extracellular pathogens and leads to indirect cell-death (Hara-Nishimura and Hatsugai, 2011).

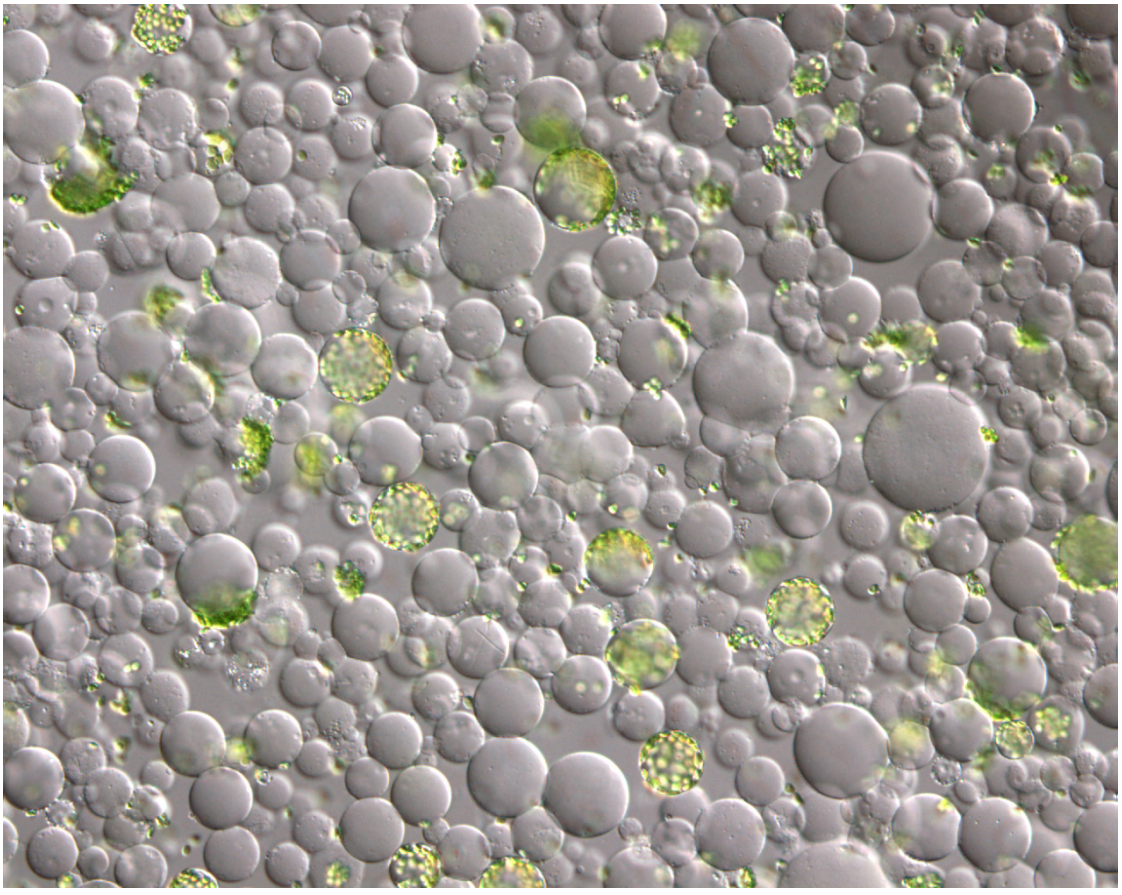

Figure 3. Isolated vacuoles from *Arabidopsis thaliana* leaf mesophyll, as they are used for vacuolar uptake assays. The green cells represent intact protoplasts (Photo by Bo Burla, 2011).

1.4 Abscisic acid

Abscisic acid (ABA) is an important plant hormone of higher plants. ABA is the central abiotic stress hormone mediating environmental stress responses, such as to drought, cold, and salt stress. Drought stress increases levels of ABA, which induces stomatal closure, thereby reducing water loss to the atmosphere (Kim et al., 2010; Figure 4). Additionally, ABA is involved in the desiccation tolerance of the embryo in the ripening seed, and is a potent inhibitor of seed germination preventing vivipary and controlling seed dormancy (Holdsworth et al., 2008). ABA is furthermore implicated in plant development, pathogen defense, plant senescence, and fruit ripening.

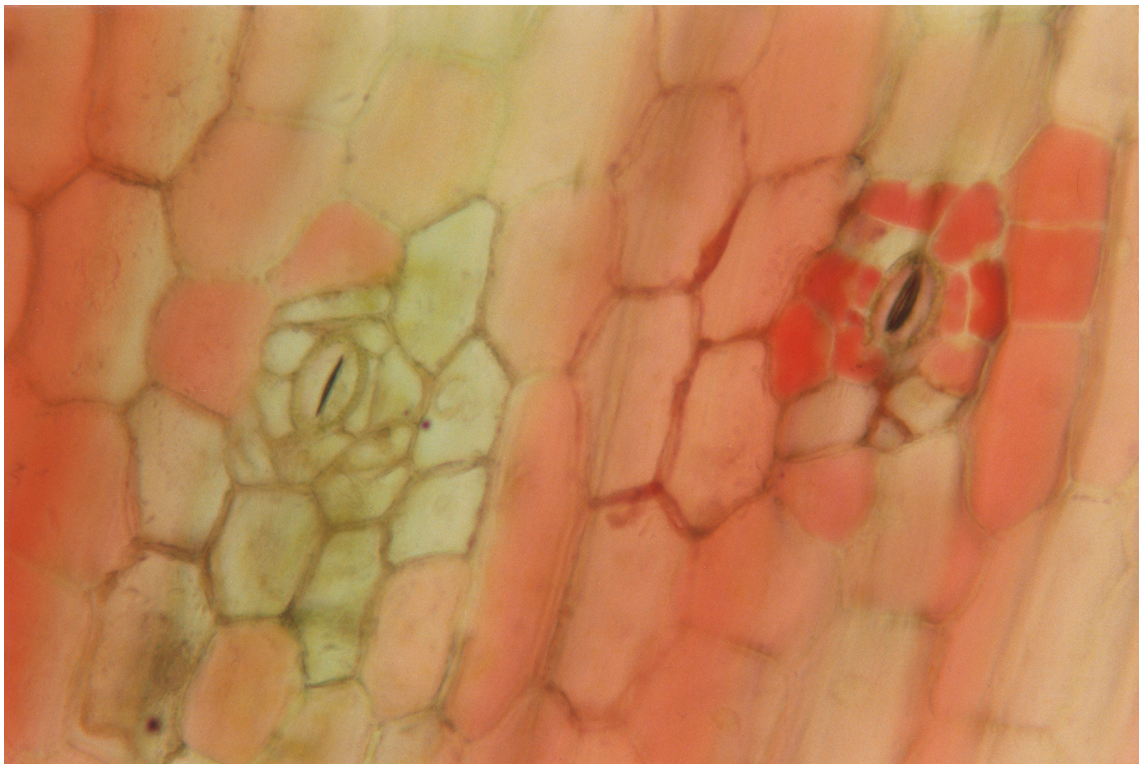

Figure 4. Epidermis from a rhubarb (*Rheum rhabarbarum*) stem with stomatal pores and cells with vacuoles containing anthocyanin pigments (Photo by Ulla Burla and Bo Burla, 1987)

ABA is also present in lower plants, including algae and the moss *Physcomitrella patens,* where it is likewise involved in abiotic stress response with partially conserved regulatory pathways as in higher plants (Johri, 2008; Khandelwal et al., 2010). Moreover, ABA functions in protozoa (Nagamune et al., 2008), in lower metazoa (Zocchi et al., 2001; Bruzzone et al., 2007), and in humans, where it has been shown to be a granulocyte-derived anti-inflammatory cytokine (Bruzzone et al., 2007; Scarfì et al., 2008). In all these species, ABA mediates the activation of the ADP-ribosyl cyclase (ADPC), which results in an increase in cyclic ADP-ribose (cADPR). cADPR mobilizes Ca^{2+} from intracellular stores, a function that is conserved across kingdoms (Lee, 1997; Guse, 2004).

The discovery of ABA goes back to the early 1960s, when Frederick Addicott and coworkers isolated a compound involved in the abscission of cotton fruits, which they called 'abscisin II'. At the same time, the group of Philip Wareing isolated 'dormin', a compound from sycamore leaves involved in leaf bud dormancy. Soon after, it was discovered that both compounds were identical, and the compound was given the name 'abscisic acid' (Addicott et al., 1967).

Abscisic acid is a 15-carbon sesquiterpene. Sesquiterpenes are isoprenoids that derive from isopentenyl diphosphate. Plastidic isoprenoids are synthesized via the mevalonic acid (MVA)-independent pathway (MEP). From these plastidic isoprenoids, the C_{40} carotenoid β-carotene is derived. β-carotene is oxidized to the xanthophyll zeaxanthin, which is subsequently enzymatically converted to violaxanthin by zeaxanthin epoxidase (ZEP). In *Arabidopsis*, ZEP is encoded by the *ABA1* gene. Afterwards, violaxanthin is converted to 9-*cis*-violaxanthin and 9'-*cis*-neoxanthin. These two compounds are then cleaved by 9-*cis*-epoxycarotenoid dioxygenases (NCED) into a C_{25} by-product and the C_{15} intermediate xanthoxin. This cleavage represents the first ABA-specific biosynthetic step. Xanthoxin is subsequently exported to the cytosol, where it is converted to abscisic aldehyde by a member of the short-chain dehydrogenase/reductase (SDR) family, which in *Arabidopsis* is encoded by the *ABA2* gene. The last step of ABA biosynthesis is the oxidation of abscisic aldehyde to ABA by

an abscisic aldehyde oxidase, which in *Arabidopsis* is encoded by the *AAO3* gene. Aldehyde oxidases are dependent on a molybdenum cofactor (MoCo). The MoCo sulfurase, which is an enzyme involved in MoCo biosynthesis, is essential for ABA biosynthesis. In *Arabidopsis*, this enzyme is encoded by the *ABA3* gene (Cutler and Krochko, 1999; Nambara and Marion-Poll, 2005; Taylor et al., 2005) (Figure 5).

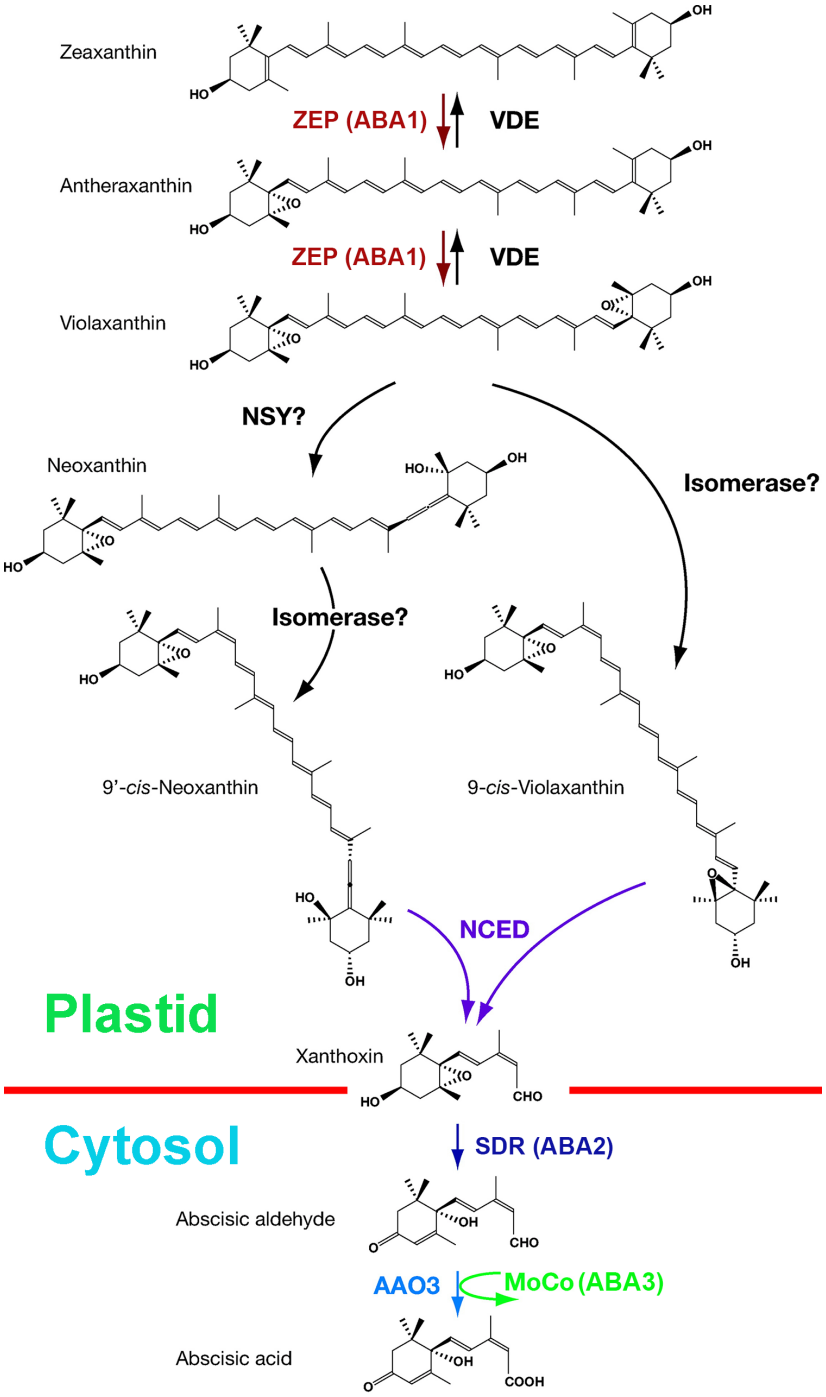

Figure 5. ABA biosynthetic pathway (Modified from Nambara and Marion-Poll, 2005).

The catabolism of ABA is mediated by two distinct pathways, hydroxylation and conjugation. The importance of each of these pathways and the composition of ABA catabolites depends on the species, tissue, developmental and physiological states (Neill et al., 1983; Zeevaart and Boyer, 1984; Hocher et al., 1991; Sauter et al., 2002; Priest et al., 2005; Okamoto et al., 2009; Seiler et al., 2011). Hydroxylation is the predominant inactivation pathway for ABA and is catalyzed by ABA 8'-hydroxylases, which are cytochrome P450 monooxygenases of the CYP707A subfamily (Figure 6). CYP707As oxidize the C-8' group of ABA, thereby producing the intermediate 8'-hydroxy-ABA, which is subsequently isomerized to phaseic acid (PA). PA is in part further converted to dihydrophaseic acid (DPA). Both, PA and DPA are considered as biologically inactive ABA catabolites.

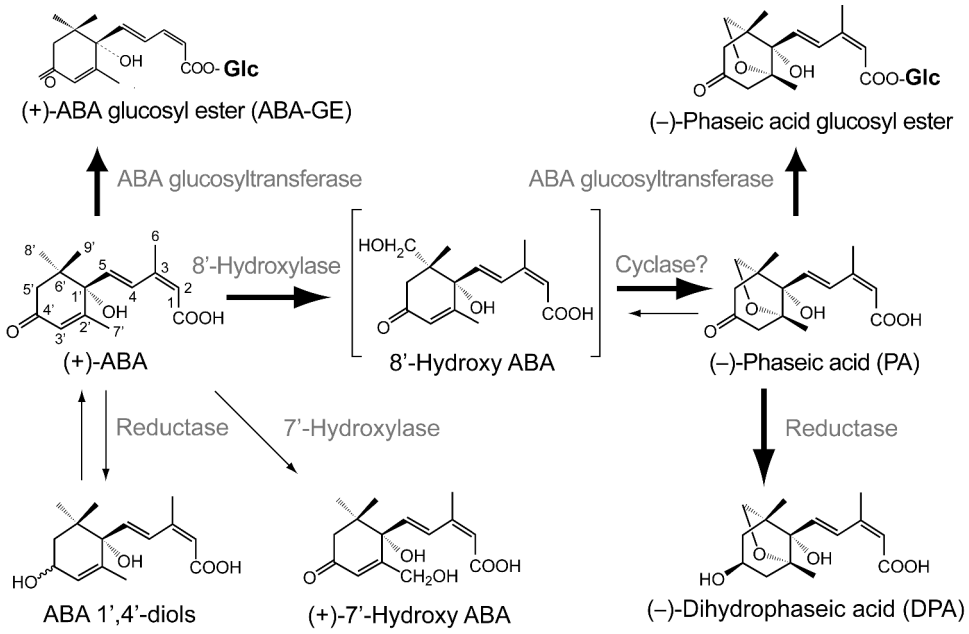

Figure 6. Pathways of ABA catabolism (Modified from Cutler and Krochko, 1999)

However, specific other oxidation products of ABA have been identified in several plant species. They include 7'-hydroxy-ABA, 9'-hydroxy-ABA and its isomer neo-phaseic acid, which are all the product of CYP707A catalyzed hydroxylation. In *Arabidopsis*, these catabolites are found in considerably lower abundance compared to PA and DPA (Cutler and Krochko, 1999; Nambara and Marion-Poll, 2005; Zaharia et al., 2005; Okamoto et al., 2009). The CYP707A ABA 8'-hydroxylases appear to be the key

enzymes of ABA catabolism and are consequently involved in the regulation of ABA levels (Kushiro et al., 2004).

Conjugation with glucose is the second inactivation pathway of ABA. The C-1' carboxyl group and the hydroxyl groups of ABA represent potential sites for glucose conjugation (Figure 6). The predominant ABA conjugate is ABA glucosyl ester (ABA-GE). However, conjugates of ABA oxidation products were also identified. ABA-GE has been found in many plants tissues, whereby it appears to be a minor ABA catabolite, compared to PA and DPA (Zeevaart and Boyer, 1984; Lehmann and Glund, 1986; Okamoto et al., 2009). However, in germinating lettuce seeds, ABA-GE was the predominant ABA catabolite (Chiwocha et al., 2003). In contrast to the oxidation of ABA to PA and DPA, the conversion of ABA to ABA-GE is reversible. Hydrolytic enzymes, i.e. β-glucosidases, can release free ABA from glucose-conjugated ABA. ABA-GE may therefore be a reservoir of free ABA and may play a role in ABA homeostasis, besides being an inactive catabolite of ABA. Indeed, ABA-GE accumulated in the ER has been shown to be a source for rapid increases in cytosolic ABA concentrations in response to drought stress. Drought stress activates ER-localized β-glucosidases, which catalyze the release of free ABA from ABA-GE within the ER, which then diffuses into the cytosol (Lee et al., 2006). Additional information on ABA-GE is presented in the Introduction of Chapter III (Section 5.1), in the context of the characterization of vacuolar ABA-GE import in *Arabidopsis thaliana*.

1.5 Plant ABC proteins

The following pages are a reprint from an article in which the author of this thesis was a joint first co-author. This article was reprinted on the 21.12.2011 from http://www.bioone.org/doi/abs/10.1199/tab.0153.

The Arabidopsis Book 9: e0153. 2011

Plant ABC Transporters

Joohyun Kang*, Jiyoung Park*, Hyunju Choi*, Bo Burla*, Tobias Kretzschmar*, Youngsook Lee and Enrico Martinoia

* Joint first co-authors

The author of this thesis contributed to this article as follows:

- Wrote Chapter II
- Performed all phylogenetic analyses presented in this publication
- Prepared Figures 1, 2 and 5
- Assisted in writing the other chapters

The Arabidopsis Book
© 2011 American Society of Plant Biologists

First published on December 06, 2011: e0153. doi: 10.1199/tab.0153

Plant ABC Transporters

Joohyun Kang[a*], Jiyoung Park[a*], Hyunju Choi[a*], Bo Burla[b*], Tobias Kretzschmar[b*], Youngsook Lee[a,c], and Enrico Martinoia[a,b,1]

[a]POSTECH-UZH Global Research Laboratory, Division of Molecular Life Sciences, Pohang University of Science and Technology, Pohang, 790-784, Korea
[b]Institute of Plant Biology, University Zurich, Zollikerstrasse 107, 8008 Zurich, Switzerland
[c]Division of Integrative Biosciences and Biotechnology, World Class University Program, Pohang University of Science and Technology, Pohang, 790-784, Korea
[1]Address correspondence to enrico.martinoia@botinst.uzh.ch

*These authors contributed equally to this book chapter

ABC transporters constitute one of the largest protein families found in all living organisms. ABC transporters are driven by ATP hydrolysis and can act as exporters as well as importers. The plant genome encodes for more than 100 ABC transporters, largely exceeding that of other organisms. In Arabidopsis, only 22 out of 130 have been functionally analyzed. They are localized in most membranes of a plant cell such as the plasma membrane, the tonoplast, chloroplasts, mitochondria and peroxisomes and fulfill a multitude of functions. Originally identified as transporters involved in detoxification processes, they have later been shown to be required for organ growth, plant nutrition, plant development, response to abiotic stresses, pathogen resistance and the interaction of the plant with its environment. To fulfill these roles they exhibit different substrate specifies by e.g. depositing surface lipids, accumulating phytate in seeds, and transporting the phytohormones auxin and abscisic acid. The aim of this review is to give an insight into the functions of plant ABC transporters and to show their importance for plant development and survival.

I. INTRODUCTION

ABC transporters constitute one of the largest protein families and are present in organisms ranging from bacteria to humans (Henikoff et al., 1997). In most cases, functional ABC transporters act as ATP-driven pumps and consist of two transmembrane domains (TMD) hydrophobic domains, which constitute the membrane-spanning pore, and two cytosolic domains, which are referred to as the nucleotide-binding domains (NBD) or nucleotide-binding folds (NBF), as they contain the ATP-binding Walker A and B motifs (Martinoia et al., 2002).

In bacteria, ABC transporters catalyze the import of many primary metabolites, such as maltose, polyols, and histidine. They also export antibiotics, lipids, and proteins, such as proteases, lipases and the RTX (repeat in toxin) cytotoxin of *Vibrio cholera*. Initially, eukaryotic ABC transporters were thought to be involved exclusively in the extrusion of compounds from the cytosol, as they were originally identified as transporters that are involved in cellular detoxification. Later studies showed that ABC transporters are present in most cell membranes. Until recently, it was assumed that eukaryotic ABC proteins transport the substrate present at the side of the NBD to the other side of a membrane. However, recent findings show that at least plant ABC transporters can also act in the opposite direction. The first demonstration was provided by Yazaki and colleagues (Shitan et al., 2003). They showed that the benzylisoquinoline alkaloid berberine, which is synthesized in roots, is taken up in the rhizome by an ABCB-type transporter.

In plants, ABC proteins were originally identified as transporters involved in the final detoxification process, i.e., vacuolar deposition (Martinoia et al., 1993). Since this finding, numerous reports have shown that the functions of this class of transporters extend far beyond detoxification. ABC transporters have frequently been shown to be involved in such diverse processes as pathogen response, surface lipid deposition, phytate accumulation in seeds, and transport of the phytohormones auxin and abscisic acid. Therefore, ABC transporters play an important role in organ growth, plant nutrition, plant development, response to abiotic stress, and the interaction of the plant with its environment.

In this review, we provide an overview of the transport functions that ABC proteins fulfill in plants, focusing primarily on knowledge gained from studies in Arabidopsis, but also including a few, well-established examples of work carried out in other plant species. In Figure 1, we present the Arabidopsis ABC transporters that have been characterized to date. Soluble ABC proteins not involved in actual transport, such as the Suf complex (Fontecave et al., 2005) or the mitochondrial AtCCMs (Rayapuram et al., 2007),

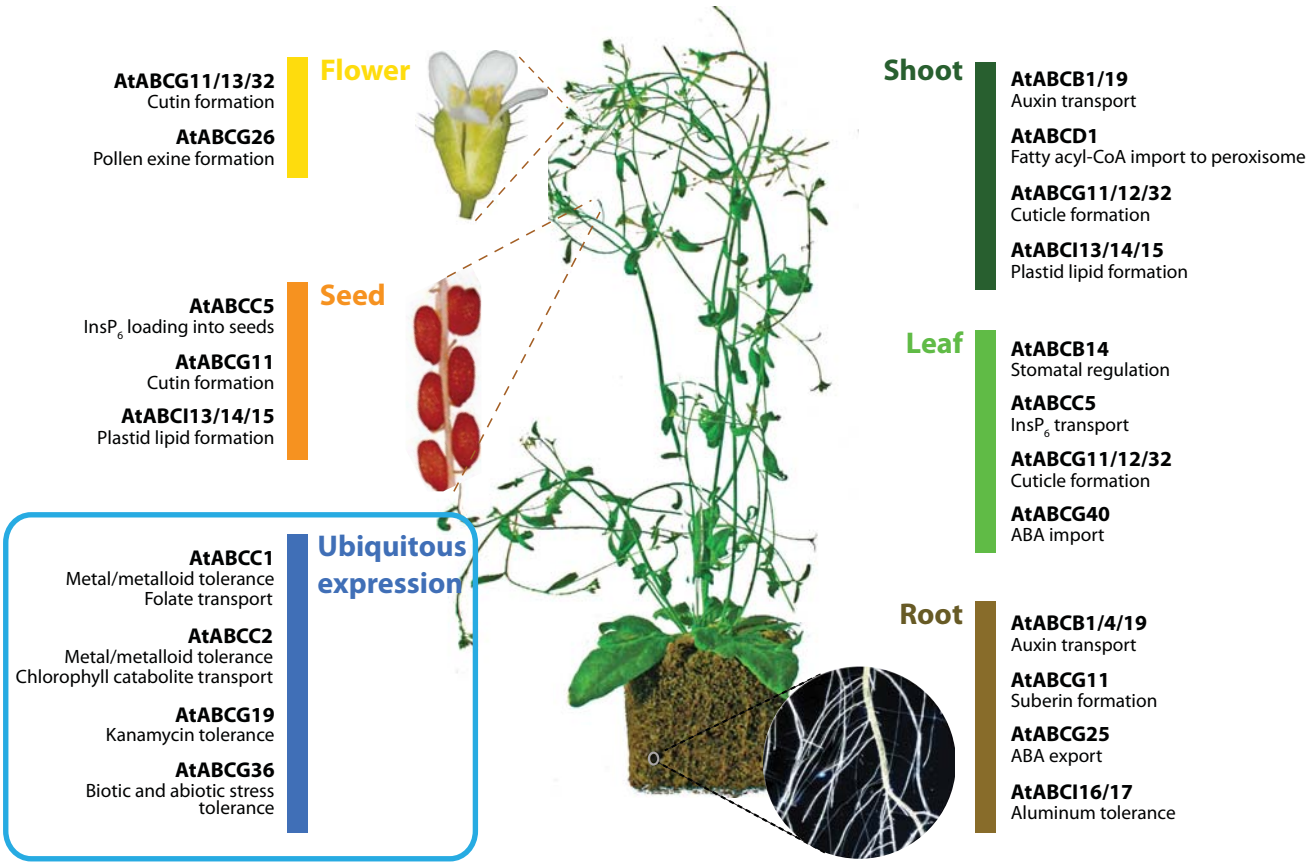

Figure 1. Overview of the Arabidopsis ABC transporters characterized to date.

ABC transporters whose functions and/or substrates have been reported are listed according to their tissue of action. Detailed information for each gene is described in the corresponding chapters. Figure modified from Kretzschmar et al. (2011).

will not be addressed here. Further information about this subset of proteins can be found in recent reviews by Rea (2007) and Yazaki et al. (2009).

II. STRUCTURAL AND PHYLOGENETIC RELATIONSHIPS OF ABC PROTEINS

Based on their domain structure and phylogenetic relationships the Arabidopsis ABC proteins are currently classified into eight subfamilies (Figure 2) in accordance with the nomenclature system for animal ABC proteins (Verrier et al., 2008). A common feature of ABC proteins is the presence of an ABC signature containing the amino acid sequence [LIVMFY]S[SG]GX3[RKA][LIVMYA]X[LIVFM][AG] as a consensus (Rea, 2007). This consensus sequence is the general case, but several exceptions have been reported (Rea, 2007).

Membrane-bound ABC proteins consist of four major subunits, two transmembrane domains (TMD) and two nucleotide-binding domains (NBD) (Higgins, 1992), which cooperate during ATP hydrolysis to drive active transport. These subunits are either encoded by individual genes (ABCI subfamily), by two genes each encoding one NBD and one TMD (half-size ABCs) that form heterodimers; by one gene encoding for one NBD and one TMD (half-size) that form homodimers or by a single gene (full-size ABCs). The subunits of ABCA to ABCD proteins have a so-called forward TMD-NBD domain organization, while those of the ABCG subfamily are characterized by reverse NBD-TMD organization. The soluble ABCE and ABCF subfamily of proteins consists only of two NBDs, whereas the ABCI subfamily comprises various genes that encode only one single domain, i.e. NBD, TMD or accessory domains. Some of these individual domains encoded by ABCIs have been shown to assemble into multi-subunit ABC transporters, in a manner similar to ABC proteins formed in prokaryotes (Verrier et al., 2008).

Within the ABCA subfamily, AtABCA1 (AOH according to the previous nomenclature) appears to be orthologous to mammalian ABC1, which is a full-size ABC transporter that harbors a large linker domain and represents the largest Arabidopsis ABC protein (Verrier et al., 2008). All of the remaining 11 Arabidopsis ABCA

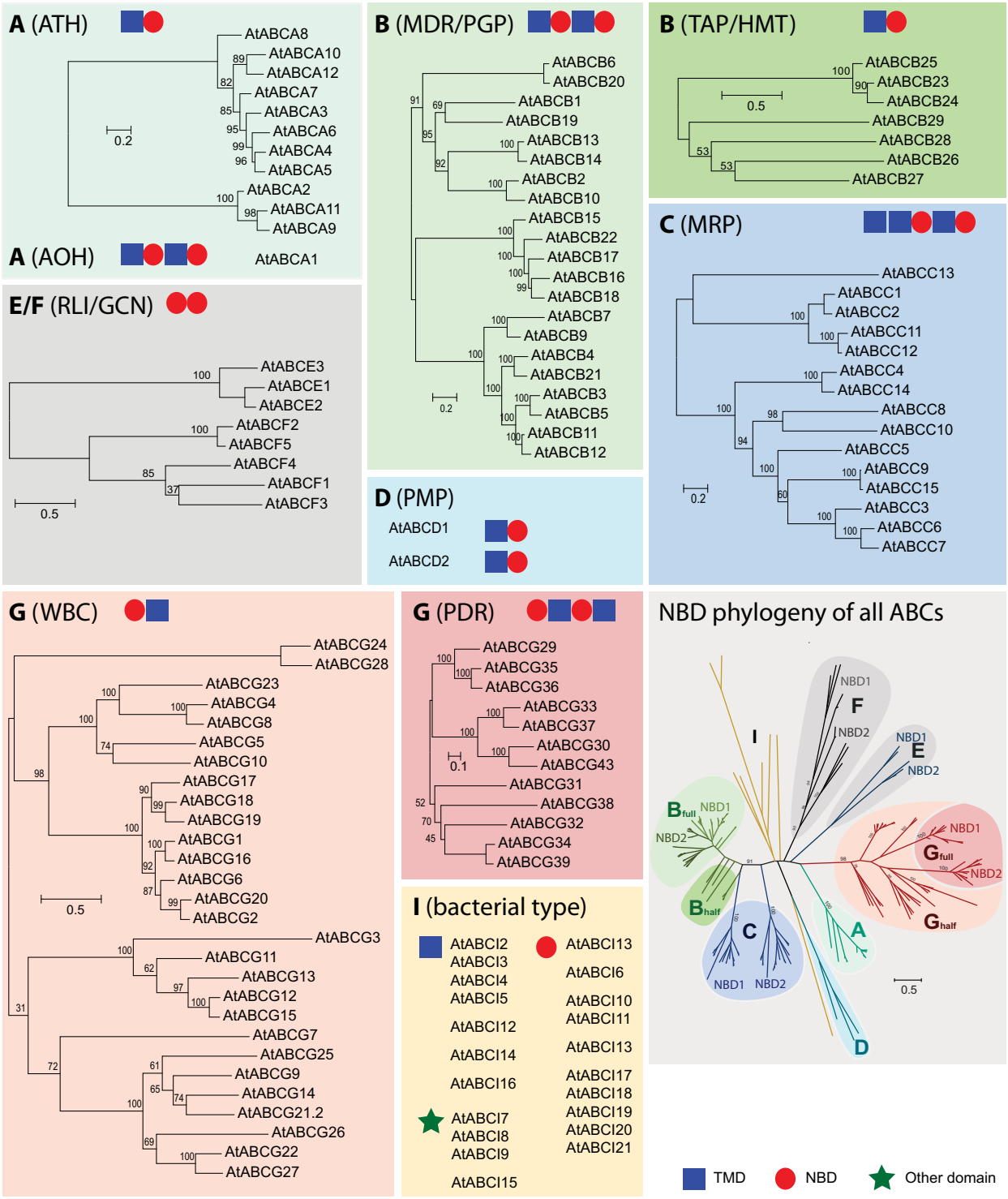

Figure 2. *Arabidopsis thaliana* ATP-binding cassette (ABC) protein subfamilies, with their maximum likelihood phylogenies, and a phylogeny of the NBDs of all Arabidopsis ABC proteins.

For the ABCI subfamily, only the encoded domain is indicated, as their divergence is too large to resolve their phylogenetic relationships. In the NBD phylogeny, both NBDs of full-size ABCs were included. NBDs of full-size ABCB show little divergence compared to NBDs of ABCCs and full-size ABCGs. Phylogenies were estimated using PhyML3.0 (Guindon et al., 2010) and the model LG+G4+I+F from a truncated protein sequence alignment generated with MUSCLE 3.8 (http://www.drive5.com/muscle). Gaps of more than 80% were removed (Capella-Gutiérrez et al., 2009). Branch support values correspond to non-parametric bootstrap values from 100 replicates. Domain organizations are indicated by colored symbols (key, bottom right).

subfamily proteins (ATH) are of the half-size type and lack the large domain found in ABCA1. Half-size ABCA proteins have only been identified in plants and prokaryotes (Peelman et al., 2003; Kovalchuk and Driessen, 2010). Further studies will be required to identify the subcellular localization of ABCA proteins.

The Arabidopsis genome encodes 21 full-size (Pgp/MDR) and seven half-size ABCBs, and has significantly more full-size ABCBs than humans, which contain only three (Vasiliou et al., 2009). So far, all characterized Arabidopsis full-size ABCB proteins have been shown to be localized at the plasma membrane (Blakeslee et al., 2007; Rea, 2007; Lee et al., 2008). Three half-size members of the ABCB subfamily (also called ATM) are localized to the mitochondria (Rea, 2007). Proteomic data indicate that AtABCB26 (TAP1) is localized to the chloroplast (Ferro et al., 2010), while AtABCB27 (TAP2) was detected in the vacuolar membrane (Jaquinod et al., 2007). The subcellular localization of the other half-size ABCBs still needs to be investigated.

The Arabidopsis ABCC protein subfamily consists only of full-size ABC proteins. Alignments and hydrophobicity profiles of TAIR10 gene models indicate that all ABCCs harbor the ABCC-specific additional N-terminal transmembrane domain (TMD0) (Tusnády et al., 2006; Klein et al., 2006). The function of TMD0 in plants is unknown; however, for certain human and yeast ABCCs this domain has been shown to be involved in protein targeting (Mason and Michaelis, 2002; Westlake et al., 2005). Most ABCC proteins localize to the vacuolar membrane (Rea, 2007; Nagy et al., 2009), and these are the only full-size ABC proteins found in the Arabidopsis tonoplast so far.

The ABCD subfamily is represented by one half-size and one full-size member, of which the latter, AtABCD1, has been shown to be located in peroxisomes (Hayashi et al., 2002).

Proteins of the Arabidopsis ABCE and ABCF subfamilies, which consist of three and five members, respectively, are thought to be soluble since they lack any detectable transmembrane domain. They probably function in processes other than transport, as is the case for their yeast and human orthologs, which participate in ribosome recycling and translational control (Vazquez de Aldana et al., 1995; Tyzack et al., 2000; Braz et al., 2004; Dong et al., 2004; Pisarev et al., 2010).

The largest ABC subfamily is ABCG, which contains 28 half-size (WBC) and 15 full-size (PDR) proteins in Arabidopsis (Verrier et al., 2008). All of them feature the characteristic, so-called, reverse organization of domains in the subunits (NBD-TMD). Genes encoding full-size ABCG proteins have only been identified in plants, fungi, oomycetes, brown algae and slime molds (Anjard and Loomis, 2002; Tyler et al., 2006; Cock et al., 2010). All characterized full-size and half-size ABCGs, except AtABCG19, localized to the plasma membrane (Lee et al., 2005; Stein et al., 2006; McFarlane et al., 2010; Kang et al., 2010b; Kuromori et al., 2010; Růžička et al., 2010; Choi et al., 2011).

The ABCH subfamily, which contains half-size transporters with a reverse domain organization, is phylogenetically unrelated to subfamily G and has not been identified in plants (Verrier et al., 2008).

Many of the 21 ABCI subfamily members are predicted to target to the chloroplast or mitochondria, and two are encoded by the mitochondrial genome (Verrier et al., 2008; Shimoni-Shor et al., 2010). ABCI19, 20 and 21, all of which encode for individual NBDs, have been shown to translate into cytosolic proteins (Marin et al., 2006) and form a distinct clade that roots to the center of the phylogenetic tree (Figure 2). The other ABCI members that encode for single NBDs also root to the center of the tree but appear to be unrelated to each other. ABCI members encoding other domains such as TMD or substrate binding domains were not included in the analysis.

In the phylogeny of NBDs from ABC genes, the sequences of two NBDs of full-size ABCB members appear to be more closely related to each other than NBDs of ABCC and full-size ABCG members (Figure 2).

III. ABC TRANSPORTERS INVOLVED IN DETOXIFICATION AND TRANSPORT OF CONJUGATED COMPOUNDS

Plants are exposed to a large number of potentially toxic compounds, such as the by-products of internal metabolic processes, certain minerals within the soil, toxins produced by pathogens, and anthropogenic compounds, such as herbicides and industrial waste. Since plants are limited in their ability to avoid toxins, they have developed versatile strategies to detoxify potentially toxic compounds. Modification of toxic compounds and their subsequent transport are well-known steps for detoxification in all living cells. Interestingly, a similar set of detoxification enzymes is used by plants for both endogenously produced organic compounds that may become toxic when accumulated within the cytosol and xenobiotics taken up from the environment. As the first step of detoxification, members of the cytochrome P450 family may catalyze the oxidation of potentially toxic endogenous and exogenous compounds, which are subsequently conjugated to a hydrophilic molecule, such as glucose or glucuronide (Kreuz et al., 1996). This conjugation step renders the potentially toxic compounds more hydrophilic and prevents the newly formed compounds from crossing membranes by diffusion. Similarly, xenobiotics are frequently conjugated to glutathione. This step is catalyzed by various glutathione S transferases (GSTs) and generally occurs without prior modification by electrophile substitution (Rouhier et al., 2008). As the last step, compound-conjugates are transported into the large central vacuole or released into the apoplast, a process known as internal or external excretion, respectively (Ishikawa, 1992; Martinoia et al., 1993). This process further reduces the toxicity of the compounds. The observations that the vacuolar transport activity for glucosylated luteolin, which is transported by ABC-type kinetics, is strongly reduced in a *Hordeum vulgare* (barley) mutant that does not synthesize this compound (Frangne et al., 2002) and that transcription of ABC-type transporters is up-regulated in a similar manner to other detoxifying enzymes in plants treated with xenobiotics suggest that modification and transport are parts of the general detoxification pathway (Gaillard et al., 1994).

III.A. Internal Excretion

Early studies suggested that xenobiotics were deposited within the central vacuole of plants (Schmitt and Sandermann Jr, 1982; Sandermann Jr, 1992). Since plants have only been exposed to industrial anthropogenic compounds for a few centuries, the question has been raised of how vacuolar transporters could recognize

such molecules. A widely distributed mechanism of detoxification in most living organisms is to conjugate a potentially toxic organic compound with the tripeptide glutathione through its thiol group (Meister, 1983). Therefore, Martinoia et al. (1993) considered the possibility that vacuoles may take up xenobiotics in their glutathionated form (GS-X), and observed that these compounds indeed efficiently accumulated in isolated barley vacuoles but only in the presence of ATP. Furthermore, they demonstrated that GS-X transport was efficiently inhibited by vanadate, an inhibitor of ABC-mediated transport processes, but not by inhibitors of the vacuolar V-ATPase or by dissipation of the electrochemical gradient generated by the latter. These observations showed that GS-X transport is not energized by the proton motive force, but is strictly ATP-dependent and is thus likely mediated by an ABC-type transporter.

III.A.1. Identification of vacuolar ABC transporters and their substrates

Based on the sequence of the human HsABCC1 protein that catalyzes the transport of GS-X (Cole et al., 1992; Jedlitschky et al., 1994), a first Arabidopsis GS-X transporter, AtABCC1/AtMRP1, was identified (Lu et al., 1997). Comparison of the peptide composition of Arabidopsis ABCC1 with that of human ABCC1 revealed a sequence identity of 41.5%. Using yeast vesicles expressing AtABCC1, the authors showed that this transporter exhibited similar transport properties to those described for isolated Arabidopsis vacuoles. This discovery was followed by the isolation and functional analysis of other members of the plant ABCC subfamily, such as AtABCC2 and AtABCC3 (Lu et al., 1998; Tommasini et al., 1998). These early publications extended the postulated range of substrates of tonoplast-localized ABC transporters from substrates of their human homologs to physiologically relevant substrates, such as chlorophyll catabolites. Chlorophyll pigments are degraded during senescence and at least the first intermediates of chlorophyll catabolism can still absorb light and transfer electrons, which results in oxidative stress if they are not efficiently detoxified. In plants, most secondary products as well as modified xenobiotics are either glucosylated or glutathionated. Compounds are rarely glucuronated, but there are some exceptions, such as the flavonoids produced in *Secale cereale* (rye) (Klein et al., 2000).

Early biochemical studies also provided insight into the transport kinetics of vacuolar ABC transporters. AtABCC2 transports both glutathionated compounds and glucuronated compounds (Klein et al., 1998; Lu et al., 1998). The two substrates do not compete for the transporter when both are present in the transport solution, but rather exhibit a trans-activation, which leads to an increase in GS-X transport by glucuronides and an enhanced affinity for glucuronides in the presence of GS-X (Liu et al., 2001). This result suggests that, when both substrates are present, the binding pocket becomes subject to steric changes that cause altered transport characteristics.

III.A.2. Inorganic compounds—Heavy metals and metalloids

A focal point regarding the study of detoxification mechanisms in plants has been heavy metal and metalloid detoxification. Contamination of agricultural soils has become a serious problem. For instance, more than 50 million people are exposed to toxic concentrations of arsenic in Bangladesh since aquifers providing drinking and agricultural water are contaminated with arsenic (Zhao et al., 2010). Similar to the P-type ATPases, proton co-transporters and proton antiporters involved in the uptake (Clemens et al., 1998; Vert et al., 2002) and vacuolar deposition (Hirschi et al., 2000; Morel et al., 2009) of several heavy metals and metalloids, ABC transporters have long been associated with heavy metal and metalloid detoxification. In *Saccharomyces cerevisiae*, it has been shown that an ABC transporter, YCF1 (Yeast Cadmium Factor1), contributes to heavy metal and metalloid tolerance (Szczypka et al., 1994; Li et al., 1997). This vacuolar transporter detoxifies bis-glutathione heavy metal/metalloid complexes, such as GS_2-Cd and GS_2-As. A similar mode of action has been postulated for human MRP1/HsABCC1, which partially complements the Cd-sensitive yeast mutant *ycf1* (Tommasini et al., 1996). Overexpression of ScYCF1 in Arabidopsis resulted in plants that were more tolerant to cadmium (Song et al., 2003), suggesting that the capacity of tonoplastic transport is a limiting factor in cadmium tolerance in this plant. In plants, some fungi, and animals, detoxification of heavy metals/metalloids is largely dependent on peptide-type chelators, the phytochelatins (PCs) (Grill et al., 1989; Clemens et al., 1999; Cobbett, 2000). These compounds are synthesized from glutathione by the heavy metal-activated phytochelatin synthase. A tonoplastic ABC transporter of *Schizosaccharomyces pombe*, HMT1, was identified as the first transporter of heavy metal-phytochelatin complexes (Ortiz et al., 1995). Functional homologs of SpHMT1 have thus far only been reported for *Caenorhabditis elegans* and Drosophila (Vatamaniuk et al., 2005; Sooksa-Nguan et al., 2009), while no homolog of this transporter was identified in the vacuolar membrane of plants.

Recently, Song et al. (2010) succeeded in identifying the plant vacuolar phytochelatin transporters. The reason why these transporters remained undiscovered for such a long time is that two ABCC proteins, AtABCC1 and AtABCC2, exhibit a redundant function, rendering reverse genetic approaches unsuitable for their identification. Both AtABCC1 and AtABCC2 transport apoPC as well as As(III)-PC_2 when expressed in yeast. Interestingly, the transport activity of these proteins does not exhibit classical saturation kinetics, but rather has a sigmoid curve, with low transport activity when substrate concentrations are low. This characteristic of the transporters probably ensures that apoPCs accumulate in the cytosol. By preventing their vacuolar sequestration before reaching a certain threshold, a larger proportion of PCs can form complexes with heavy metals in the cytosol. Vacuoles isolated from *atabcc1 atabcc2* double knockout Arabidopsis plants exhibited only 10 to 15% residual As(III)-PC_2 transport activity, strongly suggesting that these two ABC transporters are the main PC transporters in Arabidopsis (Figure 3). Overexpression of the transporters alone did not result in plants with an increased As tolerance, and the additional co-expression of phytochelatin synthase was necessary to attain this desired As-tolerant phenotype. Subsequent research on these ABC transporters revealed their roles in tolerance to Cd and Hg(II) as well (Park et al., 2011). The *atabcc1 atabcc2* double knockout was highly sensitive to Cd(II) and Hg(II). Interestingly, while *atabcc1* single knockout mutant was more sensitive than the wild type to Cd(II) and Hg(II), *atabcc2* knockout mutant did not exhibit any dramatic difference

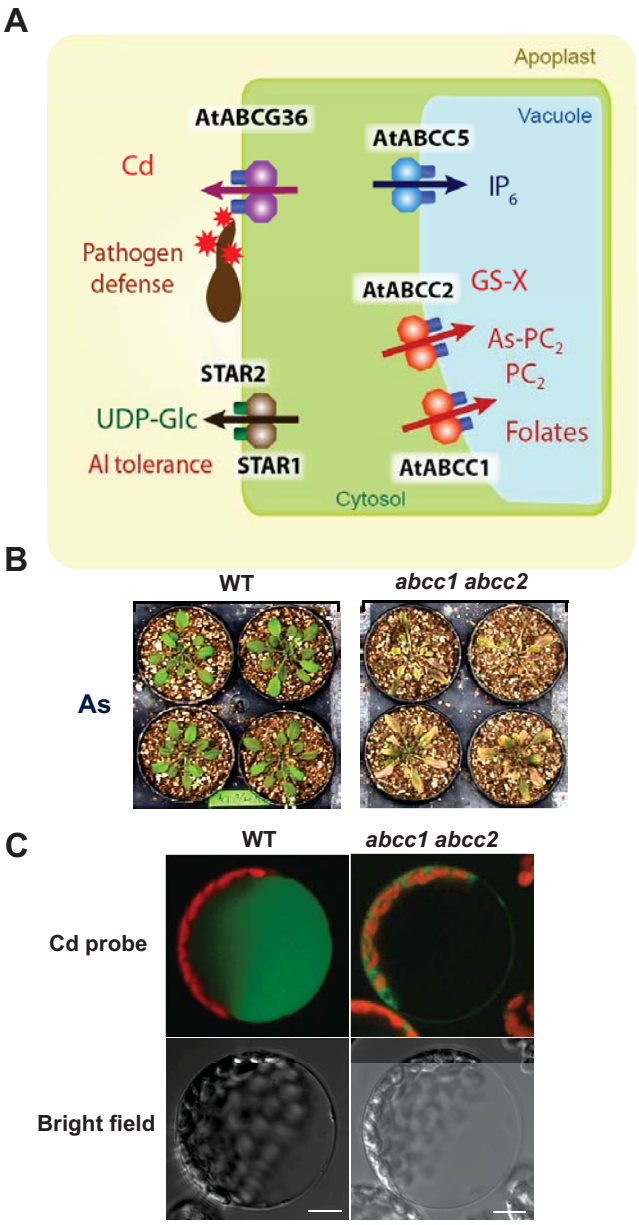

Figure 3. ABC transporters involved in cellular detoxification.

(A) At the plasma membrane, AtABCG36 mediates Cd export and is also involved in pathogen defense (Kobae et al., 2006; Stein et al., 2006; Kim et al., 2007; Bednarek et al., 2009; Clay et al., 2009). The bacterial-type ABC transporters, STAR1 and STAR2, confer aluminum tolerance by transporting UDP-glucose to the extracellular space (Huang et al., 2009; Huang et al., 2010). At the vacuolar membrane, AtABCC1 and AtABCC2 sequester arsenic-phytochelatin complexes in the vacuolar lumen and confer tolerance to toxic metals/metalloid (Song et al., 2010; Park et al., 2011). AtABCC1 is also implicated in folate transport (Raichaudhuri et al., 2009), while AtABCC2 is the major transporter of glutathione conjugate (Lu et al., 1998; Frelet-Barrand et al., 2008). AtABCC5 functions as a phytate transporter (Nagy et al., 2009).

(B-C) Loss-of-function of AtABCC1 and AtABCC2 resulted in arsenic hypersensitivity (Song et al., 2010) (B) and inhibition of vacuolar sequestration of Cd (Park et al., 2011) (C).

in the sensitivity from the wild type. These results suggest that both AtABCC1 and AtABCC2 contribute to Cd(II) and Hg(II) tolerance, and AtABCC1 can confer a significant level of tolerance to the divalent heavy metals in the absence of AtABCC2. The importance of AtABCC1 and AtABCC2 in vacuolar sequestration of Cd was clearly shown using a Cd-sensing fluorescent probe. The fluorescence was in the vacuole of wild-type cells, but mostly in the cytosol of *atabcc1 atabcc2* cells (Figure 3C). Overexpression of *AtABCC1* in Arabidopsis enhanced Cd(II) tolerance and accumulation.

AtABCC3 and AtABCC6 may also function in heavy metal tolerance. AtABCC3 has been reported to complement the Cd-sensitive phenotype of the *ycf1* mutant in *Saccharomyces cerevisiae,* suggesting that it can contribute to Cd tolerance (Tommasini et al., 1998). Growth of *atabcc6* loss-of-function mutants was slightly impaired in the presence of Cd (Gaillard et al., 2008). However, the mechanisms leading to the cadmium sensitivity or the substrates transported by AtABCC3 and AtABCC6 remain to be examined.

AtABCB25/AtATM3 is a mitochondrial ABC transporter involved in the biogenesis of iron-sulfur clusters in plants (Kushnir et al., 2001; Bernard et al., 2009), similar to its yeast homolog, Atm1p (Leighton and Schatz, 1995). In addition, AtABCB25 is also required for the biosynthesis of the molybdenum cofactor, a prosthetic group of molybdenum-containing enzymes (Teschner et al., 2010). Using a microarray for ABC transporters, Bovet et al. (2005) observed that AtABCB25 is strongly up-regulated in the roots of cadmium-treated plants. Overexpression of AtABCB25 enhanced Cd resistance, while a T-DNA insertion in this gene led to increased sensitivity (Kim et al., 2006). The observation that the *atabcb25* mutant produces more glutathione in the presence of cadmium than does the wild type also indicates that this mutant suffers higher oxidative stress. AtABCB25 is a close homolog of the vacuolar phytochelatin transporter of *Schizosaccharomyces pombe*, SpHMT1 (Ortiz et al., 1995). It is therefore tempting to speculate that AtABCB25 could transport glutathione-cadmium or cadmium-sulfur complexes as well as Fe-S clusters from the mitochondria to the cytosol, and thereby have multiple roles in biogenesis of iron-sulfur and molybdenum cofactor and heavy metal tolerance.

III.A.3. Anthocyanin transport: still an open debate

While Multidrug And Toxin Efflux (MATE)-type transporters are known to be responsible for the transport of several glucosylated flavonoids across membranes (Zhao et al., 2011), it is still debated which transport mechanism is responsible for anthocyanins accumulation within the vacuole. TT12, a MATE transporter, has been shown to catalyze the vacuolar transport of cyanidin-3-O-glucoside (Marinova et al., 2007) and epichatecin 3-O-glucoside (Zhao and Dixon, 2009). A similar substrate specificity has been shown to be mediated by Medicago MATE1, a close homolog of TT12 (Zhao and Dixon, 2009). A recent report provided evidence that transport of acylated anthocyanins in *Vitis vinifera* (grapevine) is also catalyzed by a MATE transporter (Gomez et al., 2009). In contrast, genetic evidence suggests that maize anthocyanins, which are not acylated, are transported by an ABCC protein, ZmMRP3 (Goodman et al., 2004). These observations raise the question of whether structurally different anthocyanins

are transported into the vacuole by different types of transporters or whether different plants use different transport systems. Anthocyanins are positively charged compounds and therefore not typical substrates for ABCC transporters. Furthermore, although glutathione transferases (GSTs) are apparently involved in anthocyanin transport (Alfenito et al., 1998; Mueller et al., 2000), there is no evidence that these compounds can form glutathione conjugates. However, it has been shown that animal ABCCs can transport positively charged alkaloids in the presence of the negatively charged glutathione (Versantvoort et al., 1995; Zaman et al., 1995). Alternatively, evidence has been presented that GSTs can act as ligandins of anthocyanins and it was therefore postulated they are involved in the delivery of anthocyanins to the transporter (Mueller et al., 2000). Hence, future work should address the important question of whether ZmMRP3 or its homologs can indeed catalyze the transport of anthocyanins and whether glutathione or GSTs are implicated in this process.

III.A.4. Transport of other glucosylated compounds

Besides plant secondary products, several other low molecular weight compounds, such as auxin, abscisic acid, salicylic acid, and modified xenobiotics, which were modified by cytochrome P450 in the first step of detoxification, are glucosylated within a plant cell. Salicylic acid glucoside has been shown to be taken up by an ABC-type transporter that is active in vacuolar vesicles isolated from *Glycine max* (soybean), but by a proton antiporter in *Beta vulgaris* (red beet; Dean and Mills, 2004). Similar differences were observed for two glucosylated sulfuron-based herbicides. While the transport of primisulfuron glucoside into barley vacuoles was driven by an ABC-type transporter, uptake of the closely related chlorsulfuron glucoside into vesicles isolated from red beet exhibited a proton antiport mechanism (Gaillard et al., 1994; Bartholomew et al., 2002). These results indicate that the uptake mechanism of several glucosylated compounds into the vacuole can differ between different plant species. In all of these cases, the transporters exhibiting these activities have not yet been identified and, to our knowledge, there has been no report demonstrating which ABC protein can transport glucosylated solutes.

III.A.5. Transport of antibiotics: AtABCG19 confers kanamycin resistance

A half-size member of the AtABCG family, AtABCG19, confers kanamycin resistance when overexpressed in plants (Mentewab and Stewart, 2005; Kang et al., 2010a). So far, this phenotype has only be found for AtABCG19, but not in other members in ABCG family. In the first report, AtABCG19 was proposed as a selectable marker in transgenic plants, since this gene specifically conferred resistance to kanamycin, but not to other aminoglycoside antibiotics, unlike the conventional antibiotics resistance gene, *nptII*. However, when expressed in hybrid aspen (*Populus tremuloides*), this gene conferred tolerance also to three other aminoglycoside antibiotics (Kang et al., 2010a). Mentewab and Stewart (2005) reported that AtABCG19 is targeted to the vacuolar membrane, which suggests that AtABCG19 removes kanamycin from the cytosol and stores it in the vacuole. However, this result awaits confirmation, since the N-terminal fusion of GFP used in this work might have masked the mitochondrial targeting sequence of the protein predicted from *in silico* analysis, and it therefore cannot be ruled out that this protein is localized in the mitochondrion.

III.B. External Excretion

An alternative strategy for plants to cope with toxic compounds is excretion from the cell. In particular, soil-born heavy metals that are taken up as stowaways during nutrient acquisition are excreted into apoplastic regions or directly back into the rhizosphere. External excretion can occur at a cellular level from the root epidermis, or excess compounds, such as Na^+, can be loaded into the phloem in the aboveground organs and transported back to the root (Berthomieu et al., 2003). The plasma membrane-localized full-size ABC transporter, AtABCG36/AtPDR8, which was previously connected to pathogen defense (see Chapter VII), was shown to be involved in cadmium resistance (Kim et al., 2007). Transgenic Arabidopsis plants overexpressing *AtABCG36* proved to be more tolerant to this highly toxic heavy metal. Measurement of Cd content revealed that accumulation of Cd was reduced in *AtABCG36* overexpressing plants, while it was increased in the loss-of-function mutants. Together, these results suggest that AtABCG36 excretes cadmium from roots (Figure 3A). Strong expression of *AtABCG36* in root epidermal cells (http://atted.jp/) supported this hypothesis. The direct involvement of AtABCG36 in the export of Cd ions or Cd complexes was demonstrated by flux assays using radio-labeled Cd and isolated mesophyll protoplasts. While an overexpressing line proved to be more efficient at extruding ^{109}Cd from the cell than the wild type, a silenced line was impaired in its export capacities. However, it remained unclear in which form Cd is transported by AtABCG36. Interestingly, AtABCG36 also conferred tolerance to toxic concentrations of Na^+ (Kim et al., 2010). This multi-specificity together with the involvement of AtABCG36 in pathogen defense raises the question of whether this ABC transporter exhibits broad substrate specificity, or whether AtABCG36 transports a hitherto unidentified common metabolite that links resistance to pathogens and abiotic stress.

In a screen for ABC transporters potentially involved in lead detoxification, Lee et al. (2005) observed that the transcript levels of *AtABCG40/AtPDR12* were up-regulated in the presence of lead. *AtABCG40* loss-of-function mutant plants were more susceptible to lead than the wild type, because they accumulated more of this toxic heavy metal. Accordingly, plants overexpressing *AtABCG40* were more tolerant to lead and contained less lead after exposure than the wild type. AtABCG40-mediated lead tolerance was not found to be related to glutathione-dependent detoxification mechanisms. It was hypothesized that AtABCG40 either acts as a reflux pump that extrudes lead or lead complexes directly or alternatively inhibits lead uptake into the root by excreting a chelating organic acid/agent into the rhizosphere that prevents lead uptake. The finding that AtABCG40 also acts as an ABA importer (see Chapter IV) raises the question of how these two functions are fulfilled by the same transporter. Future work is necessary to clarify whether AtABCG40 acts simultaneously and directly as a hormone importer as well as an exporter for sub-

strates involved in lead tolerance, or whether the lead tolerance is a secondary effect of the ABA transport activity of AtABCG40.

Aluminum (Al) is a toxic metal that greatly limits crop production in acidic soil. A well-known mechanism to cope with aluminum toxicity is the excretion of citrate and malate by MATE transporters (Magalhaes et al., 2007) and malate excretion by Aluminum Tolerance Transporters (ALMTs) into the rhizosphere (Delhaize et al., 2004; Meyer et al., 2010). These organic acids chelate Al, preventing the entry of toxic Al^{3+} into the root (Ryan et al., 2011). In a screen to identify genes involved in Al tolerance, several ABC transporters have been found to contribute to Al detoxification including *AtABCI16/AtALS3* and *AtABCI17/AtSTAR1* and two rice genes *OsSTAR1* and *OsSTAR2*. Mutation in *AtABCI16* resulted in hypersensitivity to Al and alteration in Al accumulation in roots (Larsen et al., 1997; Larsen et al., 2005). *AtABCI16* encodes one transmembrane domain homologous to a bacterial ABC protein, and may function to redistribute accumulated Al away from sensitive tissues, by transporting either Al directly or compounds involved in Al tolerance (Larsen et al., 1997; Larsen et al., 2005). *OsSTAR1* encodes the nucleotide-binding domain and *OsSTAR2* encodes the transmembrane domain of the transporter, which are homologous to bacterial-type ABC transporters (Huang et al., 2009). The combined ABC transporter complex is shown to localize mainly in membrane vesicles inside of root cells. Co-expression of *OsSTAR1* and *OsSTAR2* in oocytes revealed that they form a functional ABC transporter that is able to transport UDP-glucose (Figure 3A). This was a surprising result and the authors suggested that UDP-glucose may be used to alter the composition of the cell wall, and thereby prevent migration of Al into the plasma membrane. The same group recently reported that a close homolog of OsSTAR1 exists in Arabidopsis (Huang et al., 2010). The knockout mutant of *AtSTAR1* was also sensitive to aluminum. The observation that *OsSTAR1* could rescue the aluminum-sensitive phenotype of the Arabidopsis mutant indicates that the proteins encoded by these two genes exhibit similar functions. It is therefore likely that AtABCI16 and AtABCI17 make a functional transporter similar to the case of OsSTAR1 and OsSTAR2. The observation that *AtSTAR1* is expressed in the outer layers of root tips and developing leaves, however, raises the question as to whether this ABC transporter has an additional function, for instance, in pathogen resistance in Arabidopsis.

IV. TRANSPORT OF PHYTOHORMONES

IV.A. Auxin

Indole-3 acetic acid (IAA, auxin) is a phytohormone involved in a multitude of processes. It plays a role in embryogenesis, cell division, cell elongation, lateral root development, apical meristem dominance, gravitropism, phototropism, and other developmental and physiological processes (Benjamins and Scheres, 2008). Auxin is a somewhat unique growth regulator in that directional movement of the compound and is an essential component of the signaling mechanism. Tightly regulated and directed cell-to-cell transport of auxin leads to distinct auxin gradients created by asymmetric auxin distributions that are, to a large degree, responsible for the orchestration of auxin-dependent processes. Since auxin is mainly synthesized in leaf primordia and young leaves, it has to be transported to its sites of action. Polar transport of auxin from the shoot to the root apex and redirection at the root tip are essential for the programmed and plastic polarity of the plant form.

The control of differential growth by polar auxin streams was inferred from studies of tropic plant growth initiated by Charles and Francis Darwin (1880). A model for cellular auxin movement driven by chemiosmotic gradients was proposed by Rubery and Sheldrake (1974). This model predicted that auxin, which is present predominantly in the protonated, uncharged form in an acidic environment (*pKa* 4.75), can diffuse from the apoplast into a plant cell and is then released in its anionic form from this cell. The model also predicted that polarized carriers would direct the exit of auxin and, thus, the polar auxin streams. Subsequently, mutations that exhibited either reduced root gravitropism or “pinformed” inflorescences similar to those observed in Arabidopsis after treatment with the polar auxin transport inhibitor, naphthalene phthalamic acid (NPA), resulted in the identification of the PIN family of proteins (Chen et al., 1997; Gäelweiler et al., 1998; Luschnig et al., 1998). The PIN proteins exhibited a predominantly polarized cellular localization, as predicted, and were subsequently shown to exhibit auxin transport activity in heterologous systems (Petrášek et al., 2006). Earlier biochemical experiments had also predicted the presence of an auxin uptake symport activity, and this activity was subsequently associated with the AUX1/LAX family of proton symporters (Bennett et al., 1996; Yang et al., 2006). Together, PINs and AUX1/LAX proteins constitute a complex network that controls directional auxin fluxes (Křeček et al., 2009; Petrášek and Friml, 2009; Titapiwatanakun and Murphy, 2009).

IV.A.1. AtABCBs/PGPs as auxin transporters

Dudler and colleagues suggested that a subclass of ABC transporters might function in auxin transport, after observing that Arabidopsis ABCB1 localized to the plasma membrane, and that hypocotyl growth was reduced in *AtABCB1/AtPGP1* antisense lines, while *AtABCB1* overexpressing plants developed longer hypocotyls (Sidler et al., 1998). In a subsequent study, Noh et al. (2001) presented direct evidence that AtABCB1 and its closest homolog, AtABCB19/AtPGP19, participate in auxin transport. Arabidopsis *abcb1* and the more pronounced *abcb19* mutant exhibit reduced growth, decreased apical dominance, and impaired polar auxin transport (Figure 4A). *atabcb1 atabcb19* plants are very small, and the shoot basipetal auxin flux is reduced by more than 70%. Despite this strong reduction, the mutant does not exhibit the defects in organogenesis and tropic growth observed in plants treated with auxin efflux inhibitors as is the case in *pin* mutants. On the contrary, *atabcb19* hypocotyls are hyperphototropic and hypergravitropic (Noh et al., 2003; Lin et al., 2005), and *atabcb19* plants produce many more curvatures but are not agravitropic (Lewis et al., 2007). However, Arabidopsis ABCB1 and ABCB19 have been shown to act directly as auxin exporters in protoplast assays and in assays of yeast and mammalian cells expressing the Arabidopsis proteins (Geisler et al., 2005; Yang and Murphy, 2009). It is interesting to note that these transporters lost the

specificity for auxin when expressed in a heterologous system (Geisler et al., 2005). They may require some factors present in plant tissues to exhibit auxin specificity.

A third Arabidopsis ABCB transporter with an affinity for auxin, AtABCB4/AtPGP4, appears to function in auxin transport in the root, but this protein has been implicated in both auxin export and uptake activity (Santelia et al., 2005; Terasaka et al., 2005; Cho et al., 2007; Lewis et al., 2007; Wu et al., 2007). Loss of AtABCB4 function results in decreased shoot-ward auxin transport in the root (Terasaka et al., 2005; Lewis et al., 2007; Wu et al., 2007) and increased root hair elongation (Santelia et al., 2005; Cho et al., 2007). Overexpression of *AtABCB4* in root hair cells results in decreased elongation in a manner that is similar to what is seen upon overexpression of other auxin efflux transporters, and auxin efflux was enhanced in BY-2 cells overexpressing *AtABCB4* (Cho et al., 2007). However, auxin uptake activity was enhanced in *Saccharomyces cerevisiae* expressing Arabidopsis *ABCB4* (Santelia et al., 2005). When expressed in mammalian cells, AtABCB4 was shown to mediate IAA uptake at low concentrations, but to reverse to apparent efflux when treatment with NPA increased internal concentrations (Terasaka et al., 2005). A recent paper published by Yang and Murphy (2009) showed that AtABCB4 kinetics are different from those of AtABCB1 and AtABCB19. *Schizosaccharomyces pombe* cells expressing *AtABCB4* incubated in the presence of auxin initially accumulate auxin, but after a certain period of incubation, started to export auxin again. The primarily epidermal localization of AtABCB4 suggests that AtABCB4 may modulate the uptake of auxins produced by soil microorganisms (Figure 4B).

IV.A.2. Interaction of ABC transporters with PINs, PHOT1, and TWD1 modulate auxin transport activity

Evidence for the regulation of ABC protein-mediated auxin transport came from a yeast two-hybrid screen, in which the immunophilin-like TWD1 (FKBP42) was found to interact with AtABCB1. Later studies using the BRET (Bioluminescence Resonance Energy Transfer) technique provided evidence that auxin transport activity was modulated by the interaction between TWD1 and AtABCB1 (Bouchard et al., 2006; Bailly et al., 2008). Interestingly, the *twd1* loss-of-function mutant displayed a similar phenotype to the *atabcb1 atabcb19* double knock-out, except that, in addition to the dwarf phenotype, *twd1* plants exhibit a much more severe twist. NPA, an auxin transport inhibitor, as well as flavonoids, which are thought to act as endogenous auxin transport modulators, can disrupt the AtABCB1-TWD1 complex and thereby reduce the transport activity *in planta*.

Auxin transport is furthermore regulated by direct interaction between the two classes of auxin exporters, PINs and ABCBs. Localization and developmental studies suggest that these proteins mediate auxin transport independently. However, in some tissues, the two types of auxin transporters are co-localized and it was shown by a yeast two-hybrid assay as well as by co-immunoprecipitation that PIN1 can interact with AtABCB19. Similar results were obtained for PIN1 and AtABCB1. Analysis of the transport rates showed that, when present as a complex, PIN1

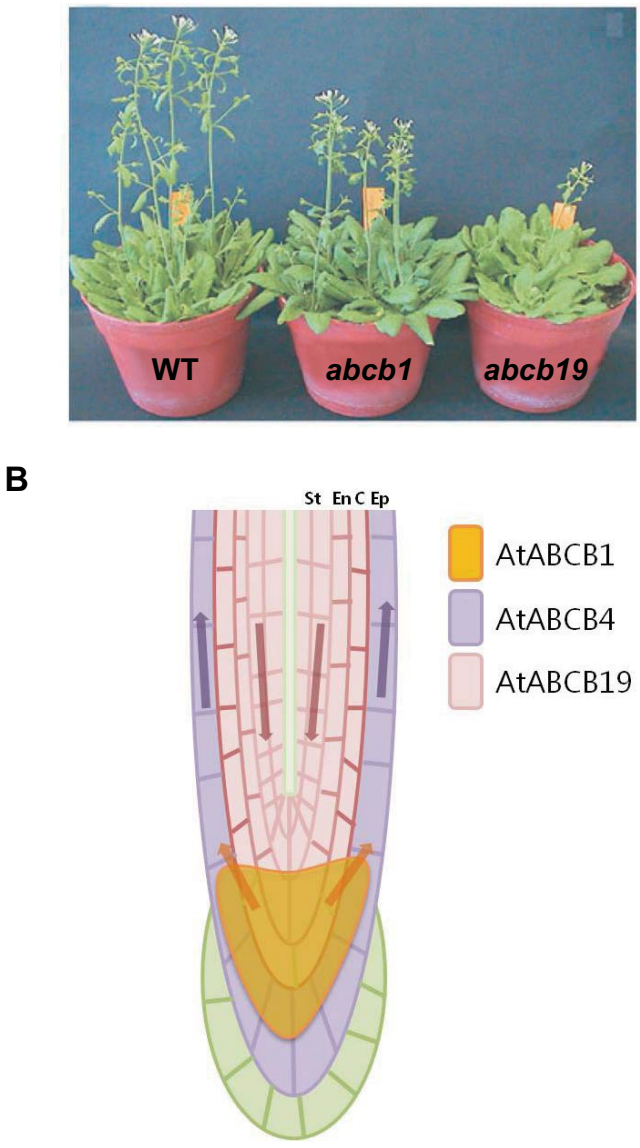

Figure 4. AtABCB1, AtABCB4, and AtABCB19 are auxin transporters.

(A) Phenotypes of the loss-of-function mutants of *AtABCB1* and *AtABCB19*. Image reprinted Geisler et al. (2005) with permission from Wiley-Blackwell Publishing.

(B) Localization of AtABCB1, AtABCB4, and AtABCB19 in roots and auxin fluxes mediated by these three ABCB proteins. AtABCB1 is expressed in the root differentiation zone (orange, columella and root apical meristem; Sidler et al., 1998). AtABCB4 localizes mainly to the epidermis (purple; Terasaka et al., 2005; Wu et al., 2007). AtABCB19 is expressed from the stele to the cortex and weakly in epidermal cells of the root (pink; Wu et al., 2007; Blakeslee et al., 2007). St : stele, En: endodermis, C: cortex, and Ep: epidermis. The arrows represent auxin flux.

and AtABCB19 exhibit a synergistic effect, and the proteins are more sensitive to inhibitors (Blakeslee et al., 2007; Rojas-Pierce et al., 2007). In contrast, an interaction between PIN2 and AtABCB1 or AtABCB19 leads to the inhibition of auxin transport. Future research should analyze these interactions *in vivo* to resolve their temporal and spatial components. This is an ambitious goal, but probably the most promising approach to further unravel the modulation of auxin fluxes.

AtABCB19 is transcriptionally regulated by photomorphogenic mechanisms (Noh et al., 2001) and both *atabcb1* and *atabcb19* exhibit a hypersensitivity to far-red, red, and blue light inhibition of hypocotyl elongation (Noh et al., 2001; Lin and Wang, 2005; Wu, 2010), a result confirming the early observations by Sidler et al. (1998). AtABCB19 is a direct phosphorylation target of the PHOT1 photoreceptor, and transient inhibition of AtABCB19 transport by PHOT1 results in the pooling of auxin in the first step of phototropic bending (Christie et al., 2011). PHOT1 interacts with the C-terminus of AtABCB19, which has been shown to be a target of the inhibitory drug gravacin (Rojas-Pierce et al., 2007) and a site of interaction with the FKBP42 immunophilin TWD1.

IV.B. Auxigenic Compounds

Auxin precursors, such as indole-3-butyric acid (IBA) or amide- or ester-linked conjugates, can rapidly be metabolized to free auxin. Thus, they constitute a rapidly available auxin pool that does not depend on *de novo* synthesis. As is the case for auxin, the regulated transport of the precursors is crucial for the normal physiology of plant. The first transporter involved in IBA transport, AtABCD1/PXA1, was identified in a screen for IBA-resistant mutants (Zolman et al., 2001). The authors showed that loss-of-function of this peroxisomal ABC transporter confers resistance to IBA, but not to IAA. Further analysis of this peroxisomal ABC transporter, also called PED3p (Hayashi et al., 2002) or COMATOSE (Footitt et al., 2007), revealed that, besides transporting IBA, it is most likely responsible for the import of substrates for peroxisomal β-oxidation (see Chapter VI).

Three reports demonstrate that two members of the ABCG family are involved in the excretion of auxigenic compounds. Ito and Gray (2006) performed a screen to identify mutants that are resistant to 2, 4-D, a synthetic auxin analogue used as an herbicide. They found that a mutation in AtABCG37/AtPDR9 conferred resistance to 2, 4-D and other structurally related compounds. This was a surprising result, since ABC transporters were thought to excrete toxic compounds and hence mutations were expected to decrease resistance rather than to enhance it. The apparent contradiction was resolved by the finding that an Ala to Thr substitution at position 1034 confers increased stability to the AtABCG37 protein. Indeed, a T-DNA insertion in the corresponding gene leads to a 2, 4-D-sensitive phenotype, while overexpression enhances tolerance to a variety of auxigenic compounds.

In a similar screen, aimed at identifying genes that lead to IBA hypersensitivity, Růžička et al. (2010) identified AtABCG37 as a potential IBA transporter. They found that loss-of-function mutants of the gene were not affected in their sensitivity to auxin, but, using heterologous expression in yeast and animal cells as well as assays with root tips, they showed that AtABCG37 indeed exports IBA and some synthetic auxins, such as 2, 4-D, from the cell. Because of its specific plasma membrane localization at the soil-exposed face of root epidermal cells, this transporter is likely to release IBA and other auxigenic compounds into the soil. Since the expression of AtABCG36 and AtABCG37 partially overlaps, the authors investigated the double knock-out mutant and observed that the sensitivity to IBA was increased even further (Růžička et al., 2010). Some microorganisms, including symbionts, produce IBA; therefore, the authors hypothesized that AtABCG37 might be involved in the cross-talk between microorganisms and plants. However, AtABCG37 may be involved in the export of a much broader range of weak organic acids and hence have a similar function to yeast PDR12. In any case, detailed studies of how AtABCG36 and AtABCG37 function affect microbial communities in the rhizosphere are pending.

Strader and Bartel (2009) performed a screen to identify mutants that specifically restore IBA, but not auxin sensitivity in the auxin signaling mutant *ibr5*. The *ibr5* mutant is defective in a protein phosphatase, which renders it insensitive to endogenous and exogenously applied auxin. Mapping of a candidate mutation revealed that loss of AtABCG36 function restores IBA sensitivity in *ibr5*. Root tips of the *atabcg36* mutant exhibit increased IBA accumulation and reduced IBA efflux, suggesting that AtABCG36 promotes IBA efflux (Strader and Bartel, 2009).

IV.C. Abscisic Acid

Abscisic acid (ABA) is a plant hormone with profound effects on seed maturation, seed dormancy, stomatal closure, drought responses, and lateral root formation (Leung and Giraudat, 1998; Rock, 2000; Rohde et al., 2000). Under drought stress, the ABA level in the shoot can increase 50-fold compared to that under turgid conditions. ABA biosynthesis is highly induced by dehydration in the vascular parenchyma cells of roots and shoots, but not in guard cells (Zimmermann et al., 2004; Christmann et al., 2005; Endo et al., 2008; https://www.genevestigator.com/gv/). Consequently, ABA has to be exported from ABA-producing cells in the roots and leaves, redistributed, and directed to guard cells. A further important developmental process regulated by ABA is the maintenance of seed dormancy. Seed dormancy is the incapacity of a viable seed to germinate under unfavorable conditions (Finch-Savage and Leubner-Metzger, 2006). To maintain dormancy, the continuous synthesis of ABA in the seed coat (endosperm) and its subsequent transport to the embryo is required (Ali-Rachedi et al., 2004).

Recently, the PYR/RCAR family has been identified as ABA receptors (Ma et al., 2009; Park et al., 2009). Since they are localized in the cytosol, ABA has to cross the plasma membrane once it arrives at the target site. Despite the fact that ABA could passively accumulate in cells by diffusion, there is also evidence that ABA uptake is mediated by a transporter (Windsor et al., 1992 ; Daeter and Hartung, 1993; Wilkinson and Davies, 1997; Jiang and Hartung, 2008).

Two approaches have recently led to the simultaneous identification of an ABA exporter and an ABA importer (Figure 5). In a forward genetic approach, Shinozaki and collaborators performed a high-throughput screen for transposon lines affected in an ABA response (Kuromori et al., 2010). A mutant line exhibiting an ABA-sensitive germination phenotype was isolated and the authors showed that the responsible transposon insertion

disrupted the AtABCG25/AtWBC26 coding sequence. This ABC transporter corresponds to a half-size ABC transporter, formerly called AtWBC26. Promoter-GUS analysis revealed that AtABCG25 is predominantly expressed in the vascular bundle. Using an N-terminal YFP-fusion protein, it was shown that AtABCG25 is targeted to the plasma membrane. Biochemical analysis of membrane vesicles isolated from *AtABCG25*-expressing insect cells showed that AtABCG25 displays high affinity and high specificity for the transport of biologically active (+) ABA. *AtABCG25*-overexpressing plants had a higher leaf temperature, indicating reduced stomatal transpiration. These results are clear evidence that AtABCG25 acts as an ABA exporter. However, knockout lines did not display a stomatal phenotype, suggesting that there is some redundancy and that a second ABA exporter may exist and work in parallel with AtABCG25.

The rationale behind the second work (Kang et al., 2010b) was that, since plant ABCG transporters had previously been shown to transport terpenoids and since ABA is a tetraterpene-derived sesquiterpene, the ABCG proteins are strong candidates for ABA transporters (Campbell et al., 2003; Rea et al., 2007). In a screen using loss-of-function *atabcg* mutants Kang et al. (2010b) observed that *atabcg40* exhibited a decreased sensitivity to ABA-induced stomatal closure. Further analysis revealed that this mutant was more drought-sensitive and, when treated with ABA, had a higher leaf temperature than the wild type. These results indicated that stomata were not able to close efficiently in this mutant. Since it was also observed that *AtABCG40/AtPDR12* is preferentially expressed in guard cells and targeted to the plasma membrane, it was suggested that the corresponding protein might act as an ABA importer. Indeed, this hypothesis was confirmed with three independent transport assays, i) using protoplasts isolated from wild-type and mutant plants, ii) using *AtABCG40*-expressing yeast, and iii) using *AtABCG40*-expressing BY2 cells. AtABCG40 imports ABA with a high affinity and is specific for the biologically active form. It has long been assumed that ABA permeates into the cell passively, and thus an ABA importer may not be required in plants. However, it should be kept in mind that, during water stress, the pH in the apoplast rises from 5.5–6.0 to about 7, and hence the protonated, freely diffusible form of ABA is present only at very low levels. The observed phenotype and the demonstration that induction of ABA-inducible genes is strongly delayed in the *atabcg40* knock-out mutant, proves that ABA import is required for a rapid and efficient response during ABA-mediated stress reactions.

Another member of the ABCG family, AtABCG22/AtWBC23, which is implicated in stomatal regulation, was identified very recently (Kuromori et al., 2011). Mutants of this transporter had a lower leaf temperature and increased water loss. However, the substrate transported by this transporter could not be determined.

Although both *atabcg40* and *atabcg25* also exhibited a germination phenotype, the precise role of *AtABCG40* and *AtABCG25* in the complex process of seed dormancy and germination has yet to be elucidated. The seed coat produces and steadily releases ABA until conditions are favorable for seed germination. The embryo, on the other hand, has to take up ABA to remain dormant. How ABA efflux and import are coordinated and which transporters are involved in this developmental process remain to be established. The same holds true for ABA transporters implicated in lateral root formation.

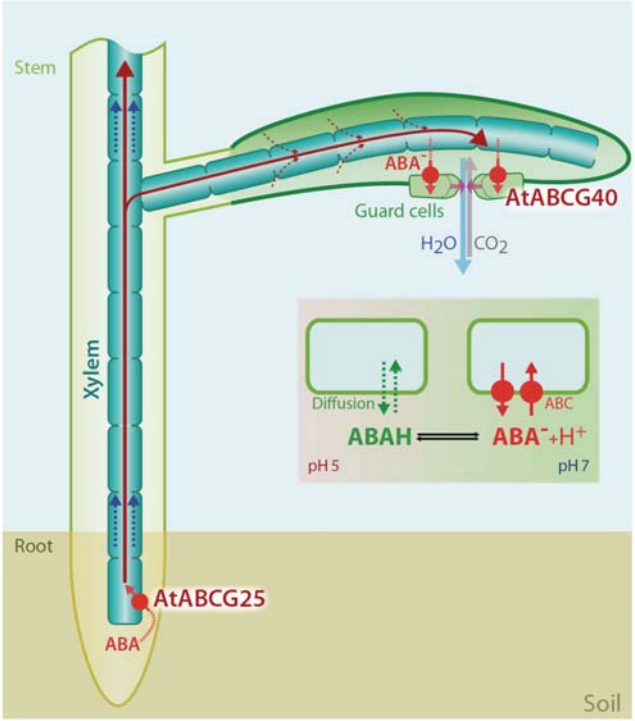

Figure 5. Abscisic acid (ABA) fluxes and the role of the ABA efflux and influx transporter.

AtABCG25 exports ABA from parenchyma cells in the vasculature into the xylem. ABA is directed with the transpiration stream to guard cells, where AtABCG40 mediates its uptake into guard cells.

V. TRANSPORT OF PRIMARY PRODUCTS

To allow for the optimal functioning of cellular metabolism, the concentration of most solutes in the cytosol and other metabolically active compartments are kept constant and transient accumulation of metabolites in excess is avoided. The large central vacuole, which exhibits only minimal metabolic activity, plays the major role as temporary storage compartment.

V.A. Folates and Folate Homologs Are Transported into the Vacuole by AtABCC1 and AtABCC4

Folates, also known as Vitamin B9 (Raichaudhuri et al., 2009), are enzymatic cofactors that are required for one-carbon transfer reactions, e.g., for amino acid and nucleotide biosynthesis. Transient accumulation of folates within the vacuole is important, primarily to maintain cytosolic concentrations of folate that are optimal for biochemical reactions. Most of the folate in the cell is conjugated to several glutamate molecules and hence bears a large number of negative charges. These can interact with cations, such as Ca^{2+}, in an unspecific manner, thus disturbing the cellular signaling pathways. Vacuolar membrane-localized ABC transporters, such as AtABCC1 (Raichaudhuri et al., 2009) and AtABCC4 (Klein et al., 2004), are involved in regulating cyto-

plasmic folate concentrations by transporting excess folates into the vacuole. Vacuoles isolated from *AtABCC1* T-DNA insertion mutants accumulated only approximately 50% of the antifolate methotrexate present in the wild type and the mutants were more sensitive when exposed to this compound. These results indicate that ABCC transporters, such as AtABCC1, are important for folate storage (Figure 3A). However, the mechanism by which folate is released from the vacuoles back into the cytosol when required remains unknown.

V.B. Phytate is Transported by AtABCC5

V.B.1. Cellular homeostasis

A similar tight regulation of cellular concentrations is also required for phytate (inositol hexa*kis*phosphate, $InsP_6$). As the main form of phosphate storage in seeds of many plant species, this compound is important for early plant growth. Phytate has six phosphate residues bound to an inositol ring, resulting in a molecule containing twelve negative charges. Consequently, phytate exhibits a considerable chelating capacity for positively charged compounds, particularly divalent cations. Therefore, the presence of high concentrations of this compound in the cytosol would adversely affect cellular metabolism. Based on sequence similarity to maize MRP4, which, when knocked-out causes a low phytate (*lpa*) phenotype in seeds (Shi et al., 2007), Nagy et al. (2009) showed that the knockout mutants of Arabidopsis AtABCC5/MRP5 also exhibit a low phytate phenotype. Transport experiments using vesicles isolated from yeast expressing *AtABCC5* confirmed that AtABCC5 acts as a phytate transporter. Several low phytate mutants, which have a mutation in homologs of AtABCC5 and ZmMRP4, have been described (Xu et al., 2009). The most drastic effect was observed in rice, where a mutation in an ABCC5 homolog is lethal (Turner et al., 2007). Manipulation of vacuolar phytate transport is of great interest to crop engineers, since reducing the phytate content in seeds would potentially allow the production of plants with a higher amount of bioavailable iron and zinc. Furthermore, a high $InsP_6$ content in seeds can have a negative impact on the environment. Monogastric animals that lack phytases in their digestive tract fail to process the phytates present in seed-based feed. As a consequence, high amounts of undigested phytates are released with the animal waste into nature, thus accentuating the phosphorus pollution from agriculture (Cromwell and Coffey, 1991).

V.B.2. Role of Inositol hexakisphosphate transport in guard cell signaling

Gaedeke et al. (2001) reported that loss-of-function mutants for *AtMRP5/AtABCC5* were no longer responsive to glibenclamide, a compound known to induce stomatal opening (Leonhardt et al., 1997). Further studies demonstrated that the guard cells of *atabcc5* mutants did not respond to ABA, Ca^{2+}, and auxin, but were still light sensitive (Klein et al., 2003). In addition, it was demonstrated that stomatal anion channel activity was reduced in *atabcc5* (Suh et al., 2007). However, it remains unclear how loss of function of a single ABC transporter could lead to such a complex stomatal phenotype. The report by Nagy et al. (2009), which demonstrates that AtABCC5 is a high affinity $InsP_6$ transporter, may provide a clue. Former studies showed that $InsP_6$ is an activator of vacuolar Ca^{2+} release and an inhibitor of K^+ influx (see references in Nagy et al. 2009). In guard cells, therefore, it was postulated that, if the $InsP_6$ signal is not readily removed from the guard cell cytosol, it would lead to the deregulation of Ca^{2+}-dependent signaling cascades and affect K^+ influx. The extremely high affinity found for this transporter (Km=0.3 µM) further supports the notion that guard cell-expressed AtABCC5 is indeed involved in the removal of this signaling compound. Further studies will be required to elucidate in detail how the integration of ABA, auxin, Ca^{2+}, and $InsP_6$ signals controls stomatal movement.

V.C. Malate Transport: Osmoregulation

In a study to identify the functions of ABC transporters highly expressed in guard cells, Lee et al. (2008) observed that loss-of-function mutants of the plasma membrane intrinsic protein AtABCB14 exhibited impaired stomatal regulation. In the presence of high levels of CO_2, stomatal closure was more pronounced in the mutant than in the wild type. This phenotype was not observed in isolated epidermal strips containing epidermal cells and guard cells only, suggesting that the aberrant stomatal movement of the mutant was not directly linked to CO_2. Based on the published literature, it is likely that the closing effect of CO_2 is on the one hand mediated directly by CO_2, and on the other by increasing malate levels in the apoplastic space (Hedrich and Marten, 1993; Hedrich et al., 1994; Hu et al., 2010). In line with these experiments, epidermal strips of *atabcb14* plants incubated in the presence of malate displayed a faster stomatal response than those of the corresponding wild type. Transport experiments using *E. coli* and HeLa cells expressing *AtABCB14* revealed that AtABCB14 is a malate importer. Since malate has dual functions as an osmoticum as well as a regulator of anion channels in guard cells (Hedrich and Marten, 1993), Lee et al. (2008) suggested that the phenotype observed for *atabcb14* was due to the accumulation of malate in the apoplast, which shifts the current-voltage curve of the guard cell anion channel, combined with the impaired import of malate into guard cells.

VI. TRANSPORT OF LIPIDS AND LIPOPHILIC COMPOUNDS

Lipids and lipophilic compounds are essential components of a plant. They are the building blocks of biological membranes, and constitute important energy reserves that are indispensable in the early phases of plant development. As surface lipids, they are also required to protect the plant from biotic and abiotic stresses.

VI.A. A Bacterial-Type ABC Transporter is Involved in the Transport of Polar Lipids from the ER to Plastids

Lipid synthesis occurs mainly in the chloroplast and endoplasmic reticulum. The plastidic stroma is the primary site for fatty acid synthesis. Fatty acids are used within the plastid for the synthesis of plastidic membranes, but are also exported to the ER, where they are used for the synthesis of building blocks for other membranes. Galactoglycerolipids, major components of plastidic lipids, are derived from phosphatidic acids by the exchange of

the phosphatidyl with a galactosyl group at the sn-3 position of the glycerol backbone. Interestingly, plastid lipids derived from phosphatidic acid are not only synthesized from plastidic phosphatidic acid, but also from phosphatidic acid assembled in the ER. Therefore, this compound has to re-enter the chloroplast.

In a screen originally aimed at identifying enzymes involved in alternative galactoglycerolipid synthesis pathways, Benning and co-workers discovered the so-called *tgd1* (trigalactosyldiacylglycerol) mutants, which exhibited a complex phenotype, including stunted growth, embryo abortion, a decrease in ER-derived plastid lipids, and accumulation of oligogalactoglycerolipids (TGDG), triacylglycerols, and phosphatidic acids in leaf tissues (Xu et al., 2005). Identification of the underlying genes revealed that *TGD1/AtABCI14* encodes a membrane-spanning protein. Two other *tgd* mutants, *tgd2* and *tgd3*, were isolated based on their altered lipid phenotypes, which resembled those of *tgd1*. *TGD2/AtABCI15* encodes a phosphatidic acid-binding protein anchored at the inner envelope of the plastid (Awai et al., 2006), and *TGD3/AtABCI13* encodes the catalytic domain of an ABC transporter located in the stroma of the plastid (Lu et al., 2007). These three subunits form a bacterial-type ABC transporter, which is proposed to be responsible for the import of phosphatidic acid into the plastid. The importance of this lipid transporter is reflected by the phenotype of the *tgd1* and *tgd2* mutants, which are consistently smaller and synthesize less chlorophyll than the wild type.

VI.B. AtABCD1 Is Required for the Import of Substrates for Beta-Oxidation

Beta-oxidation of fatty acids is an important catabolic process that is required for the generation of acetyl-CoA for entry into the citric acid cycle. In plants, this process occurs predominantly within the peroxisomes, and fatty acyl-CoAs must therefore be imported from the cytosol. At least four forward genetic screens identified an ABC transporter required for this process (Russell et al., 2000; Zolman et al., 2001; Footitt et al., 2002; Hayashi et al., 2002). In contrast to its animal and yeast counterparts, which consist of two half-size ABC proteins (Mosser et al., 1993; Shani et al., 1995; Hettema et al., 1996; Verleur et al., 1997; van Roermund et al., 2008), the plant peroxisomal ABC transporter is present as a full-size ABC protein. Arabidopsis loss-of-function mutants of *AtABCD1* are strongly impaired in several important metabolic and developmental processes, such as germination, fertility, seedling establishment, and root growth. These studies provided evidence that, besides fatty acyl-CoA, the plant peroxisomal ABC transporter can also import the auxin precursor indolbutyric acid (IBA) and precursors of jasmonic acid (Russell et al., 2000; Zolman et al., 2001; Footitt et al., 2002; Hayashi et al., 2002; Theodoulou et al., 2005). Furthermore, it was demonstrated that this transporter is also important for the peroxisomal uptake of acetate (Hooks et al., 2007). Performing a large-scale mutagenesis screen, Dietrich et al. (2009) showed that the transport activities of IBA and substrates of the β-oxidation can be separated locally. The reason for this might be that this full-length peroxisomal transporter contains two halves that are rather distinct, with each part being responsible for the recognition of certain substrates. All of these *in-planta* studies showed that β-oxidation is strongly affected in the absence of *AtABCD1*; however, no direct evidence for acyl-CoA fatty acid import was provided. To obtain direct evidence that these substrates are indeed imported by AtABCD1, Nyathi et al. (2010) expressed the Arabidopsis transporter in the yeast *pax1 pax2* mutant. This mutant yeast strain is deficient in the function of two homolgous genes of *AtABCD1* and thus fails to grow even when supplemented with exogenous fatty acids. The researchers demonstrated that the *AtABCD1*-expressing *pax1 pax2* mutant yeast was able to grow in the presence of a broad range of fatty acids. More importantly, by isolating yeast peroxisomal membranes, Nyathi et al. (2010) showed that ATP hydrolysis was stimulated in the presence of acyl-CoA fatty acids but not free fatty acids, providing direct evidence that AtABCD1 indeed has an acyl-CoA fatty acid transport activity.

VI.C. Members of the ABCG Family are Required for Deposition of Surface Lipids

Almost all plant organs are covered with hydrophobic compounds to protect the plant body against environmental stresses. As the precursors of surface lipids are mainly synthesized and modified in the endoplasmic reticulum, they must pass through the plasma membrane to reach their final destination, the cell wall, and this process requires the presence of lipid transporters at the plasma membrane. Surface compound-deficient mutants exhibiting severe defects in plant growth and plant resistance against various stresses were a promising starting point to identify transporters involved in this process. This approach led to the identification of some Arabidopsis ABCG transporters that participate in surface lipid formation.

VI.C.1. AtABCG11, 12, 13, and 32 are involved in the transport of cuticular lipid precursors from epidermal cells to the surface for cuticle layer formation

The epidermis of aerial plant organs is covered with a hydrophobic cuticle that protects the plant body from detrimental environmental conditions, such as drought and pathogen invasion. Although there are species-dependent variations in the composition of the cuticle, it generally consists of two types of highly lipophilic materials, cutins and waxes. Cutin, which is deposited on the cellulosic cell wall, is a polymer consisting mainly of glycerol and ω- and mid-chain hydroxy and epoxy C16 and C18 fatty acids (Heredia, 2003; Nawrath, 2006). Recently, α,ω-dicarboxylic acids, components known to occur in suberin, were detected in cutin (Bonaventure et al., 2004). Wax, which is formed on the cutin layer, is a complex mixture of C20 to C60 straight-chain aliphatics and may contain secondary metabolites, such as triterpenoids, phenylpropanoids, and flavonoids (Jetter et al., 2007).

The main function of cutin is to confer resistance against mechanical damage and provide a docking structure for proper wax deposition. Wax, which is directly exposed to the environment, limits non-stomatal water loss, and prevents pathogen invasion by forming a physical barrier and by inducing defense signaling pathways upon pathogen invasion (Reina-Pinto and Yephremov, 2009). The cuticle layer is also important for plant development, as many mutants impaired in cuticule formation exhibit stunted growth and post-genital organ fusion (Nawrath, 2006).

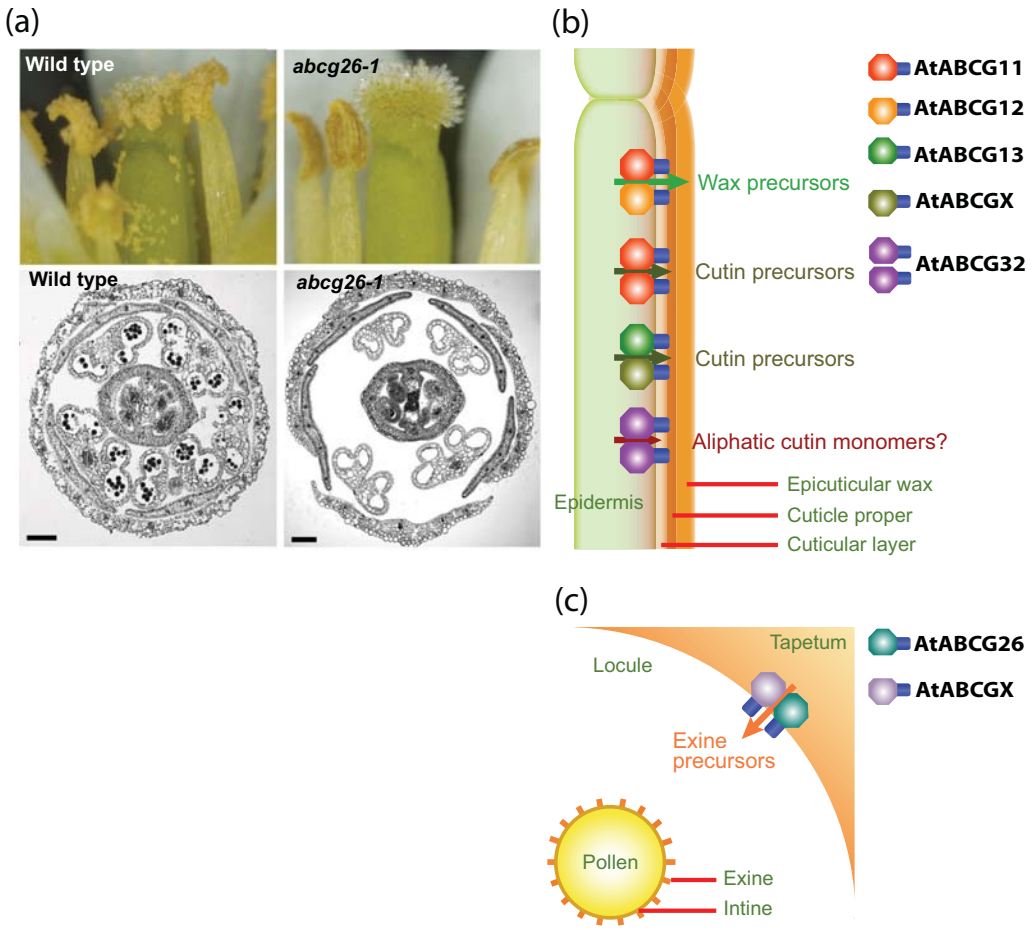

Figure 6. Surface lipids are secreted by ABC transporters of the ABCG family.

(A) Loss-of-function mutants in *AtABCG26* fail to self-pollinate due to defective pollen development caused by impaired sporopollenin formation. Scale bars = 100 µm. Figure taken from Choi et al. (2011).

(B) Members of the ABCG family that participate in cuticle formation by transporting components of the cuticular wax and/or cutin. See text for details.

(C) AtABCG26 is involved in pollen exine formation, possibly by transporting exine precursors from the tapetum to the locules.

The finding that *CER5*, a gene required for wax deposition at the outer surface of epidermal cells, encodes the half-size transporter AtABCG12 was the starting point to gain an in depth understanding of the mechanisms underlying wax deposition (Pighin et al., 2004, Figure 6B). *atabcg12* mutants contained less than 50% of the wax present in wild-type plants. AtABCG12 does not appear to be substrate-specific, since the amount of most wax components, such as alkanes, ketones, and primary and secondary alcohols, was reduced in the extracellular wax of *atabcg12* mutants. Interestingly, the strongly impaired export of these compounds did not lead to feedback inhibition of wax synthesis, as the total amount of waxes in epidermal cells and on the surface remained constant. Epidermal cells of the *atabcg12* mutant formed cytoplasmic protrusions that contained bundles of linear inclusions. These probably correspond to the precursors of cuticular waxes that cannot be exported in the absence of *AtABCG12*. AtABCG12 was localized to the plasma membrane and was specifically expressed in epidermal cells. In a subsequent study, Bird et al. (2007) showed that the *atabcg11* mutant exhibits a similar phenotype to *atabcg12*. In addition to the observations made for *atabcg12*, *atabcg11* loss-of-function mutants exhibited a stunted growth phenotype and showed post-genital organ fusions. Furthermore, the cuticle of *atabcg11* plants contained reduced amounts of both wax and cutin (Figure 6B), whereas that of *atabcg12* plants was reduced only in wax content (Panikashvili et al., 2007). The finding that the *atabcg12 atabcg11* double knockout did not display a stronger phenotype than either of the single knockouts suggests that these two half-size ABC transporters can form heterodimers. Phenotypic differences between the respective single mutants furthermore suggest that at least one of the proteins can also form a homodimer or interact with a third Arabidopsis ABCG protein. Similar studies on *atabcg11* were pre-

sented by Luo et al. (2007), Ukitsu et al. (2007), and Panikashvili et al. (2007). In an earlier study, it was shown that *AtABCG11* is responsive to stresses such as salt treatment, wounding, and ABA application (Alvarado et al., 2004). Together, these results indicate that AtABCG11 is an integral part of cuticle production and deposition, and that its activity may change in response to environmental conditions. In a subsequent study, Panikashvili et al. (2010) extended our knowledge of AtABCG11-mediated wax and cutin deposition by demonstrating that this protein also plays a role in petal and silique formation and prevents seeds from fusing during development. Furthermore, they showed that the absence of *AtABCG11* affected the expression of many genes implicated in cuticle metabolism and suberin formation in roots. Recently, McFarlane et al. (2010) provided convincing evidence that AtABCG11 and AtABCG12 indeed form heterodimers, while AtABCG11 can also form homodimers (Figure 6B). The dominant role of AtABCG11 is also reflected by the fact that AtABCG11 can traffic to the plasma membrane in the absence of AtABCG12, while the latter requires the presence of AtABCG11 to be correctly targeted.

AtABCG13, which is closely related to *AtABCG12*, is mainly expressed in petals and carpels. Accordingly, in the *atabcg13* mutant, a strong flower phenotype with inter-organ fusions was observed (Panikashvili et al., 2011). Interestingly, this ABC transporter exhibits a substrate specificity that differs from that of AtABCG11 and AtABCG12. Determination of surface compounds on flower petals revealed that flower-specific cutin components were not present in the cuticle of *atabcg13*-silenced lines, while the wax components remained unaltered (Figure 6B).

Recently, an additional member of the ABCG subfamily, AtABCG32/PEC1, a full-size ABCG protein, was reported to be involved in the formation of the cuticular layer (Bessire et al., 2011). The *atabcg32* mutant did not exhibit an obvious growth defect, and displayed organ fusions in only 2% of the population. The leaves and petals of *atabcg32* mutant plants were more permeable to toluidine blue staining, lost more water, and were hypersensitive to herbicide treatment, but resistant to infection by *Botrytis cinerea,* indicating that the mutant was defective in cuticle formation.

AtABCG32 was strongly expressed in the epidermis of expanding organs of the shoot, and the encoded protein displayed polar localization at the plasma membrane. In contrast to other mutants of *ABCG* genes that are involved in cuticle formation, the *atabcg32* mutant differed from the corresponding wild type only in the content of minor aliphatic cutin monomers (Figure 6B). The cuticles of the leaves and petals of the *atabcg32* mutant appeared to be normal; however, the cuticular layer, which is the inner boundary of the cuticle and cell wall, was more diffuse and less electron-dense. Nanoridges, which are a characteristic of the petal surface structure, exhibited an irregular shape, size, and distribution. The observation that the changes in cuticular lipids of the *atabcg32* mutant were different from those in other *abcg* cuticle mutants and that the expression of *AtABCG11* and *AtABCG13*, which are also expressed in the epidermis and involved in cutin formation, were not affected in the *atabcg32* mutant, suggests that AtABCG32 has a distinct substrate specificity and function in the cuticle formation. A homolog of *AtABCG32* was shown to be required for keeping transpiration low in barley as well as in rice (Chen et al., 2011).

VI.C.2. AtABCG26 is involved in the transport of sporopollenin precursors for pollen wall formation

Pollen grains are coated with lipophilic layers, which serve a similar protective function to the cuticle layer. The pollen wall is composed of the intine, which mainly consists of cellulose, and the exine, which mainly consists of sporopollenin, a polymer of fatty acid derivatives and phenylpropanoids. Pollen coats contain steryl ester as a main component, as well as flavonoids and alkanes as minor components (Hsieh and Huang, 2007). Most of the material in the pollen wall and coat are supplied by the tapetum, although the intine is supplied by the pollen itself. Many enzymes involved in the synthesis of sporopollenin precursors were discovered by identifying the genes responsible for pollen mutant phenotypes (Aarts et al., 1997; Morant et al., 2007; de Azevedo Souza et al., 2009; Dobritsa et al., 2009; Dobritsa et al., 2010). However, the mechanisms of the transfer of lipidic precursors have not been revealed until recently. Since the exine is formed before the tapetum degenerates by programmed cell death, it has been hypothesized that the lipophilic compounds are transported through the plasma membranes of the tapetal cells. Within the last two years, four papers were published that highlight the important role of AtABCG26 in this process (Quilichini et al., 2010; Xu et al., 2010; Choi et al., 2011; Dou et al., 2011).

Loss-of-function mutants of *AtABCG26* showed a dramatic decline in seed production. They failed to develop mature pollen (Figure 6A), which correlated with a defect in pollen exine formation. Similar to several genes encoding the synthetic enzymes of sporopollenin precursors, *AtABCG26* was exclusively expressed in the tapetum during early flower development, which corresponds with its role in pollen exine formation. In a study that identified AMS, an essential transcription factor for tapetal cell development and postmeiotic microspore formation (Xu et al., 2010), it was shown that *AtABCG26* is also regulated by this transcription factor. Locular inclusions, similar to those found in *atabcg11* and *atabcg12* mutants, were also observed in *atabcg26* (Quilichini et al., 2010). In the tapetum, electron-dense particles, which were interpreted as sporopollenin in previous reports on two other pollen wall mutants, *no exine formation* (*nef*) *1* and *defective in exine formation* (*dex*) *1* (Paxson-Sowders et al., 1997; Ariizumi et al., 2004), accumulated (Choi et al., 2011). Finally, AtABCG26 localized to the plasma membrane. Together, these observations strongly suggest that AtABCG26 exports sporopollenin precursors out of the tapetal cells and into the locules for pollen exine formation (Figure 6C). Several other ABC transporters expressed in anthers may play additional functions in pollen development or be responsible for the release of specific compounds required for the assembly of a functional sporopollenin complex.

The ABCG transporters involved in surface lipid formation are localized to the plasma membrane. Thus, it is still not clear how these lipidic compounds are transported from the endoplasmic reticulum to the plasma membrane, and then from the apoplastic space to the surface. Further, the existence of yet-to-be-identified lipid-binding and possibly also transporting families has been postulated. The next step in understanding the formation of surface lipids will include the identification of these components that cooperate with ABC transporters to bring about correct surface lipid deposition (Debono et al., 2009; Lee et al., 2009).

VII. ABC TRANSPORTERS INVOLVED IN PLANT-MICROBE INTERACTIONS

Anti-microbial plant secondary metabolites, such as phenolics, terpenoids and their derivates, alkaloids, glucosinolates, and cyanogenic glycosides form an important first line of defense against host and non-host pathogens (Osbourn, 1996). They inhibit the proliferation of fungal and bacterial microbes on aerial plant surfaces within the rhizosphere and in the apoplast around local infection sites. There is increasing evidence that the above-ground and below-ground secretion of such compounds is in part mediated by ABC transporters. Transcript profiling of ABCG full-size transporters of Arabidopsis revealed that the expression of about half of these transporters positively respond to jasmonic acid (JA) and/or salicylic acid (SA), two phytohormones that have been implicated in biotic stress responses. About half of the half-size ABCG transporters are induced by jasmonate, but only a fourth by salicylic acid (Genevestigator). Transcript levels of several ABCGs are up-regulated by jasmonate as well as salicylic acid, while others exhibit a specific induction by one of these compounds. This suggests that several ABCGs are involved in pathogen defense and/or in the cross-talk between the plant and microorganisms. This hypothesis is supported by the observation that the transcript levels of more than 50% of the ABCG transporters are up-regulated when treated with microorganisms. Indeed, loss-of-function of one full-size ABCG transporter, AtABCG30/AtPDR2, resulted in a drastic change in soil microflora in the rhizosphere that the authors attributed to an altered root-exudate composition in the mutant (Badri et al., 2008; Badri et al., 2009).

Plant-derived secondary compounds can also serve as powerful attractants of beneficial microbes, such as mycorrhizal fungi and rhizobacteria (Peters et al., 1986; Akiyama et al., 2005). Using plasma membrane vesicles from soybean, Sugiyama et al. (2007) provided evidence that the export of genestein, an isoflavonoid that acts as a plant-derived signaling molecule in the legume-rhizobia symbiosis, is catalyzed by an ABC-type transport mechanism. Since Arabidopsis does not form mycorrhizal associations and is not nodulated, insight into this fascinating topic requires that plant scientists work with other model plants that form this type of symbiotic interaction. In a study to identify genes required for correct arbuscular mycorrhiza (AM) development, Zhang et al. (2010) screened EMS mutagenized Medicago and identified a mutant producing tiny and shriveled mycorrhiza. They called this mutant *str1* for stunted arbuscules. Positional cloning revealed that the gene of interest codes for a half-size ABC transporter of the ABCG family. Interestingly, close homologues of this ABCG member are found in most plants but not in Arabidopsis, suggesting that it has a specific function in mycorrhization. The authors identified a close homologue, MtSTR2, and the *MtSTR2* RNAi plants exhibited a similar mycorrhizal phenotype to *str1*. Both genes are co-expressed and using BiFC the authors could show that they interact. However, the substrate of this transporter remains unknown.

Evidence for the involvement of a plant ABC transporter in the pathogen defense response was provided by the functional characterization of NpPDR1, a full-size ABCG protein of *Nicotiana plumbaginifolia* (Jasinski et al., 2001). NpPDR1 resides in the plasma membrane and is induced by the natural anti-fungal diterpenoid sclareol, which is also produced by *Nicotiana tabacum*. In isolated microsomes, NpPDR1 contributes to the transport of radio-labeled compounds that are closely related to sclareol, supporting the notion that sclareol is an *in vivo* substrate of NpPDR1. Transcript levels of this transporter were most abundant in the leaf epidermis and leaf trichomes (Stukkens et al., 2005), which constitute the first line of defense. Down-regulation of *NpPDR1* leads to a spontaneous and commonly lethal phenotype upon infection with the necrotropic fungus *Botrytis cinerea*. These plants were also highly susceptible to exogenously applied sclareol, indicating that NpPDR1 participates in basal plant defense. Studies on NpPDR1 have driven the idea that transporters of the ABCG subfamily are involved in the plant immune system.

In an extensive forward genetic screen of Arabidopsis mutants for increased susceptibility to the barley powdery mildew pathogen, Stein et al. (2006) identified AtABCG36/AtPDR8/PEN3 as a crucial factor in pre-invasive non-host resistance. The *AtABCG36* loss-of-function mutants were compromised in their capacity to prevent entry of two non-host biotrophs and one non-host necrotroph. On the other hand, they proved to be hyper-resistant to the compatible Arabidopsis powdery mildew pathogen, which the authors attributed to the hyperactivation of SA-dependent defense pathways observed in the mutant. Expression of an *AtABCG36-GFP* fusion construct under the control of the native promoter complemented the phenotype. The corresponding fusion protein was targeted to the plasma membrane, and displayed increased fluorescence intensity at infection sites. Two other loss-of-function mutants with a similar phenotype, *pen1* and *pen2,* were also recovered from the screen (Collins et al., 2003; Lipka et al., 2005). *PEN1* encodes a plasma membrane-located syntaxin, and *PEN2* encodes a myrosinase, a glucosyl hydrolyase implicated in the cleavage of glucose moieties from glucosinolates. By performing a detailed metabolite profiling, Bednarek et al. (2009) revealed that *pen2* mutants fail to accumulate two metabolites, the cysteine derivative, raphanusamic acid, and the tryptophan-derived indo-3-ylmethylamine. In contrast, two indole-derived glucosinolates, 4-methoxyindol-3-ylmethylglucosinolate (4MI3G), a putative precursor for raphanusamic acid and indo-3-ylmethylamine, accumulated to high concentrations in this mutant. The authors showed that cleavage of 4MI3G mediated by PEN2 is required to confer non-host-related pathogen defense. In a parallel paper, Clay et al. (2009) observed that Flg22-dependent callose deposition was strongly reduced in *pen2* and *pen3* mutants. Similarly, as in the work of Bednarek et al. (2009), Clay et al. (2009) found that the amount of 4MI3G was strongly increased in *pen2* as well as in the *pen3*/*atabcg36* mutant. These two publications showed for the first time that glucosinolates are produced not only to protect plants against herbivores, but also against pathogens. Also, these publications provide strong evidence that the cleavage product of 4-methoxyindol-3-ylmethylglucosinolate is a substrate of AtABCG36. However, if one considers that AtABCG36 is also required to protect plants against abiotic stress, such as heavy metal and salt stress (see chapter III), it is reasonable to speculate that AtABCG36 may be capable of transporting structurally unrelated compounds, as described for many ABC transporters.

Recently, a full-size ABCG transporter was identified as the responsible gene for a functional *LR34* (Leaf Rust 34) allele, which is characterized by a robust and durable pathogen resistance phenotype against leaf rust, stripe rust, and powdery mildew in

Triticum aestivum (wheat; Krattinger et al., 2009). *LR34* is predominantly expressed in adult foliar tissues, particularly of the flag leaf, and the highest transcript levels were found in the leaf tip, corresponding to the tissues that exhibit the phenotypic difference between the tolerant and susceptible wheat lines. Wheat varieties with functional *LR34* alleles can be distinguished phenotypically by the development of leaf tip necrosis in adult flag leaves. Despite its resistance-conferring properties, *LR34* is not responsive to pathogen inoculation, suggesting that it has constitutive rather than induced functions. In accordance, the expression of this gene is changed upon developmental stages not modulated by stress factors, unlike many other ABCG transporters. In contrast to NpPDR1 and AtABCG36, which are likely to be restricted to non-host resistance, LR34 is implicated in the defense against several compatible pathogens of fungal origin. LR34 is the only ABCG protein characterized to date that impedes the invasion and spread of compatible pathogens. It will be interesting to investigate whether a wheat- or *Gramineae*-specific compound is required for the tolerance, as described for PEN3.

Considering the participation of ABCG transporters in the secondary metabolite-based pathogen response, it is tempting to speculate that they also play a role in herbivore defense. This may include the deposition of a large variety of insect-deterring compounds on leaf surfaces. ABC transporters might have a role in this process, since jasmonic acid, a potent inducer of many full-size ABCGs, is also a major mediator of herbivory responses.

VIII. OUTLOOK

Throughout the last decade, different approaches such as phenotype analysis or targeted approaches have allowed considerable progress in the understanding of the role of ABC transporters in plants. However, in many cases the detailed transport studies are still missing, either due to technical problems or due to the fact that the desired radiolabeled compound is not available. Plant ABC transporters have so far been discovered in the membranes of most major plant organelles, where they contribute to a multitude of fundamental processes, such as detoxification, phytohormone transport, surface lipid deposition, and plant microbe-interactions. Thus, these transporters are indispensable for proper plant development and also for accurate signal transduction. Nevertheless, of the 130 ABC transporters annotated in the Arabidopsis genome (Verrier et al., 2008), only about 20 have been characterized on a functional level. As Arabidopsis harbors many members of this transporter family, some closely related members are predicted to have overlapping functions. In the case of ABC transporters implicated in surface lipid deposition, the mutants described still excrete a considerable amount of cutin and wax components, and it is therefore likely that additional ABCGs are involved in this important process. It is also likely that additional ABC proteins involved in auxin and abscisic acid transport are present in the Arabidopsis genome, since so far the transport of these hormones has been addressed only for some specific organs, tissues, or cell types. Despite the expected redundancies amongst the ABC transporters, we predict that many ABC proteins with novel functions will soon be discovered. Considering that there are differences in the substrates of surface lipid ABC transporters, and based on the large number of ABCGs and knowledge from the animal field, additional lipid transporters, such as sterol or brassinolide transporters, are expected to exist (Berge et al., 2000). Some of these functions will be revealed by specific screens, while for others, targeted approaches involving the creation of multiple knockouts will be required to identify a small group of genes with a specific function.

We are just starting to understand the role that ABC transporters play in plant-pathogen interactions. The data presented for PEN3/AtABCG36 and wheat LR34 indicate that ABC transporters could operate in a species-specific manner. However, the nature of the putative transported compound which is required for resistance is still elusive. On the other hand, there are some cases where biochemical analysis has demonstrated that ABC-type transport mechanisms are responsible for the transfer of certain substrates, but the corresponding transporter has not been identified. Examples of such cases include glucosylated solutes, peptides and monolignols (Gaillard et al., 1994; Bartholomew et al., 2002; Stacey et al., 2002; Dean and Mills, 2004; Miao and Liu, 2010; Ramos et al., 2011). The identification of the monolignol transporter is of particular interest, since it will not only allow for a better understanding of lignification, but may also have practical implications for biofuel production. Furthermore, it is tempting to speculate that, in some cases, ABCC transporters may be involved in the vacuolar transport of alkaloids, which can accumulate to very high concentrations in regions where it is questionable that the ion trap mechanism would be sufficient to create the predicted concentration gradient of alkaloids between the cytosol and the vacuole (Roberts et al., 1991; Martinoia et al., 2000). Xanthoxal, the precursor of ABA synthesized in the chloroplasts, is another potential substrate for the ABC transporters since it is exported to the cytosol where the last step in ABA synthesis occurs.

Finally, initial results have provided evidence that ABC transporters expressed in roots may have an impact on the interaction between plants and microorganisms. Further studies may provide insight into this cross-talk. The complex changes in root exudates observed in some ABC transporter knockout plants indicate that these transporters are integrated in the overall metabolism of the plant. Roles of many ABC transporters with subtle effects have not been recognized so far since their loss-of-function mutants do not exhibit any dramatic phenotype, but they may play an important role in the fine-tuning of metabolism. The importance of some ABC transporters for the plant survival under natural conditions might emerge only when plants with mutations in these ABC transporters are grown for several generations.

ACKNOWLEDGEMENTS

The authors would like to thank Prof. Christoph Benning and Prof. Angus Murphy for critical reading of parts of the manuscript. E. Martinoia would like to thank the Distinguished Professor Program of Pohang University of Science and Technology, which gave him the opportunity to collaborate with members of the POSTECH-UZH Global Research Laboratory, Division of Molecular Life Sciences, and contribute to this review. Y. Lee was supported by the World Class University (WCU) program through the National Research Foundation of Korea funded by the Ministry of Education, Science and Technology (R31-2008-000-10105-0 or R31-10105).

REFERENCES

Aarts, M.G., Hodge, R., Kalantidis, K., Florack, D., Wilson, Z.A., Mulligan, B.J., Stiekema, W.J., Scott, R., and Pereira, A. (1997). The Arabidopsis MALE STERILITY 2 protein shares similarity with reductases in elongation/condensation complexes. Plant J. **12:** 615-623.

Akiyama, K., Matsuzaki, K., and Hayashi, H. (2005). Plant sesquiterpenes induce hyphal branching in arbuscular mycorrhizal fungi. Nature **435:** 824-827.

Ali-Rachedi, S., Bouinot, D., Wagner, M-H., Bonnet, M., Sotta, B., Grappin, P., and Julien, M. (2004). Changes in endogenous abscisic acid levels during dormancy release and maintenance of mature seeds; studies with the Cape Verde Islands ecotype, the dormant model of *Arabidopsis thaliana*. Planta **219:** 479-488.

Alfenito, M.R., Souer, E., Goodman, C.D., Buell, R., Mol, J., Koes, R., and Walbot, V. (1998). Functional complementation of anthocyanin sequestration in the vacuole by widely divergent glutathione S-transferases. Plant Cell **10:** 1135-1149.

Alvarado, M.C., Zsigmond, L.M., Kovacs, I., Cseplo, A., Koncz, C., and Szabados, L.M. (2004). Gene trapping with firefly luciferase in Arabidopsis. Tagging of stress-responsive genes. Plant Physiol. **134:** 18-27.

Anjard, C., and Loomis, W.F. (2002). Evolutionary Analyses of ABC Transporters of *Dictyostelium discoideum*. Eukaryotic Cell **1:** 643-652.

Ariizumi, T., Hatakeyama, K., Hinata, K., Inatsugi, R., Nishida, I., Sato, S., Kato, T., Tabata, S., and Toriyama, K. (2004). Disruption of the novel plant protein NEF1 affects lipid accumulation in the plastids of the tapetum and exine formation of pollen, resulting in male sterility in *Arabidopsis thaliana*. Plant J. **39:** 170-181.

Awai, K., Xu, C., Tamot, B., and Benning, C. (2006). A phosphatidic acid-binding protein of the chloroplast inner envelope membrane involved in lipid trafficking. Proc. Natl. Acad. Sci. USA **103:** 10817-10822.

de Azevedo Souza, C., Kim, S.S., Koch, S., Kienow, L., Schneider, K., McKim, S.M., Haughn, G.W., Kombrink, E., and Douglas, C.J. (2009). A novel fatty Acyl-CoA Synthetase is required for pollen development and sporopollenin biosynthesis in Arabidopsis. Plant Cell **21:** 507-525.

Badri, D.V., Loyola-Vargas, V.M., Broeckling, C.D., De-la-Pena, C., Jasinski, M., Santelia, D., Martinoia, E., Sumner, L.W., Banta, L.M., and Stermitz, F. (2008). Altered profile of secondary metabolites in the root exudates of Arabidopsis ATP-binding cassette transporter mutants. Plant Physiol. **146:** 762-771.

Badri, D.V., Quintana, N., El Kassis, E.G., Kim, H.K., Choi, Y.H., Sugiyama, A., Verpoorte, R., Martinoia, E., Manter, D.K., and Vivanco, J.M. (2009). An ABC transporter mutation alters root exudation of phytochemicals that provokes an overhaul of natural soil microbiota. Plant Physiol. **151:** 2006–2017.

Bailly, A., Sovero, V., Vincenzetti, V., Santelia, D., Bartnik, D., Koenig, B.W., Mancuso, S., Martinoia, E., and Geisler, M. (2008). Modulation of P-glycoproteins by auxin transport inhibitors is mediated by interaction with immunophilins. J. Biol. Chem. **283:** 21817–21826.

Bartholomew, D.M., Van Dyk, D.E., Lau, S.M.C., O'Keefe, D.P., Rea, P.A, and Viitanen, P.V. (2002). Alternate energy-dependent pathways for the vacuolar uptake of glucose and glutathione conjugates. Plant Physiol. **130:** 1562-1572.

Bednarek, P., Pislewska-Bednarek, M., Svatos, A., Schneider, B., Doubsky, J., Mansurova, M., Humphry, M., Consonni, C., Panstruga, R., Sanchez-Vallet, A., Molina, A., and Schulze-Lefert, P. (2009). A glucosinolate metabolism pathway in living plant cells mediates broad-spectrum antifungal defense. Science **323:** 101-106.

Benjamins, R. and Scheres, B. (2008). Auxin: The looping star in plant development. Annu. Rev. Plant Biol. **59:** 443-465.

Bennett, M.J., Marchant, A., Green, H.G., May, S.T., Ward, S.P., Millner, P.A., Walker, A.R., Schulz, B., and Feldmann, K.A. (1996). Arabidopsis *AUX1* gene: a permease-like regulator of root gravitropism. Science **273:** 948–950.

Berge, K.E., Tian, H., Graf, G.A., Yu, L., Grishin, N.V., Schultz, J., Kwiterovich, P., Shan, B., Barnes, R., and Hobbs, H.H. (2000). Accumulation of dietary cholesterol in sitosterolemia caused by mutations in adjacent ABC transporters. Science **290:** 1771-1775.

Bernard, D.G., Cheng, Y., Zhao, Y., and Balk, J. (2009). An allelic mutant series of ATM3 reveals its key role in the biogenesis of cytosolic iron-sulfur proteins in Arabidopsis. Plant Physiol. **151:** 590-602.

Berthomieu, P., Conejero, G., Nublat, A., Brackenbury, W.J., Lambert, C., Savio, C., Uozumi, N., Oiki, S., Yamada, K., and Cellier, F. (2003). Functional analysis of AtHKT1 in Arabidopsis shows that Na^+ recirculation by the phloem is crucial for salt tolerance. EMBO J. **22:** 2004-2014.

Bessire, M., Borel, S., Fabre, G., Carraca, L., Efremova, N., Yephremov, A., Cao, Y., Jetter, R., Jacquat, A.C., Metraux, J.P., and Nawrath, C. (2011). A member of the PLEIOTROPIC DRUG RESISTANCE family of ATP binding cassette transporters Is required for the formation of a functional cuticle in Arabidopsis. Plant Cell **23:** 1958-1970.

Bird, D., Beisson, F., Brigham, A., Shin, J., Greer, S., Jetter, R., Kunst, L., Wu, X., Yephremov, A., and Samuels, L. (2007). Characterization of Arabidopsis ABCG11/WBC11, an ATP binding cassette (ABC) transporter that is required for cuticular lipid secretion. Plant J. **52:** 485-498.

Blakeslee, J.J., Bandyopadhyay, A., Lee, O.R., Mravec, J., Titapiwatanakun, B., Sauer, M., Makam, S.N., Cheng, Y., Bouchard, R., Adamec, J., Geisler, M., Nagashima, A., Sakai, T., Martinoia, E., Friml, J., Peer, W.A., and Murphy, A.S. (2007). Interactions among PIN-FORMED and P-Glycoprotein auxin transporters in Arabidopsis. Plant Cell **19:** 131–147.

Bonaventure, G., Beisson, F., Ohlrogge, J., and Pollard, M. (2004). Analysis of the aliphatic monomer composition of polyesters associated with Arabidopsis epidermis: occurrence of octadeca-cis-6, cis-9-diene-1,18-dioate as the major component. Plant J. **40:** 920-930.

Bouchard, R., Bailly, A., Blakeslee, J.J., Oehring, S.C., Vincenzetti, V., Lee, O.R., Paponov, I., Palme, K., Mancuso, S., Murphy, A.S., Schulz, B., and Geisler, M. (2006). Immunophilin-like TWISTED DWARF1 modulates auxin efflux activities of Arabidopsis P-glycoproteins. J. Biol. Chem. **281:** 30603–30612.

Bovet, L., Feller, U., and Martinoia, E. (2005). Possible involvement of plant ABC transporters in cadmium detoxification: a cDNA sub-microarray approach. Environ. Int. **31:** 263-267.

Braz, A.S.K., Finnegan, J., Waterhouse, P., and Margis, R. (2004). A plant orthologue of RNase L inhibitor (RLI) is induced in plants showing RNA interference. J. Mol. Evol. **59:** 20-30.

Campbell, E.J., Schenk, P.M., Kazan, K., Penninckx, I.A.M.A., Anderson, J.P., Maclean, D.J., Cammue, B.P.A., Ebert, P.R., and Manners, J.M. (2003) Pathogen-responsive expression of a putative ATP-binding cassette transporter gene conferring resistance to the diterpenoid sclareol is regulated by multiple defense signaling pathways in Arabidopsis. Plant Physiol. **133:**1272-11284

Chen, J.J., Janssen, B.J., Williams, A., and Sinha, N. (1997). A gene fusion at a homeobox locus: Alterations in leaf shape and implications for morphological evolution. Plant Cell **9:**1289-1304.

Chen, G., Komatsuda, T., Ma, J.F., Nawrath, C., Pourkheirandish, M., Tagiri, A., Hu, Y.-G., Sameri, M., Li, X., Zhao, X., Liu, Y., Li, C., Ma, X., Wang, A., Nair, S., Wang, N., Miyao, A., Sakuma, S., Yamaji, N., Zheng, X., and Nevo, E. (2011). An ATP-binding cassette subfamily G full transporter is essential for the retention of leaf water in both wild barley and rice. Proc. Nati. Acad. Sci. USA **108:** 12354-12359.

Cho, M., Lee, S.H., and Cho, H-T. (2007). P-glycoprotein4 displays auxin

efflux transporter-like action in Arabidopsis root hair cells and tobacco cells. Plant Cell **19:** 3930–3943.

Choi, H., Jin, J.Y., Choi, S., Hwang, J.U., Kim, Y.Y., Suh, M.C., and Lee, Y. (2011). An ABCG/WBC-type ABC transporter is essential for transport of sporopollenin precursors for exine formation in developing pollen. Plant J. **65:** 181-193.

Christie, J.M., Yang, H., Richter, G.L., Sullivan, S., Thomson, C.E., Lin, J., Titapiwatanakun, B., Ennis, M., Kaiserli, E., Lee, O.R., Adamec, J., Peer, W.A., and Murphy, A.S. (2011). Phot1 inhibition of ABCB19 primes lateral auxin fluxes in the shoot apex required for phototropism. PLOS Biol. **9:** e1001076.

Christmann, A., Hoffmann, T., Teplova, I., Grill, E., and Műller, A. (2005). Generation of active pools of abscisic acid revealed by in vivo imaging of water-stressed Arabidopsis. Plant Physiol. **137:** 209-219.

Clay, N.K., Adio, A.M., Denoux, C., Jander, G., and Ausubel, F.M. (2009). Glucosinolate metabolites required for an Arabidopsis innate immune response. Science **323:** 95-101.

Clemens, S., Antosiewicz, D.M., Ward, J.M., Schachtman, D.P., and Schroeder, J.I. (1998). The plant cDNA LCT1 mediates the uptake of calcium and cadmium in yeast. Proc. Natl. Acad. Sci. USA **95:** 12043-12048.

Clemens, S., Kim, E.J., Neumann, D., and Schroeder, J.I. (1999). Tolerance to toxic metals by a gene family of phytochelatin synthases from plants and yeast. EMBO J. **18:** 3325-3333.

Cobbett, C.S. (2000). Phytochelatin biosynthesis and function in heavy-metal detoxification. Curr. Opin. Plant Biol. **3:** 211-216.

Cock, J.M., Sterck, L., Rouze, P., Scornet, D., Allen, A.E., Amoutzias, G, Anthouard, V., Artiguenave, F., Aury, J.M., and Badger, J.H. (2010). The *Ectocarpus* genome and the independent evolution of multicellularity in brown algae. Nature **465:** 617-621.

Cole, S., Bhardwaj, G., Gerlach, J., Mackie, J., Grant, C., Almquist K., Stewart, A., Kurz, E., Duncan, A., and Deeley, R. (1992). Overexpression of a transporter gene in a multidrug-resistant human lung cancer cell line. Science **258:** 1650-1654.

Collins, N.C., Thordal-Christensen, H., Lipka, V., Bau, S., Kombrink, E., Qiu, J.L., Huckelhoven, R., Stein, M., Freialdenhoven, A., and Somerville, S.C. (2003). SNARE-protein-mediated disease resistance at the plant cell wall. Nature **425:** 973-977.

Cromwell, G., and Coffey, R. (1991). Phosphorus-a key essential nutrient, yet a possible major pollutant-its central role in animal nutrition. Biotechnology in the feed industry, T.P. Lyons, ed (Nicholasville, KY: Alltech Tech Publishers), pp. 133-145**.**

Daeter, W., and Hartung, W. (1993). The permeability of the epidermal cell plasma membrane of barley leaves to abscisic acid. Planta **191:** 41-47.

Darwin, C., and Darwin, F. (1880). The power of movement in plants.

Dean, J.V., and Mills, J.D. (2004). Uptake of salicylic acid 2-*O*-β-d glucose into soybean tonoplast vesicles by an ATP binding cassette transporter type mechanism. Physiol. Plantarum **120:** 603-612.

Debono, A., Yeats, T.H., Rose, J.K., Bird, D., Jetter, R., Kunst, L., and Samuels, L. (2009). Arabidopsis LTPG is a glycosylphosphatidylinositol-anchored lipid transfer protein required for export of lipids to the plant surface. Plant Cell **21:** 1230-1238.

Delhaize, E., Ryan, P.R., Hebb, D.M., Yamamoto, Y., Sasaki, T., and Matsumoto, H. (2004). Engineering high-level aluminum tolerance in barley with the ALMT1 gene. Proc. Natl. Acad. Sci. USA **101:** 15249-15254.

Dietrich, D., Schmuths, H., De Marcos Lousa, C., Baldwin, J.M., Baldwin, S.A., Baker, A., Theodoulou, F.L., and Holdsworth, M.J. (2009). Mutations in the Arabidopsis peroxisomal ABC transporter COMATOSE allow differentiation between multiple functions in planta: insights from an allelic series. Mol. Biol. Cell **20:** 530-543.

Dobritsa, A.A., Shrestha, J., Morant, M., Pinot, F., Matsuno, M., Swanson, R., Moller, B.L., and Preuss, D. (2009). CYP704B1 is a long-chain fatty acid ω-hydroxylase essential for sporopollenin synthesis in pollen of Arabidopsis. Plant Physiol. **151:** 574-589.

Dobritsa, A.A., Lei, Z., Nishikawa, S., Urbanczyk-Wochniak, E., Huhman, D.V., Preuss, D., and Sumner, L.W. (2010). *LAP5* and *LAP6* encode anther-specific proteins with similarity to chalcone synthase essential for pollen exine development in Arabidopsis. Plant Physiol. **153:** 937-955.

Dong, J., Lai, R., Nielsen, K., Fekete, C.A., Qiu, H., and Hinnebusch, A.G. (2004). The essential ATP-binding cassette protein RLI1 functions in translation by promoting preinitiation complex assembly. J. Biol. Chem. **279:** 42157-42168.

Dou, X.Y., Yang, K.Z., Zhang, Y., Wang, W., Liu, X.L., Chen, L.Q., Zhang, X.Q., and Ye, D. (2011). WBC27, an adenosine tri-phosphate-binding cassette protein, controls pollen wall formation and patterning in Arabidopsis. J. Integr. Plant Biol. **53:** 74-88.

Endo, A., Sawada, Y., Takahashi, H., Okamoto, M., Ikegami, K., Koiwai, H., Seo, M., Toyomasu, T., Mitsuhashi, W., Shinozaki, K., Nakazono, M., Kamiya, Y., Koshiba, T., and Nambara, E. (2008). Drought induction of Arabidopsis 9-cis-Epoxycarotenoid dioxygenase occurs in vascular parenchyma cells. Plant Physiol. **147:** 1984-1993.

Ferro, M., Brugiere, S., Salvi, D., and Seigneurin-Berny, D. (2010). AT_CHLORO, a comprehensive chloroplast proteome database with subplastidial localization and curated information on envelope proteins. Mol. Cell. Proteomics **9:** 1063-1084.

Finch-Savage, W.E., and Leubner-Metzger, G. (2006). Seed dormancy and the control of germination. New Phytol. **171:** 501-523.

Fontecave, M., Choudens, S.O., Py, B., and Baras, F. (2005). Mechanisms of iron-sulfur cluster assembly the SUF machinery. J. Biol. Inorg. Chem. **7:** 713-721.

Footitt, S., Slocombe, S.P., Larner, V., Kurup, S., Wu, Y., Larson, T., Graham, I., Baker, A., and Holdsworth, M. (2002). Control of germination and lipid mobilization by COMATOSE, the Arabidopsis homologue of human ALDP. EMBO J. **21:** 2912-2922.

Footitt, S., Dietrich, D., Fait, A., Fernie, A.R., Holdsworth, M.J., Baker, A., and Theodoulou, F.L. (2007). The COMATOSE ATP-binding cassette transporter is required for full fertility in Arabidopsis. Plant Physiol. **144:** 1467–1480.

Frangne, N., Eggmann, T., Koblischke, C., Weissenbock, G., Martinoia, E., and Klein, M. (2002). Flavone glucoside uptake into barley mesophyll and Arabidopsis cell culture vacuoles. Energization occurs by H^+-antiport and ATP-binding cassette-type mechanisms. Plant Physiol. **128:** 726-733.

Frelet-Barrand, A., Kolukisaoglu, H.U., Plaza, S., Ruffer, M., Azevedo, L., Hortensteiner, S., Marinova, K., Weder, B., Schulz, B., and Klein, M. (2008). Comparative mutant analysis of Arabidopsis ABCC-type ABC transporters: AtMRP2 contributes to detoxification, vacuolar organic anion transport and chlorophyll degradation. Plant Cell Physiol. **49:** 557-569.

Gaedeke, N., Klein, M., Kolukisaoglu, U., Forestier, C., Muller, A., Ansorge, M., Becker, D., Mamnun, Y., Kuchler, K., and Schulz, B. (2001). The *Arabidopsis thaliana* ABC transporter AtMRP5 controls root development and stomata movement. EMBO J. **20:** 1875-1887.

Gäelweiler, L., Guan, C., Műeller, A., Wisman, E., Mendgen, K., Yephremov, A., and Palme K. (1998). Regulation of polar auxin transport by AtPIN1 in Arabidopsis vascular tissue. Science **282:** 2226-2230.

Gaillard, C., Dufaud, A., Tommasini, R., Kreuz, K., Amrhein, N., and Martinoia, E. (1994). A herbicide antidote (safener) induces the activity of both the herbicide detoxifying enzyme and of a vacuolar transporter

for the detoxified herbicide. FEBS Lett. **352:** 219-221.

Gaillard, S., Jacquet, H., Vavasseur, A. Leonhardt, N., and Forestier, C. (2008). AtMRP6/AtABCC6, an ATP-Binding Cassette transporter gene expressed during early steps of seedling development and up-regulated by cadmium in *Arabidopsis thaliana*. BMC Plant Biol. **8:** 22-32

Geisler, M., Blakeslee, J.J., Bouchard, R., Lee, O.R., Vincenzetti, V., Bandyopadhyay, A., Titapiwatanakun, B., Peer, W.A., Bailly, A., Richards, E.L., Ejendal, K.F.K., Smith, A.P., Baroux, C., Grossniklaus, U., Műller, A., Hrycyna, C.A., Dudler, R., Murphy, A.S., and Martinoia, E. (2005). Cellular efflux of auxin catalyzed by the Arabidopsis MDR/PGP transporter AtPGP1. Plant J. **44:** 179–194.

Gomez, C., Terrier, N., Torregrosa, L., Vialet, S., Fournier-Level, A., Verries, C., Souquet, J.M., Mazauric, J.P., Klein, M., and Cheynier, V. (2009). Grapevine MATE-type proteins act as vacuolar H^+-dependent acylated anthocyanin transporters. Plant Physiol. **150:** 402-415.

Goodman, C.D., Casati, P., and Walbot, V. (2004). A multidrug resistance-associated protein involved in anthocyanin transport in *Zea mays*. Plant Cell **16:** 1812-1826.

Grill, E., Loffler, S., Winnacker, E.L., and Zenk, M.H. (1989). Phytochelatins, the heavy-metal-binding peptides of plants, are synthesized from glutathione by a specific gamma-glutamylcysteine dipeptidyl transpeptidase (phytochelatin synthase). Proc. Natl. Acad. Sci. USA **86:** 6838-6842.

Hayashi, M., Nito, K., Takei-Hoshi, R., Yagi, M., Kondo, M., Suenaga, A., Yamaya, T., and Nishimura, M. (2002). Ped3p is a peroxisomal ATP-binding cassette transporter that might supply substrate for fatty acid β-oxidation. Plant Cell Physiol. **43:** 1-11.

Hedrich, R., and Marten, I. (1993). Malate-induced feedback regulation of plasma membrane anion channels could provide a CO_2 sensor to guard cells. EMBO J. **12:** 897-901.

Hedrich, R., Marten, I., Lohse, G., Dietrich, P., Winter, H., Lohaus, G., and Heldt, H.W. (1994). Malate sensitive anion channels enable guard cells to sense changes in the ambient CO_2 concentration. Plant J. **6:** 741-748.

Henikoff, S., Greene, E.A., Pietrokovski, S., Bork, P., Attwood, T.K., and Hood, L. (1997). Genome families; the taxanomy of protein paralogs and chimeras. Science **279:** 609-614.

Heredia, A. (2003). Biophysical and biochemical characteristics of cutin, a plant barrier biopolymer. Biochim. Biophys. Acta **1620:** 1-7.

Hettema, E.H., van Roermund, C.W., Distel, B., van den Berg, M., Vilela, C., Rodrigues-Pousada, C., Wanders, R.J., and Tabak, H.F. (1996). The ABC transporter proteins Pat1 and Pat2 are required for import of long-chain fatty acids into peroxisomes of *Saccharomyces cerevisiae*. EMBO J. **15:** 3813-3822.

Higgins, C.F. (1992). ABC transporters: from microorganisms to man. Annu. Rev. Cell. Biol. **8:** 67-113.

Hirschi, K.D., Korenkov, V.D., Wilganowski, N.L., and Wagner, G.J. (2000). Expression of Arabidopsis CAX2 in tobacco. Altered metal accumulation and increased manganese tolerance. Plant Physiol**. 124:** 125-133.

Hooks, M.A., Turner, J.E., Murphy, E.C., Johnston, K.A., Burr, S., and Jaroslawski, S. (2007). The Arabidopsis ALDP protein homologue COMATOSE is instrumental in peroxisomal acetate metabolism. Biochem. J. **406:** 399-406.

Hsieh, K., and Huang, A.H. (2007). Tapetosomes in *Brassica* tapetum accumulate endoplasmic reticulum-derived flavonoids and alkanes for delivery to the pollen surface. Plant Cell **19:** 582-596.

Hu, H., Boisson-Dernier, A., Israelsson-Nordstrom, M., Bohmer, M., Xue, S., Ries, A., Godoski, J., Kuhn, J.M., and Schroeder, J.I. (2010). Garbonic anhydrases are upstream regulators of CO_2 –controlled stomatal movements in guard cells. Nat. Cell Biol. **12:** 87-93.

Huang, C.F., Yamaji, N., Mitani, N., Yano, M., Nagamura, Y., and Ma, J.F. (2009). A bacterial-type ABC transporter is involved in aluminum tolerance in rice. Plant Cell **21:** 655-667.

Huang, C.F., Yamaji, N., and Ma, J.F. (2010). Knockout of a bacterial-type ABC transporter gene, *AtSTAR1*, results in increased Al sensitivity in Arabidopsis. Plant Physiol. **153:** 1669-1677.

Ishikawa, T. (1992). The ATP-dependent glutathione S-conjugate export pump. Trends. Biochem. Sci. **17:** 463-468.

Ito, H., and Gray, W.M. (2006). A gain-of-function mutation in the Arabidopsis pleiotropic drug resistance transporter PDR9 confers resistance to auxinic herbicides. Plant Physiol. **142:** 63–74.

Jaquinod, M., Villiers, F., Kieffer-Jaquinod, S., Hugouvieux, V., Bruley, C., Garin, J., and Bourguignon, J. (2007). A proteomics dissection of *Arabidopsis thaliana* vacuoles isolated from cell culture. Mol. Cell. Proteomics **6:** 394-412.

Jasinski, M., Stukkens, Y., Degand, H., Purnelle, B., Marchand-Brynaert, J., and Boutry, M. (2001). A plant plasma membrane ATP binding cassette-type transporter is involved in antifungal terpenoid secretion. Plant Cell **13:** 1095-1107.

Jedlitschky, G., Leier, I., Buchholz, U., Center, M., and Keppler, D. (1994). ATP-dependent transport of glutathione S-conjugates by the multidrug resistance-associated protein. Cancer Res. **54:** 4833-4836.

Jetter, R., Kunst, L., and Samuels, A.L. (2007). Composition of plant cuticular waxes. (Blackwell Publishing Ltd).

Jiang, F., and Hartung, W. (2008). Long-distance signaling of abscisic acid (ABA): the factors regulating the intensity of the ABA signal. J. Exp. Bot. **59:** 37-43.

Kang, B.G., Ye, X., Osburn, L.D., Stewart, C.N. Jr., and Cheng, Z.M. (2010a). Transgenic hybrid aspen overexpressing the *Atwbc19* gene encoding an ATP-binding cassette transporter confers resistance to four aminoglycoside antibiotics. Plant Cell Rep. **29:** 643-650.

Kang, J., Hwang, J.U., Lee, M., Kim, Y.Y., Assmann, S.M., Martinoia, E., and Lee, Y. (2010b). PDR-type ABC transporter mediates cellular uptake of the phytohormone abscisic acid. Proc. Natl. Acad. Sci. USA **107:** 2355–2360.

Kim, D.Y., Bovet, L., Kushnir, S., Noh, E.W., Martinoia, E., and Lee, Y. (2006). AtATM3 is involved in heavy metal resistance in Arabidopsis. Plant Physiol. **140:** 922-932.

Kim, D.Y., Bovet, L., Maeshima, M., Martinoia, E., and Lee, Y. (2007). The ABC transporter AtPDR8 is a cadmium extrusion pump conferring heavy metal resistance. Plant J. **50:** 207-218.

Kim, D.Y., Jin, J.Y., Alejandro, S., Martinoia, E., and Lee, Y. (2010). Overexpression of *AtABCG36* improves drought and salt stress resistance in Arabidopsis. Physiol. Plantarum **139:** 170-180.

Klein, M., Martinoia, E., and Weissenbock, G. (1998). Directly energized uptake of beta-estradiol 17-(beta-D-glucuronide) in plant vacuoles is strongly stimulated by glutathione conjugates. J. Biol. Chem. **273:** 262-270.

Klein, M., Martinoia, E., Hoffmann-Thoma, G., and Weissenbock, G. (2000). A membrane-potential dependent ABC-like transporter mediates the vacuolar uptake of rye flavone glucuronides: regulation of glucuronide uptake by glutathione and its conjugates. Plant J. **21:** 289-304.

Klein, M., Perfus-Barbeoch, L., Frelet, A., Gaedeke, N., Reinhardt, D., Mueller-Roeber, B., Martinoia, E., and Forestier, C. (2003). The plant multidrug resistance ABC transporter AtMRP5 is involved in guard cell hormonal signalling and water use. Plant J. **33:** 119-129.

Klein, M., Geisler, M., Suh, S.J., Kolukisaoglu, H.U., Azevedo, L., Plaza, S., Curtis, M.D., Richter, A., Weder, B., Schulz, B., and Martinoia, E. (2004). Disruption of AtMRP4, a guard cell plasma membrane ABCC-type ABC transporter, leads to deregulation of stomatal opening and increased drought susceptibility. Plant J. **39:** 219-236.

Klein, M., Burla, B., and Martinoia, E. (2006). The multidrug resistance-associated protein (MRP/ABCC) subfamily of ATP-binding cassette transporters in plants. FEBS Lett. **580:** 1112-1122.

Kobae, Y., Sekino, T., Yoshioka, H., Nakagawa, T., Martinoia, E., and Maeshima, M. (2006). Loss of AtPDR8, a plasma membrane ABC transporter of *Arabidopsis thaliana*, causes hypersensitive cell death upon pathogen infection. Plant Cell Physiol. **47:** 309-318.

Kolukisaoglu, H.U., Bovet, L., Klein, M., Eggmann, T., Geisler, M., Wanke, D., Martinoia, E., and Schulz, B. (2002). Family business: the multidrug-resistance related protein (MRP) ABC transporter genes in Arabidopsis thaliana. Planta **216:** 107-119.

Kovalchuk, A., and Driessen, A.J.M. (2010). Phylogenetic analysis of fungal ABC transporters. BMC Genomics **11:** 177-197.

Krattinger, S.G., Lagudah, E.S., Spielmeyer, W., Singh, R.P., Huerta-Espino, J., McFadden, H., Bossolini, E., Selter, L.L., and Keller, B. (2009). A putative ABC transporter confers durable resistance to multiple fungal pathogens in wheat. Science **323:** 1360-1363.

Křeček, P., Skůpa, P., Libus, J., Naramoto, S., Tejos, R., Friml, J., and Zažímalová, E. (2009). The PIN-FORMED (PIN) protein family of auxin transporters. Genome Biol. **10:** 249.1-11.

Kretzschmar, T., Burla, B., Lee, Y., Martinoia, E., and Nagy, R. (2011). Functions of ABC transporters in plants. Essays Biochem. **50:** 145-160.

Kreuz, K., Tommasini, R., and Martinoia, E. (1996). Old Enzymes for a New Job (Herbicide Detoxification in Plants). Plant Physiol. **111:** 349-353.

Kuromori, T., Miyaji, T., Yabuuchi, H., Shimizu, H., Sugimoto, E., Kamiya, A., Moriyama, Y., and Shinozaki, K. (2010). ABC transporter AtABCG25 is involved in abscisic acid transport and responses. Proc. Natl. Acad. Sci. USA **107:** 2361–2366.

Kuromori, T., Sugimoto, E., and Shinozaki, K. (2011) Arabidopsis mutants of AtABCG22, an ABC transporter gene, increase water transpiration and drought susceptibility. Plant J, **67:** 885-894.

Kushnir, S., Babiychuk, E., Storozhenko, S, Davey, M.W., Papenbrock, J., De Rycke, R., Engler, G., Stephan, U.W., Lange, H., and Kispal, G. (2001). A mutation of the ABC transporter Sta1 leads to dwarfism and chlorosis in the Arabidopsis mutant starik. Plant Cell **13:** 89-100.

Larsen, P.B., Kochian, L.V., and Howell, S.H. (1997). Al inhibits both shoot development and root growth in *als3*, an Al-sensitive Arabidopsis mutant. Plant Physiol. **114**: 1207-1214.

Larsen, P.B., Geisler, M.J., Jones, C.A., Williams, K.M., and Cancel, J.D. (2005). ALS3 encodes a phloem-localized ABC transporter-like protein that is required for aluminum tolerance in Arabidopsis. Plant J. **41:** 353-363.

Lee, E.K., Kwon, M., Ko, J.H., Yi, H., Hwang, M.G., Chang, S., and Cho, M.H. (2004). Binding of sulfonylurea by AtMRP5, an Arabidopsis multidrug resistance-related protein that functions in salt tolerance. Plant Physiol. **134**: 528-538.

Lee, M., Lee, K., Lee, J., Noh, E.W., and Lee, Y. (2005). AtPDR12 contributes to lead resistance in Arabidopsis. Plant Physiol. **138:** 827-836.

Lee, M., Choi, Y., Burla, B., Kim, Y.Y., Jeon, B., Maeshima, M., Yoo, J.Y., Martinoia, E., and Lee, Y. (2008). The ABC transporter AtABCB14 is a malate importer and modulates stomatal response to CO_2. Nat. Cell Biol. **10:** 1217-1223.

Lee, S.B., Go, Y.S., Bae, H.J., Park, J.H., Cho, S.H., Cho, H.J., Lee, D.S., Park, O.K., Hwang, I., and Suh, M.C. (2009). Disruption of glycosylphosphatidylinositol-anchored lipid transfer protein gene altered cuticular lipid composition, increased plastoglobules, and enhanced susceptibility to infection by the fungal pathogen *Alternaria brassicicola*. Plant Physiol. **150:** 42-54.

Leighton, J., and Schatz, G. (1995). An ABC transporter in the mitochondrial inner membrane is required for normal growth of yeast. EMBO J. **14:** 188-195.

Leonhardt, N., Marin, E., Vavasseur, A., and Forestier, C. (1997). Evidence for the existence of a sulfonylurea-receptor-like protein in plants: modulation of stomatal movements and guard cell potassium channels by sulfonylureas and potassium channel openers. Proc. Natl. Acad. Sci. USA **94:** 14156-14161.

Leung, J., and Giraudat, J. (1998). Abscisic acid signal transduction. Annu. Rev. Plant Biol. **49:** 199-222.

Lewis, D.R., Miller, N.D., Splitt, B.L., Wu, G., and Spalding, E.P. (2007). Separating the roles of acropetal and basipetal auxin transport on gravitropism with mutations in two Arabidopsis multidrug resistance-like ABC transporter genes. Plant Cell **19:** 1838–1850.

Li, Z.S., Lu, Y.P., Zhen, R.G., Szczypka, M., Thiele, D.J., and Rea, P.A. (1997). A new pathway for vacuolar cadmium sequestration in *Saccharomyces cerevisiae*: YCF1-catalyzed transport of bis(glutathionato) cadmium. Proc. Natl. Acad. Sci. USA **94:** 42-47.

Lin, R., and Wang, H. (2005). Two homologous ATP-binding cassette transporter proteins, AtMDR1 and AtPGP1, regulate Arabidopsis photomorphogenesis and root development by mediating polar auxin transport. Plant Physiol. **138:** 949–964.

Lipka, V., Dittgen, J., Bednarek, P., Bhat, R., Wiermer, M., Stein, M., Landtag, J., Brandt, W., Rosahl, S., and Scheel, D. (2005). Pre-and postinvasion defenses both contribute to nonhost resistance in Arabidopsis. Science **310:** 1180-1183.

Liu, G., Sanchez-Fernandez, R., Li, Z.S., and Rea, P.A. (2001). Enhanced multispecificity of Arabidopsis vacuolar multidrug resistance-associated protein-type ATP-binding cassette transporter, AtMRP2. J. Biol. Chem. **276:** 8648-8656.

Lu, B., Xu, C., Awai, K., Jones, A.D., and Benning, C. (2007). A small ATPase protein of Arabidopsis, TGD3, involved in chloroplast lipid import. J. Biol. Chem. **282:** 35945-35953.

Lu, Y.P., Li, Z.S., and Rea, P.A. (1997). AtMRP1 gene of Arabidopsis encodes a glutathione S-conjugate pump: isolation and functional definition of a plant ATP-binding cassette transporter gene. Proc. Natl. Acad. Sci. USA **94:** 8243-8248.

Lu, Y.P., Li, Z.S., Drozdowicz, Y.M., Hortensteiner, S., Martinoia, E., and Rea, P.A. (1998). AtMRP2, an Arabidopsis ATP binding cassette transporter able to transport glutathione S-conjugates and chlorophyll catabolites: functional comparisons with Atmrp1. Plant Cell **10:** 267-282.

Luo, B., Xue, X.Y., Hu, W.L., Wang, L.J., and Chen, X.Y. (2007). An ABC transporter gene of *Arabidopsis thaliana*, AtWBC11, is involved in cuticle development and prevention of organ fusion. Plant Cell Physiol. **48:** 1790-1802.

Luschnig, C., Gaxiola, R.A., Grisafi, P., and Fink, G.R. (1998). EIR1, a root-specific protein involved in auxin transport, is required for gravitropism in Arabidopsis thaliana. Genes Dev. **12:** 2175–2187.

Ma, Y., Szostkiewicz, I., Korte, A., Moes, D., Yang, Y., Christmann, A., and Grill, E. (2009). Regulators of PP2C phosphatase activity function as abscisic acid sensors. Science **324:**1064–1068.

Magalhaes, J.V., Liu, J., Guimaraes, C.T., Lana, U.G.P., Alves, V.M.C., Wang, Y.H., Schaffert, R.E., Hoekenga, O.A., Pineros, M.A., and Shaff, J.E. (2007). A gene in the multidrug and toxic compound extrusion (MATE) family confers aluminum tolerance in sorghum. Nat. Genet. **39:** 1156-1161.

Marin, E., Divol, F., Bechtold, N., Vavasseur, A., Nussaume, L., and Forestier, C. (2006). Molecular characterization of three Arabidopsis soluble ABC proteins which expression is induced by sugars. Plant Science **171:** 84-90.

Marinova, K., Pourcel, L., Weder, B., Schwarz, M., Barron, D., Routaboul, J.M., Debeaujon, I., and Klein, M. (2007). The Arabidopsis

MATE transporter TT12 acts as a vacuolar flavonoid/H+ -antiporter active in proanthocyanidin-accumulating cells of the seed coat. Plant Cell **19:** 2023-2038.

Martinoia, E., Grill, E., Tommasini, R., Kreuz, K., and Amrhein, N. (1993). ATP-dependent glutathione S-conjugate export pump in the vacuolar membrane of plants. Nature **364:** 247-249.

Martinoia, E., Klein, M., Geisler, M., Sánchez-Fernández, R., and Rea, P.A. (2000). Vacuolar transport of secondary metabolites and xenobiotics. In Vacuolar Compartments. Annual Plant Reviews, D.G. Robinson and J.C. Rogers, eds (Sheffield, UK: Sheffield Academic Press), pp. 221–253.

Martinoia, E., Klein, M., Bovet, L., Forestier, C., Kolukisaoglu, Ü., Műller-Rover, B., and Schulz,B. (2002) Multifunctionality of plant ABC transporters-more than just detoxifiers. Planta **214:** 345-355.

Mason, D.L., and Michaelis, S. (2002) Requirement of the N-terminal extension for vacuolar trafficking and transport activity of yeast Ycf1p, an ATP-binding cassette transporter. Mol. Biol. Cell **13:** 4443-4455.

McFarlane, H.E., Shin, J.J., Bird, D.A., and Samuels, A.L. (2010). Arabidopsis ABCG transporters, which are required for export of diverse cuticular lipids, dimerize in different combinations. Plant Cell **22:** 3066-3075.

Meister, A. (1983). Selective modification of glutathione metabolism. Science **220:** 472-477.

Mentewab, A., and Stewart, C.N. (2005). Overexpression of an *Arabidopsis thaliana* ABC transporter confers kanamycin resistance to transgenic plants. Nat. Biotechnol. **23:** 1177-1180.

Meyer, S., De Angeli, A., Fernie, A.R., and Martinoia, E. (2010). Intra- and extra-cellular excretion of carboxylates. Trends Plant Sci. **15:** 40-47.

Miao, Y.C., and Liu, C.J. (2010). ATP-binding cassette-like transporters are involved in the transport of lignin precursors across plasma and vacuolar membranes. Proc. Natl. Acad. Sci. USA **107:** 22728-22733.

Morant, M., Jorgensen, K., Schaller, H., Pinot, F., Moller, B.L., Werck-Reichhart, D., and Bak, S. (2007). CYP703 is an ancient cytochrome P450 in land plants catalyzing in-chain hydroxylation of lauric acid to provide building blocks for sporopollenin synthesis in pollen. Plant Cell **19:** 1473-1487.

Morel, M., Crouzet, J., Gravot, A., Auroy, P., Leonhardt, N., Vavasseur, A., and Richaud, P. (2009). AtHMA3, a P1B-ATPase allowing Cd/Zn/Co/Pb vacuolar storage in Arabidopsis. Plant Physiol. **149:** 894-904.

Mosser, J., Douar, A.M., Sarde, C.O., Kioschis, P., Feil, R., Moser, H., Poustka, A.M., Mandel, J.L., and Aubourg, P. (1993). Putative X-linked adrenoleukodystrophy gene shares unexpected homology with ABC transporters. Nature **361:** 726-730.

Mueller, L.A., Goodman, C.D., Silady, R.A., and Walbot, V. (2000). AN9, a petunia glutathione S-transferase required for anthocyanin sequestration, is a flavonoid-binding protein. Plant Physiol. **123:** 1561-1570.

Nagy, R., Grob, H., Weder, B., Green, P., Klein, M., Frelet, A., Schjoerring, J.K., Brearley, C.A., Martinoia, E. (2009). The Arabidopsis ATP-binding cassette protein ATMRP5/ATABCC5 is a high-affinity inositol hexakisphosphate transporter involved in guard cell signaling and phytate storage. J. Biol. Chem. **284:** 33614-33622.

Nawrath, C. (2006). Unraveling the complex network of cuticular structure and function. Curr. Opin. Plant Biol. **9:** 281-287.

Noh, B., Murphy, A.S., and Spalding, E.P. (2001). Multidrug resistance-like genes of Arabidopsis required for auxin transport and auxin-mediated development. Plant Cell **13:** 2441–2454.

Noh, B., Bandyopadhyay, A., Peer, W.A., Spalding, E.P. and Murphy, A.S. (2003). Enhanced gravi- and phototropism in plant *mdr* mutants mislocalizing the auxin efflux protein PIN1. Nature **423:** 999–1002.

Nyathi, Y., De Marcos Lousa, C., van Roermund, C.W., Wanders, R.J., Johnson, B., Baldwin, S.A., Theodoulou, F.L., and Baker, A. (2010). The Arabidopsis peroxisomal ABC transporter, comatose, complements the *Saccharomyces cerevisiae pxa1 pxa2*Δ mutant for metabolism of long-chain fatty acids and exhibits fatty acyl-CoA-stimulated ATPase activity. J. Biol. Chem. **285:** 29892-29902.

Ortiz, D.F., Ruscitti, T., McCue, K.F., and Ow, D.W. (1995). Transport of metal-binding peptides by HMT1, a fission yeast ABC-type vacuolar membrane protein. J. Biol. Chem. **270:** 4721-4728.

Osbourn, A.E. (1996). Preformed antimicrobial compounds and plant defense against fungal attack. Plant Cell **8:** 1821-1831.

Panikashvili, D., Savaldi-Goldstein, S., Mandel, T., Yifhar, T., Franke, R.B., Hofer, R., Schreiber, L., Chory, J., and Aharoni, A. (2007). The Arabidopsis DESPERADO/AtWBC11 transporter is required for cutin and wax secretion. Plant Physiol. **145:** 1345-1360.

Panikashvili, D., Shi, J.X., Bocobza, S., Franke, R.B., Schreiber, L., and Aharoni, A. (2010). The Arabidopsis DSO/ABCG11 transporter affects cutin metabolism in reproductive organs and suberin in roots. Mol. Plant **3:** 563-575.

Panikashvili, D., Shi, J.X., Schreiber, L., and Aharoni, A. (2011). The Arabidopsis ABCG13 transporter is required for flower cuticle secretion and patterning of the petal epidermis. New Phytol. **190:** 113-124.

Park, J., Song, W.Y., Ko, D., Eom, Y., Hansen, T.H., Schiller, M., Lee, T.G., Martinoia, E., and Lee, Y. (2011). The phytochelatin transporters AtABCC1 and AtABCC2 mediate tolerance to cadmium and mercury. Plant J. doi: 10.1111/j.1365-313X.2011.04789.x

Park, S-Y., Fung, P., Nishimura, N., Jensen, D.R., Fujii, H., Zhao, Y., Lumba, S., Santiago, J., Rodrigues, A., Chow, T-F.F., Alfred, S.E., Bonetta, D., Finkelstein, R., Provart, N.J., Desveaux, D., Rodriguez, P.L., McCourt, P., Zhu, J-K., Schroeder, J.I., Volkman, B.F., and Cutler, S.R. (2009). Abscisic acid inhibits type 2C protein phosphatases via the PYR/PYL family of START proteins. Science **324:** 1068–1071.

Paxson-Sowders, D.M., Owen, H.A., and Makaroff, C.A. (1997). A comparative ultrastructural analysis of exine pattern development in wild-type Arabidopsis and a mutant defective in pattern formation. Protoplasma **198:** 53-65.

Peelman, F., Labeur, C., Vanloo, B., Roosbeek, S., Devaud, C., Duverger, N., Denèfle, P., Rosier, M., Vandekerckhove, J., and Rosseneu, M. (2003). Characterization of the ABCA Transporter Subfamily: Identification of Prokaryotic and Eukaryotic Members, Phylogeny and Topology. J. Mole. Biol. **325:** 259-274.

Peters, N.K., Frost, J.W., and Long, S.R. (1986). A plant flavone, luteolin, induces expression of Rhizobium meliloti nodulation genes. Science **233:** 977.

Petrášek, J., Mravec, J., Bouchard, R., Blakeslee, J.J., Abas, M., Seifertova, D., Wiśniewska, J., Tadele, Z., Kubes, M., Čovanová, M., Dhonukshe, P., Skúpa, P., BenKová, E., Perry L., Křeček, P., Lee, O.R., Fink, G.R., Geisler, M., Murphy, A.S., Luschnig, C., Zažímalová, E., and Friml, J. (2006). PIN proteins perform a rate-limiting function in cellular auxin efflux. Science **312:** 914–918.

Petrášek, J., and Friml, J. (2009). Auxin transport routes in plant development. Development **136:** 2675-2688.

Pighin, J.A., Zheng, H., Balakshin, L.J., Goodman, I.P., Western, T.L., Jetter, R., Kunst, L., and Samuels, A.L. (2004). Plant cuticular lipid export requires an ABC transporter. Science **306:** 702-704.

Pisarev, A.V., Skabkin, M.A., Pisareva, V.P., Skabkina, O.V., Rakotondrafara, A.M., Hentze, M.W., Hellen, C.U.T., and Pestova, T.V. (2010). The Role of ABCE1 in Eukaryotic Posttermination Ribosomal Recycling. Molecular Cell **37:** 196-210.

Quilichini, T.D., Friedmann, M.C., Samuels, A.L., and Douglas, C.J. (2010). ATP-binding cassette transporter G26 (ABCG26) is required for male fertility and pollen exine formation in *Arabidopsis thaliana*. Plant

Physiol. **154:** 678–690.

Raichaudhuri, A., Peng, M., Naponelli, V., Chen, S., Sanchez-Fernandez, R., Gu, H., Gregory, J.F., Hanson, A.D., and Rea, P.A. (2009). Plant vacuolar ATP-binding cassette transporters that translocate folates and antifolates in vitro and contribute to antifolate tolerance in vivo. J. Biol. Chem. **284:** 8449-8460.

Ramos, M.S., Abele, R., Nagy, R., Grotemeyer, M.S., Tampe, R., Rentsch, D., and Martinoia, E. (2011). Characterization of a transport activity for long-chain peptides in barley mesophyll vacuoles. J. Exp. Bot. **62:** 2403-2410.

Rayapuram, N., Hagenmuller, J., Grienenberger, J.M., Giege, P., and Bonnard, G. (2007). AtCCMA interacts with AtCcmB to form a novel mitochondrial ABC transporter involved in cytochrome c maturation in Arabidopsis. J. Biol. Chem. **282:** 21015-21023.

Rea, P.A. (2007). Plant ATP-binding cassette transporters. Annu. Rev. Plant Biol. **58:** 347-375.

Reina-Pinto, J.J., and Yephremov, A. (2009). Surface lipids and plant defenses. Plant Physiol. Biochem. **47:** 540-549.

Roberts, M.F., Homeyer, B.C., and Pham, T.D.T. (1991). Further studies of sequestration of alkaloids in *Papaver somniferum* latex vacuoles. Zeitschrift für Naturforschung **46:** 377-388.

Rock, C. (2000). Pathways to abscisic acid-regulated gene expression. New Phytol. **148:** 357–396.

van Roermund, C.W., Visser, W.F., Ijlst, L., van Cruchten, A., Boek, M., Kulik, W., Waterham, H.R., and Wanders, R.J. (2008). The human peroxisomal ABC half transporter ALDP functions as a homodimer and accepts acyl-CoA esters. Faseb. J. **22:** 4201-4208.

Rohde, A., Kurup, S., and Holdsworth, M. (2000). *ABI3* emerges from the seed. Trends Plant Sci. **5:** 418–419.

Rojas-Pierce, M., Titapiwatanakun, B., Sohn, E.J., Fang, F., Larive, C.K., Blakeslee, J., Cheng, Y., Cuttler, S., Peer, W.A., Murphy, A.S., and Raikhel, N.V. (2007). Arabidopsis P-Glycoprotein19 participates in the inhibition of gravitropism by gravacin. Chem. Biol. **14:** 1366–1376.

Rouhier, N., Lemaire, S.D., and Jacquot, J.P. (2008). The role of glutathione in photosynthetic organisms: emerging functions for glutaredoxins and glutathionylation. Annu. Rev. Plant Biol. **59:** 143-166.

Rubery, P.H., and Sheldrake, A.R. (1974). Carrier-mediated auxin transport. Planta **118:** 101-121.

Russell, L., Larner, V., Kurup, S., Bougourd, S., and Holdsworth, M. (2000). The Arabidopsis *COMATOSE* locus regulates germination potential. Development **127:** 3759-3767.

Růžička, K., Strader, L.C., Bailly, A., Yang, H., Blakeslee, J.J., Łangowski, Ł., Nejedlá, E., Fujita, H., Itoh, H., Syōno, K., Hejátko, J., Gray, W.M., Martinoia, E., Geisler, M., Bartel, B., Murphy, A.S., and Friml, J. (2010). Arabidopsis PIS1 encodes the ABCG37 transporter of auxinic compounds including the auxin precursor indole-3-butyric acid. Proc. Natl. Acad. Sci. USA **107:** 10749–10753.

Ryan, P., Tyerman, S., Sasaki, T., Furuichi, T., Yamamoto, Y., Zhang, W., and Delhaize, E. (2011). The identification of aluminium-resistance genes provides opportunities for enhancing crop production on acid soils. J. Exp. Bot. **62:** 9-20.

Sandermann, Jr. H. (1992). Plant metabolism of xenobiotics. Trends Biochem. Sci. **17:** 82-84.

Santelia, D., Vincenzetti, V., Azzarello, E., Bovet, L., Fukao, Y., Düchtig, P., Mancuso, S., Martinoia, E., and Geisler, M. (2005). MDR-like ABC transporter AtPGP4 is involved in auxin-mediated lateral root and root hair development. FEBS Lett. **579:** 5399–5406.

Schmitt, R., and Sandermann, Jr. H. (1982). Specific localization of beta-D-glucoside conjugates of 2, 4-dichlorophenoxyacetic acid in soybean vacuoles [Glycine max]. Zeitschrift fuer Naturforschung. Section C. Biosciences **37:** 772-777.

Shani, N., Watkins, P.A., and Valle, D. (1995). PXA1, a possible *Saccharomyces cerevisiae* ortholog of the human adrenoleukodystrophy gene. Proc. Natl. Acad. Sci. USA **92:** 6012-6016.

Shi, J., Wang, H., Schellin, K., Li, B., Faller, M., Stoop, J.M., Meeley, R.B., Ertl, D.S., Ranch, J.P., Glassman, K. (2007). Embryo-specific silencing of a transporter reduces phytic acid content of maize and soybean seeds. Nat. Biotechnol. **25:** 930-937.

Shimoni-Shor, E., Hassidim, M., Yuval-Naeh, N., Keren, N. (2010). Disruption of Nap14, a plastid-localized non-intrinsic ABC protein in *Arabidopsis thaliana* results in the over-accumulation of transition metals and in aberrant chloroplast structures. Plant Cell Environ. **33:** 1029-1038.

Shitan, N., Bazin, I., Dan, K., Obata, K., Kigawa, K., Ueda, K., Sato, F., Forestier, C., and Yazaki., K. (2003). Involvement of CjMDDR1, a plant multidrug-resistance-type ABA-binding cassette protein, in alkaloid transport in Coptisjaponica. Proc. Natl. Acad. Sci. USA **100:** 751-756.

Sidler, M., Hassa, P., Hasan, S., Ringli, C., and Dudler, R. (1998). Involvement of an ABC transporter in a developmental pathway regulating hypocotyl cell elongation in the light. Plant Cell 10**:** 1623–1636.

Song, W.Y., Sohn, E.J., Martinoia, E., Lee, Y.J., Yang, Y.Y., Jasinski, M., Forestier, C., Hwang, I., and Lee, Y. (2003). Engineering tolerance and accumulation of lead and cadmium in transgenic plants. Nat. Biotechnol. **21:** 914-919.

Song, W.Y., Park, J., Mendoza-Cozatl, D., Suter-Grotemeyer, M., Shim, D., Hortensteiner, S., Geisler, M., Weder, B., Rea, P., Rentsch, D., Schroder, J., Lee, Y., and Martinoia, E. (2010). Arsenic tolerance in Arabidopsis is mediated by two ABCC-type phytochelatin transporters. Proc. Natl. Acad. Sci. USA **107:** 21187-21192.

Sooksa-Nguan, T., Yakubov, B., Kozlovskyy, V.I., Barkume, C.M., Howe, K.J., Thannhauser, T.W., Rutzke, M.A., Hart, J.J., Kochian, L.V., Rea, P.A., and Vatamaniuk, O.K. (2009). Drosophila ABC transporter, DmHMT-1, confers tolerance to cadmium. DmHMT-1 and its yeast homolog, SpHMT-1, are not essential for vacuolar phytochelatin sequestration. J. Biol. Chem. **284:** 354-362.

Stacey, G., Koh, S., Granger, C., and Becker, J.M. (2002). Peptide transport in plants. Trends Plant Sci. **7:** 257-263.

Stein, M., Dittgen, J., Sánchez-Rodríguez, C., Hou, B.H., Molina, A., Schulze-Lefert, P., Lipka, V., and Somerville, S. (2006). Arabidopsis PEN3/PDR8, an ATP binding cassette transporter, contributes to nonhost resistance to inappropriate pathogens that enter by direct penetration. Plant Cell **18:** 731-746.

Strader, L.C., and Bartel, B. (2009). The Arabidopsis PLEIOTROPIC DRUG RESISTANCE8/ ABCG36 ATP binding cassette transporter modulates sensitivity to the auxin precursor indole-3-butyric acid. Plant Cell **21:** 1992–2007.

Stukkens, Y., Bultreys, A., Grec, S., Trombik, T., Vanham, D., and Boutry, M. (2005). NpPDR1, a pleiotropic drug resistance-type ATP-binding cassette transporter from *Nicotiana plumbaginifolia*, plays a major role in plant pathogen defense. Plant Physiol.**139:** 341-352.

Sugiyama, A., Shitan, N., and Yazaki, K. (2007). Involvement of a soybean ATP-binding cassette-type transporter in the secretion of genistein, a signal flavonoid in legume-Rhizobium symbiosis. Plant Physiol. **144:** 2000-2008.

Suh, S.J., Wang, Y.F., Frelet, A., Leonhardt, N., Klein, M., Forestier, C., Mueller-Roeber, B., Cho, M.H., Martinoia, E., and Schroeder, J.I. (2007). The ATP binding cassette transporter AtMRP5 modulates anion and calcium channel activities in Arabidopsis guard cells. J. Biol. Chem. **282:** 1916-1924.

Szczypka, M.S., Wemmie, J.A., Moye-Rowley, W.S., and Thiele, D.J. (1994). A yeast metal resistance protein similar to human cystic fibrosis transmembrane conductance regulator (CFTR) and multidrug resis-

tance-associated protein. J. Biol. Chem. **269:** 22853-22857.

Terasaka, K., Blakeslee, J.J., Titapiwatanakun, B., Peer, W.A., Bandyopadhyay, A., Makam, S.N., Lee, O.R., Richards, E.L., Murphy, A.S., Sato, F., and Yazaki, K. (2005). PGP4, an ATP binding cassette P-glycoprotein, catalyzes auxin transport in Arabidopsis thaliana roots. Plant Cell **17:** 2922–2939.

Teschner, J., Lachmann, N., Schulze, J., Geisler, M., Selbach, K., Santamaria-Araujo, J., Balk, J., Mendel, R.R., and Bittner, F. (2010). A novel role for Arabidopsis Mitochondrial ABC transporter ATM3 in molybdenum cofactor biosynthesis. Plant Cell **22:**468-480.

Titapiwatanakun, B., and Murphy, A.S. (2009). Post-transcriptional regulation of auxin transport proteins: cellular trafficking, protein phosphorylation, protein maturation, ubiquitination, and membrane composition. J. Exp. Bot. **60:** 1093–1107.

Theodoulou, F.L., Job, K., Slocombe, S.P., Footitt, S., Holdsworth, M., Baker, A., Larson, T.R., and Graham, I.A. (2005). Jasmonic acid levels are reduced in *COMATOSE* ATP-binding cassette transporter mutants. Implications for transport of jasmonate precursors into peroxisomes. Plant Physiol. **137:** 835-840.

Tommasini, R., Evers, R., Vogt, E., Mornet, C., Zaman, G.J., Schinkel, A.H., Borst, P., and Martinoia, E. (1996). The human multidrug resistance-associated protein functionally complements the yeast cadmium resistance factor 1. Proc. Natl. Acad. Sci. USA **93:** 6743-6748.

Tommasini, R., Vogt, E., Fromenteau, M., Hortensteiner, S., Matile, P., Amrhein, N., Martinoia, E. (1998). An ABC-transporter of *Arabidopsis thaliana* has both glutathione-conjugate and chlorophyll catabolite transport activity. Plant J. **13:** 773-780.

Turner, B.L., Richardson, A.E., Mullaney, E.J. (2007). Inositol phosphates: linking agriculture and the environment. (Wallingford UK: CABI).

Tusnády, G.E., Sarkadi, B., Simon, I., and Váradi, A. (2006). Membrane topology of human ABC proteins. FEBS Lett. **580:** 1017-1022.

Tyler, B.M., Tripathy, S., Zhang, X., Dehal, P., Jiang, R.H.Y., Aerts, A., Arredondo, F.D., Baxter, L., Bensasson, D., and Beynon, J.L. (2006). Phytophthora Genome Sequences Uncover Evolutionary Origins and Mechanisms of Pathogenesis. Science **313:** 1261-1266.

Tyzack, J.K., Wang, X., Belsham, G.J., and Proud, C.G. (2000). ABC50 Interacts with Eukaryotic Initiation Factor 2 and Associates with the Ribosome in an ATP-dependent Manner. J. Biol. Chem. **275:** 34131 -34139.

Ukitsu, H., Kuromori, T., Toyooka, K., Goto, Y., Matsuoka, K., Sakuradani, E., Shimizu, S., Kamiya, A., Imura, Y., Yuguchi, M., Wada, T., Hirayama, T., and Shinozaki, K. (2007). Cytological and biochemical analysis of COF1, an Arabidopsis mutant of an ABC transporter gene. Plant Cell Physiol. **48:** 1524-1533.

Vasiliou, V., Vasiliou, K., and Nebert, D.W. (2009). Human ATP-binding cassette (ABC) transporter family. Human genomics **3:** 281-290.

Vatamaniuk, O.K., Bucher, E.A., Sundaram, M.V., and Rea, P.A. (2005). CeHMT-1, a putative phytochelatin transporter, is required for cadmium tolerance in *Caenorhabditis elegans*. J. Biol. Chem. **280:** 23684-23690.

Vazquez de Aldana, C.R., Marton, M.J., and Hinnebusch, A.G. (1995). GCN20, a novel ATP binding cassette protein, and GCN1 reside in a complex that mediates activation of the eIF-2 alpha kinase GCN2 in amino acid-starved cells. EMBO J. **14:** 3184-3199.

Verleur, N., Hettema, E.H., van Roermund, C.W., Tabak, H.F., and Wanders, R.J. (1997). Transport of activated fatty acids by the peroxisomal ATP-binding-cassette transporter Pxa2 in a semi-intact yeast cell system. Eur. J. Biochem. **249:** 657-661.

Verrier, P.J., Bird, D., Burla, B., Dassa, E., Forestier, C., Geisler, M., Klein, M., Kolukisaoglu, U., Lee, Y., Martinoia, E., Murphy, A., Rea, P.A., Samuels, L., Schulz, B., Spalding, E.J., Yazaki, K., and Theodoulou, F.L. (2008). Plant ABC proteins--a unified nomenclature and updated inventory. Trends Plant Sci. **13:** 151-159.

Versantvoort, C., Broxterman, H., Bagrij, T., Scheper, R., and Twentyman, P. (1995). Regulation by glutathione of drug transport in multidrug-resistant human lung tumour cell lines overexpressing multidrug resistance-associated protein. Br. J. Cancer **72:** 82-89.

Vert, G., Grotz, N., Dedaldechamp, F., Gaymard, F., Guerinot, M., Briat, J., and Curie, C. (2002). IRT1, an Arabidopsis transporter essential for iron uptake from the soil and for plant growth. Plant Cell **14:** 1223-1233.

Westlake, C.J., Cole, S.P.C., and Deeley, R.G. (2005). Role of the NH_2-terminal membrane spanning domain of Multidrug Resistance Protein 1/ABCC1 in protein processing and trafficking. Mol. Biol. Cell **16:** 2483-2492.

Wilkinson, S., and Davies, W.J. (1997). Xylem sap pH increase: a drought signal received at the apoplastic face of the guard cell that involves the suppression of saturable abscisic acid uptake by the epidermal symplast. Plant Physiol. **113:** 559-573.

Windsor, M.L., Milborrow, B.V., and McFarlane, I.J. (1992). The uptake of (+)-S-and (-)-R-abscisic acid by suspension culture cells of Hopbush (*Dodonaea viscosa*). Plant Physiol. **100:** 54-62.

Wu, G., Lewis, D.R., and Spalding, E.P. (2007). Mutations in Arabidopsis multidrug resistance-like ABC transporters separate the roles of acropetal and basipetal auxin transport in lateral root development. Plant Cell **19:** 1826–1837.

Wu, G., Cameron, J.N., Ljung, K., and Spalding, E.P. (2010). A role for ABCB19-mediated polar auxin transport in seedling photomorphogenesis mediated by cryptochrome 1 and phytochrome B. Plant J. **62:** 179-191.

Xu, C., Fan, J., Froehlich, J.E., Awai, K., and Benning, C. (2005). Mutation of the TGD1 chloroplast envelope protein affects phosphatidate metabolism in Arabidopsis. Plant Cell **17:** 3094-3110.

Xu, X.H., Zhao, H.J., Liu, Q.L., Frank, T., Engel, K.H., An, G., and Shu, Q.Y. (2009). Mutations of the multi-drug resistance-associated protein ABC transporter gene 5 result in reduction of phytic acid in rice seeds. Theor. Appl. Genet. **119:** 75-83.

Xu, J., Yang, C., Yuan, Z., Zhang, D., Gondwe, M.Y., Ding, Z., Liang, W., Zhang, D., and Wilson, Z.A. (2010). The ABORTED MICROSPORES regulatory network is required for postmeiotic male reproductive development in *Arabidopsis thaliana*. Plant Cell **22:** 91-107.

Yang, H., and Murphy, A.S. (2009). Functional expression and characterization of Arabidopsis ABCB, AUX 1 and PIN auxin transporters in Schizosaccharomyces pombe. Plant J. **59:** 179–191.

Yang, Y., Hammes, U.Z., Taylor, C.G., Schachtman, D.P., and Nielsen, E. (2006). High-affinity auxin transport by the AUX1 influx carrier protein. Curr. Biol. **16:** 1123-1127.

Yazaki, K., Shitan, N., Sugiyama, A., and Takanashi, K. (2009). Cell and molecular biology of ATP-binding cassette proteins in plants. Int. Rev. Cell Mol.Biol. **276:** 264-299.

Zaman, G.J., Lankelma, J., van Tellingen, O., Beijnen, J., Dekker, H., Paulusma, C., Oude Elferink, R.P., Baas, F., and Borst, P. (1995). Role of glutathione in the export of compounds from cells by the multidrug-resistance-associated protein. Proc. Natl. Acad. Sci. USA **92:** 7690-7694.

Zhang, Q., Blaylock, L.A., and Harrison, M.J. (2010) Two Medicago trunculata half-size transporters are essential for arbuscular development in arbuscular mycorrhizal symbiosis. Plant Cell **22:** 1483-1497.

Zhao, F.J., McGrath, S.P., and Meharg, A.A. (2010). Arsenic as a food chain contaminant: mechanisms of plant uptake and metabolism and mitigation strategies. Annu. Rev. Plant Biol. **61:** 535-559.

Zhao, J., and Dixon, R.A. (2009). MATE transporters facilitate vacuolar uptake of epicatechin 3'-O-glucoside for proanthocyanidin biosynthesis in *Medicago truncatula* and Arabidopsis. Plant Cell **21:** 2323-2340.

Zhao, J., Huhman, D., Shadle, G., He, X.Z., Sumner, L.W., Tang, Y., and Dixon, R.A. (2011). MATE2 Mediates Vacuolar Sequestration of Flavonoid Glycosides and Glycoside Malonates in *Medicago truncatula*. Plant Cell **23:** 1553-1555.

Zientara, K., Wawrzynska, A., Lukomska, J., Lopez-Moya, J.R., Liszewska, F., Assuncao, A.G., Aarts, M.G., and Sirko, A. (2009). Activity of the AtMRP3 promoter in transgenic *Arabidopsis thaliana* and *Nicotiana tabacum* plants is increased by cadmium, nickel, arsenic, cobalt and lead but not by zinc and iron. J. Biotechnol. **139:** 258-263.

Zimmermann, P., Hirsch-Hoffmann, M., Hennig, L., and Gruissem, W. (2004) GENEVESTIGATOR: Arabidopsis Microarray Database and Analysis Toolbox. Plant Physiol. **136:** 2621-2632

Zolman, B.K., Silva, I.D., and Bartel, B. (2001). The Arabidopsis *pxa1* mutant is defective in an ATP-binding cassette transporter-like protein required for peroxisomal fatty acid β-oxidation. Plant Physiol. **127:** 1266-1278.

2. Aims of the Thesis

The first chapter of this thesis aimed to reveal the evolutionary relationships of genes from the *ABCC* subfamily of *ABC* genes. Genomes from eukaryotic species across kingdoms were inventoried for *ABCC* genes, which then subsequently were phylogenetically analyzed by robust methods. Consequently, these *ABCC* phylogenies were analyzed for conserved clades, for lineage-specific clades, for orthologous and paralogous relationships and other evolutionary events and mechanisms.

The second chapter of this thesis aimed to characterize the *Arabidopsis thaliana ABCC* gene *AtABCC13* on genetic and functional levels. *AtABCC13* was previously suggested to be phylogenetically and structurally distinct to the other *Arabidopsis ABCCs* genes. Preliminary data obtained in the first chapter of this thesis supported these observations and revealed unique phylogenetic characteristics of *AtABCC13*. *AtABCC13* therefore represented an interesting *ABCC* candidate gene to analyze and to obtain new insights into functions and substrates of ABCC transporters.

The third chapter of this thesis aimed to identify mechanisms by which the glucoside of the phytohormone abscisic acid is sequestered into vacuoles of *Arabidopsis thaliana*. ABA glucosyl ester (ABA-GE) is a hydrolysable ABA catabolite that accumulates in vacuoles. ABA-GE can serve as a pool for free ABA, as it was shown for ER-accumulated ABA-GE. The mechanisms of vacuolar ABA-GE uptake, however, were unknown. ABCC proteins have been demonstrated to reside on the vacuolar membrane and to transport conjugates. In view of that, it was hypothesized that ABCC transporters might also be involved in the vacuolar ABA-GE sequestration. In a first step to substantiate this hypothesis, the vacuolar transport mechanisms for ABA-GE were characterized using isolated mesophyll vacuoles from wild-type *Arabidopsis thaliana* plants. This characterization required the beforehand development of a method to economically and efficiently synthesize radiolabeled ABA-GE for the *in vitro* measurement of vacuolar ABA-GE uptake.

3. Chapter I

Evolution of the ABCC gene family

3.1 Introduction

ABC (ATP-binding cassette) transporter proteins are found in all living organisms. These proteins function as primary active membrane transporters and are involved in a multitude of cellular processes. Within the ABC protein superfamily, the ABCC subfamily forms a large group of full-size eukaryotic ABC transporters. ABCC transporters are versatile transporters that mediate the cellular export of glutathione, glucuronate and other conjugates of organic anions, i.e. of xenotoxins and endogenous compounds (Martinoia et al., 1993; Chen and Tiwari, 2011). Many ABCC transporters exhibit polyspecificity for a wide range of structurally unrelated compounds and mediate the cellular export of compounds from the cytosol to the extracellular space in animal cells and to vacuoles in plants. Consequently, particular ABCC transporters function in cellular detoxification processes (Coleman et al., 1997), in tumor multidrug resistance, and as resistance factors for various anti-cancer drugs (Chen and Tiwari, 2011), which is subject of extensive research. In addition, ABCC proteins also function in various other processes. For instance, the *Arabidopsis thaliana* AtABCC5 was shown to be a high-affinity transporter for inositol hexaphosphate that functions in guard cell signaling (Nagy et al., 2009). Furthermore, specific ABCC proteins have evolved in animals that are not involved in active membrane transport, i.e. the ATP-gated chloride channel CFTR and the ATP-controlled potassium channel regulators SUR1/2. However, despite extensive efforts, the physiological functions of most other *ABCC* genes in plants and animals are still unknown. With the availability of new sequenced genomes, *ABCC* gene repertoires from various species were published, e.g. of the algae *Chlamydomonas* (Hanikenne et al., 2005) and the water flea (Sturm et al., 2009). These and other publications comprise phylogenetic analyses comparing *ABCC* genes from a few different species and attempted to infer homologies to disclose conserved and novel functions of so far uncharacterized *ABCC* genes. However, these analyses were done at a small scale and employed methods that were not powerful enough to reliably detect orthologous relationships. This chapter aimed to obtain and compare *ABCC* gene inventories from species across eukaryotic kingdoms and to reliably identify the evolutionary relationships of the identified *ABCC* genes.

3.2 Materials and Methods

3.2.1 ABCC database

The *ABCC* gene sequences and additional information were stored in a relational database realized in Microsoft Access 2010 (Figure 7A). This database also contains data about the analyzed species and corresponding genome data in separate tables. Data summaries, e.g. number of ABCC genes per species, were retrieved using SQL queries. A program written in Microsoft Visual C#.NET was used as an interface to the database for easier data entry, data exploration, and generation of FASTA files. The database and the program are available from the author on request (Figure 7B).

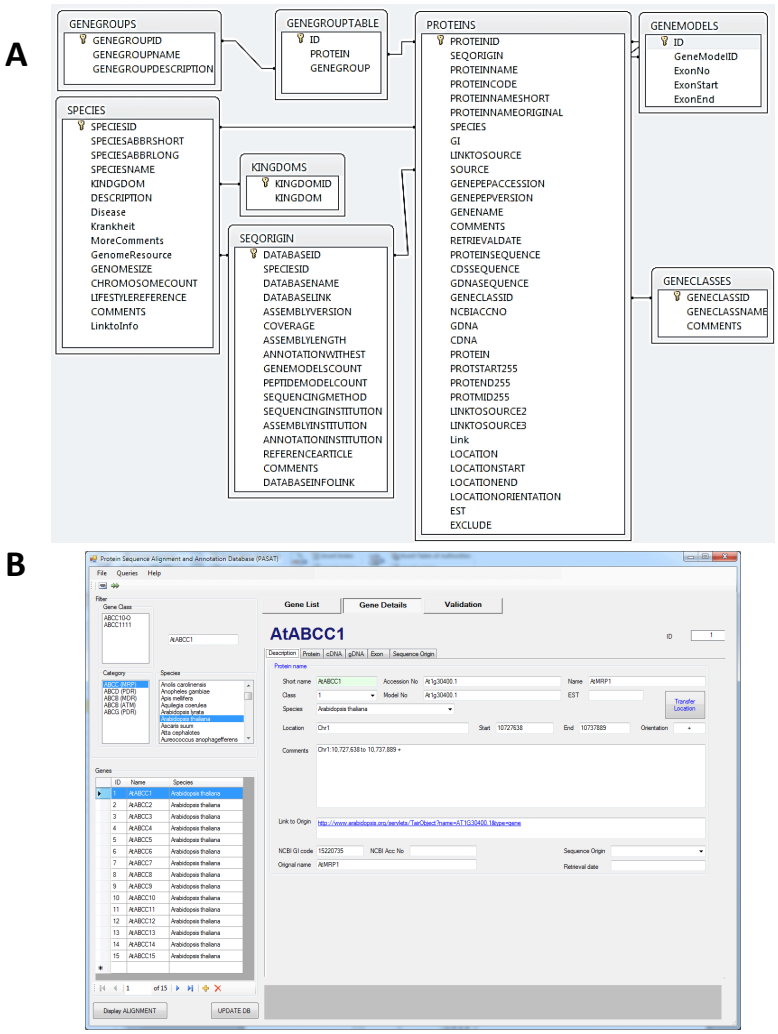

Figure 7. (A) Database schema of the relational database created for the storage of ABCC sequences and information on corresponding genome databases and sequenced species. **(B)** Graphical user interface of the program interfacing the ABCC sequence database.

3.2.2 Identification of *ABCC* genes

ABCC genes were identified using BLASTp or tBLASTn searches (Altschul et al., 1990) on protein and coding nucleotide sequence databases (Table 1) using default parameters and an *E*-value cutoff of 10^{-4}. When available, the PSI-BLAST algorithm (Altschul et al., 1997) with three iterations was used for BLASTp searches. Sequence datasets consisting of only filtered gene models were chosen if available. For *Amphimedon queenslandica, Linepithema humile* and *Pogonomyrmex barbatus*, BLASTp searches were performed on downloaded protein sequences using a locally installed NCBI BLASTP 2.2.23+ program (ftp://ftp.ncbi.nih.gov/blast) with the *use_sw_tback* option, a cutoff E-value < 10^{-4} and other parameters at their default values. Searches employed the following protein sequences as BLAST queries: *Arabidopsis thaliana AtABCC13* (At2g07680) for plants, *Saccharomyces cerevisiae CseABCC1* (YDR135C) for fungi, *Drosophila melanogaster DmABCC10* (CG7806) for invertebrates, *Homo sapiens HsABCC10* for vertebrates, and *Plasmodium falciparum PfaABCC1* (PFA0590w), *AtABCC13,* and *CseABCC1* for protozoa.

BLAST hits with a length >100 amino acids were subsequently verified as being *ABCC* genes by testing for the presence of ABCC specific domains using the NCBI Conserved Domain Database (CDD) (Marchler-Bauer et al., 2011). Following CCD domains were chosen as ABCC-defining domains: ABCC_MRP_domain1 (cd03250), ABCC_MRP_domain2 (cd03244), PLN03232 and MRP_assoc_pro (TIGR00957). BLAST hits without any detectable domains were subsequently tested by reciprocal BLAST (Moreno-Hagelsieb and Latimer, 2008) against the *Arabidopsis* (http://www.arabidopsis.org/Blast) or human (http://www.ncbi.nlm.nih.gov/BLAST) protein sequence databases. Sequences that did not result in an ABCC sequence as the top reciprocal BLAST hit were discarded. Additionally, the corresponding chromosomal, contig or scaffold locations of the identified *ABCC* genes were retrieved and compared with each other. Gene models for the same locus or overlapping models were manually curated by selecting the model that aligned with the highest identity to corresponding BLAST query sequences. Short BLAST hits that were adjacent to each other and encoded for distinct parts of an ABCC protein in the correct orientation, as

detected by alignment with the BLAST query and in CCD searches, were manually annotated as a single gene by merging the sequences. Separately located short fragments were included in the database when they encoded for more than 100 amino acids and had less than 98% identity in their corresponding genomic sequences with other identified ABCC sequences of the same species. Sequences sharing segments (>500 bp) with very high identities (≥ 98%) on coding and genomic DNA level, and which were located on individual contigs or scaffolds, were excluded from subsequent analyzes, as they are likely to represent unfiltered haplotype alleles or assembly artifacts. However, these sequences were kept in the database, but labeled with an 'x' at the end of their gene names.

For each species, all the identified ABCC sequences were aligned and those that showed obvious differences, such as exceptional insertions or deletion, or fragments with no homology, were manually inspected and curated if possible. Manual curation of gene models consisted of generation of alternative independent gene models using AUGUSTUS (http://augustus.gobics.de) (Stanke and Morgenstern, 2005), Eukaryotic GeneMark.hmm (http://exon.biology.gatech.edu/eukhmm.cgi) (Lomsadze et al.), or GENESCAN (http://genes.mit.edu/GENSCAN.html) (Burge and Karlin, 1997) with different reference organisms as options, followed by comparison of these alternative gene models in alignments with other *ABCCs*. In some cases, distinct alternative gene models were combined, if the resulting sequences had better identity to other sequences in the alignment. Detailed information of the annotation of manually curated *ABCC* genes can be found in the ABCC sequence database. As a last test, phylogenetic analyses were conducted with identified *ABCC* sequences of a species with the *Arabidopsis* ABCB1 (TAIR At2g36910.1) and/or the human ABCB1 (Ensembl ENSP00000265724) sequences as outgroup (data not shown). Sequences that clustered with the outgroup were manually verified by tBLASTn searches against the NCBI nucleotide collection and were excluded from the inventory when the top BLAST hit was not an ABCC gene.

The identified *ABCC* genes were labeled with the species identifier followed by 'ABCC' and incrementing numbers following the HUGO *ABC* gene nomenclature (http://www.genenames.org/genefamilies/ABC). If possible, the gene numbering was based on previously published gene names, such as for *Arabidopsis thaliana* and *Oryza sativa* (Verrier et al., 2008), or gene names found in corresponding genome databases (e.g. Ensembl databases for vertebrates). *ABCC* genes belonging to the *ABCC-E* orthologous group were renumbered to ABCC10 when there were 10 or more *ABCC* genes per species. Sequences of plants were numbered, if possible, according to the *Arabidopsis thaliana* and *Oryza sativa* orthologs. The numbering of the remaining sequences mainly followed the BLAST result rank. Protein, coding and genomic sequences were stored in the ABCC database together with the genome locus coordinates and orientation, the original gene names and comments on manual annotation.

Additionally, previously published *ABCC* gene counts of several species were extracted from following literature: *Phytophthora sojae* (Morris and Phuntumart, 2009); *Cyanidioschyzon merolae* and *Chlamydomonas reinhardtii* (Hanikenne et al., 2005); *Bombox mori* (Labbé et al., 2011; Liu et al., 2011); *Anopheles gambiae, Apis mellifera, Drosophila melanogaster, Tribolium castaneum* (Liu et al., 2011); *Daphnia pulex* (Sturm et al., 2009); *Schizosaccharomyces pombe* (Iwaki et al., 2006); *Saccharomyces cerevisiae* (Decottignies and Goffeau, 1997); *Dictyostelium discoideum* (Anjard and Loomis, 2002); *Batrachochytrium dendrobatidis, Chaetomium globosum, Encephalitozoon cuniculi* and *Puccinia graminis f sp tritici* (Kovalchuk and Driessen, 2010); *Strongylocentrotus purpuratus* (Goldstone et al., 2006)*; Ciona intestinalis* (Annilo et al., 2006)*; Caenorhabditis elegans* and *Caenorhabditis briggsae* (Zhao et al., 2007).

Table 1. Genome databases used for the identification and retrieval of ABCC sequences

SPECIES	DATABASE NAME	DATABASE LINK	ASSEMBLY VERSION
Acyrthosiphon pisum	AphidBase	http://www.aphidbase.com	v1.2
Aedes aegypti	VectorBase Aedes aegypti	http://www.vectorbase.org/Aedes_aegypti	AaegL1.2
Ailuropoda melanoleuca	Giant Panda Database	http://panda.genomics.org.cn	AilMel 1.0
Allomyces macrogynus	Origins of Multicellularity Database	http://www.broadinstitute.org/annotation/genome/multicellularity_project	1
Amphimedon queenslandica	Spongezome	http://spongezome.metazome.net	1
Anolis carolinensis	Ensembl Anole Lizard	http://www.ensembl.org/Anolis_carolinensis	AnoCar1.0 Database 60.1d
Anopheles gambiae	Anopheles gambiae	http://www.vectorbase.org/Anopheles_gambiae	AgamP3.6
Antonospora locustae	Antonospora locustaeDB	http://forest.mbl.edu/cgi-bin/site/antonospora01	January 2011
Apis mellifera	BeeBase	http://hymenopteragenome.org/beebase	Amel_release1_OGS
Arabidopsis thaliana	TAIR	http://www.arabidopsis.org	TAIR10
Ascaris suum	NCBI	http://www.ncbi.nlm.nih.gov/protein	
Atta cephalotes	AttaBase	http://hymenopteragenome.org/atta	Acep_OGSv1.2
Aureococcus anophagefferens	JGI Aureococcus anophagefferens	http://genome.jgi-psf.org/Auran1	Auran1
Babesia bovis	NCBI	http://www.ncbi.nlm.nih.gov/protein	
Batrachochytrium dendrobatidis	JGI Batrachochytrium dendrobatidis	http://genome.jgi-psf.org/Batde5	Batde5
Bombyx morii	SilkDB	http://silkworm.genomics.org.cn	V2.0
Bos taurus	Ensembl Cow (Bos taurus)	http://www.ensembl.org/Bos_taurus	Btau_3.1
Brachypodium distachyon	Phytozome Brachypodium distachyon	http://www.phytozome.net/brachy	JGI v1.0
Branchiostoma floridae	JGI Branchiostoma floridae	http://genome.jgi-psf.org/Brafl1	Brafl1
Brugia malayi	BROAD Institute Filarial worms	http://www.broadinstitute.org/annotation/genome/filarial_worms	V1
Caenorhabditis briggsae	WormBase	http://www.wormbase.org	WS221
Caenorhabditis elegans	WormBase	http://www.wormbase.org	WS221
Camponotus floridanus	Florida Carpenter Ant Genome Project	http://www.hymenopteragenome.org/camponotus	Cflo_OGSv3.3
Canis familiaris	Ensembl Dog (Canis familiaris)	http://www.ensembl.org/Canis_familiaris	CanFam2.0 (Ensembl 64.2)
Capitella teleta	Capitella teleta v1.0	http://genome.jgi-psf.org/Capca1	Capca1
Capsaspora owczarzaki	Origins of Multicellularity Database	http://www.broadinstitute.org/annotation/genome/multicellularity_project	1
Carica papaya	Phytozome Carica papaya (Papaya)	http://www.phytozome.net/papaya	Cpapaya_113
Cavia porcellus	Ensembl Guinea Pig (Cavia porcellus)	http://www.ensembl.org/Cavia_porcellus	cavPor3 (Ensembl 54.3)
Chaetomium globosum	JGI Chaetomium globosum	http://genome.jgi-psf.org/Chagl_1	Chagl_1
Chlamydomonas reinhardtii	Phytozome Chlamydomonas reinhardtii	http://www.phytozome.net/chlamy	v4.3
Chlorealla sp NC64A	JGI Chlorella NC64A	http://genome.jgi-psf.org/ChlNC64A_1	v 1.0
Ciona intestinalis	JGI Ciona intestinalis	http://genome.jgi-psf.org/Cioin2	Cioin2 (Ensembl 60.2p)
Ciona savignyi	Ensembl Ciona savignyi	http://www.ensembl.org/Ciona_savignyi	CSAV 2.0 (Ensembl 60.2k)
Citrus sinensis	Phytozome Citrus sinensis	http://www.phytozome.net/citrus	orange1.1
Coccomyxa sp.C-169	JGI Coccomyxa sp.C-169	http://genome.jgi-psf.org/Coc_C169_1	Annotation v2.0
Cryptosporidium parvum Iowa II	CryptoDB	http://cryptodb.org	version: 2008-08-13
Culex quinquefasciatus	VectorBase Culex quinquefasciatus	http://www.vectorbase.org/Culex_quinquefasciatus	CpipJ1.2, June 2008
Cyanidioschyzon merolae	Cyanidioschyzon merolae Genome Project	http://merolae.biol.s.u-tokyo.ac.jp	Version 1
Danio rerio	Ensembl Zebrafish (Danio rerio)	http://www.ensembl.org/Danio_rerio	Zv8 (Release 59)
Daphnia pulex	wFleaBase	http://wfleabase.org	Gene Set 2.0 beta3
Dictyostelium discoideum AX4	DictyBase	http://dictybase.org	2009
Drosophila ananassae	FlyBase	http://flybase.org	R1.3
Drosophila erecta	FlyBase	http://flybase.org	R1.3
Drosophila grimshawi	FlyBase	http://flybase.org	R1.3
Drosophila melanogaster	FlyBase	http://flybase.org	R5.32
Drosophila mojavensis	FlyBase	http://flybase.org	R1.3
Drosophila persimili	FlyBase	http://flybase.org	R1.3
Drosophila pseudoobscura	FlyBase	http://flybase.org	R2.15

Table 1 (continued). Genome databases used for the identification and retrieval of ABCC sequences

SPECIES	DATABASE NAME	DATABASE LINK	ASSEMBLY VERSION
Drosophila sechellia	FlyBase	http://flybase.org	R1.3
Drosophila simulans	FlyBase	http://flybase.org	R1.3
Drosophila virilis	FlyBase	http://flybase.org	R1.2
Drosophila willistoni	FlyBase	http://flybase.org	R1.3
Drosophila yakuba	FlyBase	http://flybase.org	R1.3
Ectocarpus siliculosus	BOGAS Ectocarpus siliculosus	http://bioinformatics.psb.ugent.be/genomes/view/Ectocarpus-siliculosus	Oktober 2010
Emiliania huxleyi	JGI Emiliania huxleyi CCMP1516	http://genome.jgi-psf.org/Emihu1	Emihu1
Encephalitozoon cuniculi	MicrosporidiaDB	http://microsporidiadb.org	version: 2008-06-19
Encephalitozoon hellem	MicrosporidiaDB	http://microsporidiadb.org	MicrosporidiaDB 1.5
Encephalitozoon intestinalis	MicrosporidiaDB	http://microsporidiadb.org	version: 2009-11-23
Entamoeba histolytica	AmoebaDB	http://amoebadb.org	version: 2009-11-27
Enterocytozoon bieneusi	MicrosporidiaDB	http://microsporidiadb.org	version: 2009-01-13
Eucalyptus grandis	Phytozome Eucalyptus grandis	http://www.phytozome.net/eucalyptus	BRASUZ1
Fragaria vesca	PFR STRAWBERRY SERVER	http://www.strawberrygenome.org	Hybrid Gene Models V 2
Fragilariopsis cylindrus	JGI Fragilariopsis cylindrus	http://genome.jgi-psf.org/Fracy1	Fracy1
Galdieria sulphuraria	The Galdieria Genome Project	http://genomics.msu.edu/galdieria	Build 3.0 (August 2007)
Gallus gallus	Ensembl Chicken (Gallus gallus)	http://www.ensembl.org/Gallus_gallus	WASHUC2 (Ensembl 64.2)
Gasterosteus aculeatus	Ensembl Stickleback	http://www.ensembl.org/Gasterosteus_aculeatus	BROAD S1 (Ensembl 64.1)
Giardia lamblia Assemblage A	GiardiaDB	http://giardiadb.org/giardiadb	GiardiaDB 2.2
Glycine max	Phytozome Glycine max (Soybean)	http://www.phytozome.net/soybean	Glyma1.0
Harpegnathos saltator	Jumping Ant Genome Project	http://hymenopteragenome.org/harpegnathos	Hsal_OGSv3.3
Helobdella robusta	JGI Helobdella robusta	http://genome.jgi-psf.org/Helro1	Helro1
Homo sapiens	Ensembl Human (Homo sapiens)	http://www.ensembl.org/Homo_sapiens	GRCh37.p5 (Ensembl 63)
Ixodes scapularis	VectorBase	http://www.vectorbase.org	IscaW1.1, December 2008
Leishmania major Friedlin	TriTrypDB	http://tritrypdb.org/	L.major 2009-09-10
Linepithema humile	ArgieBase	http://hymenopteragenome.org/linepithema	Lhum_OGSv1.2
Loa loa	BROAD Institute Filarial worms	http://www.broadinstitute.org/annotation/genome/filarial_worms	V2
Lottia gigantea	JGI Lottia gigantea	http://genome.jgi-psf.org/Lotgi1	Lotg1
Lotus japonicus	miyakogusa.jp	http://www.kazusa.or.jp/lotus	2.5
Loxodonta africana	Ensembl Elephant (Loxodonta africana)	http://www.ensembl.org/Loxodonta_africana	Loxafr3.0 (Ensembl 64.3)
Malus domestica	BOGAS Malus domestica	http://bioinformatics.psb.ugent.be/webtools/bogas/overview/Madom	01 September 2010
Manihot esculenta	Phytozome Manihot esculenta	http://www.phytozome.net/cassava	Cassava4.1
Medicago truncatula	Medicago truncatula HapMap Project	http://www.medicagohapmap.org	Mt3.5
Meloidogyne incognita	Meloidogyne incognita resources	http://www.inra.fr/meloidogyne_incognita	MincV1A1
Micromonas RC299	JGI Micromonas sp. RCC299	http://genome.jgi-psf.org/MicpuN3	MicpuN3
Mimulus guttatus	Phytozome Mimulus guttatus	http://www.phytozome.net/mimulus.php	v1.1 of assembly v1.0
Monosiga brevicollis	JGI Monosiga brevicollis	http://genome.jgi-psf.org/Monbr1	Monbr1
Mus musculus	Ensembl Mouse (Mus musculus)	http://www.ensembl.org/Mus_musculus	NCBIM37 (Ensembl 64.37)
Naegleria gruberi	JGI Naegleria gruberi	http://genome.jgi-psf.org/Naegr1	v.1.0 (October 23, 2006)
Nasonia vitripennis	NasoniaBase	http://hymenopteragenome.org/nasonia	OGS v1.2
Nematostella vectensis	JGI Nematostella vectensis	http://genome.jgi-psf.org/Nemve1	Nemve1
Nosema ceranae	MicrosporidiaDB	http://microsporidiadb.org	MicrosporidiaDB 1.5
Ornithorhynchus anatinus	Ensembl Platypus	http://www.ensembl.org/Ornithorhynchus_anatinus	5.0 (Ensembl 64.1)
Oryza sativa	Gramene	http://www.gramene.org/Oryza_sativa	MSU6, Database 60.6
Oryzias latipes	Ensembl Medaka (Oryzias latipes)	http://www.ensembl.org/Oryzias_latipes	HdrR (Ensembl 64.1)

Table 1 (continued). Genome databases used for the identification and retrieval of ABCC sequences

SPECIES	DATABASE NAME	DATABASE LINK	ASSEMBLY VERSION
Ostreococcus lucimarinus	JGI Ostreococcus lucimarinus	http://genome.jgi-psf.org/Ost9901_3	Ost9901_3 (v2.0)
Ostreococcus tauri	JGI Ostreococcus tauri	http://genome.jgi-psf.org/Ostta4	Ostta4 (v2.0)
Paramecium tetraurelia	ParameciumDB	http://paramecium.cgm.cnrs-gif.fr	Version 1
Pediculus humanus corporis	VectorBase Pediculus humanus	http://www.vectorbase.org/Pediculus_humanus	PhumU1.2
Phycomyces blakesleeanus	JGI Phycomyces blakesleeanus	http://genome.jgi-psf.org/Phybl2	Phybl2
Physcomitrella patens	Phytozome Physcomitrella patens	http://www.phytozome.net/physcomitrella.php	COSMOSS Annotation V1.6
Phytophthora sojae	JGI Phytophthora sojae	http://genome.jgi-psf.org/Physo1_1	v1.1 Filtered Models
Plasmodium falciparum 3D7	PlasmoDB	http://plasmodb.org	Version: 2010-06-01
Pleurotus ostreatus	JGI Pleurotus ostreatus	http://genome.jgi-psf.org/PleosPC15_2	PleosPC15_2 (v2.0)
Pogonomyrmex barbatus	PogoBase	http://hymenopteragenome.org/pogo	Pbar_OGSv1.2
Populus trichocarpa	Phytozome Populus trichocarpa	http://www.phytozome.net/poplar	JGI v2.2
Pristionchus pacificus	WormBase	http://www.wormbase.org	WS221
Prunus persica	Phytozome Prunus persica	http://www.phytozome.net/peach	JGI v1.0
Puccinia graminis f sp tritici	Ensembl Fungi	http://fungi.ensembl.org/Puccinia_graministritici	BROAD1 (Ensembl 64.1)
Pythium ultimum	Pythium Genome Database	http://pythium.plantbiology.msu.edu	Version 1
Ricinus communis	Phytozome Ricinus communis	http://www.phytozome.net/ricinus	v0.1
Saccharomyces cerevisiae	Saccharomyces Genome Database	http://www.yeastgenome.org	January 2011
Salpingoeca rosetta	Origins of Multicellularity Database	http://www.broadinstitute.org/annotation/genome/multicellularity_project	1
Schistosoma japonicum	GeneDB Schistosoma japonicum	http://www.genedb.org/Homepage/Sjaponicum	v4.0
Schistosoma mansoni	GeneDB Schistosoma mansoni	http://www.genedb.org/Homepage/Smansoni	v4.0h
Schizosaccharomyces pombe	Ensembl Fungi	http://fungi.ensembl.org/Schizosaccharomyces_pombe	Genebuild Dec 209
Selaginella moellendorffii	Phytozome Selaginella moellendorffii	http://www.phytozome.net/selaginella	v1.0 FilteredModels3
Solenopsis invicta	Fire Ant Genome Project	http://hymenopteragenome.org/solenopsis	Sinv_OGSv2.2.3
Sorghum bicolor	Phytozome Sorghum bicolor	http://www.phytozome.net/sorghum	v1.0 (Sbi1.4 gene set)
Sporidiobolus roseus	JGI Sporidiobolus roseus	http://genome.jgi-psf.org/Sporo1	Sporo1
Strongylocentrotus purpuratus	SpBase	http://www.spbase.org	V2.6
Takifugu rubripes	Ensembl Fugu (Takifugu rubripes)	http://www.ensembl.org/Takifugu_rubripes	FUGU 4.0 (Ensembl 64.4)
Tetrahymena thermophila	Tetrahymena Genome Database	http://www.ciliate.org	tta1_oct2008
Thalassiosira pseudonana	JGI Thalassiosira pseudonana	http://genome.jgi-psf.org/Thaps3	Thaps3
Thecamonas trahens	Origins of Multicellularity Database	http://www.broadinstitute.org/annotation/genome/multicellularity_project	1
Theileria annulata	Old GeneDB Theileria annulata	http://old.genedb.org/genedb/annulata	February 2005 Release
Theobroma cacao	Cacao Genome Database	http://www.cacaogenomedb.org	v0.9
Toxoplama gondi ME49	ToxoDB	http://toxodb.org	version: 2008-07-23
Tribolium castaneum	BeetleBase	http://beetlebase.org	Tcas 3.0
Trichinella spiralis	NCBI	http://www.ncbi.nlm.nih.gov	
Trichoplax adhaerens	JGI Trichoplax adhaerens Grell-BS-1999	http://genome.jgi-psf.org/Triad1	Triad1
Trichomonas vaginalis	TrichDB	http://trichdb.org	TrichDB 1.2
Trypanosoma brucei TREU927	TriTrypDB	http://tritrypdb.org	T.brucei927 2009-10-06
Vitis vinifera	Phytozome Vitis vinifera	http://www.phytozome.net/grape	IGGP_12x, blank
Volvox carteri	Phytozome Volvox carteri	http://www.phytozome.net/volvox	v.1.0. (June 1, 2007)
Wuchereria bancrofti	BROAD Institute Filarial worms	http://www.broadinstitute.org/annotation/genome/filarial_worms	V1
Xenopus tropicalis	Ensembl Xenopus tropicalis	http://www.ensembl.org/Xenopus_tropicalis	JGI 4.2 (Ensembl 64.42)
Zea mays	MaizeSequence	http://www.maizesequence.org	Genebuild Version 5a

3.2.3 Phylogenetic analyses

Protein sequences were aligned with MUSCLE 3.8 (http://www.drive5.com/muscle). Alignment columns with more than 20% gaps were removed using TrimAl (Capella-Gutiérrez et al., 2009). Phylogenies were estimated using RAxML 7.2.7 (Stamatakis, 2006) on the CIPRES portal V3.1 (http://www.phylo.org/index.php/portal/; Miller et al., 2010) with the protein evolution model LG+G4+F and a rapid non-parametric bootstrap analysis with 100 bootstrap replicates. The evolutionary model was determined using a ProtTest analysis (Darriba et al., 2011). Phylogenetic trees were visualized using MEGA5 (Tamura et al., 2011) and graphically decorated with the Adobe Illustrator software.

3.2.4 Chromosome maps

Circular chromosome maps were drawn using CIRCOS (Krzywinski et al., 2009) and the tandem repeat illustrations were created using the genoPlotR 0.7 package (http://genoplotr.r-forge.r-project.org/) in R 2.13.0 (http://www.R-project.org).

3.2.5 Statistical analyses and charts

R 2.13.0 (http://www.R-project.org) was used for all statistical analyses and charts.

3.2.6 HsABCC10 homology modeling

HsABCC10 models using the mouse P-glycoprotein 1 (Aller et al., 2009) (PDB ID: 3G5U) and the human ABCC1 nucleotide-binding domain 1 (Ramaen et al., 2006) (2CBZ) structures as templates were generated with Modeller 9v8 (Eswar et al., 2008), omitting the TMD0 (residues 1 to 261) and the subunit linker (residues 823 to 909). The HsABCC10 protein sequence was either aligned with sequences from the templates and SAV1866 (Dawson and Locher, 2006) or with sequences from the template structures and all other human ABCB/MDR and ABCC proteins, using Promals3D with standard parameters (Pei et al., 2008). Each of these alignments was subjected to manual iterative modeling/alignment-refinement cycles using Modeller with the DOPE potential profile as criteria. The resulting alignments were used for

estimation of 50-100 models using Modeller with increased optimization and refinement parameters (slow MD optimization, 4 optimization cycles). The model with the lowest DOPE potential was selected and consecutively regions with gaps in the alignment or regions aligning to template loop regions with no sequence identity but high DOPE potential were refined with Modeler's loop modeling function (for each region the best of 99 models based on loop DOPE potential was chosen). To verify the models, Ramachandran plots and PROCHECK G factors were obtained with PROCHECK (Laskowski et al., 1993). Additionally, the model was verified using WHAT_CHECK (http://swift.cmbi.ru.nl/gv/whatcheck/) (Hooft et al., 1996) and VADAR 1.8 (http://vadar.wishartlab.com) (Willard et al., 2003). Views of homology models were generated with PyMol (The PyMOL Molecular Graphics System, Version 1.3, Schrödinger, LLC.).

3.3 Results

3.3.1 Identification of *ABCC* gene inventories

To study the *ABCC* gene evolution, *ABCC* gene inventories of 135 annotated genomes from species of all eukaryotic lines were analyzed, with the exception of Rhizaria (Table 2). The analyzed species represent the majority of the currently sequenced and annotated protozoan, plant, invertebrate, and non-mammalian vertebrate species. Since mammals have been shown to comprise conserved *ABCC* gene families (Annilo et al., 2006), *ABCC* gene inventories were only analyzed from few of the available mammalian genomes. Moreover, only a limited number of fungal species were analyzed, since *ABC* gene inventories and phylogenies of various fungal species have been previously published (Kovalchuk and Driessen, 2010).

The search strategy of *ABCC* genes was based on already annotated genomes and employed BLAST searches with subsequent reciprocal BLAST and testing for ABCC-specific motifs. In total, 1727 putative *ABCC* genes were identified, of which 94 genes were manually reannotated. Manual annotation consisted of manual refinement of a gene model based on alignments with other *ABCC* genes. Additionally, 56 gene models were generated by merging 114 partial gene models encoding for distinct regions of an *ABCC* gene and with physical locations next to each other in the right orientation (see Material and Methods, Section 3.2.2). The remaining partial gene models were stored in the database when they had a length of more than 100 amino acids (aa) and had less than 98% identity with regions of other *ABCC* sequences of the same species. Genomes that were found to have considerably low genome assembly completeness or quality, or numerous incomplete or inaccurate *ABCC* gene models were excluded from subsequent analyses, i.e. *Lotus japonicas, Ascaris suum, Schistosoma japonicum, Phytophthora s T30-4*, *Pythium ultimum*. Comparison of the identified *ABCC* gene family sizes with published numbers reveals comparable number for most species, differing by a maximum of two genes. Only the numbers for *Chlamydomonas reinhardtii, Phytophthora sojae,* and *Strongylocentrotus purpuratus* differ considerably. In these cases, manual review of the published *ABCC* gene inventories reveals that the

search strategy used in this thesis was able to identify more complete gene models compared to the published inventories. Some of the partial genes models had been published as individual *ABCC* genes, whereas they were merged during manual curation process of *ABCC* gene models in this thesis. Differences in identified gene numbers may furthermore have resulted from the use of different, in meantime updated, versions of genome assemblies and annotations, compared to databases that were used in the published inventories.

Among the 1727 identified *ABCC* sequences, 56 (3%) were shorter than 500 aa, 194 (11%) shorter than 1000 aa, and 38 (2%) longer than 2000 aa (Figure 8). The median length was 1399 aa. The distribution of gene lengths in the database shows two maxima, one at a length of 1300 aa and another at 1450 aa. Amino acid and coding sequences, pyhysical location, original gene names, and information on manual annotations of identified *ABCC* genes were stored in the ABCC database, which is available from the author on request.

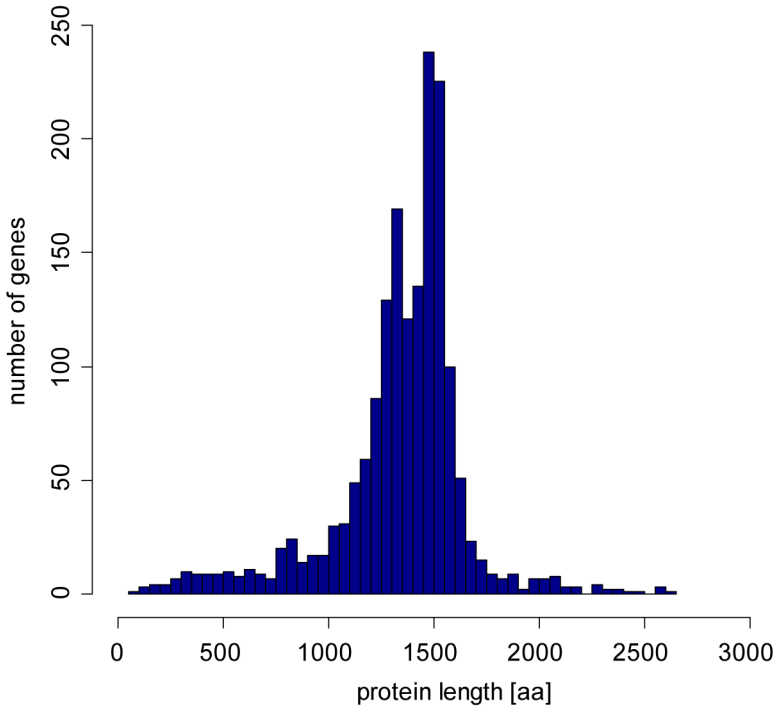

Figure 8. Distribution of protein lengths of all identified *ABCC* genes. Each bin represents 50 amino acids.

3.3.2 *ABCC* gene inventories

The numbers of *ABCC* genes identified per species varied considerably within kingdoms and taxa, and in some cases even between closely related species (Table 2). The only identified species that completely lack *ABCC* genes were *Trichomonas vaginalis* and all the analyzed microsporidian species (*Antonospora locustae, Encephalitozoon cuniculi, Encephalitozoon intestinalis, Encephalitozoon hellem, Enterocytozoon bieneusi, Nosema ceranae*). All the other analyzed species comprised between 2 and 54 *ABCC* genes. Sequences identified by the BLAST searches using different ABCC sequences against *Trichomonas vaginalis* and microsporidian genomes are all shorter than 800 bp, and none of them had any ABCC specific domain, nor resulted in ABCC protein top hits in reciprocal BLAST analyses against the NCBI database. Interestingly, the complete absence of any full-size ABC proteins, i.e. from the ABCA, ABCB, ABCB and ABCG subfamilies, was reported for *Encephalitozoon cuniculi* (Kovalchuk and Driessen, 2010).

Table 2. Numbers of identified *ABCC* genes and total number of genes per species. The total gene numbers were obtained from the literature or from genome databases. Numbers in brackets represent published ABCC gene numbers. Stars indicate that a species was included in the cross-kingdom phylogeny (Figure 11). Species in square brackets were excluded from all subsequent analysis.

Classification	Species	#Genes	#*ABCCs*	Phylo.
Viridiplantae				
Marine green algae	*Micromonas RC299*	10109	2	*
	Ostreococcus lucimarinus	7651	2	
	Ostreococcus tauri		2	*
Freshwater green algae	*Coccomyxa sp.C-169*	9629	3	*
	Chlorealla sp NC64A	9791	5	*
	Volvox carteri	14491	8	
	Chlamydomonas reinhardtii	16036	10 (7)	*
Bryophyta	*Physcomitrella patens*	32272	14	*
Lycopodiophyta	*Selaginella moellendorffii*	22273	24	*
Monocots	*Brachypodium distachyon*	25532	20	*
	Oryza sativa	40577	17	*
	Sorghum bicolor	34496	17	
	[Zea mays]	39656	13	
Eudicots	*Arabidopsis thaliana*	27228	15	*
	Carica papaya	24746	13	
	Citrus sinensis	25376	17	
	Cucumis sativa	26682	14	
	Eucalyptus grandis	44974	39	
	Fragaria vesca	34809	23	
	Glycine max	46430	39	
	[Lotus japonicas]		7	
	Malus domestica	57386	33	

Table 2 (continued). Numbers of identified *ABCC* genes and total number of genes per species.

Classification	Species	#Genes	#*ABCCs*	Phylo
	Manihot esculenta	30666	15	
	Medicago truncatula	47529	22	
	Mimulus guttatus	26718	12	
	Populus trichocarpa	45654	28	
	Prunus persica	27864	22	
	Ricinus communis	31237	13	*
	Theobroma cacao	34997	18	
	Vitis vinifera	33514	26	
Fungi				
Microsporidia				
	Antonospora locustae	2606	0	
	Encephalitozoon cuniculi	2678	0 (0)	
	Encephalitozoon hellem	2053	0	
	Encephalitozoon intestinalis	1913	0	
	Enterocytozoon bieneusi	1889	0	
	Nosema ceranae	3806	0	
Chytridiomycota				
	Allomyces macrogynus	17600	54	
	Batrachochytrium dendrobatidis	8732	18 (18)	*
Zygomycota	*Phycomyces blakesleeanus*	16528	12	*
Ascomycota	*Chaetomium globosum*	11124	9 (9)	
	Saccharomyces cerevisiae	6607	6 (6)	*
	Schizosaccharomyces pombe	5018	4 (4)	*
Basidiomycota	*Sporidiobolus roseus*	5536	7	*
	Pleurotus ostreatus	12330	10	
	Puccinia graminis f sp tritici		7 (7)	
Metazoa				
Basal metazoa	*Amphimedon queenslandica*	29867	24	
	Nematostella vectensis	27273	28	*
	Strongylocentrotus purpuratus	29129	31 (36)	
	Trichoplax adhaerens	11520	23	*
Bilateralia				
Nematoda				
Secernentea				
Ascaridida	*[Ascaris suum]*		12*	
Tylenchida	*Meloidogyne incognita*	19212	5	
Rhabditida	*Caenorhabditis elegans*	20416	9 (9)	*
	Caenorhabditis briggsae		9 (9)	
Diplogasteria	*Pristionchus pacificus*	24217	12	*
Spirurina	*Brugia malayi*	11357	3	*
	Loa loa	16318	4	
	Wuchereria bancrofti	19327	4	
Adenophorea	*Trichinella spiralis*	15808	4	
Platyhelminths	*Schistosoma mansoni*	13191	4	*
	[Schistosoma japonicum]		6*	
Mollusca	*Lottia gigantea*	23851	10	*
Annelida				
Clitellata	*Helobdella robusta*	23432	13	*
Polychaeta	*Capitella teleta*	32415	18	
Arthropoda				
Crustacea	*Daphnia pulex*	30907	8 (7)	*
Arachnida	*Ixodes scapularis*	20485	20	
Insecta				
Phthiraptera	*Pediculus humanus corporis*	10775	5	*
Hemiptera	*Acyrthosiphon pisum*	34821	17	*
Lepidoptera	*Bombyx morii*	18510	14 (14)	*

Table 2 (continued). Numbers of identified *ABCC* genes and total number of genes per species.

Classification		Species	#Genes	#*ABCCs*	Phylo
	Coleoptera	*Tribolium castaneum*	16645	33 (31)	
	Diptera				
		Aedes aegypti	15988	18	
		Anopheles gambiae	13320	12 (13)	*
		Culex quinquefasciatus	18883	15	
		Drosophila melanogaster	13827	13 (14)	*
		Drosophila ananassae		13	
		Drosophila grimshawi		14	
		Drosophila sechellia		14	
	Hymenoptera				
	Apoidea				
	Apidae	*Apis mellifera*	11062	9 (9)	*
	Formicidae	*Camponotus floridanus*	17064	10	
		Harpegnathos saltator	18564	9	
		Linepithema humile	16116	8	
		Pogonomyrmex barbatus		10	
		Solenopsis invicta		9	
	Parasitica				
		Nasonia vitripennis	18822	25	
Chordata					
		Ciona intestinalis	14002	7 (6)	*
		Ciona savignyi		6	
		Branchiostoma floridae	21955	29	
	Fish	*Danio rerio*	26096	15	
		Gasterosteus aculeatus	20787	13	
		Oryzias latipes	19686	12	
		Takifugu rubripes	18523	10	*
	Amphibia	*Xenopus tropicalis*	18429	11	
	Repitilia	*Anolis carolinensis*	16739	12	
	Birds	*Gallus gallus*	16736	11	*
		Taeniopygia guttata		12	
	Mammalia				
	Monotremata	*Ornithorhynchus anatinus*	17904	15	
	Eutheria	*Loxodonta africana*	19951	12	
		Mus musculus		11	
		Canis familiaris		13	
		Bos taurus	19262	16	
		Homo sapiens	21550	12	*
Protozoa					
Rhodophyta		*Cyanidioschyzon merolae*	5331	2 (2)	*
		Galdieria sulphuraria		2	
Apicomplexa		*Babesia bovis*	3671	4	
		Cryptosporidium parvum Iowa II	3807	14	
		Cryptosporidium hominis		12	
		Cryptosporidium muris		14	
		Neospora canium	7227	3	
		Plasmodium falciparum 3D7	6372	2	
		Theileria annulata	3792	17	
		Theileria parva strain Muguga		13	
		Toxoplama gondi ME49	9239	4	
		Toxoplama gondi GT1		4	
		Toxoplama gondi VEG		3	
Ciliophora		*Emiliania huxleyi*	33340	12	
Haptophyta		*Paramecium tetraurelia*	39642	42	
Heterokontophyta		*Aureococcus anophagefferens*	11501	14	*
		Ectocarpus siliculosus	16256	9	*
		Fragilariopsis cylindrus	27137	10	

Table 2 (continued). Numbers of identified *ABCC* genes and total number of genes per species.

Classification	Species	#Genes	#*ABCCs*	Phylo
	Phytophthora sojae	19027	27 (22)	*
	[Phytophthora s T30-4]		25	
	Pythium ultimum	15297	41	
	Thalassiosira pseudonana	11776	7	*
Excavata	*Giardia lamblia Assemblage A*	5981	6	
	Leishmania major Friedlin	9388	8	*
	Leishmania braziliensis		8	
	Leishmania infantum		9	
	Naegleria gruberi	15753	9	*
	Trichomonas vaginalis	59672	0	
	Trypanosoma brucei TREU927	11412	3	
	Trypanosoma vivax		3	
	Trypanosoma brucei gambiense		2	*
	Trypanosoma cruzinon-esmeraldo		2	
Amoebozoa	*Dictyostelium discoideum AX4*	12646	13 (14)	*
	Entamoeba histolytica	8333	8	
Holozoa	*Capsaspora owczarzaki*	8176	6	*
	Monosiga brevicollis	9196	8	*
	Salpingoeca rosetta	11597	9	*
Apusozoa	*Thecamonas trahens*	11582	9	*

3.3.3 Correlation of the *ABCC* gene numbers with total number of genes per species

A significant positive correlation of the number of predicted *ABCC* paralogs from analyzed species with the predicted total number of genes was found in this study (Poisson regression: z= 17.2, p=<0.001 n=119; Spearman's rank correlation: ρ=0.65, p<0.001, n=119) (Figure 9A).

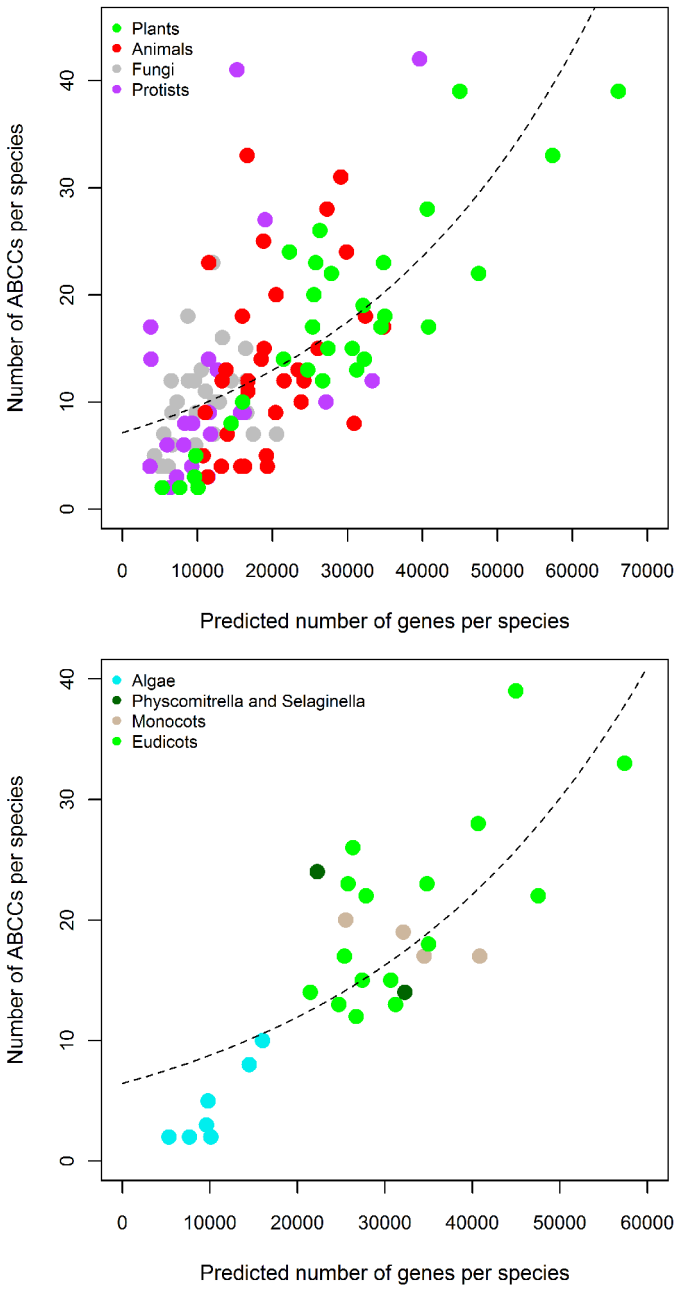

Figure 9. Correlation between the numbers of *ABCC* genes and all genes per genome. Curves represent Poisson regression. **(A)** All plant (green), fungi (grey), protist (purple) and animal (red) species. **(B)** Only plant species: Algae (blue), moss and lycophyte (dark green), monocots (brown) and eudicots (green).

Significant correlations were also observed in plants only (Poisson: z=10.99, p<0.001; Spearman's: ρ=0.82, p<0.001, n=28) (Figure 9B), non-arthropod invertebrates (Poisson: z=5.13, df=10, p<0.001; Spearman's: ρ=0.93, p<0.001, n=11), insects (Poisson: z=3.31, df=8, p<0.001; Spearman's: ρ=0.78, p<0.05, n=9), and protists (Poisson: z=7.94, df=23, p<0.001; Spearman's: ρ= 0.45, p<0.01, n=23). The correlation in fungi (Poisson: z=2.27, df=29, p<0.05; Spearman's: ρ= 0.53, p<0.05, n=29) was only moderate (Figure 10).

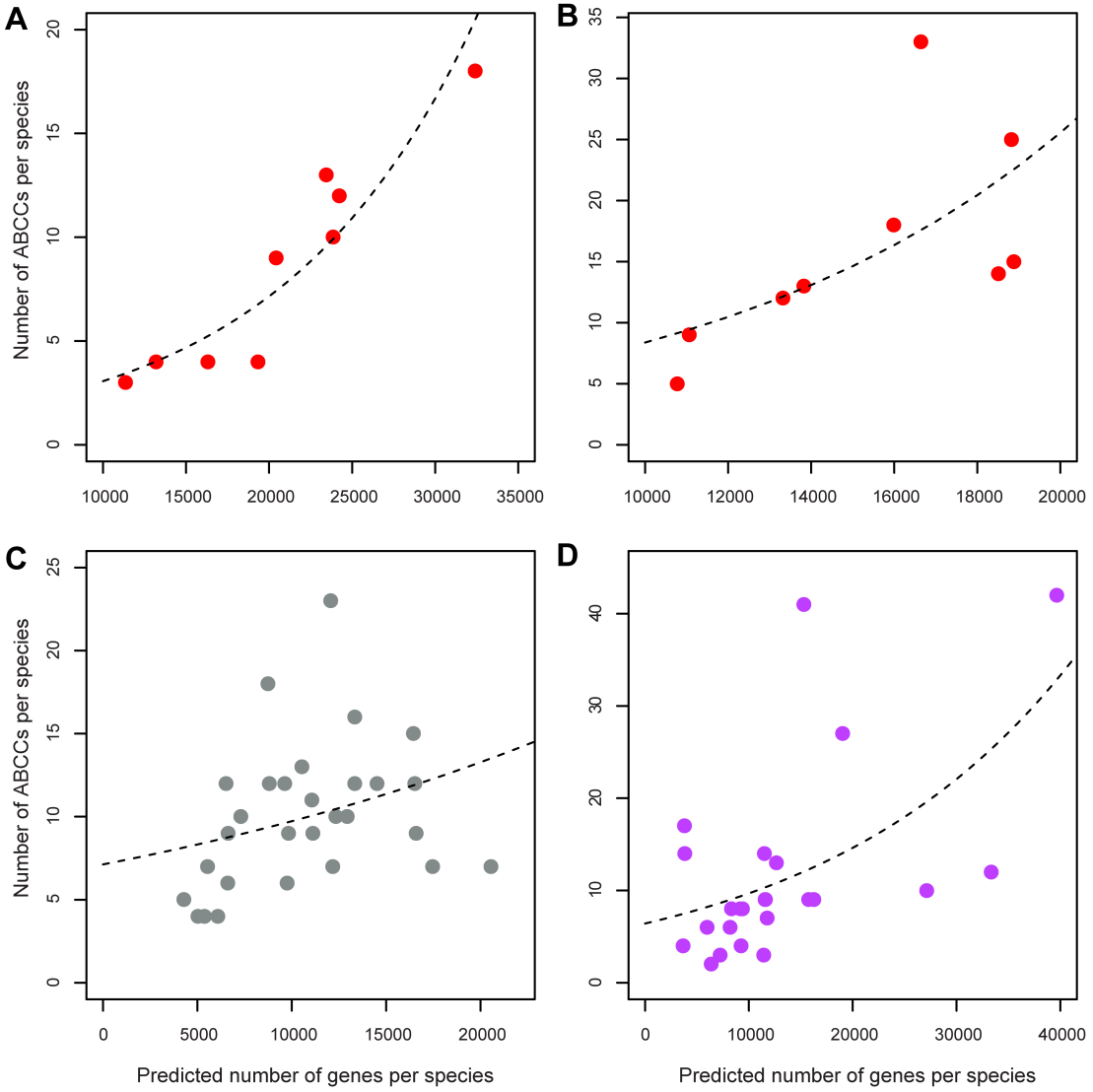

Figure 10. Correlation between the numbers of *ABCC* genes and all genes per genome. **(A)** Nematodes and non-arthropod invertebrates, **(B)** Insects, **(C)** Fungi, **(D)** Protists.

3.3.4 Evolutionary relationships of *ABCC* genes across kingdoms

To obtain an overview of the evolutionary relationships of *ABCC* genes within and across eukaryotic kingdoms, a maximum-likelihood (ML) phylogeny of ABCC protein sequences was inferred from selected plant, fungal, animal, and protist species (Table 2). To reduce the impact of protist species with highly divergent or with large numbers of *ABCC* genes on the phylogenetic inference, selected protist species were excluded from the analysis, based on preliminary phylogenetic analyses (data not shown).

The obtained *ABCC* phylogeny reveals several well-supported major clades (Figure 11). Only one of the major clades (termed *ABCC-E*), supported by 100% bootstrap (BS), comprises single gene members of all included freshwater algae, all land plant, almost all animal species and specific species from protist kingdoms. This clade represents the only major clade that harbors genes from more than two kingdoms and the only clade comprising plants and animal genes. The other major clades exclusively comprise *ABCC* genes from plants, fungi, or animals only. *ABCC* genes that are not present in major clades, assemble to clusters that do not form distinct clades (<70% BS) and root to the center of the phylogeny.

Land plant *ABCC* genes cluster into two major clades (*P1* and *P2-8*), each supported by 100% BS. The *P1* clade also comprises freshwater green algae *ABCCs,* and the *P2-8* clade clusters with a clade harboring 11 *Phytophthora sojae ABCCs* (84% BS). Specific *ABCCs* from the lycophyte *Selaginella moellendorffii* and the moss *Physcomitrella patens* form an additional distinct clade in this phylogeny. Several freshwater algae *ABCCs* cluster to the animal clades (Table 3), and the remaining *ABCCs* of algae, including those from the marine green algae *Ostreococcus tauri, Micromonas RC299,* and red algae *Cyanidioschyzon merolae ABCCs,* are found in small clusters distinct to other clades and root to the basis of the phylogeny. Fungal *ABCCs* are represented by three distinct major clades (*F1*, *F2*, and *F3*), each of them supported by 99% BS. Unlike the clades *F1* and *F2*, which harbor *ABCCs* from all analyzed fungi, the *F3* clade lacks genes from the zygomycete *Phycomyces blakesleeanus*. The *F1* clade clusters with the major animal clade *A4*, and the *F2* clade clusters with *ABCCs* from the heterokonts

Aureococcus anophagefferens and *Ectocarpus siliculosus*. Three *ABCC* genes from the chytrid fungus *Batrachochytrium dendrobatidis* are found outside the fungal clades and cluster with animal clades (Table 3). Animals *ABCC* genes cluster into four distinct major clades (*A1*, *A2*, *A3*, and *A4*), which all harbor specific human *ABCC* genes. All these clades are characterized by the presence of at least one holozoa *ABCC* gene at their roots, and some of these clades additionally harbor ABCC genes from algae, heterokonts, and/or the chytrid fungus *Batrachochytrium dendrobatidis* at their roots (Table 3). The *A1* clade (94% BS) comprising *HsABCC8/9* represents the smallest clade with each species represented by one or two paralogs, whereby nematodes and the basal metazoa do not harbor ABCC genes in this clade. The *A2* clade (100% BS) comprising *HsABCC5/11/12* has members from most animal species, except from specific insect orders. The *A3* clade (91% BS) comprising *HsABCC4/7* represents the largest animal clade, with *ABCCs* from all analyzed animal species, whereby especially basal metazoan and insect species harbor high numbers of *ABCC* paralogs in this clade. The *A4* clade (78% BS) containing *HsABCC1/2/3/6* has members from most animal species, except from certain nematode species and clusters with the fungal clade *F1*. The *Anopheles gambiae AgABCC5* represents the only animal *ABCC* gene that is found outside the animal *ABCC* clades and roots to the base of the phylogeny.

Table 3. Animal *ABCC* clades with *Homo sapiens* and non-animal *ABCC* genes clustering to these clades with a bootstrap higher than 70%. Bootstrap values of individual clades are indicated.

Clade(BS)	Homo sapiens	Holozoa+Apusozoa	Algae	Batrachochytrium	Heterokonts
E (100%)	HsABCC10	MbrABCC8, SrosABCC1 CowABCC1 TtrABCC1	CrABCC7 CspABCC1 CcoABCC1		EsiABCC1 PsoABCC10
A1 (94%)	HsABCC8/9	CowABCC4			
A2 (73% -100%)	HsABCC5/10/11	MbrABCC3/4/6 SrosABCC4 CowABCC5 TtrABCC7	CrABCC1/2 CspABCC4/5	BdeABCC10/18	
A3 (91%)	HsABCC4/7	MbrABCC2/5 SrosABCC2/5/7/9 CowABCC3 TtrABCC4	CrABCC6/9/10 CspABCC3 CcoABCC3	BdeABCC8	EsiABCC4/5/9 AanABCC8/9 TpsABCC5/6
A4 (78%)	HsABCC1/2/3/6	MbrABCC1 SrosABCC4 CowABCC2		BdeABCC1 + other fungi	PsoABCC2/7 AanABCC1 TpsABCC7

Mbr: *Monosiga brevicollis*, Sro: *Salpingoeca rosetta*, Cow: *Capsaspora owczarzaki*, Tre: *Thecamonas trahens*, Cr: *Chlamydomonas reinhardtii*, Csp: *Chlorella vulgaris*, Cco: *Coccomyxa sp*, Bde: *Batrachochytrium dendrobatidis*, Pso: *Phytophthora sojae*, Esi: *Ectocarpus siliculosus*, Aan: *Aureococcus anophagefferens*, Tps: *Thalassiosira pseudonana*

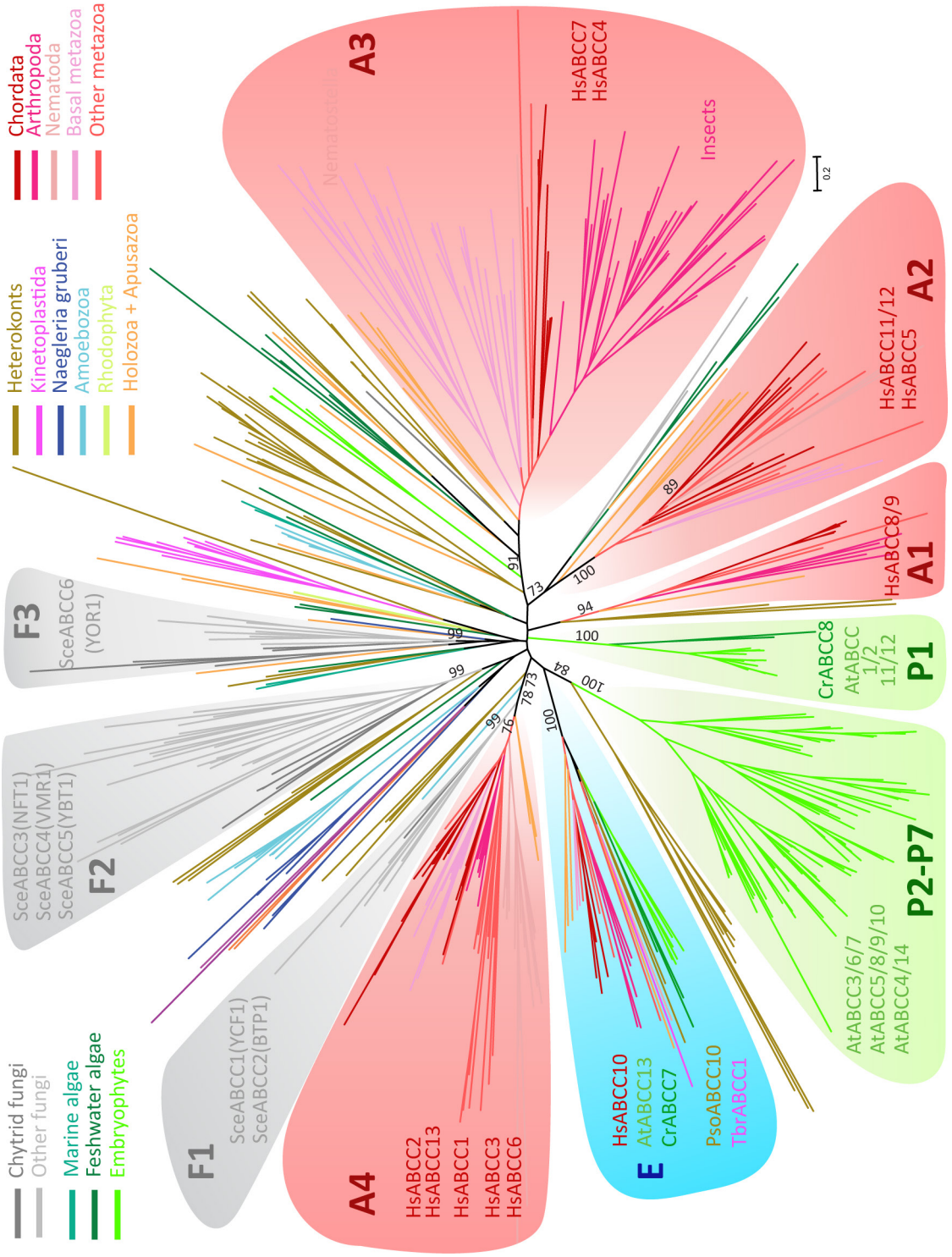

Figure 11. Maximum likelihood (ML) phylogeny of *ABCC* genes from species representing all major eukaryotic kingdoms. Clades comprising animal *ABCCs* are shaded in red, plants in green, and fungi in grey. Clades are labeled with names of *Homo sapiens (Hs), Arabidopsis thaliana (At)* and *Saccharomyces cerevisiae (Sce) ABCC* genes that are present in the clade. RAxML rapid bootstrap values higher than 70% are indicated for the main branches.

3.3.5 Plant *ABCC* genes

The number of *ABCC* genes among different plant species varies significantly (Table 2, Figure 9B). The marine green algae *Micromonas RC299 and Ostreococcus tauri* have only two *ABCC* genes, whereas the freshwater green algae *Coccomyxa sp*, *Chlorealla variabilis, Volvox carteri* and *Chlamydomonas reinhardtii* harbor 3-10 *ABCC* paralogs. Angiosperms like *Mimulus guttatus*, *Ricinus communis*, *Cucumis sativa* and *Arabidopsis thaliana* possess 12-15, whereas other angiosperms, such as *Malus domestica, Eucalyptus grandis* and *Glycine max*, harbor 33-39 *ABCCs*. The size of the *ABCC* gene family correlates with the total number of genes (Figure 9B), however, there are significant deviations. For instance, the grape *Vitis vinifera* has almost the double number of *ABCC* genes (26) compared to *Arabidopsis thaliana* (15) and *Ricinus communis* (13), whereby the total numbers of predicted genes of these species are comparable.

To analyze the phylogenetic relationship of plant *ABCC* genes, a maximum-likelihood (ML) phylogeny of *ABCCs* from selected plant species (Table 2) was estimated (Figure 12). The phylogeny reveals nine distinct, fully supported plant-specific *ABCC* clades (*E*, *P1* to *P8*) and one clade with *ABCCs* from lower plants (*P0*). Each of the angiosperm clades consists of one or more *ABCC* genes from each of the analyzed monocot and eudicot species (Table 4), with the exception of the *P7* clade that lacks *ABCCs* from *Arabidopsis thaliana*, *Medicago truncatula* and *Zea mays*. Only the *E* and the *P1* clades comprise orthologs from the green algae *Chlamydomonas reinhardtii* and *Coccomyxa sp.C-169*. Some of the other freshwater green algae *ABCCs* form a distinct clade (*P0*) that also harbors several *ABCCs* from the moss *Physcomitrella patens* and the lycophyte *Selaginella moellendorffii.* The remaining algae *ABCCs*, including those from the red and marine green algae, show no orthologous relationships to land plant *ABCCs*. The *P6*, *P7* and *P8* clades appear to be angiosperm-specific, whereas each of the *P1 to P6* clades show orthologous relationship with *ABCCs* from *Physcomitrella patens* and *Selaginella moellendorffii.* The *P1* and *P3* clades have further diverged into the eudicot-specific subclades *P1A/P1B and P3A/P3B* (Figure 13A), which harbor *ABCC* orthologs from all analyzed eudicots, except the *P3B* subclade that lacks *ABCCs* from

Arabidopsis thaliana, *Glycine max, Medicago truncatula, Mimulus guttatus* and *Cucumis sativa.* The *P2* and *P8* clades have also diverged into three and two distinct poaceae-specific subclades, respectively.

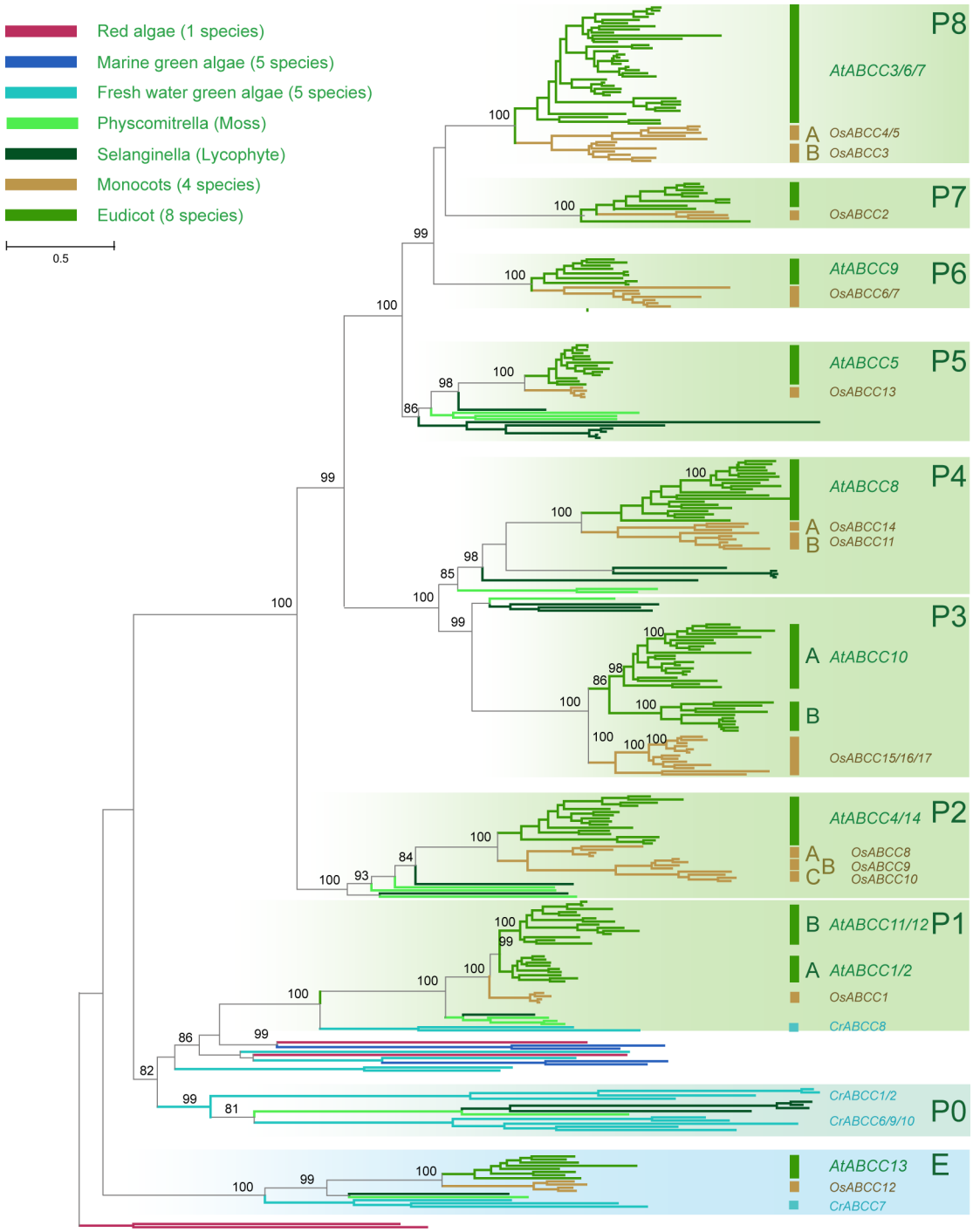

Figure 12. ML phylogeny of plant *ABCC* genes from red algae, green algae, moss, lycophyte, monocot, and eudicot species. Plant-specific clades are shaded in green and subclades are depicted with bars. *ABCC* genes from *Arabidopsis* and rice found within each of these clades are indicated. Main nodes are labeled with RAxML rapid non-parametric bootstrap values if higher than 70%.

Table 4. Species-specific distributions of *ABCC* genes in plant-specific *ABCC* clades. Clades comprising only one *ABCC* are highlighted in blue and clades with more than three paralogs are in red fonts.

Group	Order	Subfamily	Species	Total	E	P1A	P1B	P2	P3A	P3B	P4	P5	P6	P7	P8
Chlorophyta	Prasinophyceae		***Micromonas RC299***	**2**	-	-	-	-	-	-	-	-	-	-	-
			Ostreococcus lucimarinus	**2**	-	-	-	-	-	-	-	-	-	-	-
	Trebouxiophyceae		***Chlorealla sp NC64A***	**5**	1	-	-	-	-	-	-	-	-	-	-
	Chlorophyceae		***Coccomyxa sp.C-169***	**3**	1	1	-	-	-	-	-	-	-	-	-
			Chlamydomonas reinhardtii	**10**	1	1	-	-	-	-	-	-	-	-	-
Bryophyta			***Physcomitrella patens***	**13**	1	3	-	3	1	-	2	3	-	-	-
Lycopodiophyta			***Selaginella moellendorffii***	**17**	1	1	-	2	3	-	**5**	**5**	-	-	-
Monocots															
	Poales	Poaceae	***Brachypodium distachyon***	**13**	1	1	-	3	**4**	-	**4**	1	1	1	3
			Sorghum bicolor	**11**	1	1	-	3	3	-	2	1	2	1	3
			Oryza sativa	**11**	1	1	-	3	3	-	2	1	2	1	3
			Zea mays	**9**	1	1	-	3	3	-	1	1	2		2
Eudicots															
	Asterids		***Mimulus guttatus***	**12**	1	1	1	1	2	-	1	2	1	1	1
Rosids	Vitales		***Vitis vinifera***	**25**	1	1	2	1	2	**6**	3	1	1	1	**6**
Eurosids I	Myrtales		***Eucalyptus grandis***	**36**	1	1	**11**	1	2	**4**	**4**	1	3	3	**5**
	Sapindales		***Citrus sinensis***	**17**	1	1	1	1	2	1	2	1	1	1	**5**
	Malvales		***Theobroma cacao***	**17**	1	1	2	1	2	2	2	1	1	1	**3**
	Brassicales		***Carica papaya***	**13**	1	1	1	1	1	-	1	1	1	2	**3**
			Arabidopsis thaliana	**15**	1	2	2	2	1	-	1	1	2	-	3
Eurosids II	Malpighiales	Euphorbiaceae	***Manihot esculenta***	**15**	1	1	1	2	1	1	1	2	1	2	2
			Ricinus communis	**15**	1	1	1	1	1	1	1	1	2	1	**4**
		Salicaceae	***Populus trichocarpa***	**28**	1	1	3	2	**5**	3	1	2	1	3	**6**
	Fabaceae		***Medicago truncatula***	**21**	1	-	3	2	3	-	**7**	1	-	-	**4**
			Glycine max	**39**	1	2	1	**5**	**6**	-	**5**	3	2	2	**12**
	Rosaceae	Spiraeoideae	***Prunus persica***	**22**	1	1	1	1	2	3	2	1	1	3	**6**
			Malus domestica	**29**	1	2	2	3	1	**5**	3	**4**	1	2	**5**
		Rosoideae	***Fragaria vesca***	**23**	1	1	3	1	**4**	**4**	2	1	1	3	2
	Cucurbitales		***Cucumis sativa***	**14**	1	1	2	2	1	-	1	1	3	1	1

The divergence of genes varies among the clades: *ABCCs* within the *P1B* and *P5* clades exhibit only little divergence, while orthologous but also paralogous *ABCCs* of other clades display greater divergences. The plant-specific clades also differ by the variability of the number of paralogs per species they contain. Clade *ABCC-E* comprises only one gene per species, whereas clades *P1A, P1B*, *P2*, *P5*, *P6,* and *P7* mostly harbor 1-4 paralogs per species, with few exceptions. Unlike all other analyzes species, the *Eucalyptus grandis P1B* clade is greatly expanded with 11 paralogs, of which nine are located in the genome within a single cluster in a tandem arrangement (see Supplementary Table 1, Scaffold_4, in Section 3.5.1). In monocots, most species have 1-3 paralogs in each clade, with the exception of *Brachypodium distachyon* that has 4 paralogs in each of the *P3A* and *P4* clades. Within the remaining clades *P3A/B, P4* and particularly *P8,* lineage-specific expansions are frequent among the eudicot species. The *P3A* subclade displays expansions in *Fragaria vesca*, *Populus trichocarpa,* and *Glycine max;* the *P3B* subclade in *Fragaria vesca*, *Eucalyptus grandis, Malus domestica,* and *Vitis vinifera* (Figure 13A). The *P4* clade is expanded in *Eucalyptus grandis* and in the fabaceae *Medicago truncatula* and *Glycine max*. Within the *P8* clade, the majority of eudicot species exhibit lineage-specific expansions. *Glycine max* comprises 12 *ABCC* genes in this clade, which represents the largest lineage-specific expansion of *ABCCs* in plants identified in this study (Figure 13B).

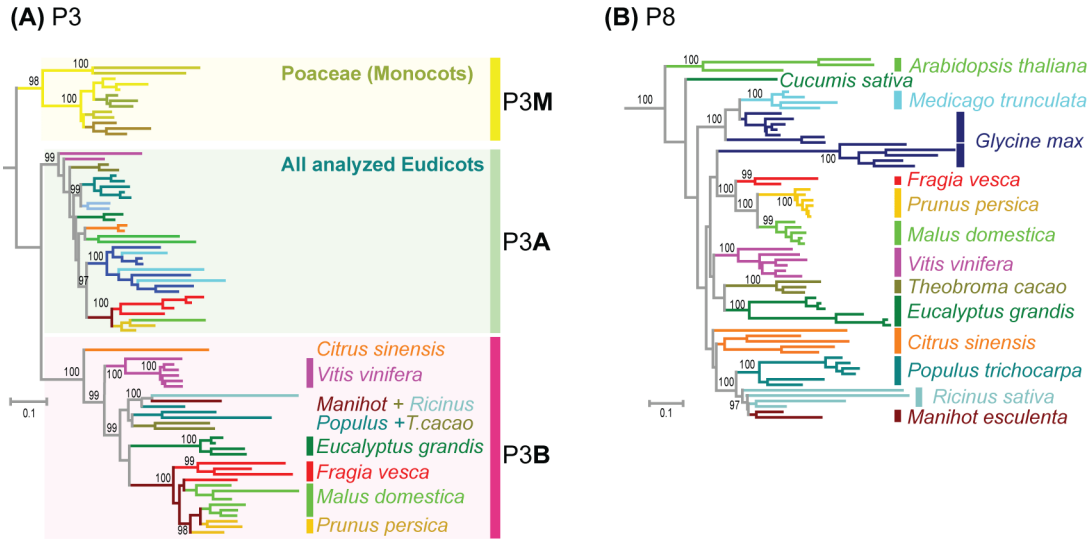

Figure 13. ML phylogenies of the *ABCC* clades *P3* and *P8* showing lineage-specific expansions. **(A)** Plant *P3* clade with the two distinct eudicot subclades *P3A* and *P3B*. **(B)** Eudicot *P8* clade. Color bars indicate lineage-specific expansions. RAxML rapid bootstrap values of main branches above 95% are indicated.

To investigate the mechanisms of *ABCC* gene expansions in plants, chromosomal locations of *ABCC* genes were analyzed in *Vitis vinifera* and *Glycine max*, which have experienced one and three whole genome duplications during their evolution, respectively (Figure 14). In *Vitis vinifera*, all *ABCC* genes from each of the plant-specific clades are located on the same chromosome. In clades that comprise more than one gene (*P1B*, *P3A*, *P3B*, *P4* and *P8*), *ABCC* genes are located in the genome in tandem configurations, adjacent to each other. The clades *P3B* and *P8* show large tandem clusters, each with six adjacent paralogs (Figure 14A). In *Glycine max*, only the clades *E* and *P1B* comprise single genes. All other clades consist of more than one paralog. These paralogs are distributed over at least two distinct chromosomes, as individual genes or as gene clusters comprising two to three genes in a tandem arrangement. The 12 *ABCC* genes of the *P8* clade from *Glycine max* are dispersed as single genes or tandem clusters on four different chromosomes (Figure 14B). Tandem duplications are also present in *Eucalyptus grandis* where 28 of the 36 *ABCCs* are found in tandem clusters (See Supplementary Table 1 in Section 3.5.1).

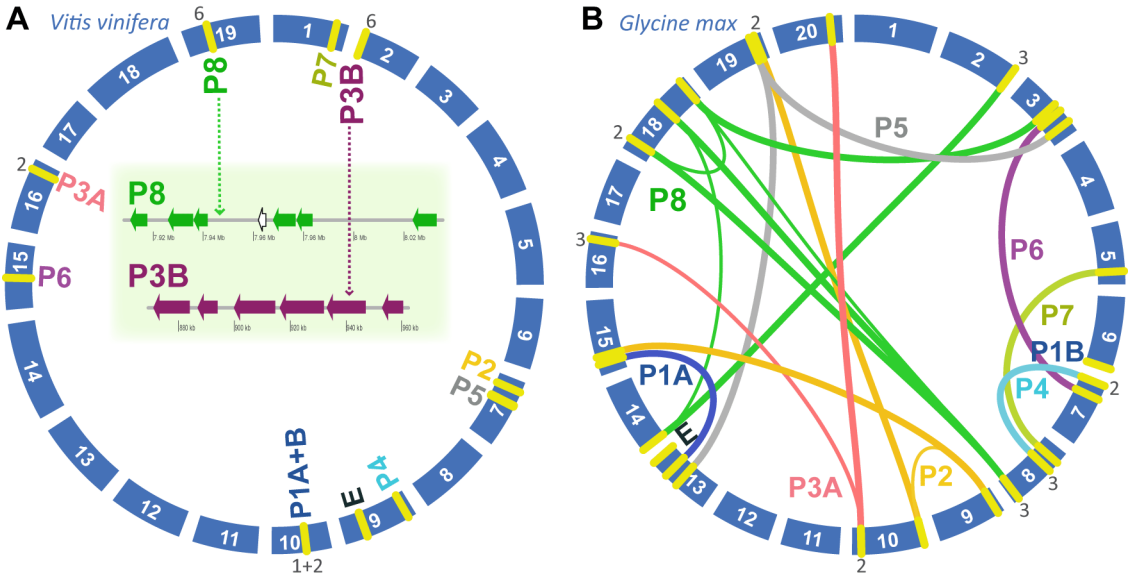

Figure 14. Chromosomal locations and paralogous relationships of *ABCC* genes from *Vitis vinifera* **(A)** and *Glycine max* **(B)**. Chromosomes are shown in blue and labeled with their numbers. *ABCC* genes are indicated by yellow bars and are labeled with the corresponding plant-specific *ABCC* clade names. Small numbers indicate number of genes present in tandem arrangement at this location. Paralogs of *ABCC* subfamily genes are connected by lines, colored and labeled by subfamily. Thicker lines indicate higher sequence similarity between paralogous genes. The tandem arrangements of genes from the *Vitis vinifera* clades *P3B* and *P8* are illustrated in the inset of A.

3.3.6 Invertebrate *ABCC* genes

Invertebrates show large variations in numbers of *ABCC* genes they comprise (Table 2). The size of the *ABCC* gene family also displays a positive correlation with the number of genes per species (Figure 10A/B). Basal marine metazoan species, such as the placozoa *Trichoplax adhaerens*, the sponge *Amphimedon queenslandica,* the sea anemome *Nematostella vectensis* and the sea urchin *Strongylocentrotus purpuratus* all have large *ABCC* gene sets, ranging from 23 to 31 *ABCC* paralogs per species. Endoparasitic nematodes (e.g. *Brugia malayi*, *Wuchereria bancrofti* and *Loa loa*) possess the fewest number of *ABCC* genes (3-4) of all analyzed animals, while the free living non-parasitic nematode *Caenorhabditis elegans* and the related insect intestinal parasite *Pristionchus pacificus* possess 9-12 *ABCCs*. The obligate parasitic body louse *Pediculus humanus* has only 5 *ABCCs*, which is the lowest number found in arthropods in this study. Large variations between related species are observed for the parasitoid wasp *Nasonia vitripennis* that harbors 25 *ABCCs*, whereas the other hymenoptera, the honeybee *Apis mellifera* and ants, only possess 9-10 *ABCCs*. The water flea *Daphnia pulex* has a small *ABCC* gene family (8) compared to its relatively high number of predicted genes (30907), thus representing one of the animals species with lowest *ABCC* densities found in this study. The red flour beetle *Tribolium castaneum* harbors 33 *ABCC* paralogs, the highest number identified for animals in this study. Compared to its small genome size with 16645 predicted genes, this beetle has a greatly enlarged *ABCC* gene family.

To analyze the evolution of invertebrate *ABCC* genes, a separate maximum-likelihood phylogeny (ML) was estimated comprising *ABCC* gene sets from various protostome phyla (Figure 15). Within this phylogeny, the four major animal *ABCC* clades (*A1* to *A4*) and the major clade *ABCC-E* were identified corresponding to the *ABCC* clades identified in the cross-kingdom phylogeny (Figure 11). The *ABCC-E* clade comprises single *ABCC* genes from all analyzed invertebrates, with the exception of *Nasonia vitripennis* and the nematodes *Caenorhabditis elegans, Brugia malayi*, *Wuchereria bancrofti* and *Loa loa*, which do not have any genes in this clade. However, an *ABCC* gene from the nematode *Pristionchus pacificus* is present in this clade.

The major clade *A1* comprises single genes from *Daphnia pulex* and all analyzed arthropods, except from *Nasonia vitripennis* and *Tribolium castaneum. Lottia gigantea*, *Helobdella robusta* and *Capitella teleta* each comprise two genes in this clade. No orthologs from the basal metazoa, nematodes, and the platyhelminth *Schistosoma mansoni* are present in this clade. The *A2* clade represents another small clade and lacks genes from diptera, *Schistosoma mansoni*, and the tick *Ixodes scapularis*, while other species are represented by 1-4 *ABCC* genes. The *A3* clade represents the largest invertebrate *ABCC* clade. The basal metazoa *Trichoplax adhaerens* and *Nematostella vectensis* possess largely expanded paralogous subclades within this clade. Substantial lineage-specific *ABCC* expansions are also detected within insects. In fact, the majority of insect *ABCCs* are found in this clade. For example, 22 of the total 25 *ABCCs* from *Nasonia vitripennis*, 14 of 17 from *Acyrthosiphon pisum*, 9 of 12 from *Drosophila melanogaster*, and 31 of 33 from *Tribolium castaneum* are present in this clade. These 31 *ABCC* paralogs from *Tribolium castaneum* are mostly present as tandem clusters of 2-8 *ABCC* genes in the genome (See Supplementary Table 2, in Section 3.5.2). *Caenorhabditis elegans* has one, while other nematodes do not have any *ABCC* genes in this clade. The remaining analyzed invertebrate species have only few *ABCC* paralogs in this clade, i.e. *Daphnia pulex*, *Ixodes scapularis*, and *Helobdella robusta* have one, *Lottia gigantean* has 2, and *Capitella teleta* has 5 *ABCCs* in this clade. In a separate phylogenetic analysis (data not shown), the *Heliothis virescens ABCC* genes involved in resistance to Bt toxin (Gahan et al., 2010) were identified of being members of the *A3* clade. The *A4* clade harbors most of nematode *ABCCs*, e.g. 7 of 9 *Caenorhabditis elegans ABCCs*, whereby the *CelABCC9* gene shows one of the largest divergences compared to other *ABCCs* observed in this phylogeny. This clade also comprises a subclade with orthologous *ABCC* genes from all analyzed insect species, comprising the *Drosophila melanogaster DmABCC1*. Furthermore, 16 of the total 20 *ABCCs* from the tick *Ixodes scapularis* are present in this clade.

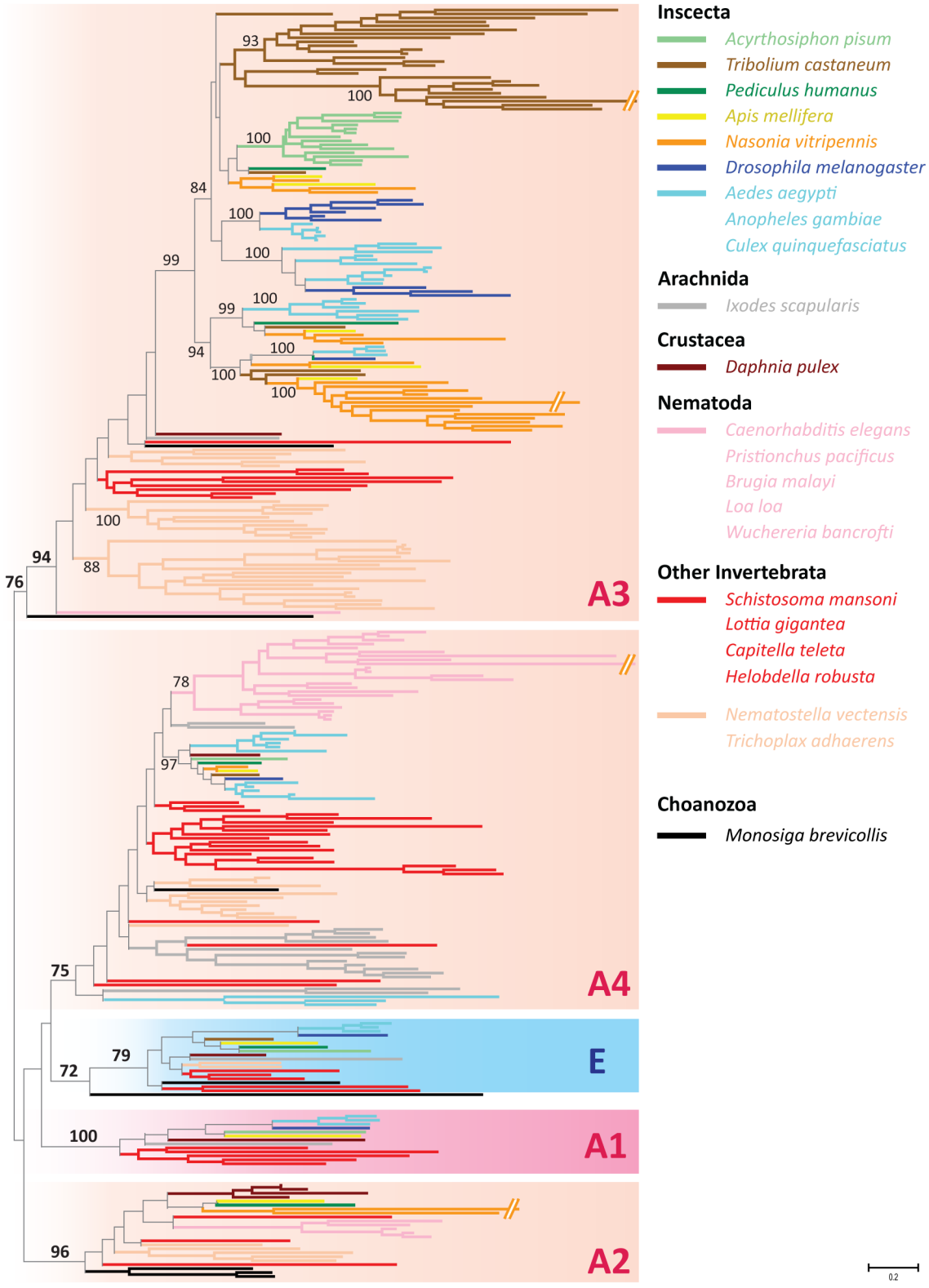

Figure 15. ML phylogeny of invertebrate *ABCC* genes. Clades corresponding to major *ABCC* clades are shaded and labeled. Main nodes are labeled with RAxML rapid non-parametric bootstrap values if higher than 70%.

3.3.7 Chordate *ABCC* genes

The majority of the analyzed vertebrates harbor 11–12 *ABCC* genes; however, the zebrafish *Danio rerio*, the platypus *Ornithorhynchus anatinus* and the cow *Bos taurus* possess 15-16 *ABCCs*. Among the analyzed non-vertebrate chordates, the tunicate *Ciona intestinalis* is predicted to have 7 *ABCC* genes, whereas 29 *ABCCs* are predicted for the lancelet *Branchiostoma floridae*.

A maximum-likelihood (ML) phylogeny comprising vertebrate and *Ciona intestinalis ABCCs* was estimated to analyze their evolutionary relationships (Figure 16). The resulting chordate *ABCC* phylogeny reveals 13 conserved clades (*ABCC1-13*), each of which generally comprising one human *ABCC* gene and mostly one or few orthologs from each of the other analyzed vertebrates. These clades can be assigned to the major animal major clades *A1-A4* and the major clade *ABCC-E*, which were identified in the cross-kingdom phylogeny (Figure 11). The *ABCC4*, *ABCC5*, *ABCC11/12* and *ABCC1/2/3/6/13* clades each harbor orthologs from *Ciona intestinalis*. Furthermore, the Ensembl Gene Orthology database (EnsemblCompara) (Vilella et al., 2009) was queried at the time of writing this thesis, to take advantage of in the meantime improved Ensembl gene annotations and orthology assignments, and to search for putative orthologs in species that were not included in the phylogeny (data not shown).

The *ABCC10* clade corresponds to the major clade *ABCC-E* and harbors single-copy *ABCCs* from all analyzed chordates. The *ABCC8* and *ABCC9* clades represent the major animal clade *A1*. Most vertebrate species have one *ABCC* in each of these two clades. However, *Danio rerio* harbors an additional paralog in the *ABCC8* clade, whereas the frog *Xenopus tropicalis* and the platypus *Ornithorhynchus anatinus* do not have any *ABCC8* orthologs. The *ABCC9* clade displays the lowest divergence among all chordate *ABCC* clades. The *ABCC7* (*CFTR*) clade comprises only single-copy vertebrate *ABCC*s and appears to have diverged from the *ABCC4* clade before the evolution of *Ciona intestinalis.* The *ABCC4* clade comprises 4 genes from *Bos taurus*, whereby 3 of them form a distinct subclade that substantially diverged from the other *ABCC4* genes. These

3 *ABCCs* are located on the *Bos taurus* chromosome 12 within a region of 4.9 Mb. Supplementary analyses using the Ensembl database furthermore revealed the presence of 2-5 *ABCC4* copies in all fish genomes, except in *Danio rerio* that appears to have only one *ABCC4* ortholog (data not shown). At the time where this phylogeny was estimated, these *ABCC4* copies were not present in the Ensembl database or were not identified, and are therefore not present in the ABCC database. However, new preliminary phylogenetic analyses indicate that these putative *ABCC4* copies indeed represent *ABCC4* paralogs. The *ABCC11* and *ABCC12* clades cluster with a clade termed *ABCC11/12*, comprising only *ABCCs* from fishes and two *ABCCs* from *Ciona intestinalis.* Birds and *Xenopus tropicalis* do not have any orthologs in the *ABCC11/12* clade. All analyzed mammals and *Anolis carolinensis* each harbor one *ABCC12* ortholog. The analyzed mammals additionally harbor an *ABCC11* ortholog, except mouse and the guinea pig *Cavia porcellus*. Supplementary Ensembl database analyses furthermore revealed that the rat *Rattus norwegicus* and the kangaroo rat *Dipodomys ordii* also lack *ABCC11* orthologs, whereas the squirrel *Spermophilus tridecemlineatu* has an *ABCC11* ortholog. Genes in the *ABCC11* clade exhibit higher divergences compared to those in the *ABCC12* clade. The *ABCC6* clade comprises single orthologs from all analyzed chordates, with the exception of *Danio rerio*, which harbors 2 genes in this clade. Eutherian *ABCC6* orthologs form a substantially diverged distinct subclade. The *ABCC13* clade represents the smallest chordate *ABCC* clade. Among the analyzed chordates, *ABCC13* orthologs were only identified in the anole *Anolis carolinensis*, the fowl *Gallus gallus*, the platypus *Ornithorhynchus anatinus*, the dog *Canis familiaris,* and the cow *Bos taurus.* Supplementary Ensembl database analyses additionally identified *ABCC13* orthologs in the western gorilla *Gorilla gorilla*, the giant panda *Ailuropoda melanoleuca*, the pig *Sus scrofa*, the rabbit *Oryctolagus cuniculus*, and the wild turkey *Meleagris gallopavo.* In human, *HsABCC13* has been characterized as a truncated pseudogene and is therefore not included in the phylogeny (Annilo and Dean, 2004). Consequently, it can also not be excluded that the other identified *ABCC13* orthologs represent pseudogenes.

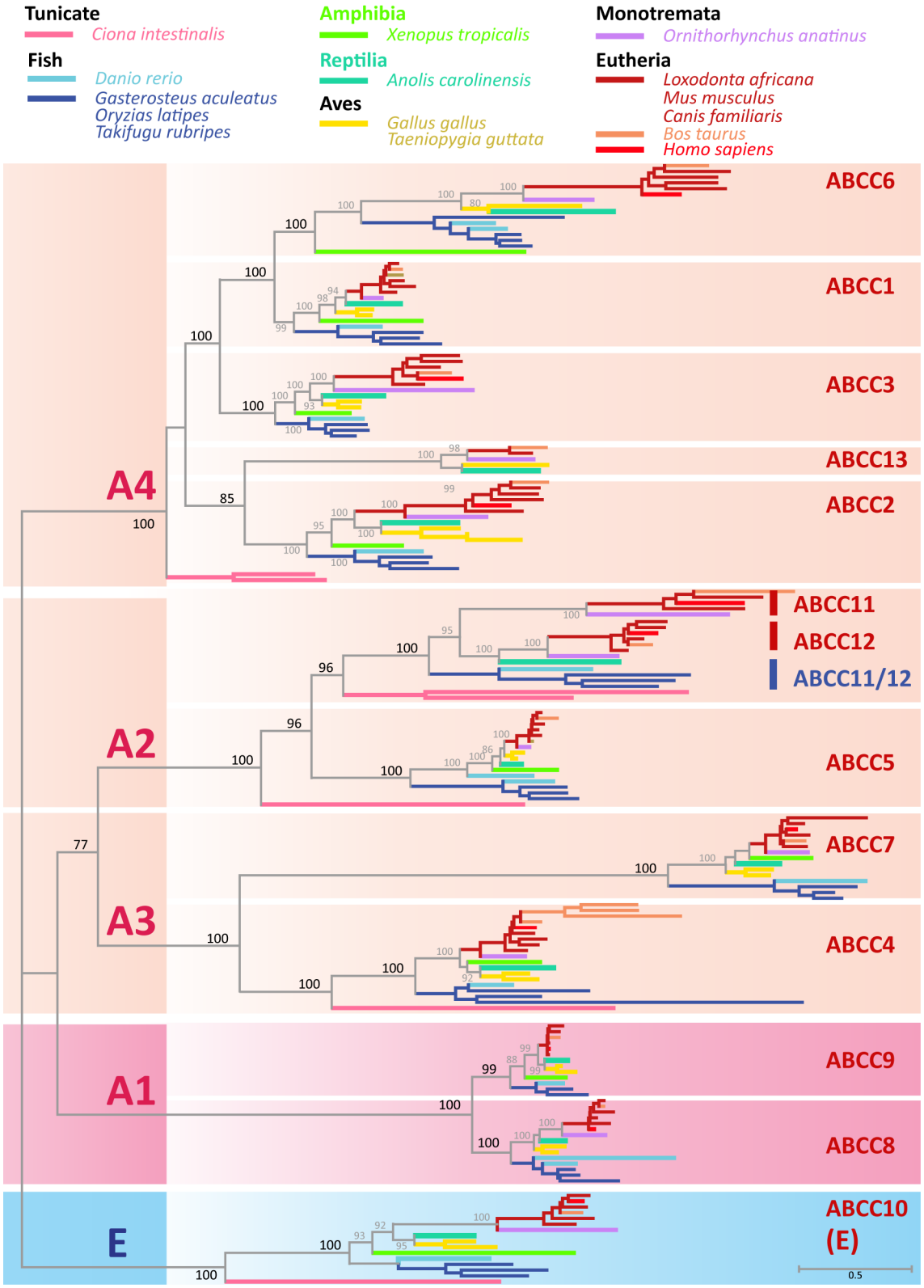

Figure 16. ML phylogeny of chordate *ABCC* genes. The major animal clades are indicated on the left and the chordate specific clades on the right. Main nodes are labeled with RAxML rapid non-parametric bootstrap values if higher than 70%.

3.3.8 Fungal *ABCC* genes

The inventories and phylogenies of *ABC* genes from various fungi have already been published (Kovalchuk and Driessen, 2010), therefore only the *ABCC* inventories of a few additional fungal species were examined (Table 2). As mentioned in Section 3.3.2, in none of the analyzed microsporidian species, *ABCC* genes were detected. The chytrid fungus *Allomyces macrogynus* has 54 predicted *ABCC* genes, representing the species with the highest number of *ABCC* genes in this study. However, the other analyzed chytrid fungi *Spizellomyces punctatus* and the amphibian pathogen *Batrachochytrium dendrobatidis* have only 12 and 18 *ABCCs*, respectively. The fungus *Aspergillus oryzae*, which represents a domesticated fungus used in Asia to ferment soybean and rice (Rokas, 2009) harbors almost twice as many *ABCCs* (23) compared to the phylogenetically related mold *Aspergillus nidulans* (12), but encodes for only 15% more genes (Kovalchuk and Driessen, 2010). Yeasts with small genomes such as *Schizosaccharomyces pombe*, *Candida albicans* and *Malassezia globosa* have 4-5 *ABCC* genes, which are the smallest numbers of *ABCCs* found within fungi (Kovalchuk and Driessen, 2010).

3.3.9 Protist *ABCC* genes

Among protist species, the apicomplexans show the greatest variance in *ABCC* gene numbers. *Plasmodium falciparum* has 2 *ABCCs* and the related piroplasms *Babesia bovis* and *Theileria annulata*, both tick-transmitted cattle blood parasites, have 4 and 17 *ABCCs*, respectively. *Neospora canium* and *Cryptosporidium parvum,* both belonging to the apicomplexan subclass of coccidia, have 3 and 14 *ABCCs*, respectively. Among the analyzed heterokonts, the brown algae *Ectocarpus siliculosus* and the diatoms *Fragilariopsis cylindrus* and *Thalassiosira pseudonana* harbor 7-10 *ABCC* genes, whereas the plant-pathogenic oomycetes *Phytophthora sojae* and *Pythium ultimum* harbor 25 and approximately 41 *ABCCs*, respectively. Among analyzed excavates, *Leishmania* species harbor 8-9, while related *Trypanosoma* species have 2-3 *ABCCs*. *Trichomonas vaginalis* does not harbor any detectable *ABCC* genes, as previously noted. All examined opisthokonta protists, i.e. holozoa and apusazoa, comprise 6-9

ABCCs. The free-living ciliate *Paramecium tetraurelia* harbors 42 *ABCC* paralogs – one of the highest numbers of *ABCC* genes per species identified in this study.

In the cross-kingdom phylogeny, protist *ABCC* genes form individual paralogous clades or clades with *ABCCs* from related species of the same phylum. The majorities of these clades root to the center of the phylogeny and do not show any relationship with other clades based on bootstrap values (Figure 11). Due to the large phylogenetic distances between the protist species, well-resolved and supported phylogenetic reconstructions of protist *ABCC* genes are difficult. Additionally, various predicted gene models of protist *ABCCs* have gaps, insertions, or regions with no homology to other *ABCCs*, which influence the quality of the alignments and the subsequent phylogenetic analyses (data not shown). Consequently, separate protist *ABCC* gene phylogenies have not been estimated in this study.

3.3.10 *ABCC-E* clade

The cross-kingdom *ABCC* phylogeny reveals the distinct major clade *ABCC-E* comprising single-copy orthologs from plants, animals, and specific protists (Figure 11).

Furthermore, in each of the previously shown kingdom-specific phylogenies of plant, invertebrate, and chordate *ABCCs*, a distinct clade (termed *E* clade) was identified that comprises single-copy orthologs only. All *ABCC* genes present in the *ABCC-E* clade of the cross-kingdom phylogeny were also present within the *E* clades of the corresponding individual kingdom-specific phylogenies. Since the *ABCC-E* clade of the cross-kingdom phylogeny and *E* clades of the separate phylogenies are all highly supported (100% bootstrap support, except in the invertebrate phylogeny, where it was 79%), it can be concluded that all the genes present in the E clades of the kingdom-specific phylogenies are part the major *ABCC-E* clade identified in the cross-kingdom phylogeny. All the identified *ABCC-E* genes strictly represent single-copy orthologs.

Among the analyzed red algae *Cyanidioschyzon merolae* and the marine green algae *Micromonas and Ostreococcus*, no *ABCC* genes clustering to the *ABCC-E* clade were

identified. However, all freshwater algae (*Coccomyxa sp.*, *Chlorealla variabilis, Chlamydomonas reinhardtii*) and all other analyzed plants harbor one *ABCC-E* ortholog. Among the analyzed animal species, the only species identified to lack *ABCC-E* orthologs are the nematodes *Caenorhabditis elegans, Brugia malayi, Wuchereria bancrofti* and *Loa loa.* However, an *ABCC-E* ortholog was identified in the nematode *Pristionchus pacificus*. For the wasp *Nasonia vitripennis* also no *ABCC-E* and no A1 clade ortholog was identified. Since all other hymenoptera harbor orthologs in both clades, it is likely that these orthologs are missing in the current annotation of the *Nasonia vitripennis* genome*. ABCC-E* orthologs were also identified in a few protist species. The two included choanoflagellates (*Monosiga brevicollis*, *Salpingoeca rosetta*), the filasterea *Capsaspora owczarzaki* and the apusazoa *Thecamonas trahens* all harbor an ortholog in the *ABCC-E* clade. Additionally, two heterokonts, the brown algae *Ectocarpus siliculosus* and the oomycete *Phytophthora sojae* each possess an *ABCC-E* ortholog, whereas the other analyzed heterokonts, the diatoms *Thalassiosira pseudonana* and *Fragilariopsis cylindrus* lack *ABCC-E* orthologs. Furthermore, *ABCC-E* orthologs were identified in the kinetoplastid *Trypanosoma brucei,* but not in the related kinetoplastid *Leishmania major*.

The protein sequences of identified *ABCC-E* orthologs from *Arabidopsis thaliana*, *Drosophila melanogaster, Homo sapiens,* and *Trypanosoma brucei* were used to search for additional *ABCC-E* orthologs in the ABCC database from species that were not included in the phylogenetic analyses (Table 2) using reciprocal BLAST. By this approach, *ABCC-E* orthologs were identified in all other animal and plant species, in *Pythium ultimum*, and in all analyzed *Phytophthora* species and *Trypanosoma* species. Furthermore, the Ensembl vertebrate database was BLASTed for *ABCC-E* orthologs in species that were not already analyzed. Single-copy *ABCC-E* orthologs were identified in all vertebrate genomes and deposited in the ABCC database.

The protein sequences from all identified *ABCC-E* orthologs were compared with other ABCC proteins by multiple sequence alignment (data not shown). In this alignment, several highly conserved, *ABCC-E* specific motifs were manually identified (Figure 17).

These motifs were not detectable in any other ABCC protein of the ABCC database, and not in any other non-ABCC protein of the NCBI protein database. The ABCC database, the NCBI and the Phytozome sequence repositories were queried for *ABCC-E* orthologs using BLAST with the consensus sequences of the identified *ABCC-E* specific motifs, PLNxFPWVxN and SSDREFxDDSLPF, as query sequence. Using this strategy, several additional putative *ABCC-E* orthologs were identified and confirmed by reciprocal BLAST analyses, e.g. in *Volvox carteri.* No protein or protein fragment sequences harboring one of these *ABCC-E* specific motifs were identified within species that were detected to be absent of *ABCC-E* orthologs by phylogenetic analyses in this study. Furthermore, using the same approach, also no additional *ABCC-E* paralogs were found in species that were identified to harboring an *ABCC-E* ortholog.

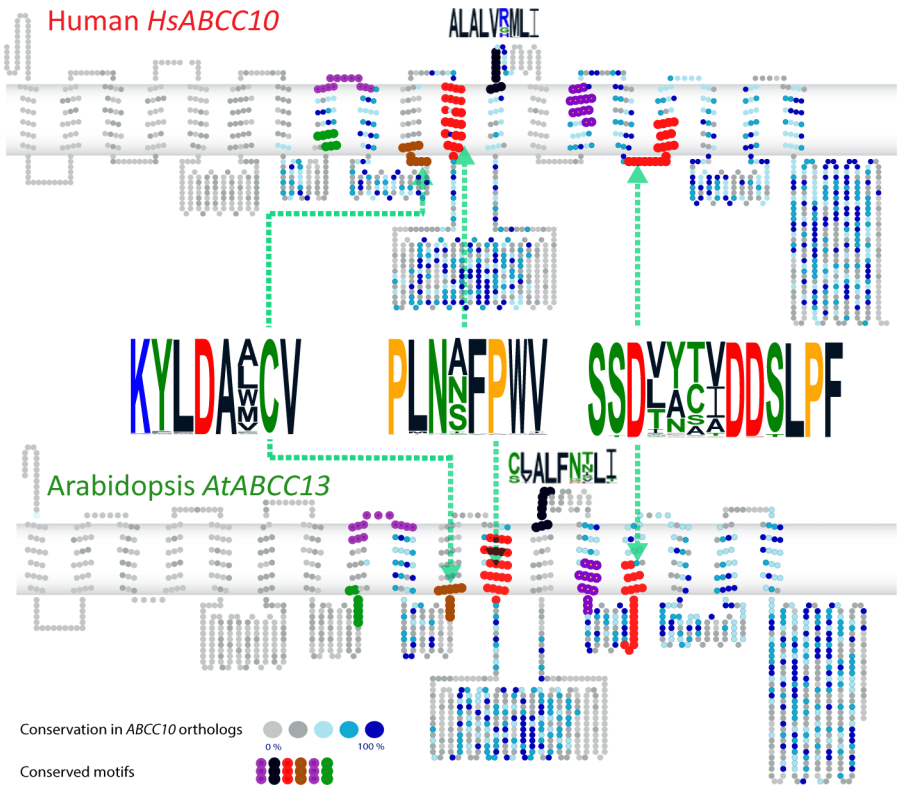

Figure 17. *ABCC-E* specific motifs. Conserved *ABCC-E* specific motifs are presented as sequence logo plots. Positions of these motifs are indicated by green dotted lines and larger symbols on the predicted transmembrane topologies of the human (HsABCC10) and *Arabidopsis* (AtABCC13) *ABCC-E* orthologs, respectively. Other residues are colored depending on their conservation within animal or plant *ABCC-E* orthologs. The HsABCC10 fragment identified to bind to the HLA-E protein (Wooden et al., 2005) and its corresponding homologous region in AtABCC13 are indicated by black symbols and by smaller logo plots obtained from the corresponding regions in various animals and plants *ABCC-E* orthologs.

3.3.11 *Homo sapiens* ABCC10 protein 3D homology-based model

A homology model of the human *ABCC-E* ortholog HsABCC10 was generated to visualize the structural position of conserved residues/regions in *ABCC-E* orthologs (Figure 19). The published 3D crystal structures of the mouse P-glycoprotein 1 (Aller et al., 2009) and the human ABCC1 nucleotide-binding domain 1 (Ramaen et al., 2006) were used as templates for homology modeling using Modeller 9v8 (Eswar et al., 2008). The TMD0 and the subunit linker region were not modeled, since no structural templates were available for these regions. Ramachandran plots of the final HsABCC10 homology model displayed more than 88% of residues in the core and 0.8% in the disallowed regions. PROCHECK G-factors of the models were -0.18, which is within acceptable values and comparable to that of the 3G5U template (-0.19) (Figure 18).

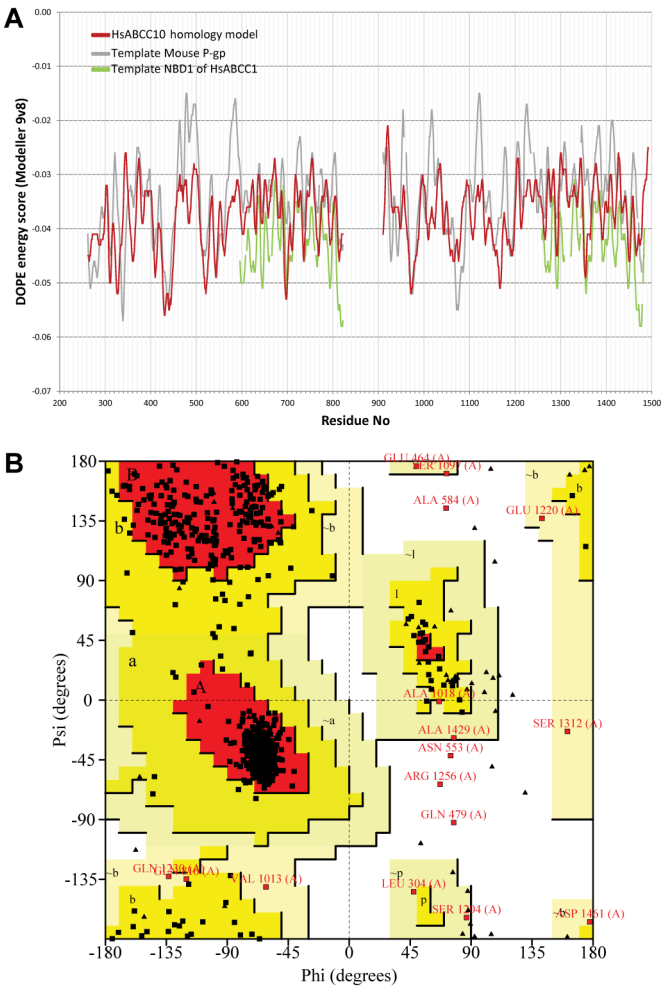

Figure 18. Verification of the HsABCC10 homology model. **(A)** Modeller's DOPE potential profile plot of the ABCC10 model (red line) and the templates mouse P-gp (grey) and HsABCC1 NBD1 (green). **(B)** Ramachandran plots of the HsABCC10 obtained with via the PROCHECK webserver.

Furthermore, the homology model has a better overall Modeller's DOPE potential profile compared to the P-glycoprotein 1 template. Additional analyses of the HsABCC10 model employed WHAT_CHECK (Hooft et al., 1996) and VADAR 1.8 (Willard et al., 2003) and did not reveal any major discrepancies to the P-gp structural model (data not shown).

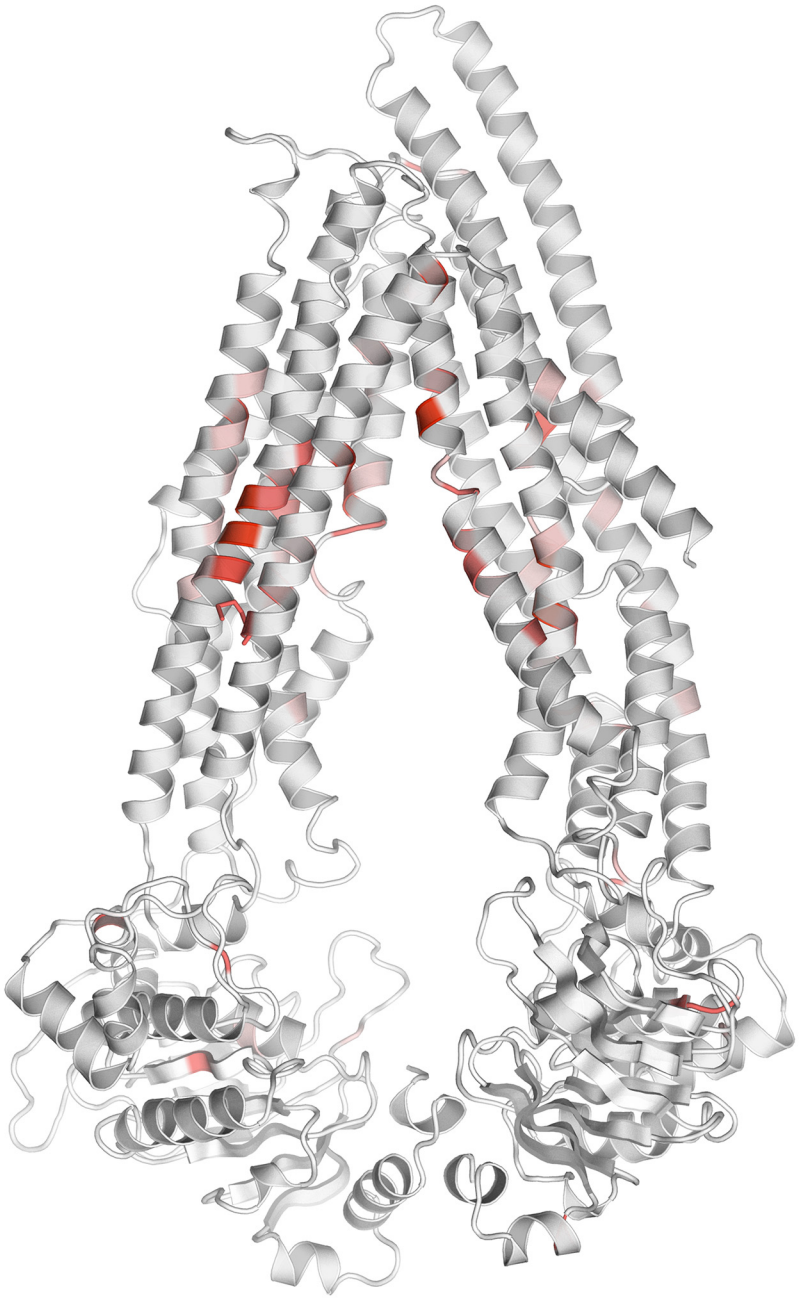

Figure 19. Human HsABCC10 homology model. The homology model is based on the structures of the mouse P-glycoprotein 1 (Aller et al., 2009) and the human ABCC1 nucleotide-binding domain 1 (Ramaen et al., 2006).

3.4 Discussion

3.4.1 Identification of *ABCC* gene inventories

In order to study the ABCC protein evolution, *ABCC* genes from 135 plant, animal, fungal and protist species, representing all major eukaryotic lines (with the exception of Rhizaria), were acquired. The identification was based on existing annotated genomes. Several species had many *ABCC* gene models that were incomplete or erroneous (data not shown). Considerable differences in annotation integrities that affect gene identification were reported for animal genomes (Creevey et al., 2011). Therefore, *ABCC* genes from selected species, e.g. from *Vitis vinifera*, were partially manually re-annotated, which resulted in more accurate gene models and in updated *ABCC* gene inventories. Furthermore, if possible, more than one species from a lineage was analyzed, in order not to draw wrong conclusions on the presence or absence of specific orthologs in specific lineages based on one single species. A distinction between pseudogenes and genes was not made in this study, since the focus was on the *ABCC* gene family evolution, rather than on genetic analyses. In total, 1727 putative *ABCC* genes were identified.

The distribution of predicted ABCC protein lengths displays two distinct peaks, which might correspond to the so-called ‘short’ and ‘long’ ABCC proteins. ‘Short’ ABCCs are N-terminally truncated ABCC proteins, which lack the first transmembrane domain (TMD0). They have been described in human (Slot et al., 2011), in yeast (Michealis and Berkower, 1995), and in the slime mold *Dictyostelium discoideum*, of which most ABCCs were predicted to be of the ‘short’ type (Anjard and Loomis, 2002).

Comparison of the species-specific *ABCC* inventories reveals large differences in *ABCC* gene numbers ranging from 2-52 paralogs per species. All red and marine algae have only 2 *ABCCs*. In land plants, the number of *ABCC* genes varies considerably, ranging from 11-15 in rice and *Arabidopsis thaliana*, and 39 in soybean. Endoparasitic animals, i.e. endoparasitic nematodes and endoparasitic protists, have the lowest number of *ABCC* genes. Basal marine metazoa such as sponge, sea anemone, and sea urchin are

among the animals with the highest number of *ABCC* genes. The only species identified to completely lack any *ABCC* genes and any partial *ABCC*-specific sequences were *Trichomonas vaginalis* and all the analyzed microsporidia. Interestingly, the extracellular parasite *Trichomonas vaginalis* has one of the highes, and the microsporidian species, which are intracellular parasites, have the smallest numbers of genes among the species analyzed in this project. However, all these species are characterized by a reduction in average protein lengths (Katinka et al., 2001; Carlton et al., 2007; Morrison et al., 2007; Corradi and Slamovits, 2010). Additionally, no full or partial sequences showing any orthologous relationship to full-size *ABC* genes were found, indicating a complete loss of full-size ABC genes in those species.

A phylogeny of *ABCC* genes from all major kingdoms reveals discrete plant, animal, and fungal-specific major clades. Furthermore, one distinct clade, termed *ABCC-E* clade, comprising single-copy *ABCC* genes from plant, animals, and few protists is apparent. All these clades root to the center of phylogeny and do not show any relationship to each other. Protist *ABCC* genes form only a few distinct small species- or lineage-specific clusters and do not show any phylogenetic relationship to the plant, fungi, and animal major *ABCC* clades. Separate preliminary phylogenetic analyses of protist *ABCCs* did not reveal any well-resolved and supported trees. Protist *ABCC* genes were therefore not separately investigated in this project. The fungal *ABCCs* were also not investigated further, as inventories and a phylogenetic analysis have already been published (Kovalchuk and Driessen, 2010). Plant, invertebrate and vertebrate *ABCCs* were further investigated by individual phylogenetic analyses.

3.4.2 The conserved *ABCC-E* clade

The *ABCC-E* clade represents a unique distinct clade of single-copy *ABCC* genes from different kingdoms, i.e. from plants, animals and a few protist species. The presence of strictly single-copy orthologs reflects a strong evolutionary selection against duplication or duplicate retention of these orthologs. *ABCC-E* orthologs are found in all analyzed freshwater algae and embryophytes. Moreover, all analyzed animals comprise an *ABCC-E* ortholog, except most analyzed nematodes, e.g. *Caenorhabditis*

elegans and the human parasitic nematodes. However, the nematode *Pristionchus pacificus* harbors an *ABCC-E* ortholog. None of analyzed fungi, including the basal chytrids and zygomycete, harbor an ABC*C-E* gene. From other kingdoms, only a few species have *ABCC-E* orthologs. All analyzed ophistokont species, i.e. holozoa and apusozoa, the brown algae *Ectocarpus siliculosus* and all analyzed oomycetes, which are both heterokonts, and all analyzed *Trypanosoma* species harbor an *ABCC-E* ortholog. However, closely related species, such as diatoms and *Leishmania* species do not have an *ABCC-E* ortholog. The selection against duplication of *ABCC-E* clade genes is illustrated by the deletion of an *ABCC* gene corresponding to the duplicate of the *ABCC-E* ortholog after a partial chromosomal duplication in *Trypanosoma brucei* (Jackson, 2007). The presence of *ABCC-E* orthologs in plants, animals, in specific heterokonts, in apusozoa and in *Trypanosoma*, suggests that *ABCC-E* orthologs have evolved very early in eukaryotic evolution, possibly at the beginning of eukaryotic life (Cavalier-Smith, 2010; Derelle and Lang, 2011). The *Arabidopsis ABCC-E* ortholog, *AtABCC13*, is further characterized and discussed in Chapter III.

3.4.3 The plant *ABCC* gene family

The plant *ABCC* gene family can be divided into the *ABCC-E* clade and eight plant-specific clades, which were termed *P1* to *P8* in this study. All analyzed monocot and eudicot plants have *ABCC* orthologs in each of these clades, with the exception of the *P7* clade that does not have members from a few specific species, including from *Arabidopsis thaliana*. The clades considerably differ in their number of paralogs per species and in the divergences of their paralogs. The *P1* clade has evolved in early viridiplantae evolution, as it contains *ABCCs* from green algae. The *P2*, *P3*, *P4* and *P5* clades evolved in embryophytes, indicated by the presence of orthologs from the moss *Physcomitrella patens* and the lycophyte *Selaginella moellendorffii*. The *P6*, *P7* and *P8* clades appear to have evolved during angiosperm evolution.

The *P1* clade has two eudicot-specific subclades (*P1A* and *P1B*). The *P1A* subclade appears to be related with the monocot and lower plant *ABCC* subclades within the *P1 clade* and its genes show smaller divergences compared to the P1B clade. The *P1A*

subclade comprises the *Arabidopsis thaliana AtABCC1/2* genes, which have been shown to encode for vacuolar phytochelatin transporters that mediate the resistance to heavy metals such arsenic and mercury (Song et al., 2010; Park et al., 2011). Additionally, AtABCC1 has been shown to transport folates and antifolates (Raichaudhuri et al., 2009) and AtABCC2 was demonstrated to transport chlorophyll catabolites and glutathione S-conjugates (Lu et al., 1998; Frelet-Barrand et al., 2008) into vacuoles. All of these compounds are found in species across the plant kingdom, from angiosperms to freshwater green algae (Aaronson et al., 1977; Gekeler et al., 1988). Therefore, the *P1* clade (in eudicots the *P1A* clade) might represent an evolutionarily conserved *ABCC* clade involved in cellular detoxification and vacuolar import of organic anions. The *P1B* subclade appears to have developed from the *P1A* subclade and its genes exhibit larger divergences compared to *P1A* clade genes. The *Arabidopsis P1B* subclade ortholog *AtABCC11* was described to have a very short transcript and possibly not to function as an ABC transporter (Yoshihisa et al., 2009). Interestingly, *Eucalyptus grandis* comprises 11 *ABCC* genes in the *P1B* clade, whereas all other analyzed plants contain one to three *ABCC* genes in this clade.

The *P5* clade represents another clade with orthologs of which the molecular function was identified. The *Arabidopsis thaliana* AtABCC5 was characterized as a vacuolar high-affinity inositol hexaphosphate transporter that is involved in phytate and phosphate storage, and in guard cell signaling (Nagy et al., 2009). *P5* orthologs from maize, soybean, and rice exhibited comparable functions and mutant phenotypes (Shi et al., 2007; Kim et al., 2008; Zhao et al., 2008). The *P5* clade typically comprises 1-2 paralogs per species and represents the plant *ABCC* clade with the lowest divergence between genes. The *P5* clade orthologs therefore appear to have conserved functions in angiosperms. Other clades are characterized by the presence of species-specific expansions. The *P8* clade harbors expanded clades of paralogs from almost all plant species. These paralogs form clusters distinct to *ABCCs* of related plant species, indicating relatively recent duplication events. Although at a smaller extend, the same was observed for the *P3* clade, which diverged into two subclades in eudicots. While one of these subclades (*P3A*) harbors orthologs from all analyzed eudicots, the other

subclade (*P3B*) lacks *ABCCs* from specific species, i.e. from fabaceae and brassicaceae. The genes from the expanded *P3B* and *P8* clades in *Vitis vinifera* are organized into tandem duplication clusters on the genome, which may reflect species-specific *ABCC* subfamily expansions driven by evolutionary pressures.

3.4.4 The animal *ABCC* gene family

The animal *ABCC* genes can be grouped into the *ABCC-E* clade and four distinct animal-specific clades, which all root the center of the cross-kingdom phylogeny. All these clades harbor orthologs from apusozoa and/or from holozoa, e.g. choanoflagellates. This suggests that the animal *ABCC* clades evolved before the evolution of animals.

Within the animal major clade *A1* harboring the human *HsABCC8/9* (*SUR1/2*), orthologs were identified in all analyzed vertebrates and in most arthropods. In vertebrates, this major clade is divided into two clades, *ABCC8* and *ABCC9*, each comprising single orthologs from all vertebrates, except from zebrafish, which appears to have two *ABCC8* clade paralogs. This evolutionarily stable clade appears to have evolved in the opisthokont lineage before the evolution of animals, but was subsequently lost again in many lineages, e.g. in the tunicate *Ciona intestinalis*. In human, HsABCC8/9 function as potassium channel regulators, whereby ABCC9 was shown to be active in the heart (Bryan et al., 2006). Similarly, one of the two *Drosophila melanogaster ABCC8/9* orthologs in this clade has also been shown to function in the heart of *Drosophila* (Akasaka et al., 2006), indicating an early functional conservation of this distinct clade of animal *ABCC* genes.

The animal major clade *A2*, harboring the human *HsABCC5*, *HsABCC11*, and *HsABCC12,* represents a relatively small clade. The human genes of this clade were all described as being 'short' *ABCCs*, lacking the TMD0 coding region (Slot et al., 2011). In invertebrates, this *ABCC* clade lacks *ABCC* genes from diptera and ticks, while other invertebrates are represented by one to four paralogs. The *ABCC5* clade has an ortholog from *Ciona intestinalis* and appears to have first evolved during chordate evolution, followed by the evolution of the *ABCC11/12* clade. The *ABCC11* clade appears to be the result of a gene duplication event from the *ABCC12* clade during

mammalian evolution. The analyses of this study indicate that *ABCC11* orthologs have been lost in the mouse-related and Ctenohystrica clades, whereas they were retained in the squirrel-related rodent clade (Churakov et al., 2010).

The animal major clade *A3* comprising the human *HsABCC4* and *HsABCC7* (*CFTR*) represents the largest animal clade. Within this animal major clade, insects exhibit partially massive expansions of *ABCC* genes. The *ABCC* genes of the moth *Heliothis virescens* shown to be involved in resistance to Bt toxin (Gahan et al., 2010) are also members of the *A3* clade. The majority of the *Drosophila melanogaster ABCCs* are found in this clade and one of these paralogs has been described being involved in response to oxygen deprivation (Huang and Haddad, 2007). In vertebrates, the animal major *A3* clade is divided into the *ABCC4* and *ABCC7* clades. The *ABCC7* clade evolved before the chordate evolution, but was then subsequently lost in all non-vertebrates. The *ABCC4* clade is the only vertebrate *ABCC* clade exhibiting species-specific expansions in more than one species. The *ABCC4* clade has expanded in fishes and in the cow, which contains five *ABCC4* paralogs. This finding may be useful for the elucidation of the endogenous function of the human HsABCC4.

The animal major clade *A4* comprises the largest number of vertebrate *ABCC* genes, and harbors the human *HsABCC1/2/3/6/13* genes and two *Ciona intestinalis ABCCs*. It also contains a distinct subclade of conserved insect *ABCCs*, including the *Drosophila melanogaster DmABCC1*, which has been shown to have a much higher transport rate compared to human ABCC transporters (Szeri et al., 2009). Furthermore, the *A4* major clade contains the largest fraction of nematode *ABCC* genes. The *Caenorhabditis elegans CelABCC9*, which represents one of the most divergent *ABCC* genes in this study, is found within this nematode clade. *CelABCC9* was named *cft-1* and was considered a putative human *ABCC7* homolog (Sheps et al., 2004). However, the analyses performed in this study revealed that *CelABCC9* does not represent an *ABCC7* ortholog. Moreover, *CelABCC1*, also named *mrp-1*, is present within the *A4* clade. *CelABCC1* has been shown to be required for efficient RNA interference in *Caenorhabditis elegans* (Sundaram et al., 2006). The vertebrate clades *ABCC1* and

ABCC6 appear to be the result of a gene duplication event preceding the evolution of fishes. *ABCC6* orthologs exhibit the largest divergences among the vertebrate clades. Zebrafish has two *ABCC6* paralogs, whereas all other vertebrates only harbor one *ABCC* copy. However, one of the zebrafish *ABCC6* paralogs may represent a pseudogene, since the presence of *HsABCC6* pseudogenes was reported in human (Pulkkinen et al., 2001). Gene conversion events between functional and pseudogenic *ABCC6* variants might be the mechanism causing the divergence of functional *ABCC6* orthologs (Symmons et al., 2008). The *ABCC2* and *ABCC13* clades appear to be the result of gene duplication event before the evolutions of fishes. While *ABCC2* orthologs are present in all vertebrates, *ABCC13* genes appear to have been subsequently lost or degenerated to pseudogenes in the majority of mammalian lineages.

3.4.5 Evolution of species-specific *ABCC* gene families

The comparison of *ABCC* gene numbers and total numbers of genes (proteome sizes) revealed significant positive correlations. Associations between proteome sizes and gene-family sizes have already been shown for other gene families (Lespinet et al., 2002; Arakaki et al., 2006; Andreini et al., 2011). Chromosomal and whole genome duplications (WGDs) result in an initial increase of gene numbers and therefore in expansions of gene families, which is subsequently followed by gene losses (Maere et al., 2005). Species that underwent relatively recent WGDs, such as the ciliate *Paramecium tetraurelia* (Aury et al., 2006) and the soybean *Glycine max* (Schmutz et al., 2010), have high numbers of predicted genes and large *ABCC* gene families. Analysis of the chromosomal locations of soybean *ABCC* genes revealed that paralogs from almost all *ABCC* clades are dispersed, apart from small tandem clusters, on at least two distinct chromosomes, indicating chromosomal duplications. The large *ABCC* gene family in soybean therefore appears to be in part the consequence of recent chromosomal duplications. Nonetheless, not all *ABCC* gene duplicates that resulted from WGDs are retained. For instance, the orthologs of the *ABCC-E* clade identified in this study only occur as single-copy orthologs, even in species that underwent recent WGDs, such as soybean. Furthermore, the gene numbers of most vertebrate *ABCC*

clades are conserved in tetrapoda, and also in ray-finned fishes (Actinopterygii), which experienced a recent additional WGD in their early evolution (Christoffels et al., 2004). Gene duplication by WGD might represent a mechanism of expansion and diversification for some specific *ABCC* clades, while there is a selection against duplication or duplicate retention in other *ABCC* clades. Nonetheless, part of the variability in *ABCC* gene family sizes might be explained by the numbers of genes per species and the evolutionary history with WGDs.

However, the analyses of this chapter also identified several species that harbor considerably more or fewer *ABCC* genes compared to other species with similar number of genes. In these cases, the increased *ABCC* gene numbers typically are the result of expansions of one or two *ABCC* clades rather than expansions of all *ABCC* clades. Genes of these expanded clades are predominantly found in tandem clusters. Numerous example of species-specific expansions or reductions of individual gene families were reported (Colangelo and Guerinot, 2006; Robertson and Wanner, 2006; Gingerich et al., 2007; Danilevskaya et al., 2008; Rispe et al., 2008; Spanu and Kämper, 2010). Such confined expansions might reflect the evolution of lineage-specific physiological and/or morphological traits, and evolutionary adaptations, e.g. to abiotic stresses, new lifestyles, symbionts, and pathogen stresses.

ABCC proteins were shown to be involved in detoxification of xenobiotics, such as heavy metals, herbicides and drugs (Gottesman, 2002; Frelet-Barrand et al., 2008; Luckenbach and Epel, 2008; Song et al., 2010). Additionally, *ABCC* genes have been shown to be factors of insect resistance to bacterial toxins (Gahan et al., 2010). Aquatic organisms are constantly exposed to various substances including toxins that are dissolved in the water. Basal aquatic animals, such as the sponge *Amphimedon queenslandica*, sea anemone *Nematostella vectensis* and sea urchin *Strongylocentrotus purpuratus* all harbor large *ABCC* gene families. The sea urchin has furthermore been shown to comprise expansions of other gene families involved in detoxification, e.g. cytochromes and conjugating enzymes (Goldstone et al., 2006). Notably, the free-living aquatic protist *Paramecium tetraurelia* has 42 *ABCCs*, which is one of the largest *ABCC*

gene families identified in this study. Hence, *ABCC* gene family expansions in these aquatic species might reflect evolutionary adaptation to the aquatic habitat. Interestingly, the water flea *Daphnia pulex* harbors only few *ABCC* genes, which may be one explanation for its sensitivity to aquatic toxins (Colbourne et al., 2011). The red flour beetle *Tribolium castaneum* was found to harbor 33 *ABCCs*, more than any other animal analyzed in this study. This high number is the result of a confined massive expansion in one single *ABCC* clade, of which the genes are all found in large tandem clusters in the genome. Large expansions were also reported for other detoxification enzyme families in *Tribolium castaneum* (Richards et al., 2008), whereas other *ABC* subfamilies, e.g. *ABCB* and *ABCG*, have comparable sizes to those of other insects (Liu et al., 2011). *Tribolium* beetles are found in various dry food stocks and other dry habitats, and they exhibit resistance to a wide range of insecticides. Consequently, the expansion of *ABCC* genes in this beetle might be the consequence of adaptations to its chemical environments, i.e. to the diverse food sources and to selective pressures from insecticide treatments. The parasitic wasp *Nasonia vitripennis* was identified in this project to possess more than twice as many *ABCCs* compared to other hymenoptera, e.g. honeybee and ants, and has been previously been shown to comprise twice as many P450 and glutathione S-transferase genes (Oakeshott et al., 2010). The parasitic lifestyle of the wasp, which is an endoparasite of flies at its larval stage and thus exposed to numerous compounds from the host, may explain the expansion of genes encoding for detoxification enzymes, including ABCCs. Additionally, the plant pathogens *Phytophthora sojae* and *Pythium ultimum*, both oomycete protists of the heterokont kingdom, harbor highly expanded *P450* gene families (Tyler et al., 2006; Lévesque et al., 2010) and three times more *ABCC* genes compared to other analyzed non-pathogenic heterokonts, such as the brown algae *Ectocarpus siliculosus*. Accordingly, the expansions in *ABCC* and other detoxification gene families possibly reflect adaptations to toxins, i.e. to components of the plant pathogen defense. Interestingly, the human body louse *Pediculus humanus* has the smallest number of detoxification related genes identified in insects so far (Kirkness et al., 2010) and is the arthropod with the lowest number of *ABCC* genes identified in this study, further

indicating an association of the *ABCC* gene family size with the sizes of other gene families involved in cellular detoxification.

In conclusion, the *ABCC* gene family size of a species in part correlates with the total number of genes. However, specific lineages or species comprise confined, partially substantial expansions within specific clades of the *ABCC* gene family. In these species, the *ABCC* gene family size is often associated with the number of other detoxification and defense-related genes. Such expansions thus possibly reflect adaptations to toxic compounds in the abiotic and biotic environment. These results are consistent with reports on the evolution of the xenobiotic cytochrome *P450* gene subfamily, for which similar evolutionary scenarios were described (Thomas, 2007).

3.5 Supplementary Information

3.5.1 Genomic locations of *Eucalyptus grandis ABCC* genes

Supplementary Table 1. Genomic locations of *Eucalyptus grandis ABCC* genes. Tandem clusters are shaded in alternating blue and grey colors.

Gene Name	Location	Start	End	Orientation
EgABCC32	scaffold_1	37333996	37340892	+
EgABCC14	scaffold_1	37366432	37375551	+
EgABCC4	scaffold_4	3330768	3346430	-
EgABCC11	scaffold_4	3385514	3399924	-
EgABCC29	scaffold_4	3419204	3434596	-
EgABCC5	scaffold_4	3470565	3493421	-
EgABCC9	scaffold_4	3504834	3526220	-
EgABCC2	scaffold_4	3540244	3556318	-
EgABCC7	scaffold_4	3624970	3636288	-
EgABCC8	scaffold_4	3704748	3717403	-
EgABCC3	scaffold_4	3752988	3769949	-
EgABCC25	scaffold_5	8626360	8632757	-
EgABCC37	scaffold_5	8662631	8667744	-
EgABCC20	scaffold_5	8698361	8703635	-
EgABCC28	scaffold_5	8728788	8734469	-
EgABCC22	scaffold_5	22456497	22463339	+
EgABCC26	scaffold_5	22466368	22473746	+
EgABCC27	scaffold_5	22479193	22486320	+
EgABCC1	scaffold_5	37919178	37942808	+
EgABCC17	scaffold_6	27747540	27753250	+
EgABCC16	scaffold_6	27812661	27824632	+
EgABCC15	scaffold_6	27928667	27940555	+
EgABCC24	scaffold_6	27998768	28004181	+
EgABCC19	scaffold_6	28041413	28048006	+
EgABCC10	scaffold_6	47895128	47912720	-
EgABCC21	scaffold_8	67005642	67011395	+
EgABCC23	scaffold_8	67018015	67023241	+
EgABCC18	scaffold_8	67062031	67067251	+
EgABCC30	scaffold_10	35853204	35859507	+
EgABCC33	scaffold_10	35879819	35886374	+
EgABCC38	scaffold_10	35890997	35896794	+
EgABCC13	scaffold_11	17299544	17309727	+
EgABCC12	scaffold_11	43792228	43799949	+
EgABCC35	scaffold_119	28994	33789	+
EgABCC36	scaffold_288	371	5396	-
EgABCC6	scaffold_288	27305	39866	-

3.5.2 Genomic locations of *Tribolium castaneum ABCC* genes

Supplementary Table 2. Genomic locations of *Tribolium castaneum ABCC* genes. Tandem clusters are shaded in alternating grey or blue colors. Individual chromosomes are alternatingly shaded in red and orange. Genes from the large expanded group within the *A3* major clade are highlighted in red font; other genes located in the *A3* major clade are in green.

Gene name	Location	Start	End	Orientation
TcABCC10	ChLG4	4956628	4964203	+
TcABCC26	ChLG5	5966333	5974377	-
TcABCC23	ChLG5	5978733	5988109	-
TcABCC24	ChLG5	5989891	5994073	-
TcABCC25	ChLG5	5995762	5999966	-
TcABCC19	ChLG5	6969497	6973765	+
TcABCC20	ChLG5	6975148	6979220	+
TcABCC21	ChLG5	6981397	6985546	+
TcABCC22	ChLG5	6989375	6993654	+
TcABCC3	ChLG5	8860574	8868920	-
TcABCC14	ChLG5	12075643	12079703	+
TcABCC13	ChLG5	12080534	12084545	+
TcABCC12	ChLG5	12085590	12089465	+
TcABCC11	ChLG5	12090049	12093099	+
TcABCC16	ChLG5	12094316	12098450	+
TcABCC17	ChLG5	12099129	12103236	+
TcABCC18	ChLG5	12103832	12107957	+
TcABCC15	ChLG5	12109821	12113956	+
TcABCC8	ChLG5	12560442	12565573	+
TcABCC2	ChLG5	15369140	15373635	+
TcABCC7	ChLG5	18589675	18598774	+
TcABCC9	ChLG5	18599335	18612030	+
TcABCC30	ChLG6	188365	195414	-
TcABCC31	ChLG6	11705126	11709007	-
TcABCC28	ChLG7	5696027	5704808	-
TcABCC4	ChLG7	13198329	13202867	+
TcABCC5	ChLG7	13205046	13210225	+
TcABCC29	ChLG8	12123192	12127192	+
TcABCC1	ChLG9	837310	846332	+
TcABCC32	ChLG9	5070045	5073909	-
TcABCC6	ChLG9	18102317	18105386	-
TcABCC27	Unknown	4003767	4007742	-
TcABCC33	Unknown	15183051	15186977	+

4. Chapter II

Genetic and functional characterization of AtABCC13 in Arabidopsis thaliana

4.1 Introduction

As detailed in Chapter I, the *Arabidopsis ABCC* gene *AtABCC13* was identified to belong to the distinct early-evolved conserved *ABCC-E* clade. Orthologs of the *ABCC-E* clade are found as strictly single-copy (singleton) genes in all analyzed plant and in almost all animal species, except in some nematode species, e.g. *Caenorhabditis elegans* and *Brugia malayi*. Moreover, *ABCC-E* clade orthologs are found in specific protozoa, such as oomycota, brown algae, trypanosoma and choanozoa.

The human *HsABCC10* (*ABCC10*, *MRP7*) and mouse *MmABCC10* (*ABCC10*) are the only *ABCC-E* clade orthologs that were so far characterized. However, *HsABCC10* has not been reported to be associated with any human diseases, and untreated *MmABCC10* knockout mice did not show any differences in their appearance, behavior, and fertility compared wild-type mice (Hopper-Borge et al., 2011). While the physiological functions of HsABCC10/MmABCC10 are still unrevealed, *HsABCC10* was found to be overexpressed in specific tumors (Kavak et al., 2010). Moreover, overexpression of *HsABCC10* was associated with vinca alkaloids resistance of carcinoma cell lines (Naramoto et al., 2007; Oguri et al., 2008; Bessho et al., 2009). Ectopic expression of *HsABCC10* in HEK293 cells conferred resistance of the cells to vinca alkaloids, nucleoside analogues, and taxanes. Overexpression of *HsABCC10* in P-glycoprotein deficient fibroblasts conferred a 116-fold increased resistance to the taxane paclitaxel (Hopper-Borge et al., 2004; Hopper-Borge et al., 2009). In addition, *MmABCC10* knockout mice were more sensitive to paclitaxel. Isolated fibroblasts from these knockout mice hyper-accumulated and were hypersensitive to paclitaxel, to the *Vinca* alkaloid vincristine, and to the nucleoside analogue cytarabine (Ara-C) (Hopper-Borge et al., 2011). In conclusion, these data indicate that *HsABCC10* and *MmABCC10* are multi-drug resistance factors for vinca alkaloids, nucleoside analogues, and taxanes. *HsABCC10* was the only *ABCC* gene that was shown to confer resistance to taxanes (Hopper-Borge et al., 2004).

HsABCC10 overexpression furthermore appeared to correlate with pathological stages of non-small cell lung tumors in untreated patients (Wang et al., 2009). Additionally,

HsABCC10 expression was shown to be p53-regulated during DNA damage-induced apoptosis (Takayanagi et al., 2004). This indicates that *HsABCC10* overexpression is not only induced by treatment with anti-cancer drugs. In addition to the results from *HsABCC10* in the context of cancer, Wooden et al. (2005) demonstrated that a peptide derived from HsABCC10 is able to bind to the MHC antigen HLA-E, which consequently inhibits natural killer cell-mediated lysis under certain conditions. These findings suggest a role of HsABCC10 beyond multi-drug resistance.

The *Arabidopsis AtABCC13* gene has been reported to be phylogenetically distinct to other *Arabidopsis ABCC* genes in previous studies. Furthermore, *AtABCC13* was described to be the only *Arabidopsis* ABCC-type gene that is truncated in the 5' region and thus to lack a corresponding putative transmembrane domain 0 (Kolukisaoglu et al., 2002; Verrier et al., 2008; Wanke and Kolukisaoglu, 2010). AtABCC13 has not been related with any physiological or molecular function, nor have orthologs of *AtABCC13* in other plant species been associated with a function. However, the fact that *AtABCC13* belongs to a conserved early-evolved group of *ABCC* genes suggests that *AtABCC13* has essential and evolutionarily conserved functions. Moreover, *AtABCC13* is phylogenetically distinct to the other *Arabidopsis ABCCs*. Thus, it was postulated that functional redundancies conferred by other *Arabidopsis ABCCs* would be less pronounced and that consequently a knockout of *AtABCC13* might reveal distinguishable phenotypes under appropriate conditions.

The aim of this thesis chapter was to characterize *AtABCC13* on a genetic and functional level. Sequences of *AtABCC13* cDNA clones were analyzed. Moreover, tissue-level expression patterns as well as the intracellular localization were investigated. The transport activities of AtABCC13 for two common ABCC transporter substrates were assessed by heterologous expression in yeast. These molecular analyses were accompanied by a phenotypic characterization of *Arabidopsis AtABCC13* knockout plants under normal conditions and in a screen for differential responses to various treatments, including cytotoxic compounds, to which the human HsABCC10 and other human ABCC transporters confer resistance in animal cells.

4.2 Materials and Methods

4.2.1 Gene accession numbers and sequence database searches

Sequences and gene structures of *Arabidopsis ABCC* transporters (except of *AtABCC13.1* and *AtABCC13.2*) were obtained from The Arabidopsis Information Resource (TAIR) (Version TAIR10; http://www.arabidopsis.org; Swarbreck et al., 2007). The sequence of *OsABCC12* (LOC_Os06g08560.1) was obtained from the Rice Genome Annotation Project (RGAP 6.1; http://rice.plantbiology.msu.edu). Human *HsABCC1* (ENSP00000382342) and *HsABCC10* (ENSP00000361608) sequences were obtained from Ensembl (http://www.ensembl.org; Flicek et al., 2010). The sequence of the *Catharanthus roseus CroABCC10* (CAO94660.1) was obtained from the NCBI GenBank (Benson et al., 2010). The *Physcomitrella patens PpABCC1* (Pp1s121_149V6.1) sequence was obtained from Phytozome 7.0 (http://www.phytozome.net).

4.2.2 Computational methods

Sequence alignment and visualization

Protein sequences were aligned using CLUSTALW Version 2.0 (Larkin et al., 2007) within the program Jalview 2 (Waterhouse et al., 2009). Alignments were visualized using Jalview 2.

Predicting the genomic intron/exon structure based on the cDNA sequence

The intron/exon structures corresponding to the cDNA sequences were determined by alignment of cDNA sequences to the genomic sequence of the *At2g07680* locus using the program Spidey on the NCBI website (http://www.ncbi.nlm.nih.gov/spidey).

Homology models of human HsABCC1 and HsABCC10

The human HsABCC1 homology model was obtained from DeGorter et al. (2008) and the human HsABCC10 model was generated as part of the project described in Chapter I. Homology models were visualized with PyMol (The PyMOL Molecular Graphics System, Version 1.3, Schrödinger, LLC.).

To map AtABCC13.1 specific residues lacking in AtABCC13.2 on these homology models, multiple sequence alignments of AtABCC13.1, AtAtABCC13.2, HsABCC1, and HsABCC10 were generated. The corresponding residues aligning to the gap in AtABCC13.2 were then highlighted within PyMol in the HsABCC1 and HsABCC10 homology models.

4.2.3 Chemicals

Unless otherwise stated, chemicals were purchased from Sigma-Aldrich in analytical grade quality. *E. coli* and yeast media components were obtained from BD, Becton Dickinson AG, Switzerland. Water used for solutions was purified using a Millipore Milli-Q™ (Millipore AG, Zug, Switzerland) water purification system.

4.2.4 Primers

Table 5. Primers used for PCR and sequencing reactions. Primer melting temperatures (Tm) were calculated using VectorNTI 5 (Invitrogen).

Primer name	Sequence	Tm [°C]
AtMRP13A-s	ATATCTGGAAGTGTAAGCCCAAAGGC	59.0
AtMRP13A-as	CCAATCAGCAAACCAGTTATCCCA	58.8
AtMRP13B-s	AGCTCAAAAGAGCCATTCCTGAGG	59.0
AtMRP13B-as	GCGGATAGTCTCTTCCCGATAACTT	57.3
AtMRP13C-s	CATGGATCTATACTATTAAATGGCTCTG	53.4
AtMRP13C-as	TCTTGATGATGTACTGAGTGCAGTG	53.6
AtMRP13D-s	GCGATATCTTGTGCAGATATGATTGTTGTG	61.7
AtMRP13D-as	TCATTAACTCAATATTAACCTTGGTGAGGG	59.1
AtMRP13E-s	CGGAGACGCACCTTTTGAGTATAC	56.0
AtMRP13E-as	TGAAGACTTAGCTGTATGTGTGGA	51.1
AtMRP13F-s	ATGGTGCAGTTGTTAGGATCAATG	54.7
AtMRP13F-as	CTGGGAGATCCTAGACAAGTGTAA	51.3
AtMRP13G-s	ACAAGTAAGCCTAAGAGTGCCAAAGGG	60.3
AtMRP13H-as	CTCTTGTTTCCTTCAACCAATCAGC	57.3
AtMRP13I-s	TCTCTATATGGATGCAAACCTGAAACG	58.7
AtMRP13I-as	ATGAGGCAAATCTCCTGTAATGTGA	55.8
AtMRP13J-s	AAAGAATTGGAACAGTTCATCGGGA	58.9
AtMRP13J-as	TGACCAAATTAGTGATGGAGTTGAG	54.1
AtMRP13-cDNA-seqP_01	GCTATCACTCTCACTAATTTCA	43.4
AtMRP13-cDNA-seqP_02	CATCCCAAAATCATTCCTTT	48.3
AtMRP13-cDNA-seqP_03	CGGTCTAGTATAATGAGTGTCA	44.0
AtMRP13-cDNA-seqP_04	CTTTTGGTCTCTTTGCTCTG	46.8
AtMRP13-cDNA-seqP_05	GGAAGCCTTTTGACTCCAAA	51.1
AtMRP13-cDNA-seqP_06	CGGATATCGTCAAATTAGAG	44.3
AtMRP13-cDNA-seqP_07	AGGTTCTATTCCTGCTTCTG	45.4
AtMRP13-cDNA-seqP_08	AAGAAGTTTCAGGTCCTCAA	45.4
AtMRP13-cDNA-seqP_09-as	CCATTTCTTCTCGTTATGGTGA	51.1
MRP13-exo01-f	ATGGCTATCACTCTCACTAATTTCAC	52.1
MRP13-exo02-f	CTCTATATGGATGCAAACCTGAAAC	53.2
MRP13-exo03-f	ACTCTTCTTCTGATTCTGATTCTCAC	51.3
MRP13-exo04-f	GTATGTAACACCTGCACTTGGAGC	54.6
MRP13-exo05-f	CTGGTGGATCTTTAGATTCCTAAC	50.2

Table 5 (continued). Primers used for PCR and sequencing reactions.

Primer name	Sequence	Tm [°C]
MRP13-exo06-f	TTGGACATTGCTTTTGGTATCTC	52.7
MRP13-exo07-f	CACTTATTGAAGACGACGATGATC	52.4
MRP13-exo08-f	CTCAACTCCATCACTAATTTGGTC	51.5
MRP13-exo09-f	CTGGACCCTTACTTCTCAACAGAC	53.0
MRP13-exo10-f	TGTTGGCTATACACTTGCTATCTC	50.2
AtMRP13Prom-attB1-A-s	GGGGACAAGTTTGTACAAAAAAGCAGGCT**TATGATTTTGTGAGCTAAAT**	39.4
AtMRP13Prom-attB2-B-as	GGGGACCACTTTGTACAAGAAAGCTGGGT**ACTCTTGGGTTTTCTACCC**	44.7
pMDC163-GUS-2-r	TCCAGACTGAATGCCCACAG	53.2
pMDC163-GUS-r	TTCACGGGTTGGGGTTTCTA	54.3
actin2-s	TGGAATCCACGAGACAACCTA	52.0
actin2-as	TTCTGTGAACGATTCCTGGAC	51.5
LBa1-2	ATGGTTCACGTAGTGGGCCATCG	61.6
RB1-s	ATTAAACTCCAGAAACCCGCGGCTGAG	65.7
DS5-3	TACCTCGGGTTCGAAATCGAT	55.0
DS3-4	CCGTCCCGCAAGTTAAATATG	53.9

4.2.5 Molecular biological methods

Genomic DNA isolation

Genomic DNA was isolated from plant leaves using a modified method from Dellaporta et al. (1983). Snap-frozen plant tissue (50-200 mg) was grinded in a 1.5 mL plastic tube and mixed with 750 µL of an extraction buffer containing 200 mM Tris-HCl pH 8.5, 50 mM EDTA, 500 mM NaCl, and freshly added 14 mM 2-mercaptoethanol and 10 g/L SDS. After incubation at 65 °C for 20 min, 250 µL potassium acetate 5 M pH 6.0 was added. Extracts were incubated 20 min on ice and centrifuged at 14'000 g and 4 °C for 3 min. The supernatant was then precipitated with 700 µl 2-propanol at 4 °C. After centrifugation at 14'000 g and 4 °C for 5 min, the pellet was washed with 70% ethanol, dried, and redissolved in 100 µL water.

Polymerase chain reactions (PCR) and gel electrophoresis

PCR reactions were performed in a final volume of 25 or 50 µl and contained 50 – 200 ng genomic DNA or 50 ng cDNA template, 1.5 mM $MgCl_2$, 500 µM of each dNTP, 0.5 µM of each primer (Table 5), 1.25 units GoTaq DNA Polymerase (Cat. No. M8305; Promega, Dübendorf, Switzerland) and 1 x GoTaq Flexi buffer (Promega M8391A). Amplification consisted of initial 2 min at 95 °C, followed by 34 cycles (except 28 cycles for *Actin2*-specific PCR) consisting of 95 °C for 30 s, 50 – 60 °C for 30 s, 72 °C for 50 s, and a final step of 7 min at 72 °C. For gel electrophoresis, 0.8% to 2.5% agarose gels in

1x TAE containing 40 ng/mL ethidium bromide were used. 1x TAE was also used as electrophoresis running buffer.

RNA isolation and RT-PCR analyses

Total RNA was extracted from adult rosette leaves or seedlings using the Promega SV total RNA isolation kit (Promega) with on-column DNAse treatment. The reverse transcription procedure followed the two-step protocol for the M-MLV reverse transcriptase system. 1 µg of isolated total RNA was incubated with 500 ng oligo-$(dT)_{15}$ primer (Promega C110A) at 70 °C for 5 min and then transferred to a water-ice bath (0 °C) for 5 min. Subsequently, M-MLV buffer 5x (Promega M531A), 50 nM of each dNTP and 240 units M-MLV Reverse Transcriptase H(-) point mutant (Promega N368B) were added to a final volume of 20 µL and the reaction was then incubated for 10 min at 40 °C, 50 min at 50 °C and 15 min at 70 °C. For subsequent PCR reactions, 50 ng cDNA were used as template.

Sequencing

Sequencing was done via the in-house sequencing service using the sequencing primers AtMRP13-cDNA-seqP_01 to 09 (Table 5) for the *AtABCC13.1* genomic and cDNA sequences, as well as for derived constructs.

Agrobacterium mediated transformation of *Arabidopsis thaliana*

All constructs for stable transformation of *Arabidopsis thaliana* were transformed into the *Agrobacterium tumefaciens* strain *GV3101* by electroporation (Weigel and Glazebrook, 2006). Transformation of *Arabidopsis thaliana* was performed according to a modified protocol described by Clough and Bent (1998). The *Agrobacterium tumefaciens* strain *GV3101* harboring the plasmid to be transformed was grown in 10 mL LB medium containing 50 µg/mL kanamycin and 50 µg/mL rifampicin in a shaker for 2 days at 28 °C and 150 rpm. 5 mL of this pre-culture was added to 400 mL LB supplemented with the same antibiotics and incubated in a shaker overnight at 28 °C and 150 rpm to an OD_{600} of 0.3. Cells were harvested by centrifugation for 10 min at 1000 g and 4 °C and resuspended to a final OD_{600} of 0.5 - 0.8 in infiltration medium containing ½MS (half strength Murashige and Skoog medium mix, modification 1B, Cat.

No. 0253, Duchefa Biochemie B.V., Haarlem, The Netherlands), 50 g/L sucrose and 5 mM $MgCl_2$. 500 µl Silwet L-77 (Lehle Seeds, Texas, USA) was added to the suspension immediately before transformation. Flowers from *Arabidopsis thaliana* wild-type plants with 10-15 cm long inflorescences were dipped for 30 seconds into the *Agrobacterium* suspension, placed for one hour in a horizontal position on a household foil, and were then covered completely with this foil. The following morning the plastic foil was removed and plants were placed back in a vertical position. The next three days the plants were watered constantly, before continuing with standard watering. Harvested seeds were sterilized, stratified, and selected on ½ MS + 1% sucrose plates containing 20 mg/L hygromycin B (Cat. No. 10687-010; Invitrogen, Zug, Switzerland).

4.2.6 *AtABCC13* cDNAs

The full-length *AtABCC13.1* cDNA had been isolated by Tobias Kretzschmar (University of Zurich, Switzerland, unpublished data) from a size-selected cDNA library of untreated four-week-old *Arabidopsis* seedlings grown in liquid culture (Tommasini et al., 1997). The 5'-UTR sequence of *AtABCC13* was determined by 5' RACE from total RNA of seedlings using the SMARTer™ RACE cDNA Amplification Kit (Clontech, Takara Bio Company, USA).

The *AtABCC13.2* cDNA was a courtesy of Miyoung Lee (University of Zurich, Switzerland, unpublished data). It had been directly amplified from *Arabidopsis* adult rosette leaf total full-length cDNA using the primers that annealed to the start and stop codons of the gene model predicated for *AtABCC13* (*At2g07680.1*) by TAIR10 (http://www.arabidopsis.org).

4.2.7 $Prom_{AtABCC13}$*::GUS* constructs and GUS staining

A 2714 bp fragment upstream of the 5'-UTR of the *AtABCC13.1* gene was amplified from genomic DNA using primers AtMRP13Prom-attB1-A-s/AtMRP13Prom-attB2B-as (Table 5) and cloned into the GATEWAY® pDONRzeo vector (Invitrogen, Zug, Switzerland) by BP recombination according to the Invitrogen GATEWAY® protocol. From this construct, the promoter fragment was subcloned into the GATEWAY®

pMDC163 GUS expression vector (Curtis and Grossniklaus, 2003) via LR reaction (Supplementary Information, Section 4.5.1). The insertion was verified by sequencing the 3' insertion site using the pMDC163-GUS-2-r primer. This construct was then stably transformed into wild-type *Arabidopsis* Col-0 plants.

Additionally, plants stably transformed with different GUS fusion constructs were obtained as a courtesy from Katsuhiro Shiratake (Nagoya University, Nagoya, Japan; unpublished data). These transformed GUS fusion constructs each harbor a 1291 bp upstream sequence fragment relative to the start codon of the *AtABCC13.1* gene model, and the first 1188 bp (*Prom*$_{AtABCC13.1}$*::AtABCC13.1*$_{1-1188}$*:GUS*) or 1750 bp (*Prom*$_{AtABCC13.1}$*::AtABCC13.1*$_{1-1750}$*:GUS*) of the *AtABCC13.1* genomic sequence. The *AtABCC13.1*$_{1-1188}$ region spans the exons 1-7 and the first 54 bp of exon 8. The corresponding transcript of the *AtABCC13.1*$_{1-1188}$ fragment has length of 621 bp (207 amino acids). The *AtABCC13.1*$_{1-1750}$ region spans the exons 1-10 and the first 89 bp of the intron between exons 10/11.

To detect GUS activity, seedlings were vacuum infiltrated and incubated overnight at 37 °C in 1 mM 5-Bromo-4-chloro-3-indolyl β-D-glucuronide cyclohexylammonium salt (Biosynth AG, Staad, Switzerland), 1.5 mM potassium ferrocyanide and 0.25 mM potassium ferricyanide in a buffer containing 0.1 M sodium phosphate buffer pH 7.0, 10 mM EDTA and 0.1 % Triton X-100. Subsequently, seedlings were destained in 70% ethanol for 2 days.

4.2.8 *AtABCC13:GFP* constructs and subcellular localization studies

All full-length *AtABCC13.1:GFP* constructs were obtained from Tobias Kretzschmar (unpublished data). Modified pART7 vectors (Endler et al., 2006) harboring the *AtABCC13.1* coding (for the *35S::cdsAtABCC13.1:GFP* construct) or the *AtABCC13.1* genomic (for the *35S::genomicAtABCC13.1:GFP* construct) sequences in-frame with a C-terminal GFP were used as transient expression vectors. Using the NotI/XhoI restriction sites, the *AtABCC13.1:GFP* fragments in the pART7 constructs were excised and ligated into the plant binary vector pART27 (Gleave, 1992) for stable transformation of *Arabidopsis* plants. All these constructs were verified by sequencing.

Additionally, a GFP fusion construct in a 35S-10H-GFP-JFH2 vector (Geisler et al., 2000) with a 5' truncated *AtABCC13.1* genomic sequence lacking the first 1188 bp, was obtained as a courtesy from Katsuhiro Shiratake (named *35S::genomicAtABCC13.1*$_{1188-}$*:GFP;* unpublished data). This construct was predicted to encode for a AtABCC13.1 protein that lacks the first 207 amino acids and thus the TMD0, according to a sequence alignment of AtABCC13.1 with the human HsABCC1 sequence and comparison with the region in HsABCC1 predicted to encode for the TMD0 (Bakos and Homolya, 2006; Supplementary Information, Section 4.5.3).

Transient expression studies employing particle bombardment were done with the epidermal layer on the inner side of onion (*Allium cepa*) bulb and on the abaxial side of *Arabidopsis* rosette leaves. Gold particles (1 mg, Ø 1.0 µm, Bio-Rad Laboratories, Hercules, CA, USA) were coated with 2.5 to 5 µg plasmid DNA, 17 mM spermidine and 1.25 mM $CaCl_2$ and subsequently washed in 100% ethanol. Tissues were bombarded with the Biolistic® PDS-1000/He particle delivery system (Bio-Rad Laboratories) using 1350 psi rupture disks at a distance of 60 mm and a vacuum of 85 kPa. Bombarded tissues were kept in a dark humidity chamber room temperature for approximately 48 hours prior to microscopic analyses. Confocal images were acquired with a Leica TCS SP2 confocal laser scanning microscope (Leica Microsystems). The GFP fluorescence and the chlorophyll auto-fluorescence were simultaneously recorded with an excitation wavelength of 488 nm and with a emission filter wavelength range of 500–530 nm for the GFP and 590–720 nm for chlorophyll fluorescence. Overlay images of the GFP and chlorophyll auto-fluorescence images were generated using the blending function of Adobe Photoshop CS4.

4.2.9 Yeast experiments

Yeast strains

Following *Saccharomyces cerevisiae* strains were used for heterologous expression of AtABCC13 and subsequent uptake studies in membrane vesicles. *Δycf1/Δbpt1* (YMK2; *MATα ura3–52 leu2–3112 his6*Δ*ycf1*::*HIS6*Δ*bpt1*::*LEU2*; Klein et al., 2002) and *Δbat1*

(*BY4741; Mat α; his3Δ1; leu2Δ0; met15Δ0; ura3Δ0; YLL048c::kanMX4*; obtained from EUROSCARF, University of Frankfurt, Germany).

Yeast pDR195-AtABCC13 expression vector and yeast transformation

For expression in yeast, the constitutively expressing, multi-copy yeast expression vector pDR195 (Rentsch et al., 1995) was used. The *AtABCC13* cDNA was excised from the previously generated pART7-AtABCC13 construct and ligated into pDR195 using the XhoI/NotI restriction sites.

Competent yeast cells of the *Δbat1* and *Δycf1/Δbpt1* (YMK2) strains were prepared from 200 mL cultures of OD_{600} = 0.6 – 0.8 in YPD (1% bacto yeast extract, 2% bacto peptone, 2% glucose). Following centrifugation for 5 min at 3000 g (4 °C), cells were washed in 4 mL ice-cold solution A (1 M sorbitol, 10 mM BICINE-KOH pH 8.35, 30 g/L ethylene glycol), centrifuged 5 min at 1000 g (4 °C), resuspended in 2 mL solution A, aliquoted and transferred to -80 °C. The *pDR195-AtABCC13* plasmid and the empty vector were transformed into yeast cells, by adding 5 µL salmon sperm solution (10 mg/mL, denatured 5 min at 95 °C), 1 µL miniprep plasmid DNA (100 ng) and 4 µL H_2O to 200 µL frozen (-80 °C) competent yeast cells. After 5 min at 37 °C, 1 mL of 400 g/L PEG-1000 in 200 mM BICINE-KOH (pH 8.35) was added. Cells were then incubated for 1 h at 28 °C, centrifuged for 5 min at 1000 g, washed with 1 mL solution C (10 mM BICINE pH 8.35, 150 mM NaCl), centrifuged for 5 min at 1000 g, and resuspended in 100 µL solution C. Transformants were selected on plates containing 1.7 g/L yeast nitrogen base, 5 g/L $(NH_4)_2SO_4$, 20 mg/mL L-tryptophan, 3 mg/L adenine, 20 g/L glucose and 14 g/L agar.

Preparation of yeast total membrane microsomes

Yeast microsomes were isolated based on a previously published method (Tommasini et al., 1996). Yeast cells were grown in 250 mL YPD (1% bacto yeast extract, 2% bacto peptone, 2% glucose) at 30 °C to an OD_{600} = 2-3, centrifuged 10 min at 1200 g (RT), washed twice with water and resuspended to OD_{600} = 10 in 1.1 M sorbitol, 20 mM Tris-HCl pH 7.6, 1 mM DTT and 57 U/mL lyticase (Sigma L4025). The suspension was incubated for 90 min at 30 °C under moderate shaking until the OD_{600} ratio of the

suspension diluted in the lysis medium vs. suspension diluted in water reached the factor 3. After centrifugation for 10 min at 1200 g (4 °C), cells were resuspended in 25 mL homogenization buffer (1.1 M glycerol, 50 mM Tris-ascorbate pH 7.4, 5 mM EDTA, 1 mM DTT, 15 g/L polyvinylpyrrolidone, 1 mM phenylmethylsulfonyl fluoride (PMSF)), and homogenized using a glass/Teflon potter with 30 movements on ice. Subsequently, the homogenate was centrifuged for 10 min at 6000 g (4 °C) and the pellet was then resuspended in 10 mL homogenization buffer, homogenized and centrifuged again. Both supernatants were pooled and centrifuged at 100'000 g for 45 min (4 °C) in an ultracentrifuge. The pellet was then resuspended to final OD_{600} of 4.0 in storage medium (1.1 M glycerol, 50 mM Tris-MES pH 7.4, 1 mM EDTA, 2 mg/mL BSA, 1 mM PMSF, 1mM DTT), aliquoted, snap frozen in liquid nitrogen and stored at -80 °C.

Yeast microsome uptake assays

The reaction mix for microsomal uptake assays contained 10 mM Tris-HCl pH 7.4, 250 mM sucrose, 10 mM creatine phosphate disodium salt (Sigma 27920), 100 µg/mL creatine phosphokinase from rabbit muscle (Sigma C3755), 10 mM $MgCl_2$, 4 mM ATP (diluted from a stock of 0.2 M ATP in 0.2 M BTP) and 50 µL/mL microsomes (OD=4), if not otherwise stated. The Tris-HCl buffer with sucrose was autoclaved and stored at 4 °C. The other compounds were prepared as 50x (200x for the creatine phosphokinase) stock solutions in H_2O, stored at -20 °C and added to the buffer immediately before use. For reactions in absence of ATP, the ATP solution was replaced with H_2O. For leukotriene C4 (LTC4) uptake, 0.025-0.13 µCi/mL (925-4810 Bq/mL) [14,15,19,20-^{3}H]leukotriene C4 (ART1672, American Radiolabeled Chemicals Inc., USA) were added, corresponding to a final LTC4 concentration of 0.19 – 1.10 nM in the reaction mix. For taurocholate uptake, 500 µM non-labeled taurocholic acid sodium salt (Sigma T4009) and 2.85 µCi/mL (105 kBq/mL; 3.5 µM) [cholic acid-2,4-^{3}H]taurocholic acid (ART 1367, American Radiolabeled Chemicals) were added.

The reaction was started by adding the microsome suspension. Incubations were performed at RT with regular mixing of suspension. Reactions were then stopped at indicated times by transferring 50 µL of the suspension into 950 µL ice-cold wash

buffer (0.4 M glycerol, 0.1 M KCl, 20 mM Tris-MES, pH 7.49). Immediately after a replicate series (n=3), 950 µL of each stopped reaction was filtered through a 0.45 µm HA nitrocellulose filter Ø25 mm (Cat. No. HAWP02500; Millipore AG, Zug, Switzerland) using a 1225 Sampling Manifold (Cat. No. XX2702550, Millipore AG) connected to a water-jet pump. Filters were washed two times with 3 mL ice-cold wash buffer. Filters were then dried at RT, transferred to scintillation counting tubes containing 3 mL Ultima Gold scintillation cocktail (PerkinElmer Inc., Schwerzenbach, Switzerland), rigorously shaken and measured in a Packard Tri-Carb liquid scintillation spectrometer (PerkinElmer Inc.).

4.2.10 Plant growth conditions

For soil-grown plants, sterilized seeds were grown on the standardized soil ED 73 ("Einheitserde Werkverband e.V." association, Germany; http://www.einheitserde.de) in climate chambers with constant temperature of 20 ± 2 °C, constant relative humidity of 60 ± 10 %RH and short day lighting (8/16 h light/dark cycle) at a light intensity of 90 - 120 µmol photons·m^{-2}·s^{-1}. Light sources consisted of three OSRAM 965 BIOLUX 58 W and one OSRAM 77 FLUORA 36 W fluorescent tubes. Plants were watered twice a week by flooding trays for one hour at half height. Every two weeks 0.03 g/L Traunem nematodes (Andermatt Biocontrol AG, Grossdietwil, Switzerland) were sprayed on plants for the bio-control of black flies.

4.2.11 Selection of homozygote *AtABCC13* insertion and wild-type lines and determination of insertion sites

AtABCC13 (At2g07680) T-DNA insertion lines were obtained from RIKEN (http://rarge.psc.riken.jp/dsmutant) (Kuromori et al., 2004) and the SALK Institute (http://signal.salk.edu/tabout.html) (Table 6).

Table 6. *AtABCC13* insertion lines used for the phenotype screening

Name	Type	Origin	Line No	Background
atabcc13-1	*Ds* transposon insertion	RIKEN	RIKEN 16-0764-1	*No-0*
atabcc13-2	T-DNA insertion	SALK	SALK_044759	*Col-6*

Corresponding wild-type lines were obtained from segregating mutant populations, designated as 'WT-like-1' (wildtype of *atabcc13-1)* and 'WT-like-2' (wildtype of *atabcc13-2*).

Mutant and wild-type plants were selected by PCR-based genotyping performed on genomic DNA. *AtABCC13* wild-type alleles were detected with primers AtMRP13D-s /AtMRP13D-as in the *atabcc13-1 line,* and with AtMRP13C-s/AtMRP13C-as for the *atabcc13-2* line, respectively. Insertions in the *atabcc13-1* line were detected with primers AtMRP13D-s and DS5-3, and in the *atabcc13-2* line with primers AtMRP13G-s/LBa1-2.

The actual sites of insertions in the *atabcc13-1* and *atabcc13-2* mutant lines were determined by sequencing the insertion flanking regions. Left border sequences of the *atabcc13-1* and *atabcc13-2* lines were amplified with primers AtMRP13D-s/Ds5-3 and AtMRP13C-s/LBa1-2. Additionally, the right border of the *atabcc13-1* was amplified using the primers DS3-4/AtMRP13D-as. After gel electrophoresis, corresponding bands were purified and directly sequenced with primers used for amplification of these fragments.

4.2.12 Screen for phenotypes of *AtABCC13* knockout mutants

The screen for differential phenotypic responses to abiotic stresses and chemical treatments was performed with both knockout (*atabcc13-1* and *atabcc13-2*) and their corresponding wild-type lines. Seeds used for an individual test were always of the same age, collected on the same day from plants of the same age and stored under identical conditions. Except for dormancy analyses, seeds were stored between 2 - 12 months prior use in the tests. Germination rates of seed batches used were always >95% when tested on ½MS + 1% sucrose plates after five days stratification. Seeds were sterilized by incubation in 70% ethanol for 5 min, followed by five subsequent washing steps with sterile deionized water. Seeds were then suspended in sterile water or 0.1% phytoagar and sown directly or after stratification at 4°C in dark for three to five days.

To test growth and development, flowering time and seed production, plants were grown in individual pots or in pots with 50 – 200 seeds under short day and long day conditions. Growth, development, flowering time, silique development and ripening, seed amount and plant senescence were visually inspected.

For plate tests, polystyrene petri dishes filled with ½MS (half-strength Murashige and Skoog medium mix, modification 1B, Cat. No. 0253, Duchefa) and 7.5 g/L phytoagar (Cat. No. P1001, Duchefa) were used, if not otherwise stated. Plates were sealed with air permeable medical tape and placed in a growth chamber at 21 °C and 16/8 h light/dark cycles of light at an intensity of 90 - 130 µmol photons·m^{-2}·s^{-1}. Light sources consisted of one OSRAM 965 BIOLUX 58 W and one OSRAM 77 FLUORA 36 W fluorescent tubes. Phenotypes were visually inspected directly from plates or from high-resolution pictures of plates that were captured using a flatbed scanner with open lid in a dimmed room. For germination tests, 50 – 120 seeds per line of either non-stratified or stratified seeds were daily scored for radicle protrusion and cotyledon emergence. For analyses of seedling growth, plant size, shape, color, root length, lateral root number, and development, 20 – 120 plants per line per test were visually inspected on a daily basis. Individual conditions and methods for tests performed in the phenotype screening are listed in the following table (Table 7).

Table 7. Experimental conditions used to screen for phenotypes of *AtABCC13* knockout mutants.

Condition	Conditions tested	Methods
Dormancy + Germination	non-stratified, stratified seeds	Seeds collected from plants with dry siliques still adhering to the plants were sterilized and directly sown on ½MS plates or after five days stratification at 4 °C in dark.
Heat	30/37 °C	½MS plates with one-week-old seedlings were placed for 24 h in an incubator at dark with a temperature of 30 or 37 °C, and then transferred to the standard growth chamber
Cold	4 °C	½MS plates with one-week-old seedlings were placed in a growth chamber with a temperature of 4 °C, 60% RH, and 8/16 h light/dark cycles of light at an intensity of 120 µmol m^{-2} s^{-1} photons.
High light + high temperature	700 µmol m^{-2} s^{-1} and 26 °C on germination	Stratified seeds were plated on ½MS plates and transferred to a growth chamber with a light intensity of 700 µmol m^{-2} s^{-1} photons and a temperature of 26 °C at plate level (12/12 h dark/light). After 7 d, plates were transferred to the standard growth chamber. Germination and growth were daily scored.
High light high temperature	700 µmol m^{-2} s^{-1} and 26 °C on seedlings	½MS plates with one-week-old seedlings were placed in a growth chamber with a light intensity of 700 µmol m^{-2} s^{-1} photons and a temperature of 26 °C at plate level (12/12 h dark/light). After 24 hours, the plate was transferred to the standard growth chamber.

Table 7 (continued). Experimental conditions used to screen for phenotypes of *AtABCC13* knockout mutants.

Condition	Conditions tested	Methods
Osmotic stress	-0.5, -0.7, -1.2 MPa (PEG plates)	Low water potential plates by overlaying PEG solution onto ½MS plates were prepared according to a protocol from the laboratory of Professor Jian-Kang Zhu, University of California, Riverside, USA (http://biocluster.ucr.edu/projects/Unknowns/external/Protocols/Stree_Zhu.doc). MS plates with 5 g/L sucrose (pH 5.7) and 1.5% phytoagar were soaked with PEG-8000 in ½MS solution as described. After equilibration, seeds were transferred onto the plates; plates were sealed with parafilm and transferred to the plate growth chamber. Three days after sowing, plates were placed vertically to observe root growth. Germination, growth and root formation were daily observed.
pH	pH 4.0, 4.2, 4.5, 7.6	½MS solution (without sucrose) was adjusted with MES or NaOH to pH 4.0/4.2/4.5/7.6. The phytoagar concentration was 2.5% to ensure solidification at such low pH values.
Glucose 6%	60 g/L	One-week-old seedlings grown on ½MS + 1% sucrose plates were transferred to ½MS medium with 0.75% phytoagar + 6% sucrose (sucrose added before autoclaving).
Sulfur deficiency	no S, 1/10 of normal [S]	For the sulfur-deficient medium, 1/2 strength Murashige and Skoog medium was prepared from single compounds, with that exception that the sulfate containing salts $MgSO_4$, $CuSO_4$, $FeSO_4$, $MnSO_4$ and $ZnSO_4$ were replaced with $MgCl_2$, $CuCl_2$, Fe(III)NaEDTA, $MnCl_2$, and $ZnNO_3$, respectively, at equal cation concentrations. For the 1/10 sulfur plates, 0.087 mM MgSO4 was added to the sulfur-free solution, which resulted in a neglected 11% increased Mg concentration.
Nitrogen deficiency	no N, 50 mM KNO_3	Nitrogen-deficient media was prepared according to Wang et al. (2003) with 0.75% phytoagar (without sucrose). Nitrate excess plate was prepared by supplementing the nitrogen-free media with 50 mM KNO_3.
ABA	0.5 µM (non-stratified, stratified seeds)	(±)-Abscisic acid (Sigma A1049) was added from a 10 mM stock solution in ethanol to autoclaved ½MS + 0.75% phytoagar medium. Sterilized, non-stratified, and stratified (5 d at 4 °C in dark) seeds were plated on freshly prepared plates.
ABA	1, 3 µM on lateral root growth	One-week-old seedlings grown on ½MS + 1% sucrose plates were transferred to ABA containing plates that were prepared by adding (±)-Abscisic acid (Sigma A1049) from a 50 mM stock solution (in H_2O, buffered with KOH, pH 7-8) to autoclaved ½MS + 0.75% phytoagar medium without sucrose. Root growth and lateral root formation were daily observed.
Tetcyclasis	3, 10, 30 µM	Tetcyclasis was a courtesy from Professor Wolfram Hartung, University Würzburg, Germany, and had a reported purity of 94.8%. A 5mM stock solution in ethanol, stored at -20 °C, was added to autoclaved ½MS + 1% sucrose + 0.75% phytoagar medium.
Epibrassinolide	30, 100, 300 nM	Epibrassinolide (Sigma E1641) stock solution (100 µM in DMSO) was added to autoclaved ½MS + 1% sucrose + 0.75% phytoagar medium.
Epibrassinolide	1, 3, 10 nM on lateral root growth	Epibrassinolide (Sigma E1641) stock solution (10 µM in DMSO) was added to autoclaved ½MS + 1% sucrose + 0.75% phytoagar medium. Plates were kept vertically in the growth chamber to observe lateral root formation.
Zeatin-Glucoside	30, 100 µM	*Trans*-Zeatin glucoside (Sigma Z0537) stock solution (10 mM in DMSO) was added to autoclaved ½MS + 1% sucrose + 0.75% phytoagar medium.
NAA	100 nM	1-naphthaleneacetic acid (Sigma N0640) stock solution (100 µM in DMSO) was added to autoclaved ½MS + 1% sucrose + 0.75% phytoagar medium.
IBA	3, 10 µM	Indole-3-butyric acid (Sigma I5386) stock solution (10 mM in H_2O) was added to autoclaved ½MS + 1% sucrose + 0.75% phytoagar medium
LiCl	10 mM	LiCl was added to ½MS + 1% sucrose + 0.75% phytoagar medium before autoclaving
$LaCl_3$	1 µM	$LaCl_3$ was added as a sterile stock solution (0.1 mM in H_2O) to autoclaved ½MS + 1% sucrose + 0.75% phytoagar medium

Table 7 (continued). Experimental conditions used to screen for phenotypes of *AtABCC13* knockout mutants.

Condition	Conditions tested	Methods
$MnSO_4$	100 µM	$MnSO_4$ was added as a sterile stock solution (100 mM in H_2O) to autoclaved ½MS + 1% sucrose + 0.75% phytoagar medium
$CsCl_2$	300 µM	$CsCl_2$ was added as a sterile stock solution (100 mM in H_2O) to autoclaved ½MS + 1% sucrose + 0.75% phytoagar medium
$ZnSO_4$	500 µM	$ZnSO_4$ was added as a sterile stock solution (100 mM in H_2O) to autoclaved ½MS + 1% sucrose + 0.75% phytoagar medium
$CaCl_2$	50, 75 µM	$CaCl_2$ was added as a sterile stock solution (10 mM in H_2O) to autoclaved ½MS + 1% sucrose + 0.75% phytoagar medium
NaCl	0, 100, 120, 150, 200 mM	NaCl was added to ½MS + 1% sucrose + 0.75% phytoagar medium before autoclaving. Freshly sterilized, non-stratified and stratified (5d at 4 °C in dark) seeds were plated on freshly prepared plates. The 150 mM condition was tested three times independently using different seed batches.
Paraquat	0, 0.2, 0.5 µM	Paraquat dichloride (Fluka 36541) stock solution (1 mM in DMSO) was added to autoclaved ½MS + 1% sucrose + 0.75% phytoagar medium
$AlCl_3$	0, 30, 100, 300 µM	$AlCl_3$ was added to ½MS + 1 % sucrose, pH adjusted to 4.2 with MES + 2.5% phytoagar before autoclaving.
UV-B	30, 60, 120, 300, 600 s	MS plates with one-week-old seedlings were opened and placed up-side-down on an electrophoresis UV transilluminator (with 6 x 15 W fluorescent tubes) set to 100% light intensity, sealed again and transferred to the standard growth chamber.
UV-C	1 x 15, 30, 50 kJ m^{-2} and 3 x 3 kJ m^{-2}	MS plates with one-week-old seedlings were opened and placed into a BIO-RAD GS Gene linker with UV-C/254 nm. Exposure to UV was calculated according to the energy emitted by the Gene Linker reported in the manual. After exposure, the plates were sealed again and transferred to the standard growth chamber. For the 3x 3 kJ m^{-2} treatments, plants were exposed once per day on three consecutive days, between and after the treatments, plates were kept in the standard growth chamber.
5-Fluorouracil	0, 10, 30, 100, 200, 500, 1000 µM	5-Fluorouracil (Sigma F6627) stock solution (20 mM in DMSO) was added to autoclaved ½MS + 1% sucrose + 0.75% phytoagar medium.
Cisplatin	0, 0.1, 1, 5, 10, 20, 30 µM	*cis*-Diammineplatinum(II) dichloride (Sigma P4394) stock solution (5 mM in 0.9% NaCl) was added to autoclaved ½MS + 1% sucrose + 0.75% phytoagar medium.
5-Flurouridine	0, 10, 30, 100, 200 µM	5-Fluorouridine (Sigma F5130) stock solution (20 mM in DMSO) was added to autoclaved ½MS + 1% sucrose + 0.75% phytoagar medium.
Ara-C	0, 1, 10, 30, 50, 100, 500 µM	Cytosine β-D-arabinofuranoside (Fluka 30399) stock solution (20 mM in DMSO) was added to autoclaved ½MS + 1% sucrose + 0.75% phytoagar medium.
MMS	0, 20, 40, 60, 100 ppm	Seedlings were grown in liquid culture by adding 10 sterilized and stratified seeds per well in wells of 24-well polystyrene tissue culture plates, filled with autoclaved ½MS (without sucrose) liquid medium. After one week, the medium of each well was exchanged with methyl methanesulfonate (Aldrich 129925) solution diluted in ½MS (without sucrose) liquid medium. Plants were left in the normal plate growth chamber on a horizontal shaker on the floor with approx. 30 µmol m^{-2} s^{-1} photons. Color and growth of seedlings was observed daily.
Hydroxyurea	0, 1, 5, 10 mM	Seedlings were grown in liquid culture by adding 10 sterilized and stratified seeds per well in wells of 24-well polystyrene tissue culture plates, filled with autoclaved ½MS (without sucrose) liquid medium. After one week, the medium of each well was exchanged with hydroxyurea (Sigma H8627) dissolved and diluted in ½MS (without sucrose) liquid medium. Plants were kept in the plate growth chamber on a horizontal shaker with approx. 30 µmol m^{-2} s^{-1} photons. Color and growth of seedlings was observed daily.

Table 7 (continued). Experimental conditions used to screen for phenotypes of *AtABCC13* knockout mutants.

Condition	Conditions tested	Methods
Adenine	0, 0.5, 1, 1.5, 2 mM	Adenine (Sigma A8626) stock solution (100 mM in HCl until dissolved, pH 4, sterile filtered) was added to autoclaved ½MS + 1% sucrose + 0.75% phytoagar medium.
Trichostatin A (HDAC inhibitor)	0, 0.5, 2, 10, 30 µM	Trichostatin A (Sigma T1952) stock solution (20 mM in DMSO) was added to autoclaved ½MS + 1% sucrose + 0.75% phytoagar medium.
Oryzalin	0, 0.1, 0.3, 1, 10 µM	Oryzalin (Fluka 36182) stock solution (20 mM in DMSO) was added to autoclaved ½MS + 1% sucrose + 0.75% phytoagar medium.
Individual leaves shaded		From 6-week-old plants grown under short day conditions, 2-3 adult rosette leaves were totally wrapped in aluminum foil to block all light. After 1, 2, 3 weeks leaf color was observed.
H_20 + dark		Adult rosette leaves from 6-week-old plants grown under short day conditions were clipped off with a razor blade and floated on their abaxial side on solutions of petri dishes filled with water. Petri dishes were stored at room temperature in dark. Leaf colors were observed daily.
Kinetin + dark	50 µM	Adult rosette leaves from 6-week-old plants grown under short day conditions were clipped off with a razor blade and floated on their abaxial side on solutions of petri dishes filled with 50 µM kinetin (Sigma K0753, 10 mM stock solution dissolved in 1M NaOH diluted in H_2O). Petri dishes were stored at room temperature in dark. Leaf colors were observed daily.
Methyljasmonate + dark	10 µL/L	Adult rosette leaves from 6-week-old plants grown under short day conditions were clipped off with a razor blade and floated on their abaxial side on solutions of petri dishes filled with 10 µL/L methyl jasmonate (Aldrich 392707) in water. Petri dishes were stored at room temperature in dark.
Ethylen + dark	1 mM ethephon	Adult rosette leaves from 6-week-old plants grown under short day conditions were clipped off with a razor blade and floated on their abaxial side on solutions of petri dishes filled with 1 mM ethephon (Fluka 45473) in water. Petri dishes were stored at room temperature in dark.
Giberellin A3 + dark	10 µM	Adult rosette leaves from 6-week-old plants grown under short day conditions were clipped off with a razor blade and floated on their abaxial side on solutions of petri dishes filled with 10 µM gibberellin A3 (Fluka 45473) in water. Petri dishes were stored at room temperature in dark.

4.3 Results

4.3.1 Gene structure of *AtABCC13* splice variants

The sequences of two cloned distinct *AtABCC13* cDNAs and their corresponding gene models were analyzed. *AtABCC13.1* was cloned from a size-selected seedling cDNA library (courtesy of Tobias Kretzschmar, see Material and Methods). The 5'-UTR had been determined using the 5'-RACE technique on total RNA isolated from seedlings. *AtABCC13.2* had been directly cloned from adult rosette leaf total cDNA, without experimental confirmation of the UTRs and the start codon (courtesy of Miyoung Lee, see Material and Methods). The TAIR10 gene model of *AtABCC13* (At2g07680.1) was not analyzed as it represents a predicted gene model without experimental cDNA or EST support (http://www.arabidopsis.org).

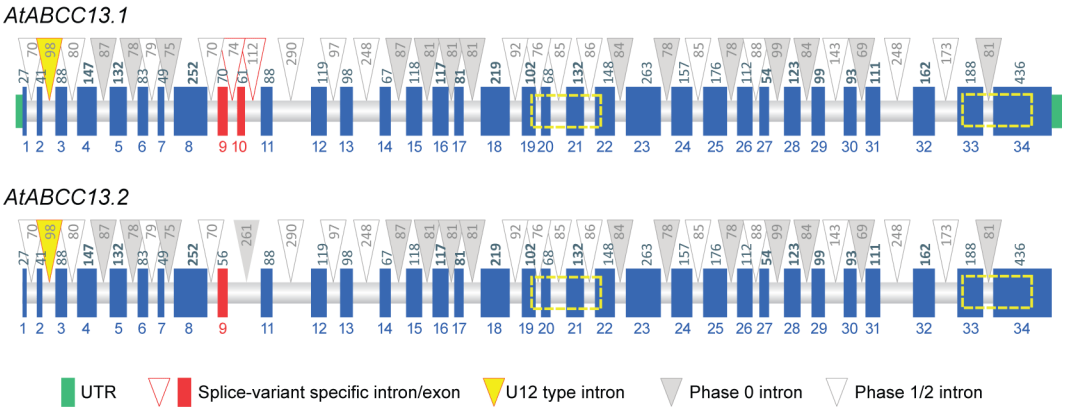

Figure 20. Gene models of the two cloned *AtABCC13* variants. Exons are represented by blue boxes, introns by triangles. Intron and exons lengths are given in base pairs. Shaded triangles and exons lengths in bold indicate phase 0 introns and exons, respectively. Exons that differ between the variants are shaded in red. The regions encompassing the Walker A and B motifs of the nucleotide-binding domains (Higgins, 1992) are illustrated by yellow dashed rectangles. The UTRs and the start codon of the *AtABCC13.2* model were not experimentally determined.

The *AtABCC13.1* coding sequence has a length of 4281 bp encoding for a 1427 amino acid protein. The 5'- and 3'-UTRs are 50 and 76 bp, respectively (Supplementary Information, Section 4.5.2). The deduced genomic region spans 7718 bp and consists of 34 exons and 33 introns, of which 29 have a length between 70 and 100 bp (Figure 20). The *AtABCC13.2* cDNA lacks the 61 bp exon 10, and its preceding exon 9 is shortened by 14 bp at the 3' end compared to *AtABCC13.1* (Figure 21A). This results in

the absence of a 75 bp segment, which does not cause a frameshift. However, homologous regions aligning to this segment were found to be present in all analyzed sequences of *AtABCC13* orthologs in plants and animals, but also in the other *Arabidopsis ABCCs* and in the human *HsABCC1* (Figure 21A and Supplementary Information, Section 4.5.2). In homology models of the human HsABCC1 (DeGorter et al., 2008) and HsABCC10, the regions aligning to this segment are located within the second transmembrane helix of TMD1 (Figure 21B/C).

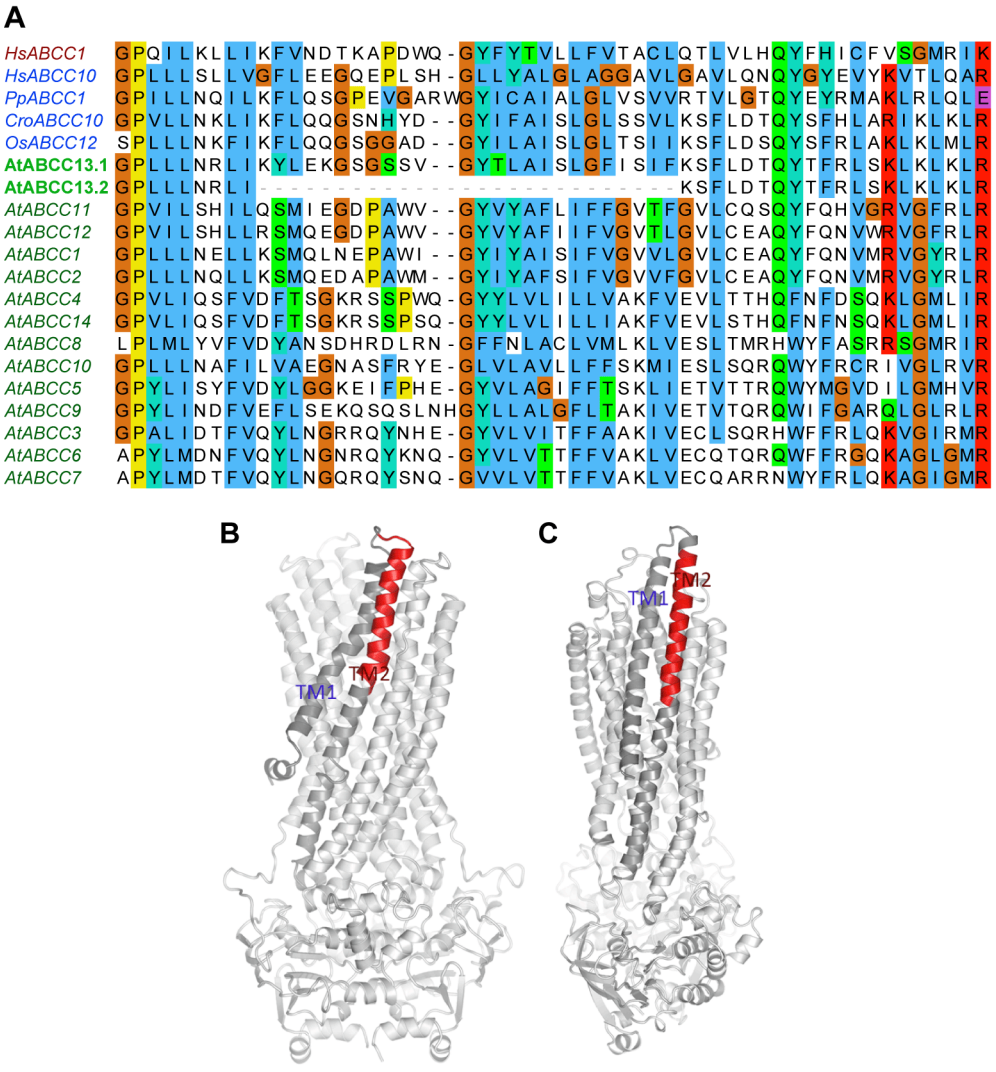

Figure 21. Region of AtABCC13.1 that is absent in AtABCC13.2. **(A)** Alignment of protein sequences deduced from the *AtABCC13.1* and *AtABCC13.2* cDNAs with sequences of *AtABCC13* orthologs from *Oryza sativa* (OsABCC12), *Catharanthus roseus* (CroABCC10), *Homo sapiens* (HsABCC10), *Physcomitrella patens* (PpABCC10) and with other *Arabidopsis* AtABCCs and the *Homo sapiens* HsABCC1. **(B & C)** Homology models of human HsABCC1 (B) and HsABCC10 (C), respectively, with the homologous region that is absent in the AtABCC13.2 variant indicated in red. The TMD0 was not modeled, since no structural templates are available.

The second intron identified in both variants (Figure 20) represents an U12-dependent intron with the non-canonical terminal dinucleotides AT–AC. Within this intron, a 5' splice (5'-ATATCCTT) and a putative branch (5'-TCCTTAAG) site sequence were identified, which correspond to reported U12 consensus 5' splice (5'-ATATCCTT) and branch (5'-TCCTTAAC) site sequences, respectively (Hall and Padgett 1994; Dietrich et al., 1997). An U12-dependent intron was also found in the *AtABCC13* ortholog of rice (*OsABCC12*). As in *Arabidopsis*, it represents the second intron and has conserved U12 5' splice (5'- ATATCCTTT) and putative branch (5'-GCCTTAAC) sites. In both orthologs, the U12-dependent intron is located within the codon after the conserved aspartic acid codon (Figure 22). The remaining 5' regions preceding the U12 intron appear not to be conserved, while the sequences downstream of the intron share several conserved residues.

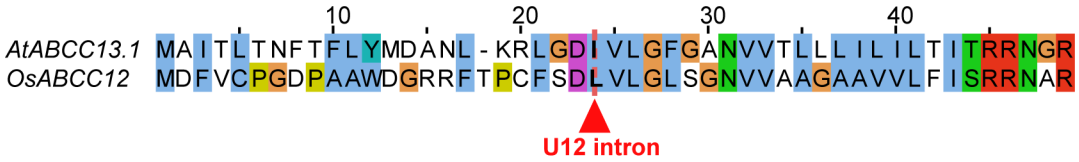

Figure 22. Alignment of the N-terminal protein sequences of AtABCC13 and its rice ortholog OsABCC12. The conserved locations of the U12-dependent introns in the corresponding genomic sequences are shown by a red dashed line.

4.3.2 The *AtABCC13* intron-exon structure compared to other plant *ABCCs*

Intron positions in the *AtABCC13* gene are mostly conserved in the rice ortholog *OsABCC12*, whereby also the encoded residues adjacent to the insertion sites are partially conserved (Figure 23). However, within the 5' region, the insertion sites of three introns show no apparent conservation on sequence level, albeit they are found in proximate locations. These introns are located in regions with low sequence conservation. The sequence alignment of this region is therefore of low confidence and consequently no conclusions can be made about the evolutionary conservation of these introns. At the 3' end, two introns found in *OsABCC12* were absent in *AtABCC13*. All other intron insertion sites are conserved in both genes.

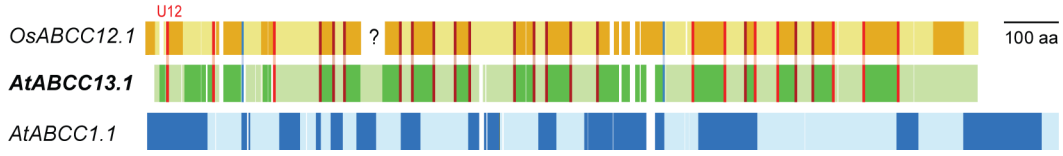

Figure 23. Comparison of intron insertion sites of *AtABCC13*, its rice ortholog *OsABCC12* and its close paralog *AtABCC1* on a graphically represented coding sequence alignment. Individual exons are indicated in alternating light and dark shades. White spaces illustrate alignment gaps. Conserved intron insertion sites that are located at the same position in the alignment, and that have at least one shared adjacent codon for the same residue are indicated by red lines. Blue lines represent intron insertion sites at the same position but with no shared adjacent codons for the same residue. The question mark depicts a segment that is absent in the *OsABCC12* gene model.

The *AtABCC13* gene has a distinct intron/exon structure and more introns compared to the other *Arabidopsis ABCCs* (Figure 23 and Figure 24). *AtABCC1* belongs to the phylogenetically closest paralogs of *AtABCC13* (see Results of Chapter I, Section 3.3.5). However, there are no apparently conserved introns shared between *AtABCC1* and *AtABCC13*. Nonetheless, ten *AtABCC1* intron sites are positioned in proximity of *AtABCC13* intron sites, within one to four codons distance.

Figure 24. Intron-exon organization of *Arabidopsis ABCC* genes including *AtABCC13*. Exons are shown as blue boxes. Genes are grouped and sorted according to their phylogenetic relationships (see Chapter I, Section 3.3.5).

4.3.3 Identification of alternatively spliced regions of *AtABCC13*

To analyze whether *AtABCC13* is alternatively spliced, PCR reactions using *Arabidopsis* adult rosette leaf total cDNA were performed with primers spanning selected exons of the *AtABCC13.1* gene model (Figure 25).

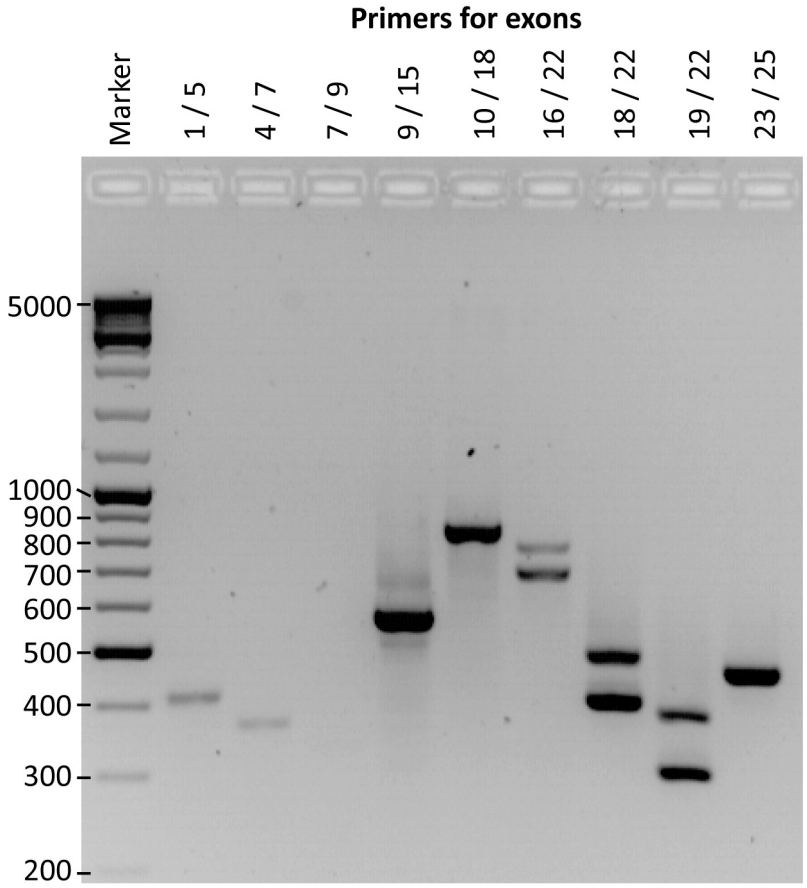

Figure 25. RT-PCR reactions for distinct regions of *AtABCC13*. PCR reactions were performed with primers for exons indicated above each lane. Exon numbers correspond to exons of the *AtABCC13.1* model (Figure 20). 80 ng of adult rosette leaf total RNA, reverse transcribed with oligo-(dT) primers, was used as template for each reaction. PCR amplification was performed with 34 cycles.

RT-PCR of *AtABCC13* fragments in the 5' region with primers for exons 1/5 and exons 4/7 resulted in single weak bands with sizes corresponding to amplicon lengths predicted based on the *AtABCC13.1* gene model. Amplification with primers for exons 7/9 did not result in any product. However, a strong band at predicted size was observed when using exon 9/15 primers, with two additional faint bands at smaller and bigger sizes. Amplification of fragments spanning exons 10/18 and 23/25 resulted in single bands with predicted sizes. However, all amplifications of fragments spanning

exons 21 and 22 (using primers for exons 16/22, 18/22 and 19/2) displayed two distinct bands, one with a size corresponding to the predicted amplicon length and another band, which was approximately 100 bp larger. Exons 21 and 22 encode parts of the nucleotide-binding domain 1 (Figure 20).

In plants transformed with the *Prom*$_{AtABCC13.1}$*::AtABCC13.1*$_{1-1188}$*:GUS* construct, which is a GUS fusion to the first 1188 bp of the *AtABCC13.1* genomic sequence, two splice variants from this construct were detected by RT-PCR (Figure 26A/B). Sequencing of the RT-PCR amplicons revealed a splice-variant corresponding to the *AtABCC13.1* gene model and another variant, in which the intron between exons 8 and 9 is retained. This intron has a length of 75 bp; its retention therefore does not cause a frameshift.

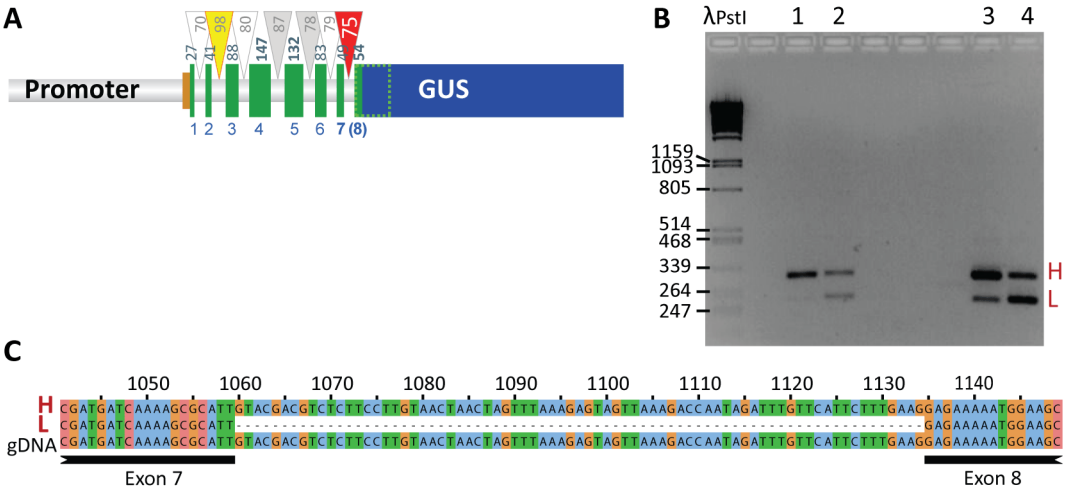

Figure 26. Alternative splicing of the *Prom*$_{AtABCC13.1}$*::AtABCC13.1*$_{1-1188}$*:GUS* construct harboring the first 1188 bp of the *AtABCC13* gene and a 1291 bp upstream promoter region, stably transformed into *Arabidopsis* (courtesy of Katsuhiro Shiratake). **(A)** Model of the *Prom*$_{AtABCC13.1}$*::AtABCC13.1*$_{1-1188}$*:GUS* construct. **(B)** RT-PCT analysis of rosette leaf total RNA from plants transformed with the *Prom*$_{AtABCC13.1}$*::AtABCC13.1*$_{1-1188}$*:GUS* construct using primers for exon 5 and the GUS gene. **(C)** Alignment of sequences of the RT-PCR amplicons H and L (see B) with the corresponding genomic sequence of the *AtABCC13* locus.

4.3.4 Analysis of available microarray data on *At*ABCC13 gene expression

Microarray gene expression data of *AtABCC13* (ATH1 Probeset ID: 266038_at) were retrieved from the Genevestigator database (Hruz et al., 2008) in October 2011. Tissue expression levels were highest in the primary root pericycle (Genevestigator level of expression: 4932 ± 451) and in the chalazal seed coat (4443 ± 885). Elevated expression values were furthermore identified in the shoot apex (2155 ± 27), root tip (2077 ± 168), and root elongation zone (2134 ± 202). The other tissues had expression levels below 1500, with the general seed coat (256 ± 16) and guard cell protoplasts (306 ± 24) having the lowest expression levels (Figure 27A). At the developmental stages defined in Genevestigator, expression levels ranged from 810 ± 35 in mature siliques to 1287 ± 22 in young rosettes. A more detailed view on *AtABCC13* expression in seed tissues at different seed developmental stages was obtained from the 'Gene Networks in Seed Development' website (http://seedgenenetwork.net). In early pre-globular and globular stages, *AtABCC13* expression was mainly confined to the chalazal seed coat and the embryo. At later stages of seed development, *AtABCC13* was also expressed in the peripheral endosperm and the general seed coat (Figure 27B).

For comparison, *Glycine max* microarray data from Genevestigator were analyzed for expression of the *Glycine max AtABCC13* ortholog *GmABCC10* (*Glyma13g44750.1*; Probeset ID: GmaAffx.56638.1.S1_s_at; see Supplementary Information, Section 4.5.4). Very high *GmABCC10* expression values were identified in the root pericycle (24431 ± 2345), parenchyma of the inner integuments (22590 ± 1335), plumule (24642 ± 340), and vascular bundles of embryonic cotyledons (17338 ± 1977). Elevated expression values were furthermore found in the shoot apical meristem (7147 ± 815), embryonic shoot and root meristem (6070 ± 133/5564 ± 500), and in cell culture syncytia (6737 ± 700). In other tissues, *GmABCC10* expression levels were below 5000.

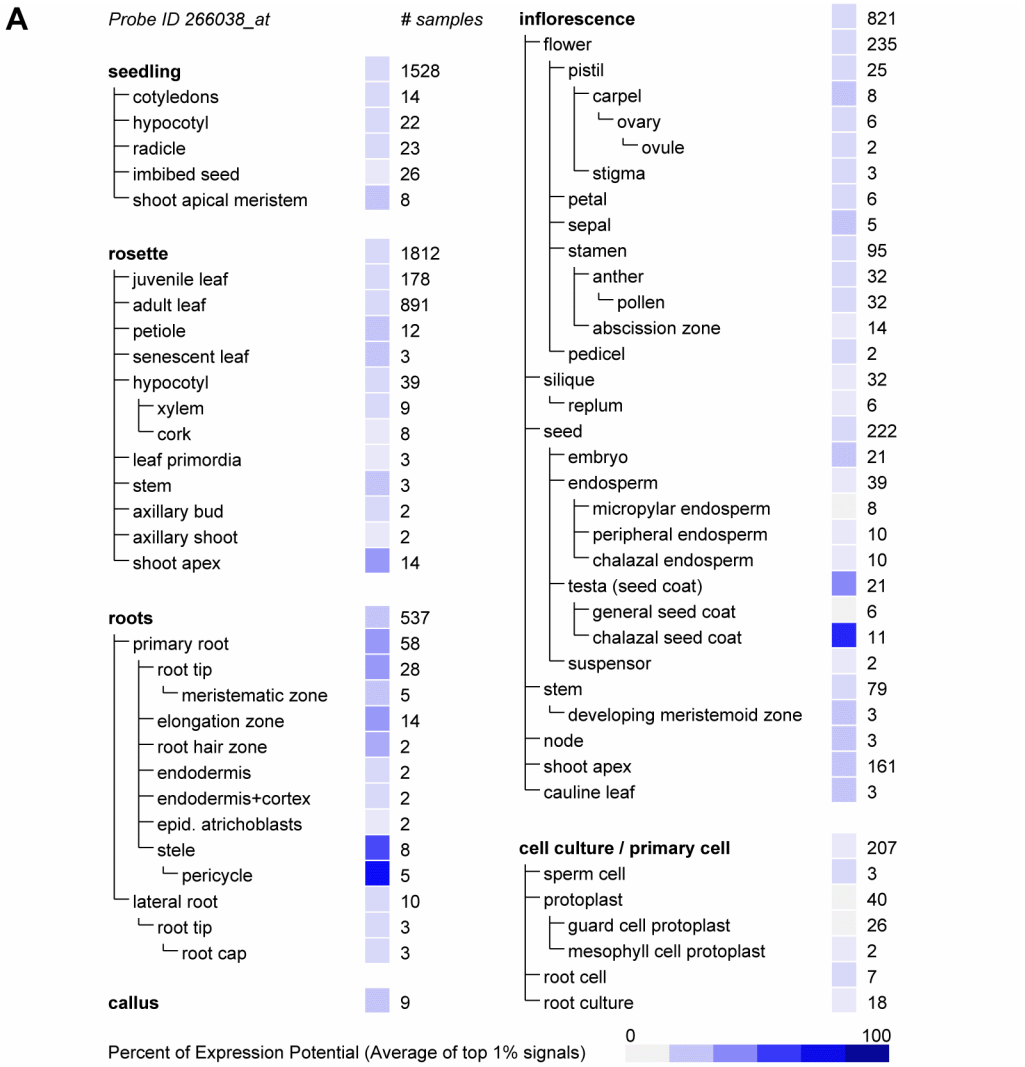

Figure 27. *AtABCC13* expression values in various organs and tissues. **(A)** Genevestigator data on *AtABCC13* expression in different organs and tissues. Illustration was obtained from Genevestigator (http://www.genevestigator.com) and modified in Abobe Illustrator. **(B)** *AtABCC13* expression patterns in different seed tissues at distinct developmental stages. Illustration was obtained from the 'Gene Networks in Seed Development' website (http://seedgenenetwork.net). Orange corresponds to highest, brown to average, and blue to low expression levels. White indicates that transcript was not detectable. Tissues names are given as abbreviations: CZE: Chalazal Endosperm, CZSC: Chalazal Seed Coat, EP: Embryo Proper, GSC: General Seed Coat, MCE: Micropylar Endosperm, PEN: Peripheral Endosperm, S: Suspensor.

A data set containing *AtABCC13* gene expression values from female gametophyte tissues, i.e. from the ovule, central cell, synergids, and egg cell, and from embryos at globular and heart stages, was obtained from Wuest et al. (2010). This data set also contained normalized *AtABCC13* expression values from various sporophytic tissues that had been obtained from publicly available microarray data (Figure 28). *AtABCC13* transcript levels were distinctly high in egg cells, where they were more than eight-fold higher compared to the average expression levels in aboveground vegetative tissues, and six fold higher than in the central cell and synergids. At early embryonic stages, *AtABCC13* expression levels were decreased compared to egg cells, but still higher than in aboveground vegetative tissues. The vegetative tissues with the highest *AtABCC13* expression levels were the root pericycle, root protophloem, root stele, and root xylem (Table 8). The male gametophytic tissues, pollen and sperm cells had *AtABCC13* expression levels comparable to values of aboveground vegetative tissues (Figure 28).

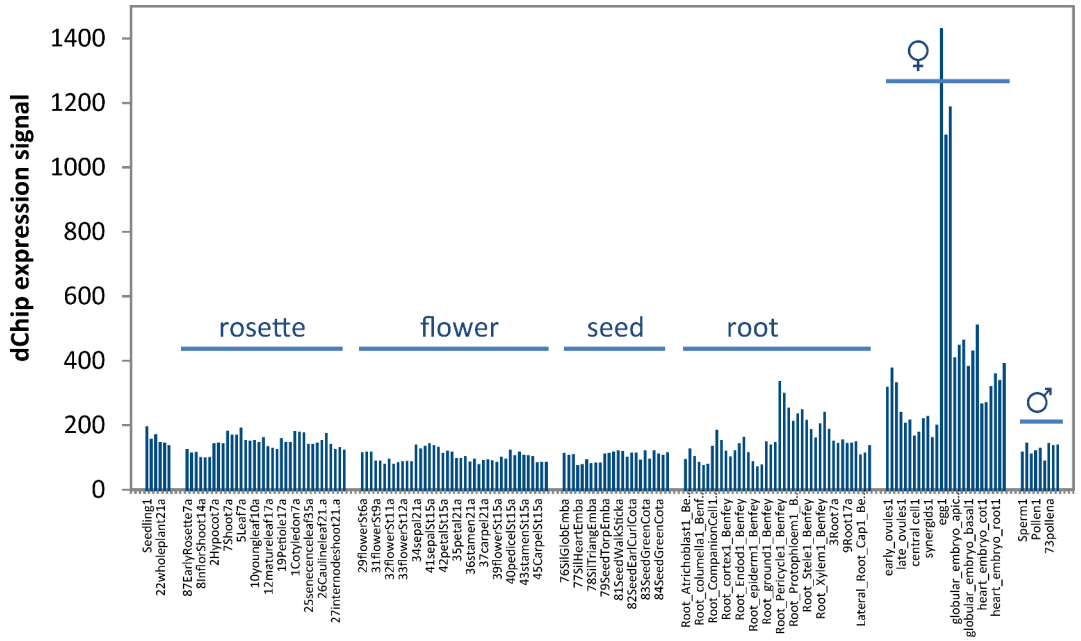

Figure 28. *AtABCC13* expression values in various *Arabidopsis* tissues including female gametophyte tissues. Each line represents one expression value of a specific tissue (three replicates per tissue). Labels are given for the third replicate (Data from Wuest et al., 2010).

Table 8. *AtABCC13* expression values of aboveground vegetative tissues and tissues with highest *AtABCC13* expression. Data are given as mean ± SD of original data obtained from Wuest et al. (2010).

Tissue	dChip expression value
Aboveground vegetative tissues	117 ± 29
Root tissues	152 ± 61
Root pericycle	293 ± 41
Early ovules	340 ± 31
Late ovules	218 ± 17
Central cell	186 ± 28
Synergids	194 ± 33
Egg	1237 ± 171
Embryo, globular stage, apical	438 ± 28
Embryo, globular stage, basal	439 ± 65
Embryo, heart stage, cotyledons	282 ± 30
Embryo, heart stage, roots	360 ± 26

4.3.5 Analysis of plants transformed with *AtABCC13* promoter–GUS fusion constructs

Arabidopsis plants stably transformed with a 2713 bp *AtABCC13* promoter fragment fused to the β-glucuronidase (GUS) gene (*Prom$_{AtABCC13.1}$::GUS*), exhibited ubiquitous GUS activity in shoot and root tissues. Highest GUS activities were observed in the vascular bundles of cotyledons, root central cylinder and emerging lateral roots (Figure 29).

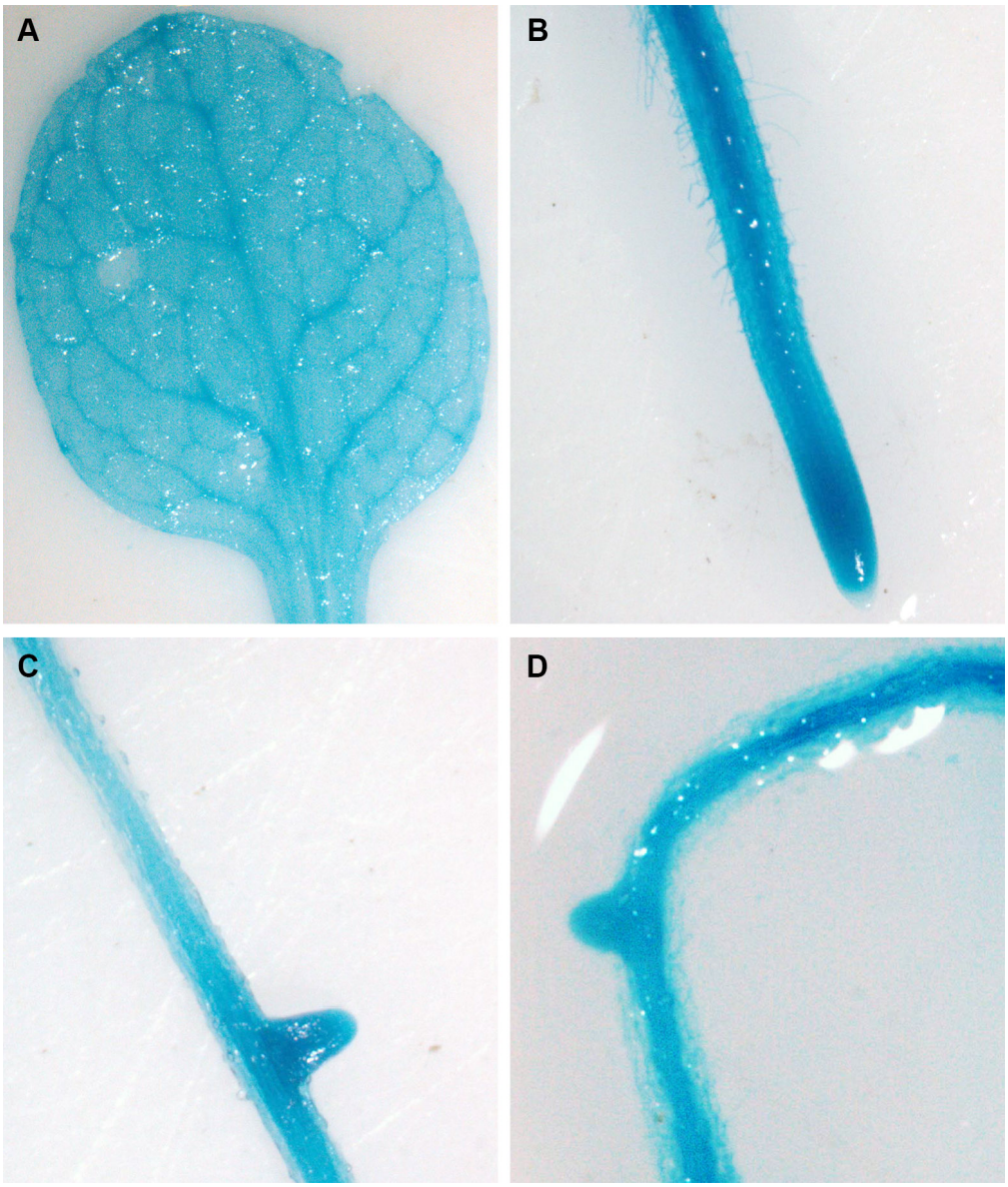

Figure 29. *Arabidopsis* seedling stably transformed with the *Prom$_{AtABCC13.1}$::GUS* construct stained for GUS activity. **(A)** Seedling cotyledon **(B)** Primary root with root tip **(C+D)** Primary root with an emerging lateral root.

Plants harboring the *Prom$_{AtABCC13.1}$::AtABCC13.1$_{1-1750}$:GUS* construct (see Material and Methods), which additionally contains the first 1750 bp of the *AtABCC13.1* genomic sequence fused to the 5' start of the GUS gene, had already been analyzed by Katsuhiro Shiratake (personal communication). This line was reanalyzed for GUS activity for comparison with the previously described *Prom$_{AtABCC13.1}$::GUS line*. GUS activities were high in vascular bundles and low in mesophyll tissues. In roots, GUS activity was only detectable in emerging lateral roots, which exhibited weak GUS signals (Figure 30).

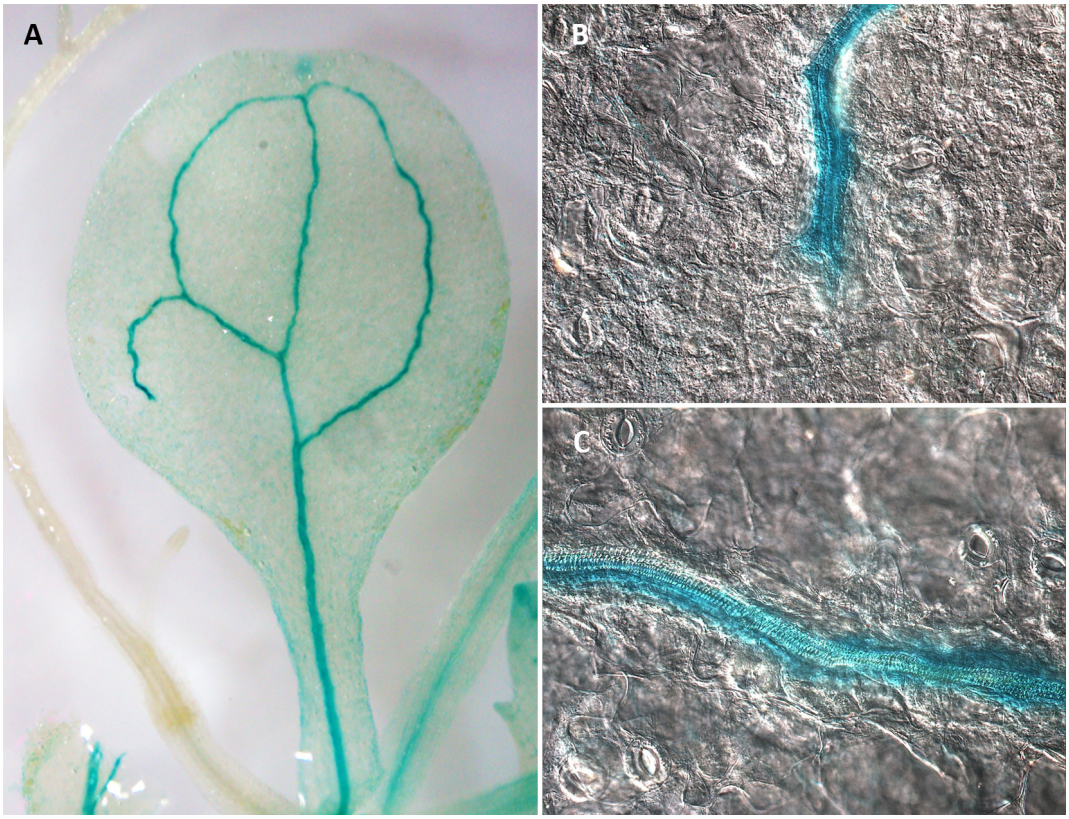

Figure 30. *Arabidopsis* seedling stably transformed with the *Prom$_{AtABCC13.1}$::AtABCC13.1$_{1-1750}$:GUS* construct (courtesy of Katsuhiro Shiratake) stained for GUS activity **(A)** Cotyledon and sections of the primary root **(B+C)** Phase-contrast microscopic pictures of a cotyledon with leaf veins displaying high GUS activities.

4.3.6 AtABCC13 subcellular localization

To elucidate the subcellular localization of AtABCC13, C-terminal GFP fusion constructs of the genomic (*35S::genomicAtABCC13.1:GFP*) and coding (*35S::cdsAtABCC13.1:GFP*) sequence of *AtABCC13* were generated and tested in transient (particle bombardment) and stable expression systems. In both systems, the expression of the GFP fusion constructs was under the control of a 35S promoter. Onion epidermal cells transiently transformed with *35S::cdsAtABCC13.1:GFP* showed a GFP fluorescence signal in the vacuolar membrane, but also in endosomal membrane compartments (Figure 31A).

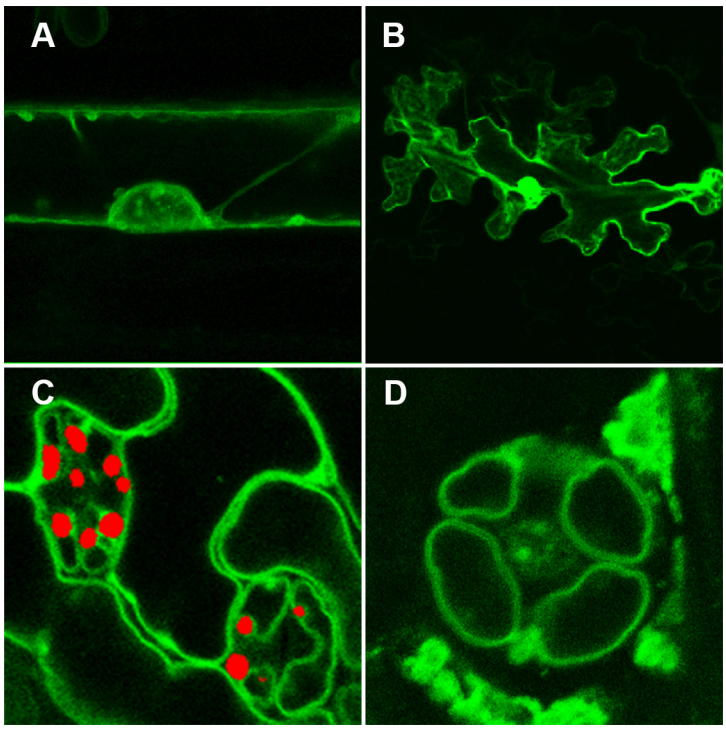

Figure 31. Confocal microscopy images of plant epidermal tissues transformed with *35S::AtABCC13:GFP* fusion constructs. **(A)** Onion epidermal cell transiently transformed with the *35S::cdsAtABCC13.1:GFP* construct. **(B)** *Arabidopsis* leaf epidermal cell transiently transformed with the *35S::genomicAtABCC13.1*$_{1188}$*:GFP* construct, which additionally harbors a 5' truncated genomic *AtABCC13.1* sequence. The arrow shows the mesh-like structure indicating ER localization. **(C-D)** Young rosette leaf epidermal cells from *Arabidopsis* plants stably transformed with the *35S::genomicAtABCC13.1:GFP* construct. Overlay imagine of the GFP signal and the chlorophyll auto-fluorescence. The arrow shows the membrane-localized GFP signal surrounding a chloroplast indicating vacuolar membrane localization (C). Detail image of a pair of guard cells (D). Constructs were courtesy from Tobias Kretzschmar (A, C, D) and Katsuhiro Shiratake (B), respectively.

However, when the *35S::cdsAtABCC13.1:GFP* construct was bombarded on *Arabidopsis* leaf epidermal cells, no transformed cells were detected. Likewise, the particle

bombardment of the *35S::genomicAtABCC13.1:GFP* construct did not result in any recognizable transformed epidermal cells, neither in onion nor in *Arabidopsis* leaf epidermal cells.

Additionally, a GFP-fusion construct with a 5' truncated genomic sequence of *AtABCC13,* lacking the first 1188 bp that presumably encode for the TMD0 (*35S::genomicAtABCC13*$_{1188-}$*:GFP*; see Material and Methods), was tested by transient transformation of *Arabidopsis* leaf epidermal cells. In transformed cells, the GFP signal had high intensities in the nucleus and in net-like structures (Figure 31B), corresponding to reported ER localization patterns (Held et al., 2008).

In stably transformed *Arabidopsis* plants, GFP signals were only observed in lines harboring the *35S::genomicAtABCC13.1:GFP* construct. In these lines, a strong GFP fluorescence was observed in the cotyledons and leaves of seedlings. On subcellular level, the GFP fluorescence showed a localization typical for the vacuolar membrane with the GFP signal surrounding the chloroplasts (Figure 31C) and with a pattern typical for fragmented vacuoles of guard cells (Figure 31D) (Gao et al., 2009). However, in adult plants, the GFP signal was undetectable. Plants stably transformed with the *35S::cdsAtABCC13.1:GFP* construct did not exhibit any GFP fluorescence.

4.3.7 Transport activities of AtABCC13 heterologously expressed in yeast

To test whether AtABCC13 transports the common ABCC substrates leukotriene C4 (LTC4) and taurocholate (see Discussion, Section 4.4.4), AtABCC13 was heterologously expressed in the yeast *Saccharomyces cerevisiae.* AtABCC13 was constitutively expressed in yeast cells using the yeast plasma membrane ATPase *PMA1* promoter of the yeast expression vector pDR195 (Rentsch et al., 1995). Total membrane microsomes were used for uptake experiments, as the intracellular localization of heterologously expressed AtABCC13 in yeast cells was not determined.

LTC4 uptake was tested at LTC4 concentrations between 0.14 to 1.07 nM (see figure legends). First, the experimental conditions for measuring LTC4 uptake were tested using microsomes of the *Δbat1* yeast strain, which lacks the ABCC gene *BAT1* (*YBT1*, YLL048C) encoding a bile acid transporter. The LTC4 uptake was proportional up to a vesicle concentration of 50 µL/mL vesicles of OD=4 (Figure 32A). The addition of an ATP-regeneration system (creatine kinase and creatine phosphate) increased the LTC4 uptake by a factor of 1.6 (Figure 32B). Consequently, for all uptake assays, creatine kinase/creatine phosphate, and a vesicle concentration of 50 µL/mL were used.

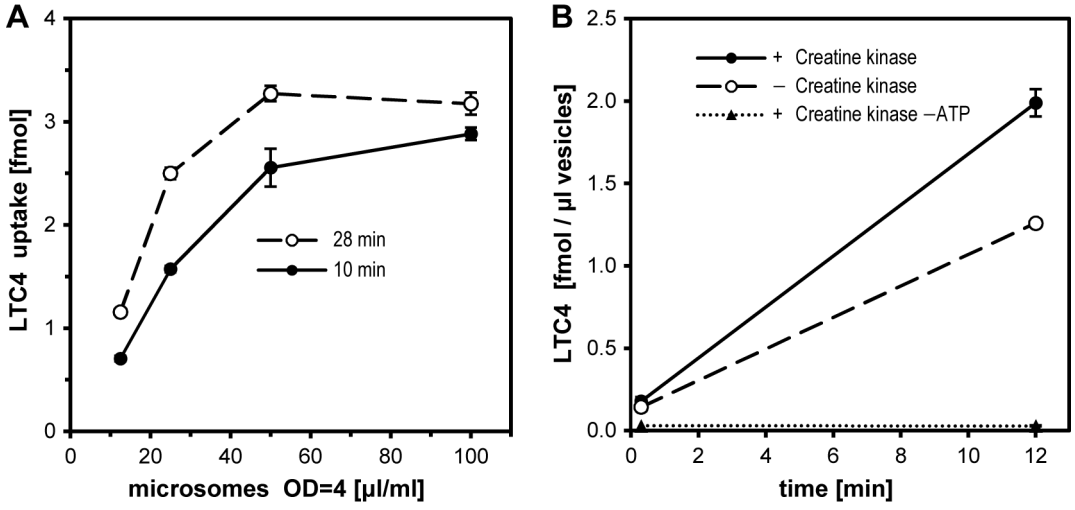

Figure 32. LTC4 uptake of *Δbat1* yeast microsomes. **(A)** Effect of the microsomal concentration on the LTC4 uptake measured after an incubation of 10 min (filled circles) and 28 min (open circles) in the presence of MgATP, but without creatine kinase and creatine phosphate. **(B)** Effect of creatine kinase (CK) and creatine phosphate (CP) on the LTC4 uptake in absence (triangle) and presence (filled circles) of MgATP, compared with uptake without CK and CP but in presence of MgATP (open circle). The LTC4 concentrations at the start of assays were 0.14 nM for (A) and 0.28 nM for (B).

Transformation of the *pPDR195-AtABCC13* construct into the *Δbat1* yeast strain did not result in an increased MgATP-depended LTC4 uptake of microsomes after 15 min, compared to a *Δbat1* strain transformed with the empty vector pPDR195 (EV). A slight increase in uptake compared to the EV strain was observed at 3 and 8 min. In absence of MgATP, the EV strain only showed a minimal LTC4 uptake (Figure 33A).

LTC4 transport in yeast has been shown to be predominantly mediated by the ABCC transporter YCF1 (Falcón-Pérez et al., 1999). Indeed, microsomes from the *Δycf1/Δbpt1* (YMK2) strain, which lacks *YCF1* and another *ABCC* gene, *BPT1,* showed a 6.7-fold reduced MgATP-dependent LTC4 uptake compared to microsomes from the *Δbat1* strain (Figure 33B). To analyze whether *AtABCC13* can complement LTC4 uptake, the *pPDR195-AtABCC13* construct was transformed into the *Δycf1/Δbpt1* yeast strain. Microsomes from this strain did not show any substantial differences in LTC4 uptake compared to microsomes from a *Δycf1/Δbpt1* line transformed with the empty vector (Figure 33B).

The bile acid taurocholate has been shown to be transported by the yeast ABCC transporter BAT1 (Ortiz et al., 1997). The yeast BAT1 knockout strain *Δbat1* showed a more than nine fold decreased microsomal taurocholate uptake compared to the *Δycf1/Δbpt1* strain, which contains a functional BAT1 (Figure 33C). The *pPDR195-AtABCC13* construct was transformed into the *Δbat1* strain to test whether it complements taurocholate uptake. This line did not exhibit an increased microsomal taurocholate uptake compared to the empty vector transformed *Δbat1* line (Figure 33C/D). Transformation of the *pPDR195-AtABCC13* construct into the *Δycf1/Δbpt1* strain, however, resulted in a 46% reduced microsomal uptake of taurocholate compared to the empty vector transformed strain (Figure 33D). Taurocholate uptake rates were measured at a taurocholate concentration o 504 µM.

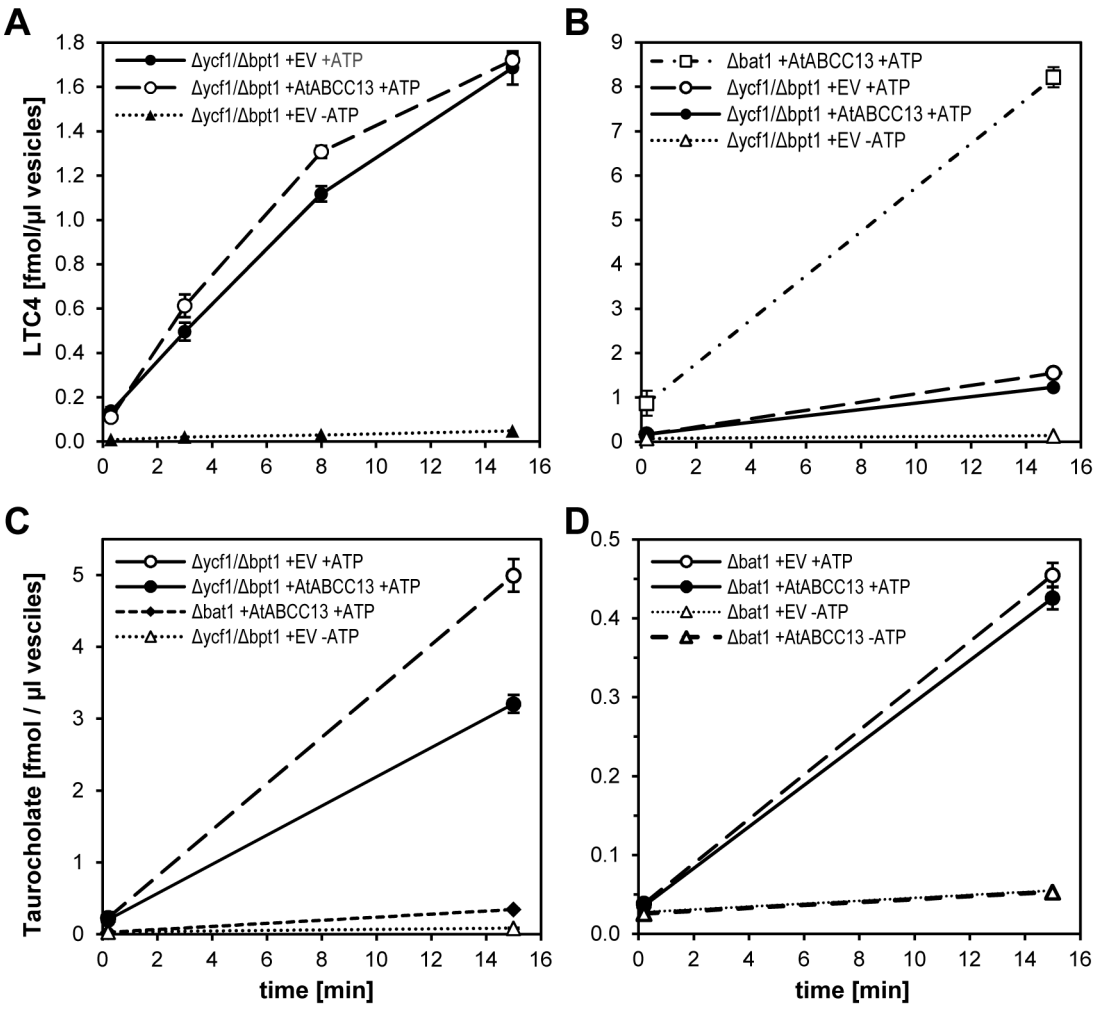

Figure 33. LTC4 and taurocholate uptake of *AtABCC13* or empty vector transformed yeast microsomes **(A+B)** LTC4 uptake of the *Δycf1/Δbtp1* (YMK2) strain (A) and the *Δbat1* strain (B), which were transformed with the *pDR195* empty vector (open symbols) or with the *pDR195-AtABCC13* construct (filled symbols), in absence (triangle) or presence of 4 mM MgATP (circles and square). The LTC4 concentrations at the start of the assays were 0.19 nM for (A) and 1.07 nM for (B). **(C+D)** Taurocholate uptake in microsomes from the *Δycf1/Δbtp1* strain (C) and *Δbat1* strain (C+D) transformed with the *pDR195* empty vector (open symbols) or with the *pDR195-AtABCC13* construct (filled symbols); in absence (triangle) or presence of 4 mM MgATP (circles and square). The taurocholate concentrations at the start of assays were 504 µM.

4.3.8 Selection and verification of homozygous *AtABCC13* knockout lines

Mutants homozygous for *atabcc13* insertions (named *atabcc13-1* and *atabcc13-2)* and corresponding wild-type lines (named WT-like-1 and WT-like-2) harboring two *AtABCC13* wild-type alleles were selected from segregating mutant populations by PCR-based genotyping. The *atabcc13-1* mutant harbors a DS transposon insertion within intron 22, and *atabcc13*-2 harbors a T-DNA insertion within exon 20, three base pairs before the 3'-exon/intron border. Both insertions are within the region encoding for the nucleotide-binding domain 1 (NBD1). The exact insertion sites were verified by sequencing the insertions' flanking regions (Figure 34).

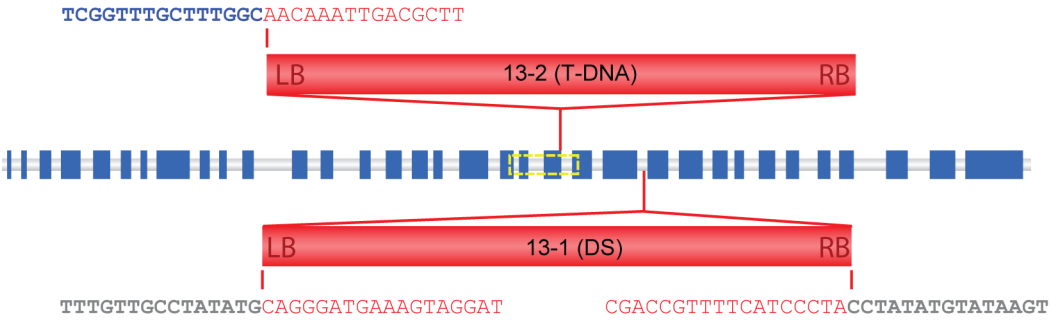

Figure 34. Insertion site of the Ds transposon in the *atabcc13-1* and the T-DNA in the *atabcc13-2* mutant lines. Sequences of insertion flanking regions are indicated for both borders of the *atabcc13-1* insertion and for the left border of the *atabcc13-2* insertion. Flanking insertion sequences are shown in red, exonic sequences in blue and intronic sequences in grey fonts. The yellow dashed box indicates the region encoding for the Walker A and B motifs of the nucleotide-binding domain 1 (see Figure 20).

Semi-quantitative RT-PCR was used to test mutant and wild-type lines for the absence or presence of *AtABCC13* wild-type transcript (Figure 35). Full-length cDNA from total RNA isolated from 2-week-old seedlings was synthesized by reverse transcription using oligo-(dT) primers. Primers used for subsequent PCR analyses were intron spanning and flanked the insertion sites. For the analysis of *atabcc13-1*, primers binding to exons 22 and 25, and for *atabcc13-2*, primers binding to exons 18 and 22 were used (see Results, Section 4.3.1). PCR reactions were performed with 34 cycles and an extension time of 90 seconds. Expected cDNA amplicon lengths were 472 bp for the *atabcc13-1* and 412 bp for the *atabcc13-2* specific PCR reactions. For genomic DNA, expected amplicon lengths were 635 and 751 bp, respectively. The *atabcc13-2* specific RT-PCR resulted in a second band additional to the expected band. This additional

band was also found in analyses of alternative splicing (see Results, Section 4.3.3). *AtABCC13* wild-type transcript was not detectable in both knockout lines. As a cDNA loading control and an additional check for genomic DNA contamination, PCRs specific for the *actin2* (At3g18780) gene were performed with 28 cycles using the same cDNAs used for the insertion specific PCR. Expected amplicon lengths were 302 bp for the cDNA and 388 bp for the genomic DNA.

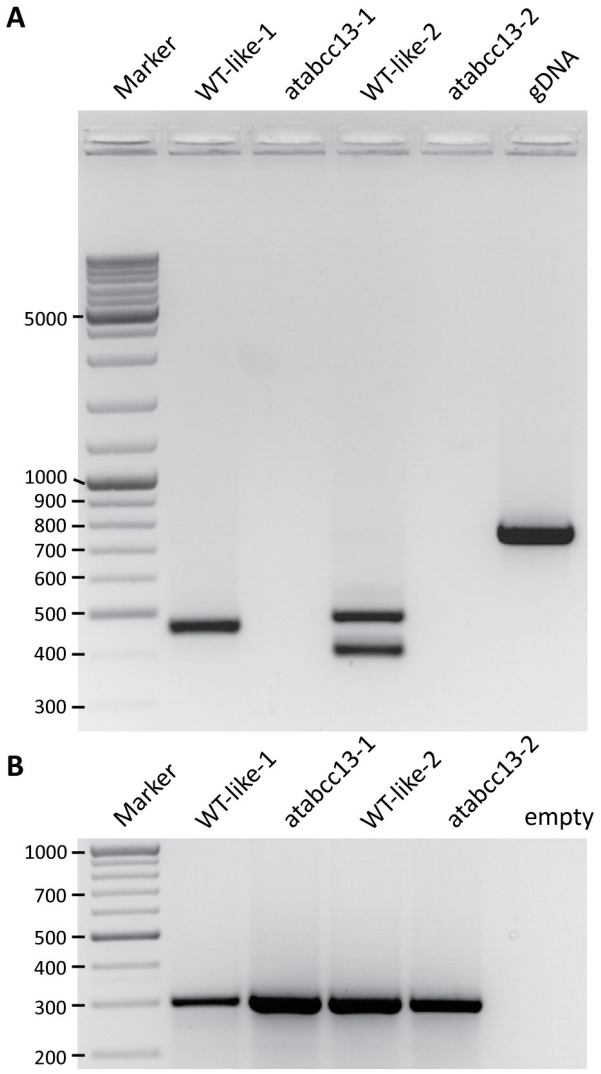

Figure 35. RT-PCR analyses of *AtABCC13* knockout mutant and corresponding wild-type plant lines. **(A)** RT-PCR using *atabcc13-1* and *atabcc13-2* insertion and intron spanning primers for the *AtABCC13* gene (34 cycles). The gDNA lane corresponds to genomic DNA amplified using the same primers as for the *atabcc13-2* specific RT-PCR **(B)** *Actin2* specific RT-PCR of the same cDNA used for A (28 cycles).

4.3.9 *AtABCC13* mutant phenotype screening

Both *AtABCC13* knockout lines (*atabcc13-1* and *atabcc13-2*) and their corresponding wild-type lines were screened for differential responses to various conditions (Table 9). The genotypes of mutant and wild-type lines were regularly verified. Depending on the test, plant growth, development and appearance, root length, lateral root number and development, flowering time, silique ripening, seed germination and seed production were qualitatively examined and compared without statistical evaluation. In all tested conditions, the two *AtABCC13* knockout lines did not exhibit any differences in the analyzed parameters (Table 9) compared to the corresponding wild-type lines.

Table 9. Summary of conditions under which *AtABCC13* knockout lines were screened for altered phenotypes. G: germination rate, P: plant growth and appearance, L: lateral root number and appearance

Category	Treatment	Tested conditions	Examined parameters
Dormancy	Dormancy + Germination	non-stratified, stratified seeds	G, P
Environmental stress	Heat	30/37 °C	P
	Cold	4 °C	P
	High light + temperature	700 µmol m^{-2} s^{-1} and 26 °C	G/P
	Osmotic stress	-0.5, -0.7, -1.2 MPa (PEG plates)	G, P, L
	pH	pH 4.0, 4.2, 4.5, 7.6	G, P
	Glucose 6%	60 g/L	P
Nutrient deficiency	Sulfur deficiency	no S , 1/10 of normal [S] of ½MS	G, P
	Nitrogen deficiency	no N, 50 mM KNO_3	G, P
Phytohormones	ABA	0.5 µM (non-stratified, stratified seeds)	G, P
	ABA	1, 3 µM on lateral root growth	L
	Tetcyclasis	1, 3, 10 µM	G, P
	Epibrassinolide	1, 3, 10, 30, 100, 300 nM	G, P, L
	Zeatin-Glucoside	30, 100 µM	G, P
	NAA	100 nM	G, P, L
	IBA	3, 10 µM	G, P, L
Salt stress, Toxic ions	$LiCl_2$	10 mM	G, P
	$LaCl_3$	1 µM	G, P
	$MnSO_4$	100 µM	G, P
	$CsCl_2$	300 µM	G, P
	$ZnSO_4$	500 µM	G, P
	$CaCl_2$	50, 75 µM	G, P
	NaCl	0, 100, 120, 150, 200 mM	G, P
Oxidative stress	Paraquat	0, 0.2, 0.5 µM	G, P
Genotoxic conditions	$AlCl_3$	0, 30, 100, 300 µM	G, P
	UV-B	30, 60, 120, 300, 600 s	P
	UV-C	1 x 15, 30, 50 and 3 x 3 kJ m^{-2}	P
	5-Fluorouracil	0, 10, 30, 100, 200, 500, 1000 µM	G, P
	Cisplatin	0, 0.1, 1, 5, 10, 20, 30 µM	G, P
	5-Flurouridine	0, 10, 30, 100, 200 µM	G, P

Table 9 (continued). Summary of conditions under which *AtABCC13* knockout lines were screened for altered phenotypes

Category	Treatment	Tested conditions	Examined parameters
	Ara-C	0, 1, 10, 30, 50, 100, 500 µM	G, P
	MMS	0, 20, 40, 60, 100 ppm	P
	Hydroxyurea	0, 1, 5, 10 mM	P
	Adenine	0, 0.5, 1, 1.5, 2 mM	G, P
Miscellaneous	Trichostatin A (HDAC inhibitor)	0, 0.5, 2, 10, 30 µM	G, P, L
	Oryzalin (microtubuli depolymeriser)	0, 0.1, 0.3, 1, 10 µM	G, P, L
Senescence	Individual leaves shaded		C
	H_20 + dark		C
	Kinetin + dark	50 µM	C
	Methyljasmonate + dark	10 µL/L	C
	Ethylene + dark	1 mM ethephon	C
	Gibberellin A3 + dark	10 µM	C

4.4 Discussion

4.4.1 Genetic characteristics of *AtABCC13*

The sequences of two distinct *AtABCC13* cDNAs clones were analyzed. The *AtABCC13.1* cDNA had been cloned from a size-selected cDNA library of *Arabidopsis* seedlings (courtesy of Tobias Kretzschmar); the *AtABCC13.2* cDNA had been cloned from adult rosette leaf total cDNA (courtesy of Miyoung Lee). The *AtABCC13.1* coding sequence has a comparable length to other analyzed *ABCCs* genes and comprises all regions conserved in analyzed *ABCC* genes. The *AtABCC13.2* sequence lacks a 75 bp segment within the 5' region, which is present and conserved in all other analyzed *ABCC* sequences. Consequently, the *AtABCC13.1* cDNA and its deduced coding sequence and genomic structure were used for designing and cloning of *AtABCC13-GFP* and *AtABCC13* promoter-GUS fusion constructs, and for sequence analyses.

The *AtABCC13.1* cDNA has a deduced open-reading frame of 4281 bp, which is flanked by a 50 bp 5'-UTR and a 76 bp 3'-UTR. It encodes for a 1427 amino acid protein, which corresponds to the length of 'long' ABCC proteins from Arabidopsis and human that comprise a TMD0 domain (Klein et al., 2006; Tusnády et al., 2006). Moreover, the entire *AtABCC13.1* sequence aligns to sequences of 'long' *ABCCs*, therefore it presumably comprises a region encoding the transmembrane domain 0 (TMD0). These findings are in contrast to earlier publications describing *AtABCC13* to be truncated in the 5' region and hence to lack a coding region for the TMD0 (Kolukisaoglu et al., 2002; Verrier et al., 2008; Wanke and Kolukisaoglu, 2010). These publications, however, were based on older TAIR (http://www.arabidopsis.org) models of the *AtABCC13* gene, which had no cDNA and EST support.

The *AtABCC13.1* cDNA is encoded by 34 exons that span a genomic region of 7718 bp. The presence of 34 introns distinguishes *AtABCC13* from all other *Arabidopsis ABCC* genes, which have fewer introns and do not share any conserved intron positions with *AtABCC13*. On the other hand, most of the *AtABCC13* intron positions are conserved in the *AtABCC13* ortholog of rice, *OsABCC12,* whereby two introns found in *OsABCC12*

have presumably been lost in *AtABCC13*. The intron-density of *AtABCC13.1 with* 7.94 introns/kb coding sequence is considerably higher than the average 2.38 introns/kb of *Arabidopsis* genes (calculated based on the average exon length obtained from TAIR10 Gene Annotation Data, http://www.arabidopsis.org/portals/genAnnotation) and the median 6.2 introns/kb (95% CI = 6.1 – 6.2) of angiosperm genes (Csuros et al., 2011). A recent intron-gain appears to be unlikely, as intron-gain rates during plant evolution were low (Roy and Penny, 2007). However, the high intron-density of *AtABCC13* may be the consequence of its ancient evolutionary origin (see Discussion of Chapter I, Section 3.4.2), as it has been shown that many evolutionarily conserved genes originally were intron-rich (Roy and Gilbert, 2005) and/or accumulated introns during their early evolution (Carmel et al., 2007).

AtABCC13 and its rice ortholog *OsABCC12* both harbor an U12-dependent intron as the second intron. The positions and the flanking regions of the U12-dependent intron insertions are conserved between *AtABCC13* and *OsABCC12*. U12-dependent introns represent a low-abundance class of introns that are spliced by the U12-type spliceosome (Hall and Padgett, 1994; Tarn and Steitz, 1996). They are characterized by conserved branch point and branch splice sites. U12-class introns may possess non-canonical terminal dinucleotides, including AT-AC, however the universal GT-AG terminal dinucleotides were also found (Lewandowska et al., 2004; Lin et al., 2010). In the *Arabidopsis* genome, only 216 U12-dependent introns were identified (Lin et al., 2010). U12 introns have been implicated in alternative splicing in plants and humans, whereby in some cases the alternative splicing was found to be tissue-specific (Zhu and Brendel, 2003; Lewandowska et al., 2004; Chang et al., 2007). Moreover, U12-dependent introns were implicated in the post-transcriptional regulation of gene expression (Patel et al., 2002). However, RT-PCR analyses of *Arabidopsis* rosette leaf total RNA did not reveal any *AtABCC13* transcript variants in which the U12-dependent intron was retained. Correspondingly, the U12-dependent intron was also spliced out of transcripts from a stably transformed construct harboring the first eight exons of *AtABCC13* fused to a GUS gene under the transcriptional control of the *AtABCC13* native promoter. In *AtABCC13*, retention of the 98 bp long U12-dependent intron

causes a frameshift resulting in premature stop codons. The mRNA comprising these stop codons might be subject to nonsense-mediated mRNA decay (McGlincy and Smith, 2008) and may therefore not have been detectable by RT-PCR analyses. Consequently, the U12-dependent intron in *AtABCC13* might be involved in post-transcriptional regulation of *AtABCC13* expression. Interestingly, the U12-dependent intron in the rice *OsABCC12* has a length of 129 bp, thus retention of this intron does not cause a frameshift.

The cloned *AtABCC13.2* cDNA represents a splice-variant of *AtABCC13*. It lacks a 75 bp segment within the 5' region that is encoded by exon 10 and parts of exon 9 of the *AtABCC13.1* gene model. This segment encodes for a region corresponding to the N-terminal half of the second transmembrane helix (TM) of the transmembrane domain 1 (TMD1) of human HsABCC1 and HsABCC10. This transmembrane helix represents the TM7 of the human HsABCC1 protein (DeGorter et al., 2008), of which residues have been shown to be involved in substrate binding and specificity (Koike et al., 2002; Wu et al., 2005). However, there are no reports on ABCC variants that have deletions within the TM7, neither in *Arabidopsis* nor in other species. Even though *AtABCC13.2* was cloned from leaf total RNA, RT-PCR analyses with primers annealing to the exons spanning this segment resulted in no detectable product with this segment missing. Furthermore, this segment was found to be present in a cDNA sequence of the *AtABCC13* ortholog in *Catharanthus roseus* (EMBL CAO94660.1), which is so far the only experimentally determined full-length cDNA sequence of a plant *AtABCC13* ortholog deposited in public databases. *AtABCC13.2* may therefore represent a minor splice-variant that was cloned by chance, and/or that was cloned from a sample in which this transcript variant was present in higher abundance. Consequently, the physiological and functional significance of the *AtABCC13.2* splice-variant is unknown.

RT-PCR analyses of rosette leaf total RNA revealed two distinct transcript fragments from a region spanning exons 21 and 22 that encode parts of the NDB1. Both transcripts appeared to be present at similar abundance. One transcript fragment has a size corresponding to the estimated size based on the *AtABCC13.1* gene model. The

second fragment is approximately 100 bp longer. No transcripts corresponding to any of these two fragments were identified in the *Arabidopsis atabcc13-1* mutant line, which harbors a transposon insertion in the intron downstream of exon 22, indicating that the second amplified fragment is not the result of nonspecific primer binding. The amplified longer fragment has to be sequenced in order investigate whether the 86 bp intron between exons 21 and 22 is retained. Retention of this intron would cause a frameshift. Consequently, the full-length sequence of the transcript variant harboring this additional sequence between exons 21 and 22 has to be determined to elucidate whether this transcript represents a functional *AtABCC13* transcript.

Another alternatively spliced region of *AtABCC13.1* was identified in plants transformed with the $Prom_{AtABCC13.1}$*::AtABCC13.*$1_{1\text{-}1188}$*:GUS* construct. Using RT-PCR with primers specific for this construct, partial intron-retention of the 75 bp intron between exons 7 and 8 was detected. The retention of this intron does not cause a frameshift. Nevertheless, an RT-PCR analysis of rosette leaf total RNA from wild-type plants did not reveal any transcript fragment with an intron-retention between exons 7 and 8. The fusion of the GUS gene 54 bp downstream from the 5' end of exon 8 might affect the splicing efficiency of the preceding intron and may therefore lead to partial intron-retention and to the presence of two different transcripts. Hence, no conclusions on the occurrence and significance of alternative splicing of intron 8 in wild-type plants can be made based on these data.

However, RT-PCR analysis on rosette leaf total RNA from wild-type plants revealed that transcript segments originating from the *AtABCC13* 5' region comprising the first eight exons are significantly lower expressed compared to those originating from downstream regions of *AtABCC13*. This might be explained by a lower efficiency of the reverse transcription of long transcripts in RT-PCR protocols that use oligo-(dT) primers (Hawkins et al., 2003). Alternatively, truncated *AtABCC13* transcript variants may be overrepresented compared to full-length *AtABCC13* transcripts. The RT-PCR amplifications of downstream segments of *AtABCC13* may therefore have resulted in more PCR product compared to amplifications of *AtABCC13* 5' segments. This

hypothesis is supported by the findings obtained from the expression of the *Prom$_{AtABCC13.1}$::AtABCC13.1$_{1-1750}$:*GUS construct in plants. In this construct, the GUS gene is fused to the first 1750 bp of the *AtABCC13.1* genomic sequence. The last 89 bp of *AtABCC13.1$_{1-1750}$*, which precede the GUS gene, belong to the 5' end of the 290 bp intron 11. It is likely that this partial intronic sequence is retained in the mRNA from the *Prom$_{AtABCC13.1}$::AtABCC13.1$_{1-1750}$:GUS* construct, as a 3' splice site is presumably missing in this partial intron. With this intronic sequence, the GUS gene of the *AtABCC13.1$_{1-1750}$:GUS* construct is out-of-frame. However, plants stably transformed with this construct exhibited strong GUS expression in vascular tissues (see Results, Section 4.3.5). Therefore, the expression of functional GUS apparently must be the result of an alternative transcription start site in the *AtABCC13* locus. Taken together, these data indicate the existence of truncated *AtABCC13.1* gene transcripts, which might even be present at higher abundance than the full-length *AtABCC13.1* transcript.

4.4.2 Expression patterns of *AtABCC13*

Seedlings harboring a *AtABCC13* Promoter-GUS construct (*Prom$_{AtABCC13.1}$::GUS*) displayed strong GUS activities in the root central cylinder, emerging lateral roots, in vascular bundles of leaves and stems, and lower but ubiquitous activities in other tissues. Seedlings harboring the previously discussed *AtABCC13* Promoter-GUS fusion construct that additionally comprises the first 1750 bp of the *AtABCC13.1* genomic sequence (*Prom$_{AtABCC13.1}$::AtABCC13.1$_{1-1750}$:GUS*), had less GUS activity in mesophyll tissues and in the root central cylinder compared to *Prom$_{AtABCC13.1}$::GUS* plant lines. This difference in GUS expression apparently is the result of alternative transcription start sites present in the *Prom$_{AtABCC13.1}$::AtABCC13.1$_{1-1750}$:GUS* construct (see Discussion, Section 4.4.1), and, possibly, also of altered promoter activities due to presence of additional genomic sequence. The N-terminal AtABCC13 fragment fused to the GUS protein, which presumably comprises transmembrane helices, might also influence the GUS expression and distribution.

Analysis of publicly available microarray data using Genevestigator (Hruz et al., 2008) revealed that transcripts of *AtABCC13* and its *Glycine max* ortholog *GmABCC10* were

present in all organs and in most tissues specified by Genevestigator. In sporophytic tissues, the highest expression values of *AtABCC13* and *GmABCC10* were found in the pericycle. These data are in accordance with the observed high GUS activities in the root central cylinder and emerging lateral roots of plants transformed with the *Prom$_{AtABCC13.1}$::GUS* construct. The pericycle represents the outmost layer of the root central cylinder, which is formed in *Arabidopsis* by approximately 12 cells (Dolan et al., 1993). The pericycle cells are not all identical; they rather possess different properties, i.e. different cell cycle state, cell division competence, plasmodesmatal connections, and gene expression patterns, depending on their position (Parizot et al., 2008). A specific subset of pericycle cells can postembryonically differentiate into lateral root primordia that develop into lateral roots (Péret et al., 2009). Elevated *AtABCC13* and *GmABCC10* expression levels were also found in other tissues. In *Glycine max*, particularly the plumule, which harbors the embryonic shoot meristem, displayed high *GmABCC10* expression values. In the vascular bundles of embryonic cotyledons, in the embryonic shoot and root meristems, and in the shoot apical meristem, *GmABCC10* expression levels were elevated as well. In *Arabidopsis*, *AtABCC13* expression was elevated in the shoot apex and root tip. Furthermore, GUS activity was higher in leaf vascular bundles compared to the leaf mesophyll tissue of plants transformed with the *Prom$_{AtABCC13.1}$::GUS* construct. These findings indicate an elevated transcriptional activity of *AtABCC13*/*GmABCC10* in tissues containing meristematic cells, such as the shoot meristem and vascular cambium.

The other tissues with high *AtABCC13*/*GmABCC10* expression values were the chalazal seed coat of *Arabidopsis* and the inner integument parenchyma of *Glycine max*. In early pre-globular and globular seed stages, *AtABCC13* transcript was only present in the chalazal seed coat and in the embryo. At later embryo developmental stages, *AtABCC13* expression was also observed in the general seed coat and in the dividing peripheral endosperm cells. The chalazal seed coat develops from the chalaza. The chalaza is the sporophytic tissue of the ovule, from which the integuments, the progenitors of the seed coat, emerge and differentiate (Groß-Hardt et al., 2002). The chalaza thus also represents a tissue with meristematic activity.

Wuest et al. (2010) analyzed the transcriptomes of *Arabidopsis* female gametophytic tissues and compared them with reanalyzed publicly available *Arabidopsis* microarray data. Within these data, *AtABCC13* gene expression levels were found to be distinctively high in egg cells and increased in the developing embryo, while being low in other gametophytic and sporophytic tissues. The *AtABCC13* expression levels in egg cells are four times higher than in the root pericycle, which is the tissue with the second highest *AtABCC13* expression level identified in this analysis. Similarities in expression patterns between female gametes of plant and animals have been revealed by Wuest et al. (2010). Therefore, the question was raised, whether transcripts of *AtABCC13* orthologs are also present in high abundance in oocytes of animals. However, the transcript level of the human *AtABCC13* ortholog *HsABCC10* was not significantly increased in human oocytes (Kocabas et al., 2006; Reich et al., 2011).

In summary, *AtABCC13* was particularly highly expressed in unfertilized egg cells and in many tissues comprising cells with mitotic activity or meristematic potential. In other tissues, *AtABCC13* was expressed at low levels.

4.4.3 Subcellular localization of AtABCC13

The subcellular localization of AtABCC13 was studied using N-terminal GFP fusion constructs under the control of a 35S promoter. AtABCC13 was localized to the tonoplast when overexpressed as a genomic *AtABCC13.1:GFP* fusion construct. However, plants transformed with *AtABCC13 cDNA:GFP* fusion constructs did not display any GFP fluorescence signal. This may be due to post-transcriptional silencing resulting from abnormal high *AtABCC13 cDNA* transcript levels caused by the 35S-driven overexpression that activate the post-transcriptional antiviral defense system (Vaucheret et al., 1998). Likewise, the overexpression may also lead to an enhanced degradation of the fusion protein. Introns were shown to be involved in regulation of gene expression and specific introns were implicated in the intron-mediated enhancement (IME) of mRNA accumulation (Rose, 2008). Consequently, the genomic *AtABCC13.1:GFP* fusion construct may contain introns involved in IME, which enhance the *AtABCC13.1:GFP* expression sufficiently enough to detect GFP fluorescence.

Furthermore, it may be possible that in plants transformed with the genomic *AtABCC13.1:GFP* construct, the observed GFP signal originated from *AtABCC13:GFP* variants that were alternatively spliced or had different transcriptional starts compared to the *AtABCC13.1* cDNA.

The transient expression of the genomic *AtABCC13.1:GFP* fusion construct was not successful. The construct harboring the full genomic *AtABCC13* fragment may be too long for efficient transcription under the employed conditions. Alternatively, splicing under transient expression conditions may not have worked properly and yielded too low levels of functional transcript. However, transient transformation of Arabidopsis leaves with the 5' truncated genomic *AtABCC13.1:GFP* fusion construct (*35S::genomicAtABCC13.1*$_{1188\text{-}}$*:GFP*) resulted in a GFP signal typical for ER-typical localization pattern. This truncated genomic *AtABCC13*$_{1188\text{-}}$ sequence encodes for an AtABCC13.1 protein lacking the first 207 amino acids and thus presumably lacks the TMD0. This suggests that the TMD0 might be involved in the targeting of AtABCC13. However, since the localization of the full-length AtABCC13:GFP construct could not be determined in this transient expression system, no definite conclusions can be drawn on the role of TMD0 in membrane targeting of AtABCC13.

The tonoplast localization of the genomic AtABCC13.1:GFP fusion product suggests that the evolutionarily conserved AtABCC13 already exhibited a tonoplast localization, corresponding to the tonoplast localization of other characterized plant ABCCs that appeared later in evolution (Nagy et al., 2009; Song et al., 2010; see also Discussion of Chapter I, Section 3.4.3).

4.4.4 Transport activities of AtABCC13 heterologously expressed in yeast

Leukotrienes are fatty acid signaling molecules derived from arachidonic acid. The glutathione *S*-conjugated Leukotriene C4 (LTC4) belongs to the cysteinyl leukotrienes, which additionally comprise a cysteine in their structure (Berg and Stryer, 2006a). LTC4 has been shown to be a substrate of several characterized ABCC transporters such as of the human HsABCC1 (Leier et al., 1994), HsABCC2 (Cui et al., 1999), HsABCC3 (Zeng et al., 2000), HsABCC4 (Yang et al., 2003), HsABCC6 (Belinsky et al., 2002), HsABCC11

(Chen et al., 2005) and the yeast YCF1 (Falcón-Pérez et al., 1999). The bile acid taurocholic acid is a taurin (2-aminoethanesulfonic acid)-conjugated choline (Berg and Stryer, 2006b). Taurocholate, the salt of taurocholic acid, is a substrate of several ABCC transporters, such as of the HsABCC11 (Chen et al., 2005), the rat ABCC3 (Hirohashi et al., 2000) and the yeast BAT1 (Ortiz et al., 1997).

Since AtABCC13 represents an evolutionarily conserved ABCC protein, it was analyzed for its ability to mediate transport of the common ABCC substrates Leukotriene C4 and taurocholate. To assess this, AtABCC13 was heterologously expressed in the two different *Saccharomyces cerevisiae* strains: *Δycf1/Δbtp1* (YMK2), which lacks the yeast endogenous LTC4 transporter YCF1, and *Δbat1*, which lacks the yeast endogenous taurocholate transporter BAT1. Uptake was assayed using total membrane microsomes to include all membranes where AtABCC13 might be expressed, as the intracellular localization of heterologously expressed AtABCC13 in yeast cells was not determined.

LTC4 uptake was strongly MgATP-dependent, but nine-fold reduced in microsomes from the *Δycf1/Δbtp1* (YMK2) strain, compared to microsomes from the *Δbat1* strain. Transformation of *AtABCC13* into both of these strains did not result in any detectable enhanced microsomal LTC4 uptake compared to microsomes from strains transformed with the corresponding empty vector. The reported K_m for LTC4 transport varied between 97 nM for human HsABCC1 and 820 nM for yeast YCF1 (Leier et al., 1994; Falcón-Pérez et al., 1999). A low and not always consistent LTC4 transport activity was also reported for the human AtABCC13 ortholog HsABCC10 expressed in HEK293 cells (Chen et al., 2003). The LTC4 concentrations used in the presented yeast microsomal uptake experiments were only approximately 1 nM, therefore a possibly low-affinity LTC4 transport by AtABCC13 may have been undetectable under the employed experimental conditions. Due to the cost of labeled LTC4, uptake experiments with higher LTC4 concentrations were not performed.

Taurocholate uptake was also strongly MgATP-dependent in microsomes from the *Δycf1/Δbtp1* and *Δbat1* strains, but was six to ten-fold reduced in *Δbat1* strain

microsomes. Transformation of *AtABCC13* into the *Δbat1* strain did not result in any detectable enhanced microsomal taurocholate uptake compared to microsomes from the *Δbat1* strain transformed with the corresponding empty vector, both in presence and in absence of MgATP. The transformation of *AtABCC13* into the *Δycf1/Δbtp1* strain resulted in a 46% decreased microsomal taurocholate uptake compared to the empty vector transformed *Δycf1/Δbtp1* strain. However, the uptake rate was still nine times higher compared to *AtABCC13* transformed into the *Δbat1* strain. This might be due to the expression of *AtABCC13* in the *Δycf1/Δbtp1* strain, which may interfere with the BAT1 transporter or cause artifacts in the vesicle preparation. The taurocholate concentrations used in the assays were 500 µM, which is approximately eight times higher than the apparent K_m of 63 µM of the yeast endogenous taurocholate transporter BAT1 (Ortiz et al., 1997). The taurocholate concentration should therefore have been sufficient to detect transport activities also of low affinity taurocholate transporters.

In summary, heterologously expressed AtABCC13 did not exhibit any transport activities for the amphipathic compounds LTC4 and taurocholate under the tested conditions. It is possible that the used substrate concentrations were too low to detect low-affinity transport, at least in the case for LTC4. Additionally, the actual expression levels and the amount of correctly folded and post-translationally modified AtABCC13 in the yeast cells used for microsome preparations were unknown. It may therefore be that the amount of functional AtABCC13 in the yeast microsomal preparation was too low to measure transport of LTC4 and taurocholate. On the other hand, lack of transport affinities for LTC4 and/or taurocholate was shown for several human ABCC transporters (Keppler, 2011). However, the human AtABCC13 ortholog ABCC10 was shown to transport the glucuronated steroid 17β-estradiol-(17-β-d-glucuronide) ($E_2$17βG) at a much higher than LTC4 when ectopically expressed in HEK293 cells (Chen et al., 2003). $E_2$17βG uptake by AtABCC13 has not yet been tested, but compounds of this family or other glucuronides may represent interesting candidates for *AtABCC13* substrates. Given the evolutionary conservation of *AtABCC13* in plants and animals, it

is probable that *AtABCC13* transports compounds with shared structural determinants that occur in both kingdoms.

4.4.5 Characterization of *AtABCC13* knockout plants

The drug resistance profile of the human AtABCC13 ortholog ABCC10 and the fact that other human ABCC transporters were also implicated in resistance to cytotoxic compounds including cisplatin and 5-fluorouracil (Cui et al., 1999; Guo et al., 2003) lead to the hypothesis that AtABCC13 may also have a function in responses of *Arabidopsis* to genotoxic and cytotoxic compounds. To test whether AtABCC13 confers *in vivo* resistance to exogenously applied cytotoxic compounds and to elucidate its endogenous function, *Arabidopsis* plants knocked-out in *AtABCC13* were screened for differential responses to treatments with cytotoxic and genotoxic compounds, and to a wide range of additional compounds and abiotic conditions. Given the high *AtABCC13* expression in the pericycle, chalazal seed coat and egg cell, several conditions focused on seed germination and lateral root formation. Other conditions aimed to investigate whether the general abiotic stress tolerances were affected.

Two independent *AtABCC13* transposon/T-DNA insertion lines (*atabcc13-1* and *atabcc131-2*) in different backgrounds (Nossen-0 and Columbia-0) were compared with their corresponding wild-types lines. Both lines carried the insertion in a region encoding for the nucleotide domain 1. The insertion was located within an intron of the *atabcc13-1* and within an exon of the *atabcc13-2* line. In RT-PCR analyses, transcript corresponding to the wild-type *AtABCC13* allele was completely absent in both knockout lines. *AtABCC13* knockout and wild-type plants were qualitatively identical with respect to seed dormancy, germination, seedling development, plant appearance, growth rate, root length, lateral root formation, flowering time, seed production, and senescence. Likewise, no differences were identified in the tested genotoxic and/or cytotoxic conditions, abiotic stress treatments (i.e. osmotic, salt, heat and cold, high light and pH), phytohormone treatments (i.e. ABA, epibrassinolide, zeatin-glucoside, NAA), treatments with toxic ions and oxidative stress inducing compounds, growth conditions with sulfur and nitrogen-deficient media, senescence

assays and other conditions mentioned. The absence of any phenotype identified in this screening is supported by Hanada et al. (2009), who analyzed single-copy and duplicate gene knockout effects in *Arabidopsis*. In this article, the *AtABCC13* knockout line was classified as having no seed, reproductive, vegetative, and conditional phenotypes. In addition, transgenic mice in which the mouse *AtABCC13* ortholog *MmABCC10* was knocked out, were reported to be healthy and to exhibit no observable phenotype under normal breeding conditions (Hopper-Borge et al., 2011).

The presence of single-copy *AtABCC13* orthologs in all plant, almost all animal and specific protozoan species indicate conserved functions of *AtABCC13* in universal, early-evolved processes. The strong selection against duplication of *AtABCC13* throughout its evolution could be the result of gene-dosage constraints (Veitia et al., 2008). It has been shown that dosage imbalances of multi-protein components resulting from gene duplications may be deleterious and decrease fitness (Veitia, 2002; Papp et al., 2003; Veitia et al., 2008). Similarly, it has been demonstrated that genes encoding for under-wrapped proteins, which are proteins requiring stabilization by interaction with other proteins, have a decreased duplicability (Liang et al., 2008). In *Arabidopsis*, knockouts in single-copy genes were shown in a study by Hanada et al. (2009) to have significantly higher ratio of phenotypic effects than knockouts of individual duplicated genes. Nevertheless, the overall proportion of knockouts with identified phenotypes was only 13% for single-copy and 5% for duplicate genes in this study. Functional redundancy resulting from paralogous ABCC proteins may explain the absence of a detectable phenotype in *AtABCC13* knockout lines. Alternatively, and more likely, the specific conditions to reveal phenotypes of *AtABCC13* mutants have not been found in this screening. Due to limited resources and time, only a restricted number of conditions were tested. Conditions such as biotic stress and different growth conditions were not included. Furthermore, phenotypes were generally qualitatively scored, without quantification and statistical evaluation. Weak phenotypes may therefore have been undetected in the screening.

4.4.6 Summary

The evolutionarily conserved *Arabidopsis* ABCC/MRP-type ABC protein AtABCC13 was characterized with respect to genetic and functional properties. In contrast to earlier publications, sequence analyses revealed that AtABCC13 represents a full-length ABCC protein that harbors a putative TMD0, a feature typical for specific ABCCs. There are evidences for *AtABCC13* transcript variants resulting from alternative transcription starts and from alternative splicing, i.e. from intron retention. The gene structure of *AtABCC13* comprises 33 introns, distinguishing it from other *Arabidopsis ABCC* genes and possibly reflecting its ancient evolutionary origin. The second intron belongs to the rare U12-dependent intron family, which has been implicated in alternative splicing and post-transcriptional regulation. However, there was no evidence for alternative splicing of this intron in *AtABCC13*. AtABCC13 was localized to the vacuolar membrane as a C-terminal GFP fusion protein in stably transformed plants, which corresponds to the tonoplast localization of already characterized *Arabidopsis* ABCCs. *AtABCC13* promoter-GUS activity was ubiquitous but highest in vascular veins, root central cylinder and in lateral roots. Microarray data on *AtABCC13* expression indicated a ubiquitous but low expression in most organs and tissues. However, distinctive high *AtABCC13* expression levels were identified in the egg cell, chalazal seed coat and root pericycle. Microarray data from the *AtABCC13* ortholog in *Glycine max* displayed similar patterns of expression. These data indicate a higher *AtABCC13* expression in tissues with potential or actual meristematic/mitotic activities. Heterologously expressed AtABCC13 in yeast did not mediate the transport of leukotriene C4 and taurocholate, two common substrates of several human and yeast ABCCs. Two independent *Arabidopsis AtABCC13* knockout lines were screened for differential responses to various abiotic and chemical treatments, including cytotoxic compounds for which the human AtABCC13 ortholog HsABCC10 was shown to confer resistance. None of the tested conditions revealed differences between the *AtABCC13* knockout lines and wild-type plants. Given the data obtained within this project, no conclusions on the endogenous function and substrate of AtABCC13 can be made.

4.5 Supplementary Information

4.5.1 *PromAtABCC13::GUS* construct

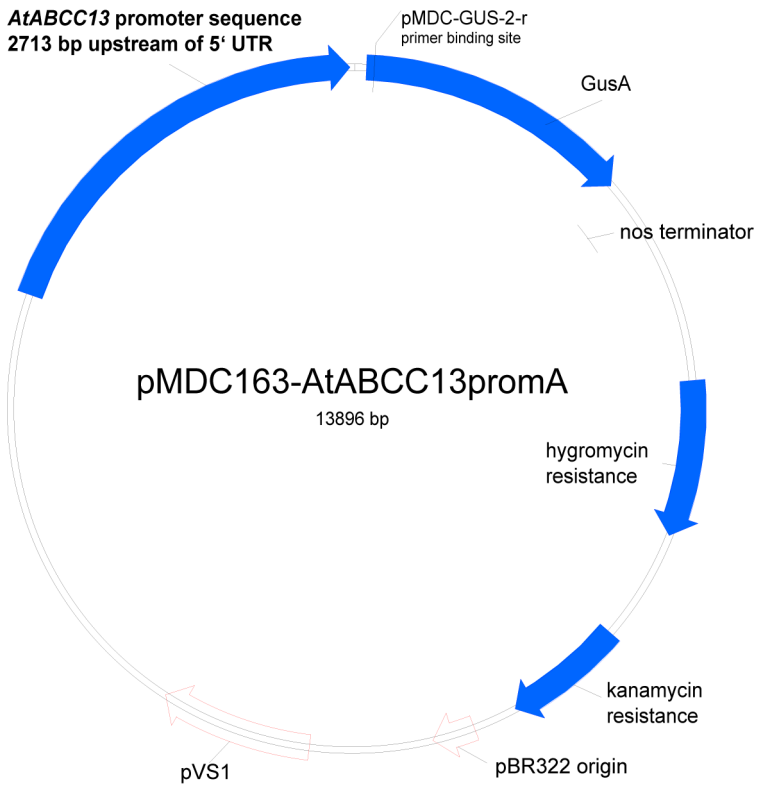

4.5.2 Genomic, coding and deduced protein sequences of *AtABCC13*.1 and *AtABCC13*.2

Sequences are given in the FASTA format. UTRs are in grey font. Exons within the genomic sequences are highlighted by capital letters and red font color.

```
>AtABCC13.1_PEP
MAITLTNFTFLYMDANLKRLGDIVLGFGANVVTLLLILILTITRRNGRCNRRKSYIEKCLLYVTPALGACLSCVDLVLLVRTNRRREV
ILCFVPLSGFVMWIAVILSLKFACCACHVFTSQILCFWWIFRFLTDALHLNMIFTLQEICLIMLDIAFGISINVLRIKQAHPKIIPLE
DPLIEDDDDQKRIEKNGSWWDLFTFGYIGSIMKHGSVKQLELENLLTLPPEMDPFTCCENLLRCWQLQECNNYSTPSLIWSIYGVYGW
PYFRLGLLKVFNDCIGFAGPLLLNRLIKYLEKGSGSSVGYTLAISLGFISIFKSFLDTQYTFRLSKLKLKLRSSIMSVIYRKCLWVNT
ANRSGFSEGEIQTFMSVDADRIVNLCNSLHDLWSLPLQIGIALYLLYTQVKFAFLSGLAITILLIPVNKWISVLIASATEKMMKLKDE
RIRKTGELLTNIRTLKMYGWDNWFADWLKETRATEVTHLATRKYLDAWCVFFWATTPTLFSLCTFGLFALMGHQLDAATVFTCLALFN
SLISPLNSFPWVINGLIDAFISTRRVSKFLCCLEHSRDFSIDSGFTSEDLAVCVEDASCTWSSNVEEDYNLTIKQVSLRVPKGSFVAV
IGEVGSGKTSLLNSLLGEMRCVHGSILLNGSVAYVPQVPWLLSGTVRENILFGKPFDSKRYFETLSACALDVDISLMVGGDMACIGDK
GLNLSGGQRARFALARAVYHGSDMYLLDDVLSAVDSQVGCWILQRALLGPLLNKKTRVMCTHNIQAISCADMIVVMDKGKVNWSGSVT
DMPKSISPTFSLTNEFDMSSPNHLTKRKETLSIKEDGVDEISEAAADIVKLEERKEGRVEMMVYRNYAVFSGWFITIVILVSAVLMQG
SRNGNDLWLSYWVDKTGKGVSHYSTSFYLMVLCIFCIINSILTLVRAFSFAFGGLKAAVHVHNALISKLINAPTQFFDQTPSGRILNR
FSSDLYTIDDSLPFILNILLANFVGLLGIIVVLSYVQVLFLLLLLPFWYIYSKLQVFYRSTSRELRRLDSVSRSPIYASFTETLDGSS
TIRAFKSEEHFVGRFIEHLTLYQRTSYSEIIASLWLSLRLQLLGSMIVLFVAVMAVLGSGGNFPISFGTPGLVGLALSYAAPLVSLLG
SLLTSFTETEKEMVSVERVLQYMDVPQEEVSGPQSLSDKWPVHGLVEFHNVTMRYISTLPPALTQISFTIQGGMHVGVIGRTGAGKSS
ILNALFRLTPVCSGEILVDGKNISHLPIRELRSCLAVVPQSPFLFQGSLRDNLDPLGLSEDWRIWEILDKCKVKAAVESVGGLDSYVK
ESGCSFSVGQRQLLCLARALLKSSKILCLDECTANIDVHTASLLHNTISSECKGVTVITIAHRISTVVDLDSILILDRGILVEQGKPQ
HLLQDDSSTFSSFVRASQ-
```

>AtABCC13.2_PEP
MAITLTNFTFLYMDANLKRLGDIVLGFGANVVTLLLILILTITRRNGRCNRRKSYIEKCLLYVTPALGACLSCVDLVLLVRTNRRREV
ILCFVPLSGFVMWIAVILSLKFACCACHVFTSQILCFWWIFRFLTDALHLNMIFTLQEICLIMLDIAFGISINVLRIKQAHPKIIPLE
DPLIEDDDDQKRIEKNGSWWDLFTFGYIGSIMKHGSVKQLELENLLTLPPEMDPFTCCENLLRCWQLQECNNYSTPSLIWSIYGVYGW
PYFRLGLLKVFNDCIGFAGPLLLNRLIKSFLDTQYTFRLSKLKLKLRSSIMSVIYRKCLWVNTANRSGFSEGEIQTFMSVDADRIVNL
CNSLHDLWSLPLQIGIALYLLYTQVKFAFLSGLAITILLIPVNKWISVLIASATEKMMKLKDERIRKTGELLTNIRTLKMYGWDNWFA
DWLKETRATEVTHLATRKYLDAWCVFFWATTPTLFSLCTFGLFALMGHQLDAATVFTCLALFNSLISPLNSFPWVINGLIDAFISTRR
VSKFLCCLEHSRDFSIDSGFTSEDLAVCVEDASCTWSSNVEEDYNLTIKQVSLRVPKGSFVAVIGEVGSGKTSLLNSLLGEMRCVHGS
ILLNGSVAYVPQVPWLLSGTVRENILFGKPFDSKRYFETLSACALDVDISLMVGGDMACIGDKGLNLSGGQRARFALARAVYHGSDMY
LLDDVLSAVDSQVGCWILQRALLGPLLNKKTRVMCTHNIQAISCADMIVVMDKGKVNWSGSVTDMPKSISPTFSLTNEFDMSSPNHLT
KRKETLSIKEDGVDEISEAAADIVKLEERKEGRVEMMVYRNYAVFSGWFITIVILVSAVLMQGSRNGNDLWLSYWVDKTGKGVSHYST
SFYLMVLCIFCIINSILTLVRAFSFAFGGLKAAVHVHNALISKLINAPTQFFDQTPSGRILNRFSSDLYTIDDSLPFILNILLANFVG
LLGIIVVLSYVQVLFLLLLLPFWYIYSKLQVFYRSTSRELRRLDSVSRSPIYASFTETLDGSSTIRAFKSEEHFVGRFIEHLTLYQRT
SYSEIIASLWLSLRLQLLGSMIVLFVAVMAVLGSGGNFPISFGTPGLVGLALSYAAPLVSLLGSLLTSFTETEKEMVSVERVLQYMDV
PQEEVSGPQSLSDKWPVHGLVEFHNVTMRYISTLPPALTQISFTIQGGMHVGVIGRTGAGKSSILNALFRLTPVCSGEILVDGKNISH
LPIRELRSCLAVVPQSPFLFQGSLRDNLDPLGLSEDWRIWEILDKCKVKAAVESVGGLDSYVKESGCSFSVGQRQLLCLARALLKSSK
ILCLDECTANIDVHTASLLHNTISSECKGVTVITIAHRISTVVDLDSILILDRGILVEQGKPQHLLQDDSSTFSSFVRASQ-

>AtABCC13.1_CDNA
aaagaattggaacagttcatcgggaagggttttgggaccctagagaatccATGGCTATCACTCTCACTAATTTCACTTTTCTCTATAT
GGATGCAAACCTGAAACGTTTAGGCGACATAGTTTTAGGGTTTGGAGCAAATGTAGTTACTCTTCTTCTGATTCTGATTCTCACCATA
ACGAGAAGAAATGGTAGATGTAACAGAAGGAAAAGCTACATTGAGAAGTGTTTGTTGTATGTAACACCTGCACTTGGAGCTTGTTTGT
CATGTGTGGACTTGGTGTTACTTGTGAGAACAAACCGTAGGAGAGAAGTCATTCTCTGTTTTGTCCCCTTGTCTGGTTTCGTAATGTG
GATTGCCGTCATCCTCTCATTGAAGTTTGCTTGTTGTGCGTGCCACGTTTTCACTAGCCAGATTCTATGTTTCTGGTGGATCTTTAGA
TTCCTAACAGATGCCCTTCATCTTAACATGATTTTCACATTACAGGAGATTTGCCTCATCATGTTGGACATTGCTTTTGGTATCTCTA
TTAATGTCCTCAGGATAAAGCAGGCACATCCCAAAATCATTCCTTTGGAAGATCCACTTATTGAAGACGACGATGATCAAAAGCGCAT
TGAGAAAAATGGAAGCTGGTGGGACTTATTCACTTTTGGGTACATTGGTTCAATAATGAAACATGGCTCGGTGAAGCAGCTAGAATTG
GAAAATCTACTTACACTACCACCTGAAATGGATCCTTTTACATGTTGTGAGAATTTATTGAGATGTTGGCAACTTCAAGAGTGTAATA
ATTACTCAACTCCATCACTAATTTGGTCAATATATGGTGTATATGGATGGCCATATTTTCGTCTTGGACTGTTAAAGGTGTTCAATGA
TTGCATTGGATTTGCTGGACCCTTACTTCTCAACAGACTTATCAAGTATCTTGAAAAAGGTTCAGGAAGTTCTGTTGGCTATACACTT
GCTATCTCCTTGGGCTTCATATCTATCTTTAAGTCTTTTCTTGATACACAATACACGTTTCGTCTTTCAAAGCTGAAACTCAAGCTAC
GGTCTAGTATAATGAGTGTCATCTACAGGAAGTGTTTGTGGGTGAACACAGCAAACCGGTCAGGATTTTCTGAAGGCGAGATTCAAAC
ATTTATGTCGGTAGATGCTGACCGCATTGTTAACTTGTGCAACAGTTTGCATGACTTGTGGAGCCTGCCTTTGCAAATTGGGATAGCT
TTGTATCTTTTGTATACTCAAGTCAAGTTTGCTTTTCTTTCTGGACTTGCAATCACCATCTTGCTGATACCAGTGAATAAATGGATAT
CGGTGCTGATTGCATCTGCAACAGAGAAAATGATGAAGCTTAAAGATGAGAGGATTAGAAAAACAGGAGAGCTTTTAACAAACATACG
CACACTTAAAATGTATGGATGGGATAACTGGTTTGCTGATTGGTTGAAGGAAACAAGAGCCACCGAAGTGACTCACTTAGCGACTCGG
AAGTATTTAGATGCTTGGTGTGTTTTCTTTTGGGCAACAACACCAACTCTTTTTTCTCTTTGCACTTTTGGTCTCTTTGCTCTGATGG
GTCATCAACTTGATGCAGCAACGGTGTTTACTTGTCTTGCTTTGTTTAATAGCTTAATCTCTCCATTAAACTCGTTTCCATGGGTCAT
CAACGGTCTCATTGATGCCTTTATATCCACCAGGCGTGTGAGCAAGTTCTTGTGTTGTTTGGAGCATAGTAGAGATTTTTCTATAGAT
TCTGGATTTACATCTGAAGACTTAGCTGTATGTGTGGAAGATGCATCTTGTACTTGGTCAAGTAACGTAGAAGAGGATTATAACTTGA
CAATAAAACAAGTAAGCCTAAGAGTGCCAAAGGGATCTTTTGTTGCAGTTATCGGGGAGGTTGGTTCAGGTAAAACATCGTTGTTGAA
TTCACTTTTAGGCGAAATGCGGTGTGTTCATGGATCTATACTATTAAATGGCTCTGTGGCATATGTACCACAGGTCCCATGGCTTTTG
TCTGGAACTGTACGTGAAAACATTTTATTCGGGAAGCCTTTTGACTCCAAAAGGTATTTCGAGACATTGAGTGCTTGTGCACTAGATG
TGGATATTTCACTTATGGTCGGAGGAGACATGGCGTGTATAGGTGATAAAGGACTAAACTTATCCGGAGGACAGAGAGCTCGGTTTGC
TTTGGCCAGGGCTGTTTATCATGGTTCAGACATGTACCTTCTTGATGATGTACTGAGTGCAGTGGATTCACAAGTAGGATGTTGGATA
TTGCAAAGAGCACTTCTGGGTCCTCTGTTGAACAAAAAGACTCGTGTTATGTGCACTCACAACATTCAGGCGATATCTTGTGCAGATA
TGATTGTTGTGATGGACAAAGGAAAAGTGAATTGGTCAGGAAGTGTTACTGATATGCCCAAATCCATTTCTCCAACATTTTCTTTAAC
CAATGAATTTGATATGTCATCACCAAATCACTTGACCAAAAGAAAAGAGACTCTATCTATCAAGGAAGATGGTGTAGATGAAATTAGT
GAAGCTGCGGCGGATATCGTCAAATTAGAGGAACGAAAAGAGGGTCGAGTTGAAATGATGGTTTATAGGAACTATGCTGTGTTTTCTG
GTTGGTTCATTACTATTGTAATATTGGTTTCAGCGGTTTTAATGCAAGGGTCTCGTAATGGAAATGATTTGTGGCTATCATATTGGGT
TGACAAGACAGGAAAAGGAGTATCGCATTACTCAACCTCGTTTTATTTGATGGTTCTCTGTATCTTTTGCATCATTAACTCAATATTA
ACCTTGGTGAGGGCATTCTCATTTGCATTTGGAGGATTAAAAGCAGCAGTGCATGTTCATAATGCATTAATCAGTAAGCTTATAAATG
CACCTACACAGTTCTTTGATCAGACACCAAGTGGAAGAATACTTAATAGGTTTTCCTCTGATCTATATACCATCGACGACTCTCTCCC
GTTTATTCTCAACATTCTTCTAGCAAATTTTGTTGGCTTGTTAGGGATTATTGTAGTATTGTCTTATGTTCAGGTTCTATTCCTGCTT
CTGCTTCTGCCATTTTGGTACATATACAGCAAGCTTCAGGTCTTCTACAGGTCTACTTCAAGGGAACTACGAAGGTTGGACAGTGTTT
CACGATCACCGATATATGCATCGTTCACGGAGACACTTGATGGGTCATCAACTATCAGGGCTTTTAAGTCTGAGGAGCATTTTGTAGG
TAGATTTATTGAGCATTTGACGCTATACCAGCGGACTTCTTACTCAGAGATAATCGCAAGCTTGTGGCTCTCCTTGCGTCTTCAGTTG
TTAGGATCAATGATTGTCTTATTTGTCGCTGTAATGGCTGTCCTCGGCTCCGGGGGGAACTTTCCAATCAGTTTTGGTACACCTGGAC
TGGTGGGATTAGCGCTCTCATATGCAGCTCCATTGGTTTCTCTGTTAGGAAGCTTGTTAACAAGTTTTACTGAAACAGAAAAAGAAAT
GGTTTCTGTTGAAAGGGTTCTCCAGTACATGGATGTGCCTCAAGAAGAAGTTTCAGGTCCTCAATCTCTCAGCGATAAGTGGCCTGTT
CACGGATTAGTTGAGTTTCACAATGTGACAATGAGATACATCTCAACTCTGCCTCCGGCCCTCACCCAAATTTCTTTTACAATCCAAG
GAGGAATGCATGTAGGAGTAATTGGAAGAACTGGTGCCGGGAAGTCCTCGATCTTGAATGCGCTTTTCCGGCTTACTCCTGTTTGTAG
TGGAGAGATATTGGTGGATGGAAAAAACATAAGCCATCTTCCGATAAGAGAACTCCGTTCTTGCCTCGCTGTTGTTCCTCAGAGCCCT
TTTCTGTTTCAAGGATCACTGAGGGATAACCTTGATCCTCTTGGGTTGAGTGAGGATTGGAGAATCTGGGAGATCCTAGACAAGTGTA
AAGTTAAGGCAGCGGTAGAAAGTGTAGGAGGGTTAGATTCATATGTAAAGGAATCTGGTTGTTCCTTTTCTGTTGGACAGAGACAGCT
TTTGTGCCTTGCTCGTGCTTTGCTCAAGTCATCTAAGATCCTATGCCTTGATGAATGCACCGCCAACATCGATGTTCACACAGCTTCC
CTACTCCACAACACGATATCGAGTGAATGCAAAGGCGTAACCGTCATTACCATTGCTCACCGCATTTCTACGGTTGTTGATTTAGACA
GCATCCTAATTCTTGATCGTGGAATTCTTGTTGAACAAGGAAAACCACAACATCTTTTGCAAGATGACTCCTCAACTTTTTCAAGCTT
TGTCAGAGCTTCTCAGTGAaatgttgttagaatctgatcacttgtaacttctgatctctgctataattatcttgtcatggaaattaag
aaaaact

>AtABCC13.2_CDS
ATGGCTATCACTCTCACTAATTTCACTTTTCTCTATATGGATGCAAACCTGAAACGTTTAGGCGACATAGTTTTAGGGTTTGGAGCAA
ATGTAGTTACTCTTCTTCTGATTCTGATTCTCACCATAACGAGAAGAAATGGTAGATGTAACAGAAGGAAAAGCTACATTGAGAAGTG
TTTGTTGTATGTAACACCTGCACTTGGAGCTTGTTTGTCATGTGTGGACTTGGTGTTACTTGTGAGAACAAACCGTAGGAGAGAAGTC
ATTCTCTGTTTTGTCCCCTTGTCTGGTTTCGTAATGTGGATTGCCGTCATCCTCTCATTGAAGTTTGCTTGTTGTGCGTGCCACGTTT
TCACTAGCCAGATTCTATGTTTCTGGTGGATCTTTAGATTCCTAACAGATGCCCTTCATCTTAACATGATTTTCACATTACAGGAGAT
TTGCCTCATCATGTTGGACATTGCTTTTGGTATCTCTATTAATGTCCTCAGGATAAAGCAGGCACATCCCAAAATCATTCCTTTGGAA
GATCCACTTATTGAAGACGACGATGATCAAAAGCGCATTGAGAAAAATGGAAGCTGGTGGGACTTATTCACTTTTGGGTACATTGGTT
CAATAATGAAACATGGCTCGGTGAAGCAGCTAGAATTGGAAAATCTACTTACACTACCACCTGAAATGGATCCTTTTACATGTTGTGA
GAATTTATTGAGATGTTGGCAACTTCAAGAGTGTAATAATTACTCAACTCCATCACTAATTTGGTCAATATATGGTGTATATGGATGG
CCATATTTTCGTCTTGGACTGTTAAAGGTGTTCAATGATTGCATTGGATTTGCTGGACCCTTACTTCTCAACAGACTTATCAAGTCTT
TTCTTGATACACAATACACGTTTCGTCTTTCAAAGCTGAAACTCAAGCTACGGTCTAGTATAATGAGTGTCATCTACAGGAAGTGTTT
GTGGGTGAACACAGCAAACCGGTCAGGATTTTCTGAAGGCGAGATTCAAACATTTATGTCGGTAGATGCTGACCGCATTGTTAACTTG
TGCAACAGTTTGCATGACTTGTGGAGCCTGCCTTTGCAAATTGGGATAGCTTTGTATCTTTTGTATACTCAAGTCAAGTTTGCTTTTC
TTTCTGGACTTGCAATCACCATCTTGCTGATACCAGTGAATAAATGGATATCGGTGCTGATTGCATCTGCAACAGAGAAAATGATGAA
GCTTAAAGATGAGAGGATTAGAAAAACAGGAGAGCTTTTAACAAACATACGCACACTTAAAATGTATGGATGGGATAACTGGTTTGCT
GATTGGTTGAAGGAAACAAGAGCCACCGAAGTGACTCACTTAGCGACTCGGAAGTATTTAGATGCTTGGTGTGTTTTCTTTTGGGCAA
CAACACCAACTCTTTTTTCTCTTTGCACTTTTGGTCTCTTTGCTCTGATGGGTCATCAACTTGATGCAGCAACGGTGTTTACTTGTCT
TGCTTTGTTTAATAGCTTAATCTCTCCATTAAACTCGTTTCCATGGGTCATCAACGGTCTCATTGATGCCTTTATATCCACCAGGCGT
GTGAGCAAGTTCTTGTGTTGTTTGGAGCATAGTAGAGATTTTTCTATAGATTCTGGATTTACATCTGAAGACTTAGCTGTATGTGTGG
AAGATGCATCTTGTACTTGGTCAAGTAACGTAGAAGAGGATTATAACTTGACAATAAAACAAGTAAGCCTAAGAGTGCCAAAGGGATC
TTTTGTTGCAGTTATCGGGGAGGTTGGTTCAGGTAAAACATCGTTGTTGAATTCACTTTTAGGCGAAATGCGGTGTGTTCATGGATCT
ATACTATTAAATGGCTCTGTGGCATATGTACCACAGGTCCCATGGCTTTTGTCTGGAACTGTACGTGAAAACATTTTATTCGGGAAGC
CTTTTGACTCCAAAAGGTATTTCGAGACATTGAGTGCTTGTGCACTAGATGTGGATATTTCACTTATGGTCGGAGGAGACATGGCGTG
TATAGGTGATAAAGGACTAAACTTATCCGGAGGACAGAGAGCTCGGTTTGCTTTGGCCAGGGCTGTTTATCATGGTTCAGACATGTAC
CTTCTTGATGATGTACTGAGTGCAGTGGATTCACAAGTAGGATGTTGGATATTGCAAAGAGCACTTCTGGGTCCTCTGTTGAACAAAA
AGACTCGTGTTATGTGCACTCACAACATTCAGGCGATATCTTGTGCAGATATGATTGTTGTGATGGACAAAGGAAAAGTGAATTGGTC
AGGAAGTGTTACTGATATGCCCAAATCCATTTCTCCAACATTTTCTTTAACCAATGAATTTGATATGTCATCACCAAATCACTTGACC
AAAAGAAAAGAGACTCTATCTATCAAGGAAGATGGTGTAGATGAAATTAGTGAAGCTGCGGCGGATATCGTCAAATTAGAGGAACGAA
AAGAGGGTCGAGTTGAAATGATGGTTTATAGGAACTATGCTGTGTTTTCTGGTTGGTTCATTACTATTGTAATATTGGTTTCAGCGGT
TTTAATGCAAGGGTCTCGTAATGGAAATGATTTGTGGCTATCATATTGGGTTGACAAGACAGGAAAAGGAGTATCGCATTACTCAACC
TCGTTTTATTTGATGGTTCTCTGTATCTTTTGCATCATTAACTCAATATTAACCTTGGTGAGGGCATTCTCATTTGCATTTGGAGGAT
TAAAAGCAGCAGTGCATGTTCATAATGCATTAATCAGTAAGCTTATAAATGCACCTACACAGTTCTTTGATCAGACACCAAGTGGAAG
AATACTTAATAGGTTTTCCTCTGATCTATATACCATCGACGACTCTCTCCCGTTTATTCTCAACATTCTTCTAGCAAATTTTGTTGGC
TTGTTAGGGATTATTGTAGTATTGTCTTATGTTCAGGTTCTATTCCTGCTTCTGCTTCTGCCATTTTGGTACATATACAGCAAGCTTC
AGGTCTTCTACAGGTCTACTTCAAGGGAACTACGAAGGTTGGACAGTGTTTCACGATCACCGATATATGCATCGTTCACGGAGACACT
TGATGGGTCATCAACTATCAGGGCTTTTAAGTCTGAGGAGCATTTTGTAGGTAGATTTATTGAGCATTTGACGCTATACCAGCGGACT
TCTTACTCAGAGATAATCGCAAGCTTGTGGCTCTCCTTGCGTCTTCAGTTGTTAGGATCAATGATTGTCTTATTTGTCGCTGTAATGG
CTGTCCTCGGCTCCGGGGGGAACTTTCCAATCAGTTTTGGTACACCTGGACTGGTGGGATTAGCGCTCTCATATGCAGCTCCATTGGT
TTCTCTGTTAGGAAGCTTGTTAACAAGTTTACTGAAACAGAAAAAGAAATGGTTTCTGTTGAAAGGGTTCTCCAGTACATGGATGTG
CCTCAAGAAGAAGTTTCAGGTCCTCAATCTCTCAGCGATAAGTGGCCTGTTCACGGATTAGTTGAGTTTCACAATGTGACAATGAGAT
ACATCTCAACTCTGCCTCCGGCCCTCACCCAAATTTCTTTTACAATCCAAGGAGGAATGCATGTAGGAGTAATTGGAAGAACTGGTGC
CGGGAAGTCCTCGATCTTGAATGCGCTTTTCCGGCTTACTCCTGTTTGTAGTGGAGAGATATTGGTGGATGGAAAAAACATAAGCCAT
CTTCCGATAAGAGAACTCCGTTCTTGCCTCGCTGTTGTTCCTCAGAGCCCTTTTCTGTTTCAAGGATCACTGAGGGATAACCTTGATC
CTCTTGGGTTGAGTGAGGATTGGAGAATCTGGGAGATCCTAGACAAGTGTAAAGTTAAGGCAGCGGTAGAAAGTGTAGGAGGGTTAGA
TTCATATGTAAAGGAATCTGGTTGTTCCTTTTCTGTTGGACAGAGACAGCTTTTGTGCCTTGCTCGTGCTTTGCTCAAGTCATCTAAG
ATCCTATGCCTTGATGAATGCACCGCCAACATCGATGTTCACACAGCTTCCCTACTCCACAACACGATATCGAGTGAATGCAAAGGCG
TAACCGTCATTACCATTGCTCACCGCATTTCTACGGTTGTTGATTTAGACAGCATCCTAATTCTTGATCGTGGAATTCTTGTTGAACA
AGGAAAACCACAACATCTTTTGCAAGATGACTCCTCAACTTTTTCAAGCTTTGTCAGAGCTTCTCAGTGA

>AtABCC13.1_genomic
aaagaattggaacagttcatcgggaagggttttgggaccctagagaatccATGGCTATCACTCTCACTAATTTCACTgtaagtacact
atttctttactttctctatggtttgttgatgatgaaaaatttatcaatctttgtctcagTTTCTCTATATGGATGCAAACCTGAAACG
TTTAGGCGACATatatccttccttgaacttcatgggtttataggagtttgcgtatgtatatagatacatgaatgctcaattttggatt
gttgttccttaagaatgattacAGTTTTAGGGTTTGGAGCAAATGTAGTTACTCTTCTTCTGATTCTGATTCTCACCATAACGAGAAG
AAATGGTAGATGTAACAGAAGGgtaagagtaagcctaattttctactttggttttggtaaaaaaaaagaactgattcgtcctcatttg
attttctttattagAAAAGCTACATTGAGAAGTGTTTGTTGTATGTAACACCTGCACTTGGAGCTTGTTTGTCATGTGTGGACTTGGT
GTTACTTGTGAGAACAAACCGTAGGAGAGAAGTCATTCTCTGTTTTGTCCCCTTGTCTGGTTTCGTAATGTGGgtaagcttcttgtta
ccaaacacgaacagaactctgtctttgtctttctcttttgtttctgctttgaaggtttttttttaccttgtagATTGCCGTCATCCTCT
CATTGAAGTTTGCTTGTTGTGCGTGCCACGTTTTCACTAGCCAGATTCTATGTTTCTGGTGGATCTTTAGATTCCTAACAGATGCCCT
TCATCTTAACATGATTTTCACATTACAGgtaattaagttgtctttatgaatctgtcacattctccatataagtagagttggttaaccg
aatttggagcgtgtacagGAGATTTGCCTCATCATGTTGGACATTGCTTTTGGTATCTCTATTAATGTCCTCAGGATAAAGCAGGCAC
ATCCCAAAATCATgtatatgctttaatatggttctcttatttaatatttttttccttttcatttcttgtttaattccttattctcctt
gtagTCCTTTGGAAGATCCACTTATTGAAGACGACGATGATCAAAAGCGCATTgtacgacgtctcttccttgtaactaactagtttaa
agagtagttaaagaccaatagatttgttcattctttgaagGAGAAAAATGGAAGCTGGTGGGACTTATTCACTTTTGGGTACATTGGT
TCAATAATGAAACATGGCTCGGTGAAGCAGCTAGAATTGGAAAATCTACTTACACTACCACCTGAAATGGATCCTTTTACATGTTGTG
AGAATTTATTGAGATGTTGGCAACTTCAAGAGTGTAATAATTACTCAACTCCATCACTAATTTGGTCAATATATGGTGTATATGGATG
GCCATATTTTCGTCTTGGACTGTTAAAGgtacgttgcttatttgactttcttatataatctttgttaatattgctactacaaaacatg
aattttgcagGTGTTCAATGATTGCATTGGATTTGCTGGACCCTTACTTCTCAACAGACTTATCAAGTATCTTGAAAAAGgttgagaa
tctttttaaagatttagtaaatatgattactaatggaatcattgacactgtttataaactaaacagGTTCAGGAAGTTCTGTTGGCTA
TACACTTGCTATCTCCTTGGGCTTCATATCTATCTTTAAgtaaatatagtgcatagtcatcatatttctacatttttttgtcatctca
aatgtgttccaagtgtagcaatagttactaggcacttgtgatgtatgctttttttgtcttgtagGTCTTTTCTTGATACACAATACACG
TTTCGTCTTTCAAAGCTGAAACTCAAGCTACGGTCTAGTATAATGAGTGTCATCTACAGGAAGgtaaaacatgtgaaaagtgaaaact
tttattgtgagtggtagtaattggttccataatttcttgaaagtgaactattatcacaagaattttgtatatatacagtatggttttg

gaaatttgtgctttgcttcagcgagtattcggttaaagatatcgatatctccttgccgttactacaaacggagacgcacctttgagt
atacgatatataacttcatacatagtatcaaacgttttggttcttttggtaaagagctgtttttgtttatgaaattatattgtatgca
gTGTTTGTGGGTGAACACAGCAAACCGGTCAGGATTTTCTGAAGGCGAGATTCAAACATTTATGTCGGTAGATGCTGACCGCATTGTT
AACTTGTGCAACAGTTTGCATGACTTGTGGAGgtaagaacatttgcctgtaaacaatgaaagtgcttccaatattgagtaacaataaa
ttggccactcttacaatttttcattcaaatatatgtctcagCCTGCCTTTGCAAATTGGGATAGCTTTGTATCTTTTGTATACTCAAG
TCAAGTTTGCTTTTCTTTCTGGACTTGCAATCACCATCTTGCTGATACCAGgtacccagtttacattatcgtaactacaatatagaat
gcccatttttttctttgaatatctggaagtgtaagcccaaaggccatacatctcctagaggcgagacccacaccattttagattcat
ctcctttgaaaaagaaatccctcccaacgtgcctcgaacctatcacctccacggagatttagtattgggccaatagctcgttggtgat
gccagtttttctcattttccctttttttttggcagTGAATAAATGGATATCGGTGCTGATTGCATCTGCAACAGAGAAAATGATGAAG
CTTAAAGATGAGAGgtgtgagaaaacgtttagtaagtgttgatcataagagggatgttagtagtaatttctcacattgtaaaaagttt
tgttatctatcagGATTAGAAAAACAGGAGAGCTTTTAACAAACATACGCACACTTAAAATGTATGGATGGGATAACTGGTTTGCTGA
TTGGTTGAAGGAAACAAGAGCCACCGAAGTGACTCACTTAGCGgttaggtcttcgtatccttccttttgctgttttgtccaagtactt
tgtattaacgtttaagtcttcgtttggctttctagACTCGGAAGTATTTAGATGCTTGGTGTGTTTTCTTTTGGGCAACAACACCAA
CTCTTTTTTCTCTTTGCACTTTTGGTCTCTTTGCTCTGATGGGTCATCAACTTGATGCAGCAACGgtacttttgaatctgctctata
acattttctgattcaaatatgtaaaatttttcttgacaatcctgtttttttttttccagGTGTTTACTTGTCTTGCTTTGTTTAATAGC
TTAATCTCTCCATTAAACTCGTTTCCATGGGTCATCAACGGTCTCATTGATgtaagattatctttcgatcatattaagaagcattttt
atctaccattttagttatatatcatttttgttaccttgttgcagGCCTTTATATCCACCAGGCGTGTGAGCAAGTTCTTGTGTTGTTT
GGAGCATAGTAGAGATTTTTCTATAGATTCTGGATTTACATCTGAAGACTTAGCTGTATGTGTGGAAGATGCATCTTGTACTTGGTCA
AGTAACGTAGAAGAGGATTATAACTTGACAATAAAACAAGTAAGCCTAAGAGTGCCAAAGGGATCTTTTGTTGCAGTTATCGGGGAGg
tatacgaatcgtccccaccgttagagctgcatagttcgattaaattatgattaggtgtttcttaaactctttttgtttgcttaatttt
cagGTTGGTTCAGGTAAAACATCGTTGTTGAATTCACTTTTAGGCGAAATGCGGTGTGTTCATGGATCTATACTATTAAATGGCTCTG
TGGCATATGTACCACAGgtttgtaaactggttaaatactttctttttggtttccactatgagaagtcttacatgtacctcactcacct
tcaagGTCCCATGGCTTTTGTCTGGAACTGTACGTGAAAACATTTTATTCGGGAAGCCTTTTGACTCCAAAAGgtttagtaagtttgc
ttcatcaactcttaaagttatgatctagtgtaactgatagacaaagctagtggtgactttgttaaactagGTATTTCGAGACATTGAG
TGCTTGTGCACTAGATGTGGATATTTCACTTATGGTCGGAGGAGACATGGCGTGTATAGGTGATAAAGGACTAAACTTATCCGGAGGA
CAGAGAGCTCGGTTTGCTTTGGCCAGgtttgctatatatctcctatgctctttcaccatccatagacttgagtgttgtgtttctgatg
attttgtgtgtgctttatcaatagGGCTGTTTATCATGGTTCAGACATGTACCTTCTTGATGATGTACTGAGTGCAGTGGATTCACAA
GTAGGATGTTGGATATTGCAAAGAGCACTTCTGGGTCCTCTGTTGAACAAAAAGACTCGTGTTATGTGCACTCACAACATTCAGgtct
caaatctctctacacgttaaatatttatctatctcaatttaatttttctcataccgtcaagctgtttctactatgacagGCGATATC
TTGTGCAGATATGATTGTTGTGATGGACAAAGGAAAAGTGAATTGGTCAGGAAGTGTTACTGATATGCCCAAATCCATTTCTCCAACA
TTTTCTTTAACCAATGAATTTGATATGTCATCACCAAATCACTTGACCAAAAGAAAAGAGACTCTATCTATCAAGGAAGATGGTGTAG
ATGAAATTAGTGAAGCTGCGGCGGATATCGTCAAATTAGAGGAACGAAAAGAGGGTCGAGTTGAAATGATGGTTTATAGgtaaacaaa
atttgcttaaccatgtctttttttttgttgcctatatgtataagtaagtgattgttatctgtttatgcagGAACTATGCTGTGTTTTCT
GGTTGGTTCATTACTATTGTAATATTGGTTTCAGCGGTTTTAATGCAAGGGTCTCGTAATGGAAATGATTTGTGGCTATCATATTGGG
TTGACAAGACAGGAAAAGGAGTATCGCATTACTCAACCTCGTTTTATTTGgtattaaactcgcgcataaaaccacgaaacgtaactct
tatgtctctgtgtttttctagtttaataataactactaatcttgcagATGGTTCTCTGTATCTTTTGCATCATTAACTCAATATTAAC
CTTGGTGAGGGCATTCTCATTTGCATTTGGAGGATTAAAAGCAGCAGTGCATGTTCATAATGCATTAATCAGTAAGCTTATAAATGCA
CCTACACAGTTCTTTGATCAGACACCAAGTGGAAGAATACTTAATAGgttagacacaaggaaactctttgaatcatgtgtcttgttct
tcatcttaacttctttttttggttttactctgttcagGTTTTCCTCTGATCTATATACCATCGACGACTCTCTCCCGTTTATTCTCAA
CATTCTTCTAGCAAATTTTGTTGGCTTGTTAGGGATTATTGTAGTATTGTCTTATGTTCAGgtttgtctgaaactcttctctcttttt
gctaagtattaactcttctgttttgttggagaagttacattaatgtataatatgtatacagGTTCTATTCCTGCTTCTGCTTCTGCCA
TTTTGGTACATATACAGCAAGCTTCAGgtacatatacaacttcttgtagccaatctgatttcatatttggtgtcccttagagaagaag
aagagttcaaattttctactaactgaaaattgcttcagGTCTTCTACAGGTCTACTTCAAGGGAACTACGAAGGTTGGACAGTGTTTC
ACGATCACCGATATATGCATCGTTCACGGAGACACTTGATGGGTCATCAACTATCAGGGCTTTTAAGTCTGAGgtagttttggttctg
cttctaaatgtcaggttttgcttctccattaatgacaaaactgtatgctaattccggtttgcatgacagGAGCATTTTGTAGGTAGAT
TTATTGAGCATTTGACGCTATACCAGCGGACTTCTTACTCAGAGATAATCGCAAGCTTGTGGCTCTCCTTGCGTCTTCAGgtacacta
atacatctttgcttacatttttgtagaacatttttcattcacctttttgagaattggtaacaatgtttagtttcatgtgtctgcaataaa
tatggaaatctcgaaaaatcgctgataagttgagtaaaatggtgcagTTGTTAGGATCAATGATTGTCTTATTTGTCGCTGTAATGGC
TGTCCTCGGCTCCGGGGGGAACTTTCCAATCAGTTTTGGTACACCTGGACTGgtaagaaactgcagttttcataaatatataggaaag
tgaaaagcatactatttataatttggatcacagGTGGGATTAGCGCTCTCATATGCAGCTCCATTGGTTTCTCTGTTAGGAAGCTTGT
TAACAAGTTTTACTGAAACAGAAAAAGAAATGGTTTCTGTTGAAAGGGTTCTCCAGgtaatgattctgattctttttttggtttgtca
accgaaattaattgcagctcaaaagagccattcctgaggaatgttgtttacatatatgatatgatgtggttcggtacaaattcgtcgt
gccaaattatccacttctacattcgcactacgagaaatcaaagataaagataatgattctgattcattaagtaatttttgtatgttag
tgttactaattacatgaaccatgctctcctgtgttattagTACATGGATGTGCCTCAAGAAGAAGTTTCAGGTCCTCAATCTCTCAGC
GATAAGTGGCCTGTTCACGGATTAGTTGAGTTTCACAATGTGACAATGAGATACATCTCAACTCTGCCTCCGGCCCTCACCCAAATTT
CTTTTACAATCCAAGGAGGAATGCATgtacgtgtatcgccgagcactctacaacagacttgacttttttctgtttttatctttttctccc
aacatatacaatttatatgaagttatcgggaagagactatccgctagagagagcactctacaacagaattgacttttttctgtctcatg
attgttttgttttcatttatcagGTAGGAGTAATTGGAAGAACTGGTGCCGGGAAGTCCTCGATCTTGAATGCGCTTTTCCGGCTTAC
TCCTGTTTGTAGTGGAGAGATATTGGTGGATGGAAAAAACATAAGCCATCTTCCGATAAGAGAACTCCGTTCTTGCCTCGCTGTTGTT
CCTCAGAGCCCTTTTCTGTTTCAAGGATCACTGAGgtgagaacttaactccttcaattcactaaccaaaggtgttgcctgcagtttca
taatgaaaaaaagttgtggttctcgtagGGATAACCTTGATCCTCTTGGGTTGAGTGAGGATTGGAGAATCTGGGAGATCCTAGACAA
GTGTAAAGTTAAGGCAGCGGTAGAAAGTGTAGGAGGGTTAGATTCATATGTAAAGGAATCTGGTTGTTCCTTTTCTGTTGGACAGAGA
CAGCTTTTGTGCCTTGCTCGTGCTTTGCTCAAGTCATCTAAGATCCTATGCCTTGATGAATGCACCGCCAACATCGATGTTCACACAG
CTTCCCTACTCCACAACACGATATCGAGTGAATGCAAAGGCGTAACCGTCATTACCATTGCTCACCGCATTTCTACGGTTGTTGATTT
AGACAGCATCCTAATTCTTGATCGTGGAATTCTTGTTGAACAAGGAAAACCACAACATCTTTTGCAAGATGACTCCTCAACTTTTTCA
AGCTTTGTCAGAGCTTCTCAGTGAaatgttgttagaatctgatcacttgtaacttctgatctctgctataattatcttgtcatggaaa
ttaagaaaaact

4.5.3 Protein sequence alignment of AtABCC13 with orthologs and paralogs

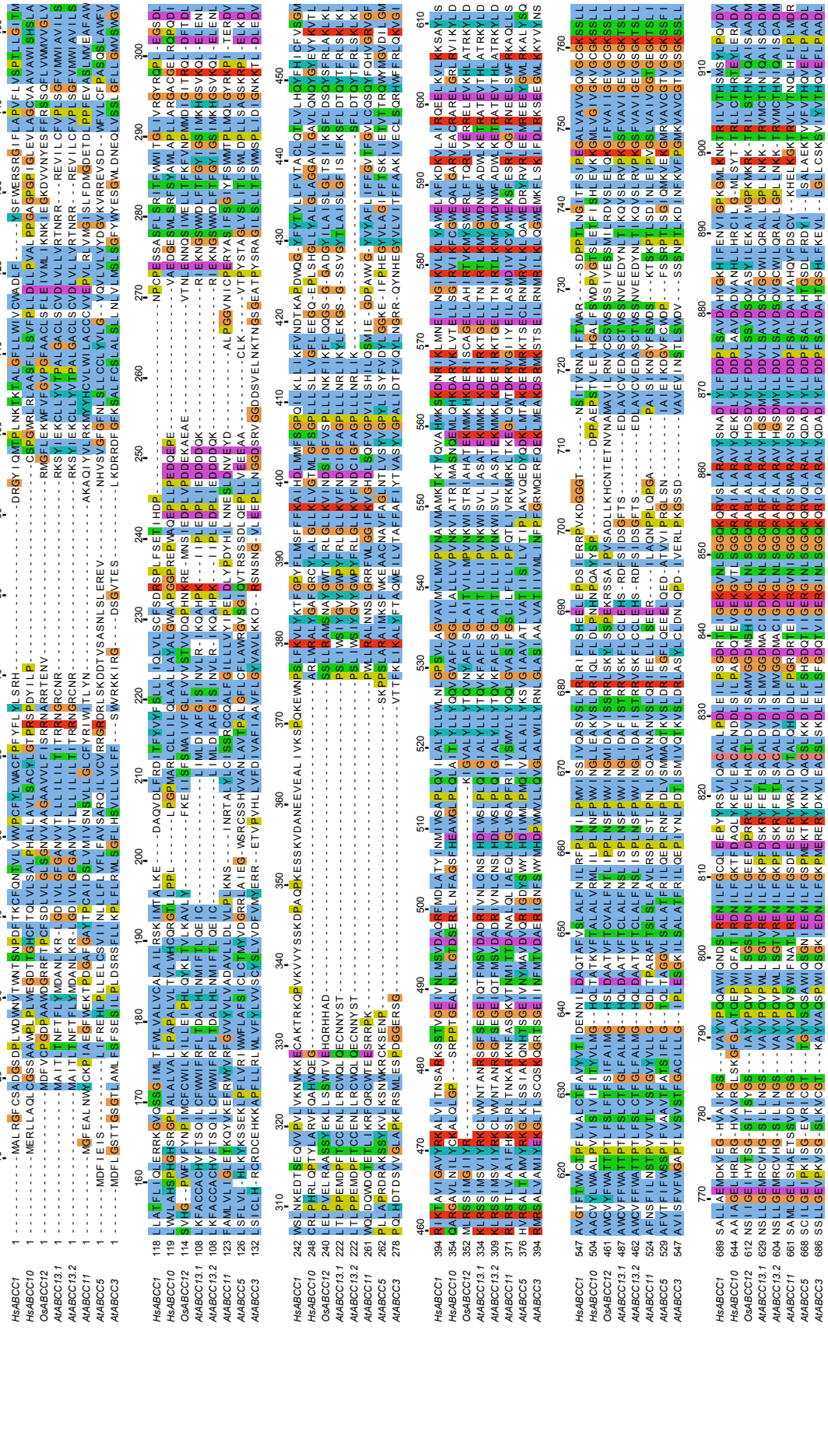

Protein sequence alignment of AtABCC13 with orthologs and paralogs (continued)

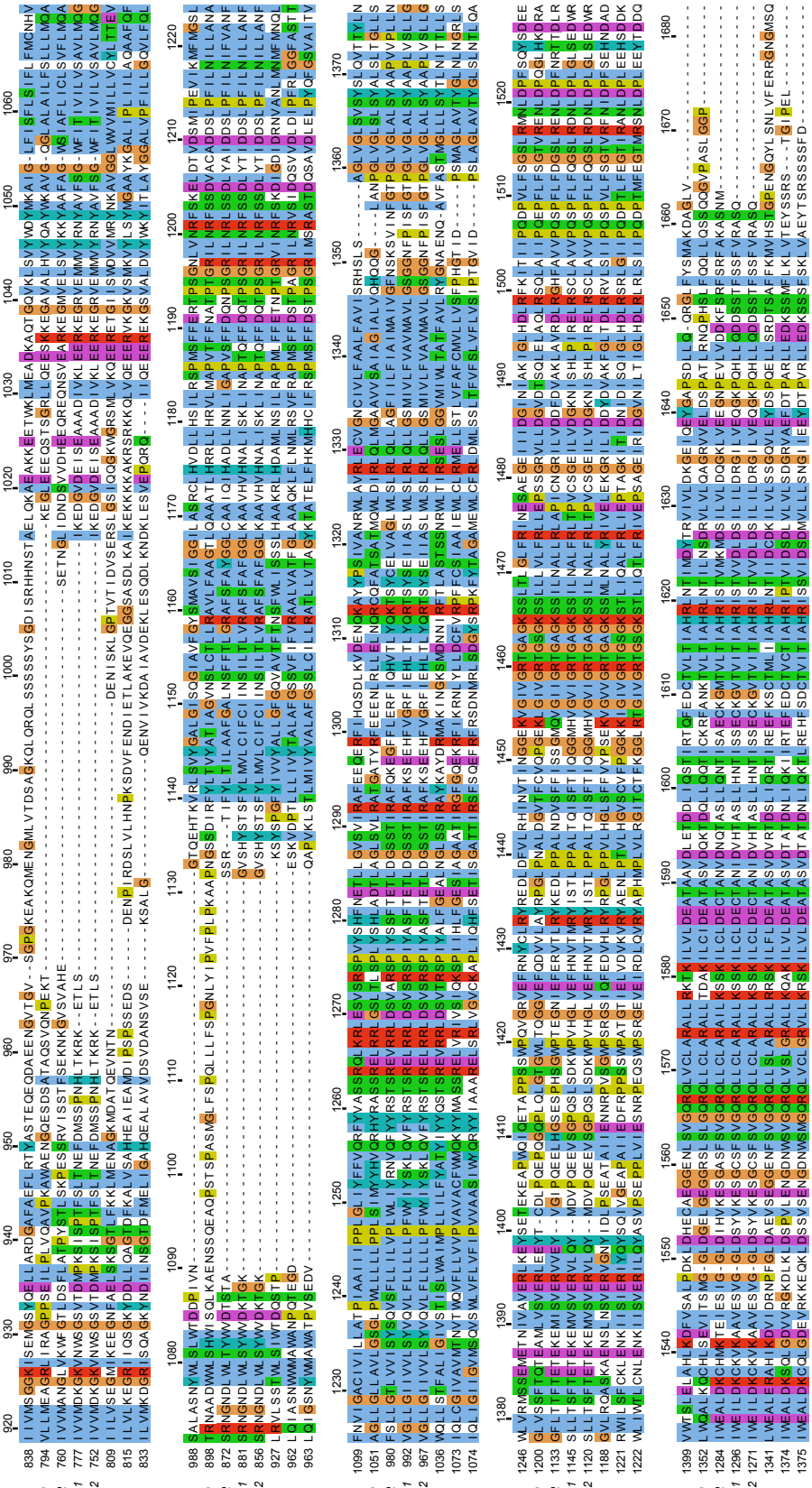

4.5.4 Expression pattern of the *Glycine max GmABCC10*

Tissue-specific expression values of *Glyma13g44750.1,* the *Glycine max* ortholog of *AtABCC13*, obtained from Genevestigator (http://www.genevestigator.com) and modified in Abobe Illustrator.

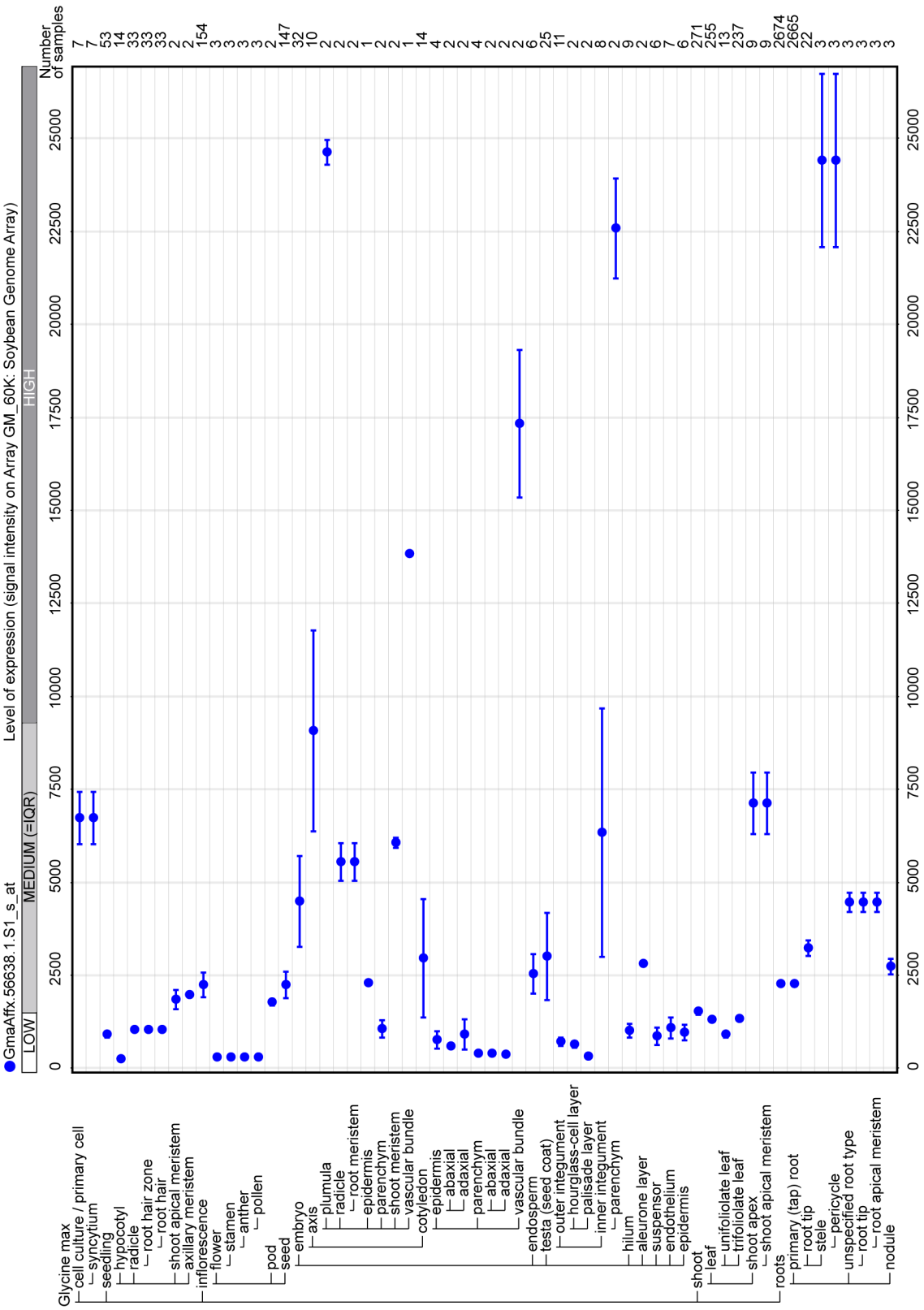

5. Chapter III

Characterization of vacuolar ABA-GE uptake in Arabidopsis thaliana

This chapter represents a manuscript for an article, which will be submitted in future after additional analyses.

5.1 Introduction

Abscisic acid (ABA) is a major phytohormone of higher plants with an important function in signaling and modulating responses to cellular water availability. It controls stomatal movement and regulates cellular dehydration tolerance during seed desiccation and abiotic stress conditions (i.e. drought, osmotic and salt). Furthermore, it functions in seed development, seed dormancy and germination (Holdsworth et al., 2008), lateral root formation (Galvan-Ampudia and Testerink, 2011), pathogen resistance (Ton et al., 2009), leaf senescence and in fruit ripening (Jia et al., 2011). ABA also functions in algae, protozoa, lower metazoa and humans, where it has been shown to be a granulocyte-derived anti-inflammatory cytokine (Zocchi et al., 2001; Bruzzone et al., 2007; Johri, 2008; Nagamune et al., 2008; Khandelwal et al., 2010). A common action of ABA found in all these species is the activation of the ADP-ribosyl cyclase (ADPC), leading to an increase in cyclic ADP-ribose, which is an universal Ca^{2+} mobilizer (Lee, 1997; Guse, 2004).

ABA is a sesquiterpene derived from the carotenoid zeaxanthin. In plants, zeaxanthin is converted to xanthoxin in chloroplast, which is then exported to the cytosol, where the two final ABA biosynthesis steps occur.

Catabolism of ABA occurs via two mechanisms, hydroxylation mediated by P450 cytochromes of the CYP707A subfamily and conjugation mediated by UDP-glucosyltransferases. The importance of each of these pathways and the resulting composition in ABA catabolites is species and tissue-specific, and depends on developmental and physiological states (Neill et al., 1983; Zeevaart and Boyer, 1984; Hocher et al., 1991; Sauter et al., 2002; Priest et al., 2005; Okamoto et al., 2009; Seiler et al., 2011).

ABA 8'-hydroxylation represents the major catabolic pathway of ABA and has been shown to be a key regulatory step in ABA action (Kushiro et al., 2004). The intermediate oxidation product 8'-OH-ABA is rapidly isomerized to phaseic acid (PA), which is partially reduced to dihydroxyphaseic acid (DPA), depending on the tissue. PA

and DPA have been shown to exhibit lower or no biological activity (Sharkey and Raschke, 1980; Nambara and Marion-Poll, 2005). ABA 7'- and 9'-hydroxylations catalyzed by CYP707As resulting in 7'-OH-ABA, 9'-OH-ABA and neo-PA appear to be only minor ABA catabolic pathways in *Arabidopsis thaliana* (Okamoto et al., 2011).

Conjugation of ABA and its oxidative catabolites with glucose represents the other mechanism of ABA inactivation. The major conjugated form appears to be ABA glucosyl ester (ABA-GE) (Koshimizu et al., 1968; Loveys, 1979; Weiler, 1980; Boyer and Zeevaart, 1982; Lehmann and Glund, 1986; Xu et al., 2002; del Refugio Ramos et al., 2004), but a wide range of other conjugates, e.g. of 8'-OH-ABA, epi-DPA, DPA and PA have been identified (Milborrow, 1978; Lehmann and Glund, 1986; Carrington et al., 1988; del Refugio Ramos et al., 2004). While these conjugates are all hydrolysable under alkaline conditions, additional non-hydrolysable ABA conjugates were described in barley leaf protoplasts and in *Fagus sylvatica* seeds (Kaiser et al., 1985; Le Page-Degivry et al., 1997). In *Arabidopsis*, ABA-GE was found in considerable amounts in leaves and seeds (Priest et al., 2005; Okamoto et al., 2011), therefore appearing to be an important ABA conjugate. However, comprehensive data on ABA conjugate composition in *Arabidopsis* are not available.

ABA-GE is present in the apoplast and in the xylem (Dietz et al., 2000; Sauter et al., 2002; Christmann et al., 2005). Xylem ABA-GE was found to increase under drought, salt and osmotic stress. Due to its hydrophilic properties, ABA-GE may be transported over longer distances, without loss from diffusion into neighboring tissues. Therefore, ABA-GE was proposed to be a root-to-shoot signaling molecule (Sauter et al., 2002). This hypothesis was supported by the detection of ABA β-glucosidase activity in the extracellular space of barley leaves that may be involved in release of free ABA from xylem-borne ABA-GE (Dietz et al., 2000).

However, at least in *Arabidopsis*, root formation and root-to-shoot translocation of ABA or ABA-GE are not required for drought-stress response. Under drought stress, ABA *de-novo* biosynthesis leading to stomatal closure occurs independently of root ABA biosynthesis (Christmann et al., 2005; Christmann et al., 2007). Therefore, the

significance of ABA or ABA-GE mediated root-to-shoot signaling needs to be further elucidated (Goodger and Schachtman, 2010).

Intracellular compartmentalization of ABA and its catabolites is important in ABA homeostasis. In tomato cell culture protoplasts, free ABA, PA and DPA were found mainly in the extra-vacuolar compartments, whereas conjugated ABA was mostly found in the vacuole (Lehmann and Glund, 1986). Vacuoles isolated from *Vicia faba* leaf protoplasts, contained 91% of the total cellular ABA-GE and 22% of the total free ABA (Bray and Zeevaart, 1985).

However, at least in *Arabidopsis*, ABA-GE is also sequestered in the ER where it serves as a pool for the rapid release and increase of cytosolic free ABA, as suggested from the function of the ER-localized β-glucosidase AtBG1 that specifically hydrolyses ABA-GE (Lee et al., 2006). AtBG1 polymerizes under drought-stress resulting in an increased glucosidase activity, and plants lacking functional AtBG1 show impaired stomatal responses to day/night cycles and drought-stress conditions. There are evidences for an ABA-GE transporter in the ER membrane; however, no ABA-GE transporter protein, neither the transporter type has been characterized yet (Lee et al., 2006).

Except for the ER, there are no evidences that intracellular ABA-GE is hydrolyzed to release free ABA. ABA-GE has been shown to accumulate in leaves and cell cultures after drought-stress cycles (Milborrow, 1978; Zeevaart, 1980; Pierce and Raschke, 1981; Boyer and Zeevaart, 1982; Zeevaart, 1983; Priest et al., 2005). Vacuolar ABA-GE was therefore proposed to be a stable inactive end product of the ABA catabolism (Boyer and Zeevaart, 1982; Lehmann and Glund, 1986; Zeevaart, 1999). Since ABA-GE has a very low permeability for biological membranes (Boyer and Zeevaart, 1982; Baier et al., 1990), the accumulation of vacuolar ABA-GE must be the result of a transporter-mediated ABA-GE uptake or an intra-vacuolar conjugation of free ABA.

In this study, we characterized the transport of ABA-GE across the tonoplast by using isolated *Arabidopsis* leaf mesophyll vacuoles.

5.2 Materials and Methods

5.2.1 Solutions

For the vacuole isolation, following solutions were used: Mesophyll buffer (500 mM sorbitol, 1 mM $CaCl_2$, 10 mM MES-KOH pH 5.6). Sorbitol buffer (400 mM sorbitol, 30 mM potassium gluconate, 20 mM HEPES, pH 7.2 adjusted with imidazole, 1 mg/mL BSA, 1 mM DTT); Percoll pH 6 100% (500 mM sorbitol, 1 mM $CaCl_2$, 20 mM MES in Percoll 100% (GE Healthcare 17-0891-01)); Percoll pH 7.2 100% (500 mM sorbitol, 20 mM HEPES in Percoll 100%); Lysis buffer (200 mM sorbitol, 20 mM EDTA, 10 mM HEPES pH 8.0 with KOH, 10% Ficoll (GE Healthcare 17-0300-50), 0.2 mg/mL BSA, 1 mM DTT); Betaine buffer (400 mM betaine, 30 mM potassium gluconate, 20 mM HEPES, pH 7.2 adjusted with imidazole, 1 mg/mL BSA, 1 mM DTT). BSA and DTT were always added before use.

For the [^{14}C]ABA-GE synthesis and transport experiments following solutions were used: ABA 50 mM stock solution ((±)-Abscisic acid, Sigma A1049, was added to water and titrated with KOH until the compound was fully dissolved, pH was verified to be between 7.0 – 8.0, and aliquots were stored at –20 °C); UDP glucose 10 mM (Uridine 5'-diphosphoglucose disodium salt (Sigma 94335) dissolved in water, aliquoted and stored at -20 °C for a maximum of six months); ABA-GE 20 mM ((±)-*cis,trans*-Abscisic acid glucosyl ester (OlChemIm Ltd, Olomouc, Czech Republic) dissolved in ethanol and stored at -20 °C). [^{14}C]UDP glucose (Uridine diphosphate glucose, [glucose-14C(U)], American Radiolabeled Chemicals, Inc., ARC 0154). Bafilomycin A1 1 mM (dissolved in ethanol and stored at -20 °C); Quercetin 50 mM and quercetin 3-O-glucoside 50 mM (dissolved in DMSO and stored at -20 °C). For each experiment, fresh stock solutions were prepared for glibenclamide (10 mM in DMSO) and sodium orthovanadate (100 mM in water, boiled 5 min at 95 °C).

LB and YT media were prepared according to the GST Gene Fusion System Handbook (GE Healthcare Life Sciences). Other chemicals were purchased from Sigma-Aldrich in analytical grade quality.

5.2.2 Analysis of [^{14}C]UDP glucose purity

We have observed varying purities of the purchased [^{14}C]UDP glucose lots. Therefore, we assessed the lot quality by HPLC, according to a previously described method (Lazarowski et al., 2000). Briefly, 1 µCi [^{14}C]UDP glucose were separated by reversed-phase HPLC on a Hypersil C18 ODS-2 (5 µm, 250 x 4.6 mm) column (Thermo Scientific Ltd) and a mobile phase consisting of 8 mM tetrabutylammonium hydrogen sulfate, 60 mM KH_2PO_4, pH 5.3, and 15% methanol. The flow was set to 1 ml/min. Absorbance at 264 nm was detected using a PDA-100 photodiode array detector (Dionex, Olten, Switzerland) and the radioactivity was measured in-line with a Packard Radiomatic Flo-One Chromatograph Detector (PerkinElmer Inc.).

5.2.3 Expression and purification of recombinant UGT71B6

The intron-free UGT71B6 (At3g21780) gene was directly amplified from *Arabidopsis* (Col-0) genomic DNA using the primers At3g21780-EcoRI-ATG (5'-CCGGAATTCATGAA-AATAGAGCTAGTATTCATTCCCTC-3' and At3g21780-TGA-XhoI (5'-CCCGCTCGAGC-TAGCTTTCAGTTTCCGACCAA-3'), and ligated into the GST gene fusion vector pGEX-4T-1 (GE Healthcare Life Sciences) using the BamHI/XhoI restriction sites. The resulted plasmid was verified by sequencing (for sequencing primers see Section 5.5.2) and transformed into the *Escherichia coli* BL21-CodonPlus(DE3)-RIL strain (Agilent Technologies). From an overnight preculture of a fresh transformant colony in LB + 100 µg/mL ampicillin, 4 mL were added to 400 mL 2×YT + 100 µg/mL ampicillin, and grown at 37 °C to an OD_{600} of 0.5 - 0.6. Recombinant protein expression was induced by adding 0.4 mM IPTG and incubation at 14 °C for 16 h. Cells were harvested by centrifugation at 7700 × g for 10 min at 4 °C, resuspended in 20 mL ice-cold 1 x PBS + 0.1 % Triton X-100 and frozen overnight at -20 °C. Next day, the suspension was thawed on ice, briefly sonicated with five short bursts, and centrifuged at 12'000 × g for 10 min at 4 °C. The supernatant was used for purification of the fusion protein using Glutathione Sepharose 4B beads (GE Healthcare Life Sciences). Purification was performed according the manufacturer's instruction, except that fusion proteins were eluted with 20 mM reduced glutathione, 120 mM NaCl in 100 mM TRIS-HCl pH 8.0, and

concentrated to 50 µL using an Amicon Ultra-0.5 mL 30 kDa centrifugation ultrafilter (Millipore AG). After adding glycerol to a final concentration of 100 µL/mL, the recombinant enzyme preparation was aliquoted and stored at -80 °C. Protein concentrations were determined using the Bradford Protein Assay (Bio-Rad Laboratories) standardized against BSA.

5.2.4 [^{14}C]ABA-GE synthesis

The synthesis is based on a previously described protocol (Lim et al., 2005). The reaction was performed in a 1.5 mL polypropylene tube with a final volume of 100 µL. It contained 10 to 30 nmol (3.3 to 10 µCi) [^{14}C]UDP glucose (evaporated to dryness under a N_2 stream) or 30 nmol cold UDP glucose for control reactions, 100 mM TRIS-HCl pH 7.0, 10 mM DTT, 5 mM $MgCl_2$, 5 mM ABA and 4 - 5 µg UGT71B6 recombinant protein, added in the indicated order. After incubation for 12 h at 30 °C, the reaction was stopped by adding 20 µL of trichloroacetic acid (240 mg/mL) and centrifugation at 12'000 x g for 2 min (4 °C). The supernatant was immediately used for subsequent HPLC purification.

5.2.5 Reverse-phased HPLC purification of [^{14}C]ABA-GE

Reversed-phase HPLC employed a Hypersil C18 ODS-2 (5 µm, 250 x 4.6 mm) column (Thermo Scientific Ltd) and a mobile phase consisting of a linear gradient of 10 to 80% methanol in 0.1 M acetic acid (pH 3.5, adjusted with triethylamine) at a flow of 0.5 ml/min over 30 min. Detection was performed with a PDA-100 photodiode array detector (Dionex, Olten, Switzerland) at 270 nm. Authentic ABA-GE was used as reference for the retention time of synthesized ABA-GE. The mobile phase containing the eluted peak corresponding to ABA-GE was collected in a glass vial, evaporated to dryness under a N_2 stream at 30 °C, and stored for a maximum of one week at -20 °C. Immediately before use, 50 - 100 µL water was added and the compound was redissolved by sonification in an ultrasonic bath for 2 x 5 s and by vortexing.

5.2.6 Plant material

Wild-type *Arabidopsis thaliana* plants of the Col-0 accession were grown on standardized soil ED 73 ('Einheitserde Werkverband e.V.' association, Germany) in climate chambers with a constant temperature of 20 ± 2 °C, a relative humidity of 60 ± 10 %RH and short day conditions (8 /16 h light/dark cycle) with a light intensity of 100 µmol quanta m^{-2} s^{-1}. One week before vacuole isolation, the light intensity was reduced to 50 µmol quanta m^{-2} s^{-1}.

5.2.7 Isolation of *Arabidopsis* mesophyll vacuoles

The isolation of intact *Arabidopsis* leaf mesophyll vacuoles followed a previously described procedure (Frangne et al., 2002). Leaves from 5-6 weeks old plants were sandpapered at their abaxial side, washed with mesophyll buffer + 1 mg/mL BSA and incubated for 2 h at 30 °C on mesophyll buffer containing 10 mg/mL cellulase R10 and 5 mg/mL macerozyme R10 (SERVA Electrophoresis GmbH). Released protoplasts were collected by centrifugation at 50 g and 4 °C for 8 min, and mixed with 100% Percoll pH 6 to a Percoll concentration of 40%. The suspension was overlaid with 30% Percoll pH 7.2 (100% Percoll pH 7.2 diluted with protoplast buffer) and an additional layer of protoplast buffer. Following centrifugation for 8 min at 50 g and 4 °C, washed protoplasts were collected, warmed to 37 °C, mixed with an equal volume of lysis buffer (pre-warmed to 42 °C) and incubated at room temperature under gentle mixing by inversing the tube. Release of vacuoles was surveyed under the microscope and reaction was stopped after 5 – 10 min by cooling the lysate to 4 °C. The lysate was then overlaid with lysis buffer/betaine buffer (1:1) and a layer of betaine buffer. After centrifugation at 260 g and 4 °C for 8 min, vacuoles were collected into a new tube and kept on ice. The purity and density of the vacuole suspension was examined under the microscope. Immediately before use, vacuoles were supplemented with Percoll pH 7.2 to a Percoll concentration of 30%. A representative photo of isolated vacuoles used for uptake experiments is presented in Figure 3.

5.2.8 ABA-GE uptake assays

Determination of ABA-GE import into isolated vacuoles was based on the previously described silicon oil centrifugation method (Rentsch and Martinoia, 1991; Frangne et al., 2002). Each reaction contained 70 µl of 47% Percoll pH 7.2, 2.8 mg/mL BSA, 1.4 mM DTT, 0.05 µCi $^{3}H_2O$, and 1.4 mM $MgCl_2$ for the –ATP reactions, or 7.1 mM $MgCl_2$ and 5.7 mM ATP for the +ATP reactions. [^{14}C]ABA-GE concentration was between 0.7 and 2 µM (corresponding to 21 – 60 µCi). For transport kinetics determinations, corresponding amounts of cold ABA-GE were added (evaporated under a N_2 stream). Uptake experiments were performed by adding 30 µl vacuole suspension. The vacuolar volume for each reaction was calculated using the counts originating from $^{3}H_2O$.

5.2.9 Estimation of enzyme kinetic parameters

The Michaelis-Menten nonlinear regression fits were calculated using the nls and SSmicmen functions of R 2.13.0 (http://www.R-project.org).

5.2.10 Analysis of substrate stability during uptake experiments

Pooled vacuoles from five uptake experiment replicates were mixed with trichloroacetic acid at a final concentration of 48 mg/mL and centrifuged at 12’000 x g for 5 min (4 °C). From the supernatant, 200 µl were injected into the same HPLC system used for [^{14}C]ABA-GE purification. Fractions were collected each 3 min, concentrated to 0.5 mL under a N_2 stream at 30 °C, and after addition of 3 mL Ultima Gold scintillation cocktail (PerkinElmer Inc), measured in a Packard Tri-Carb liquid scintillation spectrometer (PerkinElmer Inc.).

5.3 Results

5.3.1 Enzymatic synthesis of [^{14}C]ABA-GE from ABA and [^{14}C]UDP glucose using the recombinant ABA glucosyltransferase UGT71B6

The recombinant *Arabidopsis* ABA glucosyltransferase UGT71B6 was expressed as a GST-fusion protein in *Escherichia coli* and affinity purified. Approximately 250 – 500 µg protein was obtained from a 400 mL culture. The enzymatic synthesis of [^{14}C](+)ABA-GE was based on a previously published method (Priest et al., 2005) and optimized for highest [^{14}C]UDP glucose to [^{14}C](+)ABA-GE conversion efficiency by using a saturating ABA concentration, a prolonged incubation time and a high enzyme amount. To confirm the purity of the synthesized (+)ABA-GE, a synthesis using cold UDP glucose was prepared and a fraction of it was hydrolyzed with 1M NaOH. In the subsequent HPLC analyses, only one peak corresponding to ABA-GE was visible in the original substrate, while the ABA-GE peak was absent in the NaOH treated substrate, while a peak appeared corresponding to ABA (Figure 36).

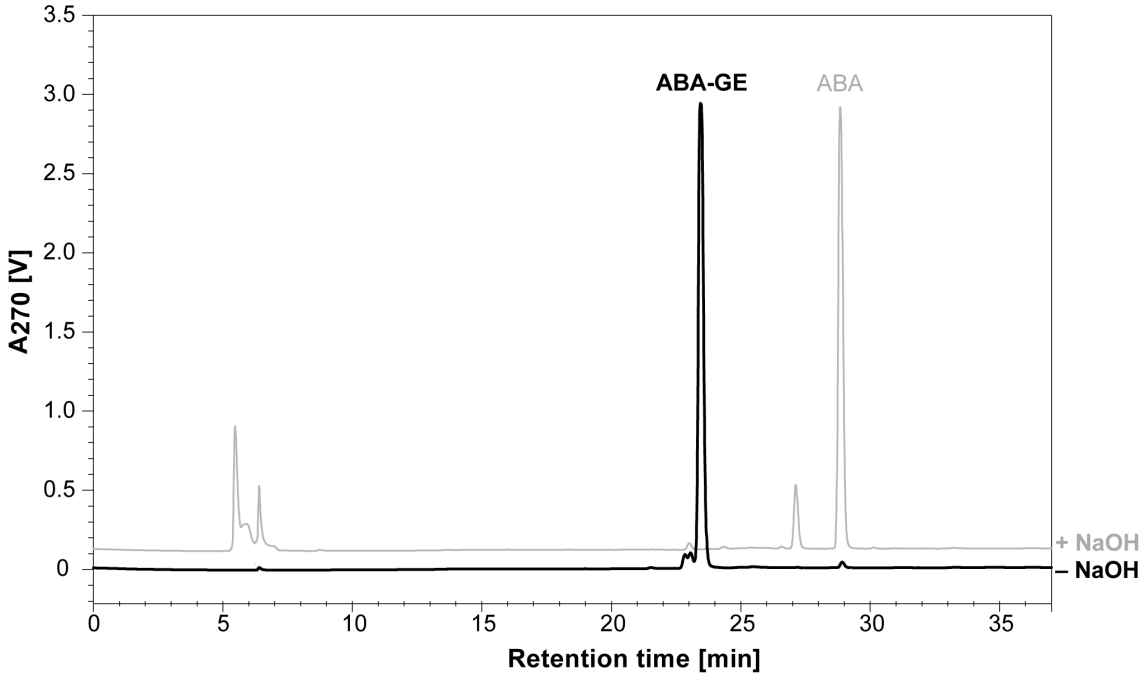

Figure 36. HPLC separation of the enzymatically synthesized and purified ABA-GE substrate, before (black chromatogram) and after (grey) hydrolysis with 1M NaOH.

5.3.2 Time-dependent uptake of ABA-GE into *Arabidopsis* vacuoles in the presence and absence of MgATP

Isolated *Arabidopsis* vacuoles accumulated (+)ABA-GE in a time-dependent manner (Figure 37). The presence of 4 mM MgATP enhanced the uptake by a factor 3.14 ± 0.82, mean ± SD from six experiments compared to the experimental conditions without MgATP. In both cases, the uptake was linear for at least 18 min. The extrapolated (+)ABA-GE uptake value at 0 min represents (+)ABA-GE that is nonspecifically associated to vacuoles. In following experiments, ABA-GE uptake rates were calculated from the uptake between 3 and 18 min.

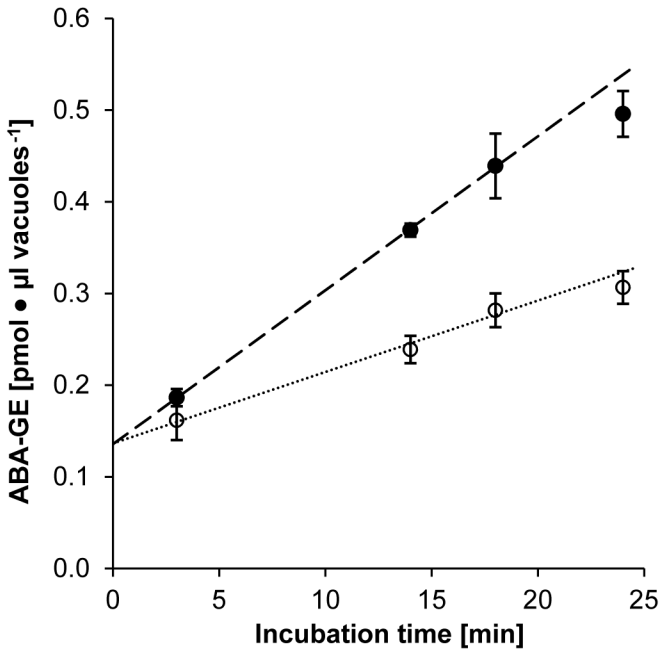

Figure 37. Time-dependent uptake of ABA-GE into *Arabidopsis* vacuoles in the presence (close circles) and absence (open circles) of 4 mM MgATP. The ABA-GE concentration in this assay was 0.77 µM.

5.3.3 Stability of [^{14}C]ABA-GE during uptake experiments

ABA-GE is prone to hydrolysis by ABA-β-glucosidases that cleave off the glucose at its β-(1-4) bond (Dietz et al., 2000; Lee et al., 2006). β-glucosidases released from lysed protoplasts and glucosidase contaminants from hydrolytic enzymes used during protoplast isolation may still be present in the vacuole preparation, despite that protoplasts and vacuoles are washed during their preparation. Additionally, other enzymes such as P450 cytochromes present in the vacuole suspension may degrade

ABA-GE before it is taken up by vacuoles. In order to verify that the measured ^{14}C radioactivity originated from labeled (+)ABA-GE and not from [^{14}C]ABA-GE degradation products, we separated lysed vacuoles obtained from transport experiment (after incubation time of 18 min) by HPLC and measured the radioactivity of collected fractions (Figure 38). In the presence of MgATP, 80% of the total radioactivity was found in the faction corresponding to ABA-GE, the remaining activity was distributed over the fractions from 3 – 15 min. In the absence of MgATP, 57% of the total activity was found in the ABE-GE fraction and 24% in the 3 – 6 min fractions. However, the total amount of degraded ABA-GE was similar under both conditions.

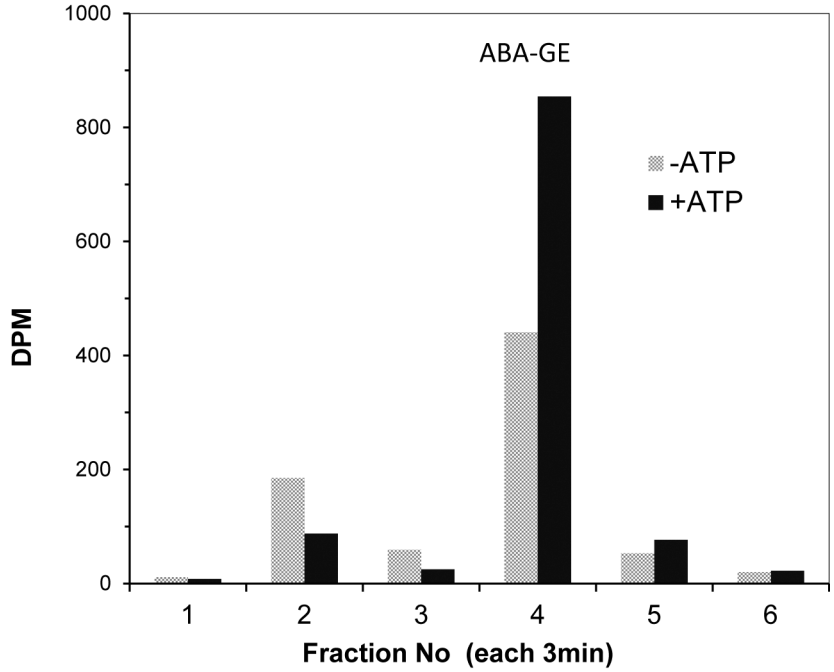

Figure 38. HPLC analysis of *Arabidopsis* vacuoles incubated with [^{14}C]ABA-GE for 18 min. Vacuoles obtained from five assay replicates were mixed with 48 mg/mL trichloroacetic acid and separated by HPLC. Fractions collected every 3 min were counted in liquid scintillation counter. Fraction 4 corresponds to the fraction in which ABA-GE elutes.

5.3.4 Distinct mechanisms energize ABA-GE uptake by *Arabidopsis* vacuoles

To discriminate whether the enhancement of vacuolar (+)ABA-GE uptake by MgATP is the result of a direct or indirect energization we analyzed the effects of ABC transporter inhibitors and compounds dissipating the proton gradient (Table 10). The tested individual compounds and combinations of which, partially inhibited the vacuolar ABA-GE uptake. The known ABC transporter inhibitors orthovanadate and glibenclamide (Martinoia et al., 1993; Payen et al., 2001) reduced the (+)ABA-GE uptake by 30 and 47%, respectively. Ammonium chloride, which dissipates the proton gradient over the membrane, reduced the uptake by 34%, and the vacuolar proton pump (V-ATPase) inhibitor Bafilomycin A1 (Bowman et al., 1988) by 43%. Combination of the ABC inhibitor orthovanadate and the V-ATPase inhibitor Bafilomycin A1 resulted in 57% reduction of the ABA-GE uptake, which is more than the effects of the individual compounds, but still higher than the uptake without addition of MgATP. Based on the total transport activity, inhibition was 57%. When related to the ATP-dependent transport activity, inhibition was 79.3%.

Table 10. Effect of ABC transporter inhibitors and membrane-potential modifiers on the vacuolar ABA-GE uptake of *Arabidopsis* vacuoles. n=3 or 4 if not otherwise stated.

Treatment		ABA-GE uptake % of +ATP	ABA-GE uptake % ATP dependent
+	ATP	**100**	**100**
-	ATP	**28.4 ± 12.0**	**0**
+	NH_4Cl (500 mM)	**66.4 ± 7.3**	**51.3**
+	Bafilomycin A1 (0.5 µM)	**56.9 ± 15.6**	**39.8**
+	Vanadate (1 mM)	**69.7 ± 13.0**	**57.7**
+	Glibenclamide (100 µM)	**52.9 (n=2)**	**34.2**
+	Bafilomycin A1 (50 µM) + Vanadate (1 mM)	**43.2 (n=2)**	**20.7**

5.3.5 Specificity of ABA-GE uptake mechanisms

To test the specificity of the (+)ABA-GE transport mechanisms, free ABA, glucose, sucrose and UDP-glucose were tested for their ability to compete with the ABA-GE uptake. None of these substances was able to significantly inhibit the (+)ABA-GE uptake. While 5 mM glucose inhibited the uptake by 11%, ABA (5 mM) and sucrose (5 mM) inhibited the transport by less than 6%. Additionally, quercetin was tested, as it

has been shown to inhibit ABC and other transporters (Otsuka et al., 2005; van Zanden et al., 2005). Quercetin (0.5 mM) and quercetin 3-O-glucoside (0.5 mM) strongly inhibited (+)ABA-GE uptake by 78 and 73%, respectively, which is more than any other compound tested in this work.

Table 11. Effect of ABA and Glucose analogs on vacuolar ABA-GE uptake. ABA-GE concentration in the uptake medium was 2 µM.

Treatment		ABA-GE uptake % of +ATP
+	ATP	**100**
-	ATP	**28.4 ± 12.0 (n=4)**
+	UDP glucose (0.1 mM)	**96.7 (n=1)**
+	Glucose (5 mM)	**89.3 (n=1)**
+	Sucrose (5 mM)	**95.3 (n=1)**
+	ABA (0.5 mM)	**94.4 (n=1)**
+	ABA-GE (1 mM)	**38.2 (n=2)**
+	Quercetin (0.1 mM)	**60.6 (n=1)**
+	Quercetin (0.5 mM)	**22.6 (n=1)**
+	Quercetin 3-O-glucoside (0.5 mM)	**27.0 (n=2)**

5.3.6 Kinetics of the vacuolar ABA-GE uptake

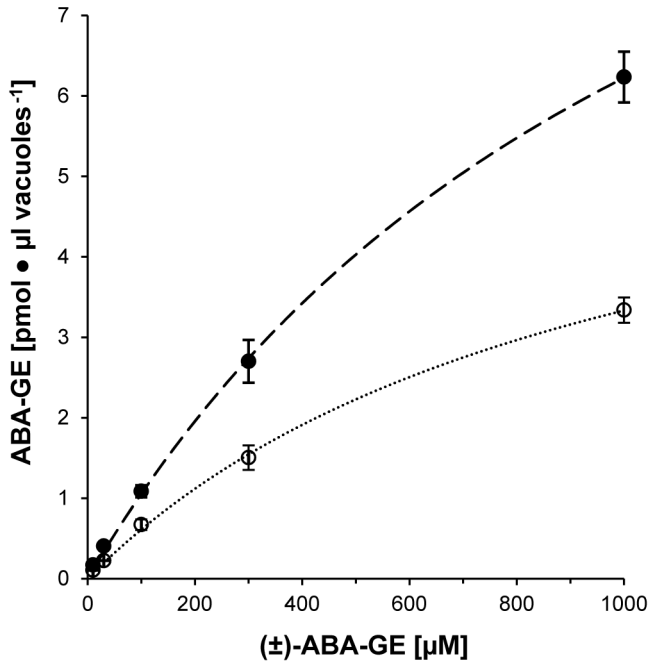

Figure 39. Representative saturation curves for the uptake of ABA-GE in dependence of the ABA-GE concentration, in presence of Bafilomycin A1 (0.5 µM, open circles) or vanadate (1 mM, closed circles).

The fact that (+)ABA-GE uptake was reduced by inhibitors affecting different pumps indicated that distinct transporter systems work in parallel, one corresponding to an ABC transporter type (the vanadate inhibited) and the second to an uptake by a secondary energized process (Bafilomycin A1 and NH_4^+). To analyze the anticipated ABC and proton-gradient driven transport mechanisms, distinct kinetics were determined in the presence of the ABC transport inhibitor vanadate and the V-ATPase inhibitor Bafilomycin A1, respectively. Both kinetics displayed Michealis-Menten saturation curves with statistically significant non-linear Michealis-Menten regression fits (Figure 39). In a representative analysis, the estimated K_m was 1.20 ± 0.1 mM (±)ABA-GE in presence of Bafilomycin A1 and 0.98 ± 0.12 mM (±)ABA-GE in the presence of vanadate. The estimated V_{max} was higher for the uptake in presence of Bafilomycin A1 (13.69 ± 0.66 pmol (±)ABA-GE · µl vacuoles^{-1}) than in the presence of vanadate (6.61 ± 0.44 pmol · (±)ABA-GE µl vacuoles^{-1}).

5.4 Discussion

In mesophyll cells, ABA-GE is mainly compartmentalized to vacuoles (Bray and Zeevaart, 1985; Lehmann and Glund, 1986). This ABA-GE accumulation must occur via transporter-mediated mechanisms or by intra-vacuolar conjugation of free ABA, as ABA-GE has a low permeability for biological membranes (Boyer and Zeevaart, 1982; Baier et al., 1990). In this work, we demonstrated that ABA-GE is transported into *Arabidopsis* vacuoles by two distinct directly energized mechanisms.

To characterize ABA-GE transport, we established a method to efficiently synthesize radiolabeled [^{14}C](+)ABA-GE from commercially available [^{14}C]UDP glucose. We determined the uptake of (+)ABA-GE into intact vacuoles isolated from *Arabidopsis* leaf mesophyll protoplasts. The ATP-enhanced uptake indicated the presence of actively energized transport mechanisms for (+)ABA-GE (Figure 37). This active transport appears to be mediated by two distinctly energized mechanisms. On one hand, the partial inhibition of transport by ABC transporter inhibitors indicated ABC transporter mediated mechanisms, and on the other hand, the partial inhibition by compounds altering the proton gradient indicated the presence of a proton-gradient energized mechanism (Table 10).

The ABC and proton-gradient driven ABA-GE uptake characterized in this work exhibited comparable K_m values of 800 and 1200 µM, respectively (Figure 39). In isolated *Vicia faba* mesophyll protoplasts 91% of the total ABA-GE was found in vacuoles (Bray and Zeevaart, 1985) and based on this a vacuolar ABA-GE concentration of approximately 3 µM can be calculated supposing a vacuolar volume of 20 pL. The cytoplasmic ABA-GE concentration is expected to be lower than the vacuolar concentration, assuming the vacuolar volume being 80% of the protoplast volume and that also the ER contains ABA-GE. While this estimated cytosolic ABA-GE concentration is considerably lower than the apparent K_m of the ABA-GE transport systems characterized here, these transport systems would nevertheless allow the accumulation of ABA-GE within 3 to 4 hours to the reported concentration assuming a cytosolic concentration of 0.5 µM.

Vacuolar sequestration via ABC transporter and proton dependent mechanisms have been shown for glucose conjugates of various secondary metabolites and xenobiotic compounds, including flavone glycosides (Frangne et al., 2002), epicatechins (Zhao et al., 2011), salicylic acid glucose (Dean and Mills, 2004; Dean et al., 2004) and xenobiotics (Klein et al., 1996; Bartholomew et al., 2002). So far, the only unequivocally tonoplast-localized ABC proteins identified in *Arabidopsis* belong to the ABCC subfamily, aside from the half-size ABCB protein AtABCB27 (TAP2) (Jaquinod et al., 2007; Nagy et al., 2009; Song et al., 2010).

Members of the ABCC subfamily (Verrier et al., 2008), previously named multidrug-resistance proteins, may be candidates for the ABC transporter mediated ABA-GE uptake, as they have been shown to function in the cellular detoxification mechanism and to transport various organic anions and their conjugates (Ton et al., 2009). Proton antiporters of the multidrug and toxic compound extrusion protein (MATE) family (Omote et al., 2006), of which some reside on the tonoplast and were shown to transport glycosylated flavonoids (Jaquinod et al., 2007; Zhao and Dixon, 2009) may be candidates for the proton dependent ABA-GE uptake.

Recently, two plasma-membrane localized ABC proteins catalyzing ABA transport have been identified (Kang et al., 2010; Kuromori et al., 2010). However, under our experimental conditions free ABA at concentrations well above the Km (5 mM) did not inhibit ABA-GE transport (Table 11), showing that the transport mechanisms are specific for the glucosylated ABA but not for free ABA.

The flavonoids quercetin and its 3-O-glucoside strongly inhibited ABA-GE uptake into vacuoles, to the level when ATP was absent (Table 11). Quercetin and its glucoside have been shown to be inhibitors as well as substrates of ABC transporters (van Zanden et al., 2005; An et al., 2011). Therefore, these compounds may competitively and non-competitively inhibit ABC transporters involved in vacuolar ABA-GE uptake. In addition, quercetin and quercetin glucosides were shown to inhibit MATE transporters in human and plants (Otsuka et al., 2005; Zhao et al., 2011). The strong inhibitory

effect of quercetin supports the findings that ABC transporters and other transporters, i.e. MATEs, are involved in ABA-GE uptake.

Quercetin and quercetin glucosides are also substrates of the animal sodium-dependent glucose transporter SGLT1 (Walgren et al., 2000; Wolffram et al., 2002), which was shown to transport other glucosides as well (Lostao et al., 1994; Díez-Sampedro et al., 2000). In plants, such transporters have not been found. The only identified proteins involved in the plant vacuolar import of glucose are the tonoplast monosaccharide transporters (TMT) (Wormit et al., 2006; Cho et al., 2010) and the vacuolar glucose transporters (VGT) (Aluri and Büttner, 2007), which function as glucose/H^+ antiporters. However, 5 mM glucose did not inhibit vacuolar ABA-GE uptake (Table 11), suggesting that these monosaccharide transporters are not involved in ABA-GE sequestration.

In this work, we have characterized the vacuolar sequestration mechanisms for ABA-GE, a membrane-impermeable ABA catabolite. ABA-GE appears to be mainly imported via ABC transporter and proton antiporter mechanisms, which may be part of broad-spectrum sequestration system for conjugated metabolites.

5.5 Supplementary Information

5.5.1 Vector map of the pGEX-4T-1-UGT71B6 expression construct

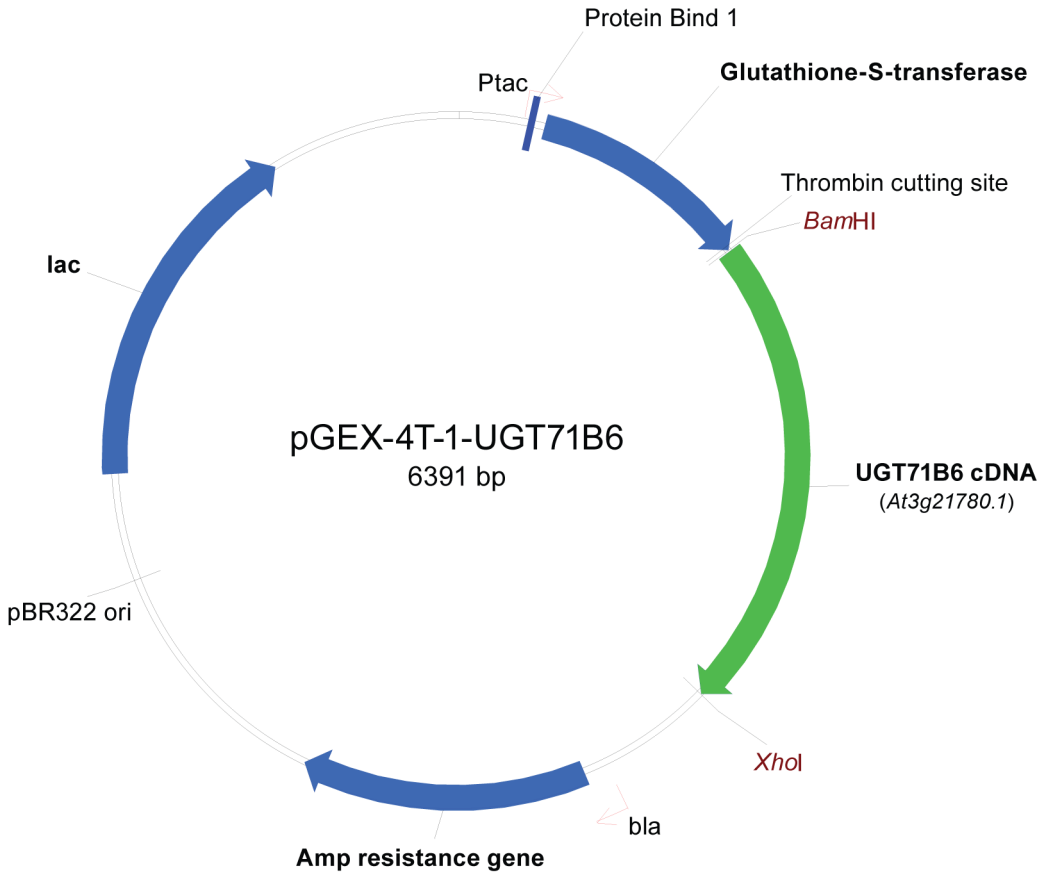

5.5.2 Cloning and sequencing primers.

Primer name	Sequence	T melt [°C]
At3g21780-EcoRI-ATG	CCGGAATTCATGAAAATAGAGCTAGTATTCATTCCCTC	54.8
At3g21780-TGA-XhoI	CCCGCTCGAGCTAGCTTTCAGTTTCCGACCAA	54.2
UGT71B6-SqP1	TCCGGCAATTAGTCATCTCA	50.5
UGT71B6-SqP2	GTTGACATGTACTGCACGTC	45.6
UGT71B6-SqP3	AACACGGTTCCTGACTTGGA	51.8
UGT71B6-SqP4	AGAGCCTCCCGGAGAATTCA	55.1
UGT71B6-SqP5	GGGAGGTCGGAGATTGTGAC	53.1
UGT71B6-SqP6r	TGGATGTGGGAATCAGTTGC	53.0

Primer melting temperatures (Tm) were calculated using VectorNTI 5 (Invitrogen)

6. General Conclusions

6.1 Evolution of the *ABCC* gene family

In Chapter I of this thesis, *ABCC* gene inventories of 135 species from most eukaryotic kingdoms were identified. Robust phylogenetic analyses were then performed on the identified *ABCC* genes. A phylogeny comprising *ABCC* genes from all kingdoms revealed ten distinct *ABCC* clades. One of these clades (termed *ABCC-E* clade) presumably evolved very early in eukaryotic evolution and comprises single-copy *ABCC* genes from all analyzed plant, most animal and a few protozoan species. All other *ABCC* clades comprise plant, fungal, or animal *ABCCs* only. The four animal-specific *ABCC* clades apparently evolved independently before the emergence of animals.

A phylogeny of plant *ABCC* genes revealed the existence of eight distinct plant-specific *ABCC* clades, additional to the plant *ABCC-E* clade. All analyzed angiosperms comprise *ABCCs* in each of these clades. Additionally, five of the plant-specific clades comprise *ABCC* genes from the moss *Physcomitrella patens,* whereas only one plant-specific clade contains *ABCC* genes from algae. The other plant-specific clades probably evolved during evolution of angiosperms. The plant-specific *ABCC* clades can furthermore be categorized into evolutionarily 'stable' and 'dynamic' clades. The 'stable' clades harbor only one or few *ABCC* genes per species, whereas the 'dynamic' clades usually comprise multiple paralogous *ABCCs* per species and lineage-specific *ABCC* gene expansions. Interestingly, all plant ABCC transporters for which a function has been published are members of 'stable' clades. The fact that these ABCC genes function in central physiological processes may explain why knockout mutants of these genes exhibit detectable phenotypes. The lack or reduced redundancy resulting from the absence or presence of only few paralogs within the same clade may furthermore explain the dominance of these *ABCC* genes. On the other hand, *ABCC* paralogs from expanded 'dynamic' clades possibly have evolved in a species-specific context. Lineage-specific expansions in these clades may reflect adaptations, e.g. to pathogens or environmental conditions, and/or the evolution of specific physiological and anatomical traits. Knockout mutants of *ABCC* genes from these 'dynamic' clades may exhibit phenotypes that cannot be identified in screenings that do not target lineage-

specific traits, such as screenings for general abiotic stress responses. The identification of mutant phenotypes of these *ABCC* genes may further be hampered by the presence of paralogs in the same clade, which exhibit functional redundancy.

A phylogenetic analysis of invertebrate *ABCC* genes likewise revealed 'stable' clades that are relatively small with only few paralogs per species, and 'dynamic' clades in which most species have, in some cases even greatly, expanded *ABCC* gene families. The chordate *ABCC* phylogeny revealed 12 distinct clades, which all, except one, comprise one human *ABCC* gene member. All chordate *ABCC* clades represent 'stable' clades, which comprise no species-specific expansions, except of the *ABCC4* clade, which is expanded in cow and in most of the analyzed fish.

The sizes of the *ABCC* gene families display large differences between species, but positively correlate with the total numbers of genes per species. The majority of species with reduced genomes, such as endoparasites, comprise few *ABCC* genes. Likewise, species that underwent multiple or recent whole genome duplications (WGD) and that have high numbers of genes, such as the ciliate *Paramecium tetraurelia* and the soybean *Glycine max,* harbor large *ABCC* gene families. Phylogenetic analyses of the *Glycine max ABCC* gene family showed that most of the *ABCC* clades comprise multiple paralogs, which is likely the result of the recent WGD. On the other hand, several species with relatively small genomes, including the grape *Vitis vinifera* and the red flour beetle *Tribolium castaneum,* also comprise large *ABCC* gene families. Phylogenetic analyses revealed that these large *ABCC* gene families are the result of massive expansions in one or very few specific clades. The paralogs of these clades were all found in local tandem clusters in the genome, suggesting that these expansions are the result of specific evolutionary processes, e.g. lineage-specific adaptations.

The reconstruction of the evolutionary history of the *ABCC* gene family may help for a better understanding of ABCC functions and evolution. The identification of distinct clades and orthologous/paralogous groups of ABCC genes may be useful to elucidate functions of so far uncharacterized *ABCC* genes and to find functional orthologs of

already characterized *ABCC* genes. From a biotechnological point of view, the information on orthologous relationships between *ABCC* genes may help in the identification of gene variants exhibiting the highest activity or other desired properties, based on a 'lead-gene', e.g. a gene that was first discovered in a model species, such as *Arabidopsis*. Furthermore, this work established new or updated *ABCC* gene inventories and improved gene models for various species. Finally, the findings of this chapter advocate for an extension of the current plant *ABCC* gene nomenclature in order to indicate the orthologous group to which an *ABCC* gene belongs.

6.2 *AtABCC13* - the *Arabidopsis* ortholog of the conserved *ABCC-E* clade

In Chapter II of this thesis, the *Arabidopsis ABCC* gene *AtABCC13* was characterized. *AtABCC13* is the *Arabidopsis* ortholog of the above-mentioned distinct *ABCC-E* clade identified in Chapter I, which comprises single-copy orthologous *ABCC* genes from plant, animals and protozoa. *AtABCC13* is phylogenetically distinct to all other *Arabidopsis ABCC* genes and has previously been reported to be truncated compared to other Arabidopsis *ABCC* genes. This suggested that *AtABCC13* represents an *ABCC* gene with distinct and evolutionarily conserved functions. It was expected that *AtABCC13* deletion mutants would have identifiable phenotypes, since there are no close paralogs that may exhibit redundant functions. An extensive phenotypic screening has been conducted with various conditions, including treatments with genotoxic compounds and exposures to abiotic stresses. However, under all tested conditions, the *AtABCC13* knockout lines did not exhibit any altered phenotypes compared to the wild-type lines. The absence of an identifiable phenotype is in contrast to the evolutionary conservation of *AtABCC13* and its presence as a single-copy gene, suggesting a functional importance of *AtABCC13*. The absence of a phenotype of *AtABCC13* knockout lines is furthermore in contrast to other characterized ABCC transporters from 'stable clades', which produce phenotypes when knocked out, e.g. the *Arabidopsis* phytate transporter gene *AtABCC5*. Consequently, *AtABCC13* may function in processes that were not targeted by the phenotype

screening, or *AtABCC13* knockout phenotypes were not detectable under the tested conditions. Biotic stresses, such as infections with pathogens, and evidently numerous other possible conditions have not been tested due to time and infrastructural restrictions. The absence of phenotypes identified in *AtABCC13* knockout lines is in accordance with recent data from mice in which *MmABCC10*, the mouse ortholog of *AtABCC13,* was knocked out. These *MmABCC10* knockout mice were reported to be healthy and to exhibit no observable phenotype under normal breeding conditions. Even a small selective advantage conferred by a gene can result in its conservation during evolution. It is therefore conceivable that the *Arabidopsis AtABCC13* and the mouse *MmABCC10* confer small selective advantages, which are only detectable over several generations and were thus not identified in screens for phenotypes.

Several genetic characteristics of *AtABCC13* were revealed in this thesis. In contrast to earlier publications, *AtABCC13* was characterized to encode a full-length 'long' *ABCC* protein that comprises a putative transmembrane domain 0 (TMD0). Several transcript variants of *AtABCC13* were identified, indicating alternative splicing and alternative transcription start sites. *AtABCC13* has a distinctive high intron density with 33 introns, whereby its second intron belongs to the rare U12-dependent intron class. The AtABCC13 protein is targeted to the vacuolar membrane, as other characterized *Arabidopsis* ABCC proteins. This suggests that the vacuolar localization of *Arabidopsis* ABCC proteins has evolved early in plant evolution. *AtABCC13* appears to be expressed at low level in most tissues, but is particularly highly expressed in the egg cell, parts of the developing seed, root pericycle and vascular bundles. The expression patterns suggest an increased expression of *AtABCC13* in tissues comprising cells with mitotic activity. Unfortunately, many of these expression data were only available after the phenotype screening had been completed. Therefore, a new screen with tests involving tissues where *AtABCC13* is highly expressed, as well as morphological and biochemical analyses of these tissues may be steps towards the identification of processes in which AtABCC13 functions. The characterization of *AtABCC13* and orthologs in other plant and animal species may also be valuable to understand the evolution and functions of other *ABCC* genes.

6.3 Mechanisms of vacuolar ABA-GE uptake

In Chapter III, the vacuolar uptake of abscisic acid glucosyl ester (ABA-GE) into *Arabidopsis* vacuoles was characterized. ABA-GE is a hydrolysable catabolite of the phytohormone abscisic acid that preferentially accumulates in the plant vacuole. Vacuolar ABA-GE sequestration may play a role in ABA homeostasis. However, the mechanisms by which ABA-GE is imported into the vacuole have not yet been identified. ABCC transporters were considered as candidates for vacuolar ABA-GE import, because they have been demonstrated to mediate the transport of glucose conjugates, and are so far the only ABC proteins that have been shown to reside on the vacuolar membrane, aside from the half-size ABC protein AtABCB27 (TAP2).

In order to perform uptake experiments with isolated *Arabidopsis* leaf mesophyll vacuoles using radiolabeled ABE-GE, an enzymatic method was developed to efficiently synthesize radiolabeled ABA-GE in high purity from radiolabeled UDP-Glucose. The conducted uptake experiments revealed that two distinct active transport mechanisms work in parallel: a proton gradient-dependent and an ABC transporter-mediated mechanism. Both transport mechanisms have an apparent Km of approximately 1 mM, which possibly is sufficient for the vacuolar sequestration of ABA-GE synthesized in the cytoplasm. Furthermore it was shown, that the vacuolar ABA-GE uptake is not inhibited by free ABA and glucose. Nevertheless, both transporter systems may be elements of a broad-spectrum sequestration system for conjugated metabolites.

The findings from this thesis project provide a starting point for the identification of transporters involved in vacuolar ABA-GE sequestration. To determine whether and which ABCC transporters are involved in vacuolar ABA-GE uptake, *Arabidopsis* ABCCs proteins will be tested for ABA-GE transport activity using a heterologous yeast expression system. Additionally, vacuolar ABA-GE levels of *Arabidopsis ABCC* gene knockout mutants will be determined.

Besides, the developed enzymatic method to efficiently synthesize radiolabeled ABA-GE in high purity may be valuable to other researchers working on ABA metabolism.

7. References

Aaronson S, Dhawale SW, Patni NJ, Deangelis B, Frank O, Baker H (1977) The cell content and secretion of water-soluble vitamins by several freshwater algae. Arch. Microbiol. **112**: 57-59

Addicott FT, Lyon JL, Ohkuma K, Thiessen WE, Carns HR, Smith OE, Cornforth JW, Milborrow BV, Ryback G, Wareing PF (1968) Abscisic acid: a new name for abscisin II (dormin). Science **159**: 1493

Akasaka T, Klinedinst S, Ocorr K, Bustamante EL, Kim SK, Bodmer R (2006) The ATP-sensitive potassium (KATP) channel-encoded dSUR gene is required for Drosophila heart function and is regulated by tinman. Proc. Natl. Acad. Sci. U.S.A. **103**: 11999-12004

Aller SG, Yu J, Ward A, Weng Y, Chittaboina S, Zhuo R, Harrell PM, Trinh YT, Zhang Q, Urbatsch IL, et al (2009) Structure of P-Glycoprotein Reveals a Molecular Basis for Poly-Specific Drug Binding. Science **323**: 1718-1722

Altschul SF, Gish W, Miller W, Myers EW, Lipman DJ (1990) Basic local alignment search tool. J. Mol. Biol. **215**: 403-410

Altschul SF, Madden TL, Schäffer AA, Zhang J, Zhang Z, Miller W, Lipman DJ (1997) Gapped BLAST and PSI-BLAST: a new generation of protein database search programs. Nucleic Acids Res. **25**: 3389-3402

Aluri S, Büttner M (2007) Identification and functional expression of the Arabidopsis thaliana vacuolar glucose transporter 1 and its role in seed germination and flowering. Proc. Natl. Acad. Sci. U.S.A. **104**: 2537-2542

An G, Gallegos J, Morris ME (2011) The Bioflavonoid Kaempferol Is an Abcg2 Substrate and Inhibits Abcg2-Mediated Quercetin Efflux. Drug Metab. Dispos. **39**: 426-432

Andreini C, Banci L, Bertini I, Rosato A (2011) Zinc through the Three Domains of Life. J. Proteome Res. **5**: 3173-3178

Anjard C, Loomis WF (2002) Evolutionary Analyses of ABC Transporters of Dictyostelium discoideum. Eukaryot. Cell **1**: 643-652

Annilo T, Chen Z-Q, Shulenin S, Costantino J, Thomas L, Lou H, Stefanov S, Dean M (2006) Evolution of the vertebrate ABC gene family: Analysis of gene birth and death. Genomics **88**: 1-11

Annilo T, Dean M (2004) Degeneration of an ATP-binding cassette transporter gene, ABCC13, in different mammalian lineages. Genomics **84**: 34-46

Arakaki AK, Tian W, Skolnick J (2006) High precision multi-genome scale reannotation of enzyme function by EFICAz. BMC Genomics **7**: 315

Aury J-M, Jaillon O, Duret L, Noel B, Jubin C, Porcel BM, Segurens B, Daubin V, Anthouard V, Aiach N, et al (2006) Global trends of whole-genome duplications revealed by the ciliate Paramecium tetraurelia. Nature **444**: 171-178

Baier M, Gimmler H, Hartung W (1990) The Permeability of the Guard Cell Plasma Membrane and Tonoplast. J. Exp. Bot. **41**: 351-358

Bakos É, Homolya L (2006) Portrait of multifaceted transporter, the multidrug resistance-associated protein 1 (MRP1/ABCC1). Pflugers Arch. **453**: 621-641

Barbier-Brygoo H, De Angeli A, Filleur S, Frachisse J-M, Gambale F, Thomine S, Wege S (2011) Anion Channels/Transporters in Plants: From Molecular Bases to Regulatory Networks. Annu. Rev. Plant Biol. **62**: 25-51

Bartholomew DM, Van Dyk DE, Lau S-MC, O'Keefe DP, Rea PA, Viitanen PV (2002) Alternate Energy-Dependent Pathways for the Vacuolar Uptake of Glucose and Glutathione Conjugates. Plant Physiol. **130**: 1562-1572

Belinsky MG, Chen Z-S, Shchaveleva I, Zeng H, Kruh GD (2002) Characterization of the Drug Resistance and Transport Properties of Multidrug Resistance Protein 6 (MRP6, ABCC6). Cancer Res. **62**: 6172-6177

Benson DA, Karsch-Mizrachi I, Lipman DJ, Ostell J, Sayers EW (2010) GenBank. Nucl. Acids Res. **38**: D46-51

Berg JM, Stryer L Leukotrienes *In* Biochemistry, 6th ed. W.H. Freeman and Co, 2006a, pp 643

Berg JM, Stryer L Taurocholate *In* Biochemistry, 6th ed. W.H. Freeman and Co, 2006b, pp 749

Bessho Y, Oguri T, Ozasa H, Uemura T, Sakamoto H, Miyazaki M, Maeno K, Sato S, Ueda R (2009) ABCC10/MRP7 is associated with vinorelbine resistance in non-small cell lung cancer. Oncol. Rep. **21**: 263-268

Bowman EJ, Siebers A, Altendorf K (1988) Bafilomycins: a class of inhibitors of membrane ATPases from microorganisms, animal cells, and plant cells. Proc. Natl. Acad. Sci. U.S.A. **85**: 7972-7976

Boyer GL, Zeevaart JAD (1982) Isolation and Quantitation of β-d-Glucopyranosyl Abscisate from Leaves of Xanthium and Spinach. Plant Physiol. **70**: 227-231

Bray EA, Zeevaart JAD (1985) The Compartmentation of Abscisic Acid and β-d-Glucopyranosyl Abscisate in Mesophyll Cells. Plant Physiol. **79**: 719-722

Bruzzone S, Moreschi I, Usai C, Guida L, Damonte G, Salis A, Scarfì S, Millo E, De Flora A, Zocchi E (2007) Abscisic acid is an endogenous cytokine in human granulocytes with cyclic ADP-ribose as second messenger. Proc. Natl. Acad. Sci. U.S.A. **104**: 5759-5764

Bryan J, Muñoz A, Zhang X, Düfer M, Drews G, Krippeit-Drews P, Aguilar-Bryan L (2006) ABCC8 and ABCC9: ABC transporters that regulate K+ channels. Pflugers Arch. **453**: 703-718

Buchanan BB, Gruissem W, Jones RL Chapter 1 Membrane Structure and Membranous Organelles. *In* Biochemistry & Molecular Biology of Plants, John Wiley & Sons Ltd, 2002, pp 25-29

Burge C, Karlin S (1997) Prediction of complete gene structures in human genomic DNA. J. Mol. Biol. **268**: 78-94

Capella-Gutiérrez S, Silla-Martínez JM, Gabaldón T (2009) trimAl: a tool for automated alignment trimming in large-scale phylogenetic analyses. Bioinformatics **25**: 1972-1973

Carlton JM, Hirt RP, Silva JC, Delcher AL, Schatz M, Zhao Q, Wortman JR, Bidwell SL, Alsmark UCM, Besteiro S, et al (2007) Draft Genome Sequence of the Sexually Transmitted Pathogen Trichomonas vaginalis. Science **315**: 207-212

Carmel L, Rogozin IB, Wolf YI, Koonin EV (2007) Evolutionarily conserved genes preferentially accumulate introns. Genome Res. **17**: 1045-1050

Carrington NJ, Vaughan G, Milborrow BV (1988) β-d-Glucopyranosyl phaseic acid from shoots of Lycopersicon esculentum. Phytochemistry **27**: 673-676

Cavalier-Smith T (2010) Kingdoms Protozoa and Chromista and the eozoan root of the eukaryotic tree. Biol. Lett. **6**: 342-345

Chang W-C, Chen Y-C, Lee K-M, Tarn W-Y (2007) Alternative splicing and bioinformatic analysis of human U12-type introns. Nucleic Acids Res. **35**: 1833-1841

Chen Z-S, Guo Y, Belinsky MG, Kotova E, Kruh GD (2005) Transport of Bile Acids, Sulfated Steroids, Estradiol 17-β-d-Glucuronide, and Leukotriene C4 by Human Multidrug Resistance Protein 8 (ABCC11). Mol. Pharmacol. **67**: 545-557

Chen Z-S, Hopper-Borge E, Belinsky MG, Shchaveleva I, Kotova E, Kruh GD (2003) Characterization of the Transport Properties of Human Multidrug Resistance Protein 7 (MRP7, ABCC10). Mol. Pharmacol. **63**: 351-358

Chen Z, Tiwari AK (2011) Multidrug resistance proteins (MRPs/ABCCs) in cancer chemotherapy and genetic diseases. FEBS J. **278**: 3226-3245

Chiwocha SDS, Abrams SR, Ambrose SJ, Cutler AJ, Loewen M, Ross ARS, Kermode AR (2003) A method for profiling classes of plant hormones and their metabolites using liquid chromatography-electrospray ionization tandem mass spectrometry: an analysis of hormone regulation of thermodormancy of lettuce (Lactuca sativa L.) seeds. Plant J. **35**: 405-417

Cho J, Burla B, Lee D, Ryoo N, Hong S, Kim H, Eom J, Choi S, Cho M, Bhoo SH, et al (2010) Expression analysis and functional characterization of the monosaccharide transporters, OsTMTs, involving vacuolar sugar transport in rice (Oryza sativa). New Phytol. **186**: 657-668

Christmann A, Hoffmann T, Teplova I, Grill E, Müller A (2005) Generation of Active Pools of Abscisic Acid Revealed by In Vivo Imaging of Water-Stressed Arabidopsis. Plant Physiol. **137**: 209-219

Christmann A, Weiler EW, Steudle E, Grill E (2007) A hydraulic signal in root-to-shoot signalling of water shortage. Plant J. **52**: 167-174

Christoffels A, Koh EGL, Chia J-ming, Brenner S, Aparicio S, Venkatesh B (2004) Fugu Genome Analysis Provides Evidence for a Whole-Genome Duplication Early During the Evolution of Ray-Finned Fishes. Mol. Biol. Evol. **21**: 1146-1151

Churakov G, Sadasivuni MK, Rosenbloom KR, Huchon D, Brosius J, Schmitz J (2010) Rodent Evolution: Back to the Root. Mol. Biol. Evol. **27**: 1315-1326

Clark R, Proks P (2010) ATP-sensitive potassium channels in health and disease. Adv. Exp. Med. Biol. **654**: 165-192

Cobbett CS (2000) Phytochelatins and Their Roles in Heavy Metal Detoxification. Plant Physiol. **123**: 825-832

Colangelo EP, Guerinot ML (2006) Put the metal to the petal: metal uptake and transport throughout plants. Curr. Opin. Plant Biol. **9**: 322-330

Colbourne JK, Pfrender ME, Gilbert D, Thomas WK, Tucker A, Oakley TH, Tokishita S, Aerts A, Arnold GJ, Basu MK, et al (2011) The Ecoresponsive Genome of Daphnia pulex. Science **331**: 555-561

Cole S, Bhardwaj G, Gerlach J, Mackie J, Grant C, Almquist K, Stewart A, Kurz E, Duncan A, Deeley R (1992) Overexpression of a transporter gene in a multidrug-resistant human lung cancer cell line. Science **258**: 1650-1654

Cole SPC, Deeley RG (2006) Transport of glutathione and glutathione conjugates by MRP1. Trends Pharmacol. Sci. **27**: 438-446

Coleman J, Blake-Kalff M, Davies E (1997) Detoxification of xenobiotics by plants: chemical modification and vacuolar compartmentation. Trends Plant Sci. **2**: 144-151

Corradi N, Slamovits CH (2010) The intriguing nature of microsporidian genomes. Brief. Funct. Genomics **10**:115-124

Creevey CJ, Muller J, Doerks T, Thompson JD, Arendt D, Bork P (2011) Identifying Single Copy Orthologs in Metazoa. PLoS Comput. Biol. **7**: e1002269

Csuros M, Rogozin IB, Koonin EV (2011) A Detailed History of Intron-rich Eukaryotic Ancestors Inferred from a Global Survey of 100 Complete Genomes. PLoS Comput. Biol. **7**: e1002150

Cui Y, König J, Buchholz U, Spring H, Leier I, Keppler D (1999) Drug Resistance and ATP-Dependent Conjugate Transport Mediated by the Apical Multidrug Resistance Protein, MRP2, Permanently Expressed in Human and Canine Cells. Mol. Pharm. **55**: 929-937

Curtis MD, Grossniklaus U (2003) A Gateway Cloning Vector Set for High-Throughput Functional Analysis of Genes in Planta. Plant Physiol. **133**: 462-469

Cutler AJ, Krochko JE (1999) Formation and breakdown of ABA. Trends Plant Sci. **4**: 472-478

Danilevskaya ON, Meng X, Hou Z, Ananiev EV, Simmons CR (2008) A Genomic and Expression Compendium of the Expanded PEBP Gene Family from Maize. Plant Physiol. **146**: 250-264

Darriba D, Taboada GL, Doallo R, Posada D (2011) ProtTest 3: fast selection of best-fit models of protein evolution. Bioinformatics **27**: 1164-1165

Dawson RJP, Locher KP (2006) Structure of a bacterial multidrug ABC transporter. Nature **443**: 180-185

Dean JV, Mills JD (2004) Uptake of salicylic acid 2-O-β-D-glucose into soybean tonoplast vesicles by an ATP-binding cassette transporter-type mechanism. Physiol. Plant. **120**: 603-612

Dean JV, Mohammed LA, Fitzpatrick T (2004) The formation, vacuolar localization, and tonoplast transport of salicylic acid glucose conjugates in tobacco cell suspension cultures. Planta **221**: 287-296

Decottignies A, Goffeau A (1997) Complete inventory of the yeast ABC proteins. Nat Genet. **15**: 137-145

DeGorter MK, Conseil G, Deeley RG, Campbell RL, Cole SPC (2008) Molecular modeling of the human multidrug resistance protein 1 (MRP1/ABCC1). Biochem. Biophys. Res. Commun. **365**: 29-34

Dellaporta SL, Wood J, Hicks JB (1983) A plant DNA minipreparation: Version II. Plant. Mol. Biol. Rep. **1**: 19-21

Derelle R, Lang BF (2011) Rooting the eukaryotic tree with mitochondrial and bacterial proteins. Mol. Biol. Evol. **29** 1277-1289

Dietz K, Sauter A, Wichert K, Messdaghi D, Hartung W (2000) Extracellular β-glucosidase activity in barley involved in the hydrolysis of ABA glucose conjugate in leaves. J. Exp. Bot. **51**: 937-944

Díez-Sampedro A, Lostao MP, Wright EM, Hirayama BA (2000) Glycoside binding and translocation in Na(+)-dependent glucose cotransporters: comparison of SGLT1 and SGLT3. J. Membr. Biol. **176**: 111-117

Dolan L, Janmaat K, Willemsen V, Linstead P, Poethig S, Roberts K, Scheres B (1993) Cellular organisation of the Arabidopsis thaliana root. Development **119**: 71-84

Endler A, Meyer S, Schelbert S, Schneider T, Weschke W, Peters SW, Keller F, Baginsky S, Martinoia E, Schmidt UG (2006) Identification of a Vacuolar Sucrose Transporter in Barley and Arabidopsis Mesophyll Cells by a Tonoplast Proteomic Approach. Plant Physiol. **141**: 196-207

Eswar N, Eramian D, Webb B, Shen M-Y, Sali A (2008) Protein structure modeling with MODELLER. Methods Mol. Biol. **426**: 145-159

Falcón-Pérez JM, Mazón MJ, Molano J, Eraso P (1999) Functional Domain Analysis of the Yeast ABC Transporter Ycf1p by Site-directed Mutagenesis. J. Biol. Chem. **274**: 23584-23590

Flicek P, Amode MR, Barrell D, Beal K, Brent S, Chen Y, Clapham P, Coates G, Fairley S, Fitzgerald S, et al (2010) Ensembl 2011. Nucleic Acids Res. **39**: D800-D806

Frangne N, Eggmann T, Koblischke C, Weissenböck G, Martinoia E, Klein M (2002) Flavone Glucoside Uptake into Barley Mesophyll and Arabidopsis Cell Culture Vacuoles. Energization Occurs by H+-Antiport and ATP-Binding Cassette-Type Mechanisms. Plant Physiol. **128**: 726-733

Frelet-Barrand A, Kolukisaoglu HU, Plaza S, Rüffer M, Azevedo L, Hörtensteiner S, Marinova K, Weder B, Schulz B, Klein M (2008) Comparative mutant analysis of Arabidopsis ABCC-type ABC transporters: AtMRP2 contributes to detoxification, vacuolar organic anion transport and chlorophyll degradation. Plant Cell Physiol. **49**: 557-569

Gahan LJ, Pauchet Y, Vogel H, Heckel DG (2010) An ABC Transporter Mutation Is Correlated with Insect Resistance to Bacillus thuringiensis Cry1Ac Toxin. PLoS Genet. **6**: e1001248

Galvan-Ampudia CS, Testerink C (2011) Salt stress signals shape the plant root. Curr. Opin. Plant Biol. **14**: 296-302

Gao X, Wang X, Ren F, Chen J, Wang X (2009) Dynamics of vacuoles and actin filaments in guard cells and their roles in stomatal movement. Plant Cell Environ. **32**: 1108-1116

Gaxiola R, Palmgren M, Schumacher K (2007) Plant proton pumps. FEBS Lett. **581**: 2204-2214

Geisler M, Frangne N, Gomès E, Martinoia E, Palmgren MG (2000) The ACA4 Gene of Arabidopsis Encodes a Vacuolar Membrane Calcium Pump That Improves Salt Tolerance in Yeast. Plant Physiol. **124**: 1814-1827

Gekeler W, Grill E, Winnacker E-L, Zenk MH (1988) Algae sequester heavy metals via synthesis of phytochelatin complexes. Arch Microbiol. **150**: 197-202

Gingerich DJ, Hanada K, Shiu S-H, Vierstra RD (2007) Large-Scale, Lineage-Specific Expansion of a Bric-a-Brac/Tramtrack/Broad Complex Ubiquitin-Ligase Gene Family in Rice. Plant Cell **19**: 2329-2348

Gleave AP (1992) A versatile binary vector system with a T-DNA organisational structure conducive to efficient integration of cloned DNA into the plant genome. Plant Mol. Biol. **20**: 1203-1207

Goldstone JV, Hamdoun A, Cole BJ, Howard-Ashby M, Nebert DW, Scally M, Dean M, Epel D, Hahn ME, Stegeman JJ (2006) The chemical defensome: environmental sensing and response genes in the Strongylocentrotus purpuratus genome. Dev. Biol. **300**: 366-384

Goodger JQ, Schachtman DP (2010) Re-examining the role of ABA as the primary long-distance signal produced by water-stressed roots. Plant Signal. Behav. **5**: 1298-1301

Goodman CD, Casati P, Walbot V (2004) A Multidrug Resistance-Associated Protein Involved in Anthocyanin Transport in Zea mays. Plant Cell **16**: 1812-1826

Gottesman MM (2002) Mechanisms of cancer drug resistance. Annu. Rev. Med. **53**: 615-627

Groß-Hardt R, Lenhard M, Laux T (2002) WUSCHEL signaling functions in interregional communication during Arabidopsis ovule development. Genes Dev. **16**: 1129-1138

Guo Y, Kotova E, Chen Z-S, Lee K, Hopper-Borge E, Belinsky MG, Kruh GD (2003) MRP8, ATP-binding Cassette C11 (ABCC11), Is a Cyclic Nucleotide Efflux Pump and a Resistance Factor for Fluoropyrimidines 2′,3′-Dideoxycytidine and 9′-(2′-Phosphonylmethoxyethyl)adenine. J. Biol. Chem. **278**: 29509-29514

Guse AH (2004) Regulation of calcium signaling by the second messenger cyclic adenosine diphosphoribose (cADPR). Curr. Mol. Med. **4**: 239-248

Gutmann DAP, Ward A, Urbatsch IL, Chang G, van Veen HW (2010) Understanding polyspecificity of multidrug ABC transporters: closing in on the gaps in ABCB1. Trends Biochem. Sci. **35**: 36-42

Hall SL, Padgett RA (1994) Conserved Sequences in a Class of Rare Eukaryotic Nuclear Introns with Non-consensus Splice Sites. J. Mol. Biol. **239**: 357-365

Hanada K, Kuromori T, Myouga F, Toyoda T, Li W-H, Shinozaki K (2009) Evolutionary Persistence of Functional Compensation by Duplicate Genes in Arabidopsis. Genome Biol. Evol. **1**: 409-414

Hanikenne M, Krämer U, Demoulin V, Baurain D (2005) A Comparative Inventory of Metal Transporters in the Green Alga Chlamydomonas reinhardtii and the Red Alga Cyanidioschizon merolae. Plant Physiol. **137**: 428-446

Hara-Nishimura I, Hatsugai N (2011) The role of vacuole in plant cell death. Cell Death Differ. **18**: 1298-1304

Hawkins PR, Jin P, Fu GK (2003) Full-length cDNA synthesis for long-distance RT-PCR of large mRNA transcripts. BioTechniques **34**: 768-770, 772-773

Hediger MA, Romero MF, Peng J-B, Rolfs A, Takanaga H, Bruford EA (2004) The ABCs of solute carriers: physiological, pathological and therapeutic implications of human membrane transport proteins. Pflugers Arch. **447**: 465-468

Held MA, Boulaflous A, Brandizzi F (2008) Advances in Fluorescent Protein-Based Imaging for the Analysis of Plant Endomembranes. Plant Physiol. **147**: 1469-1481

Herman EM, Larkins BA (1999) Protein Storage Bodies and Vacuoles. Plant Cell **11**: 601-614

Higgins CF, Haag PD, Nikaido K, Ardeshir F, Garcia G, Ames GF-L (1982) Complete nucleotide sequence and identification of membrane components of the histidine transport operon of S. typhimurium. Nature **298**: 723-727

Higgins CF (1992) ABC transporters: from microorganisms to man. Annu. Rev. Cell Biol. **8**: 67-113

Higgins CF, Linton KJ ABC transporters: an introduction and overview. *In* ABC Proteins from Bacteria to Man, Academic Press, 2003, pp xvii-xxii

Hirohashi T, Suzuki H, Takikawa H, Sugiyama Y (2000) ATP-dependent Transport of Bile Salts by Rat Multidrug Resistance-associated Protein 3 (Mrp3). J. Biol. Chem. **275**: 2905-2910

Hocher V, Sotta B, Maldiney R, Miginiac E (1991) Changes in abscisic acid and its β-D-glucopyranosyl ester levels during tomato (Lycopersicon esculentum Mill.) seed development. Plant Cell Rep. **10**: 444-447

Holdsworth MJ, Bentsink L, Soppe WJJ (2008) Molecular networks regulating Arabidopsis seed maturation, after-ripening, dormancy and germination. New Phytol. **179**: 33-54

Hooft RWW, Vriend G, Sander C, Abola EE (1996) Errors in protein structures. Nature **381**: 272

Hopper-Borge EA, Churchill T, Paulose C, Nicolas E, Jacobs JD, Ngo O, Kuang Y, Grinberg A, Westphal H, Chen Z-S, et al (2011) Contribution of Abcc10 (Mrp7) to In Vivo Paclitaxel Resistance as Assessed in Abcc10−/− Mice. Cancer Res. **71**: 3649-3657

Hopper-Borge E, Chen Z-S, Shchaveleva I, Belinsky MG, Kruh GD (2004) Analysis of the Drug Resistance Profile of Multidrug Resistance Protein 7 (ABCC10). Cancer Res. **64**: 4927-4930

Hopper-Borge E, Xu X, Shen T, Shi Z, Chen Z-S, Kruh GD (2009) Human multidrug resistance protein 7 (ABCC10) is a resistance factor for nucleoside analogues and epothilone B. Cancer Res. **69**: 178-184

Hörtensteiner S (2006) Chlorophyll degradation during senescence. Annu. Rev. Plant Biol. **57**: 55-77

Hruz T, Laule O, Szabo G, Wessendorp F, Bleuler S, Oertle L, Widmayer P, Gruissem W, Zimmermann P (2008) Genevestigator V3: A Reference Expression Database for the Meta-Analysis of Transcriptomes. Adv. Bioinformatics **420747**

Huang H, Haddad GG (2007) Drosophila dMRP4 regulates responsiveness to O2 deprivation and development under hypoxia. Physiol. Genomics. **29**: 260-266

Iglesias A Jr Vacuoles and plant defense *In* Vacuolar Compartments in Plants, Sheffield Academic Press, 2000, pp 112-132

Iwaki T, Giga-Hama Y, Takegawa K (2006) A survey of all 11 ABC transporters in fission yeast: two novel ABC transporters are required for red pigment accumulation in a Schizosaccharomyces pombe adenine biosynthetic mutant. Microbiology **152**: 2309-2321

Jackson A (2007) Evolutionary consequences of a large duplication event in Trypanosoma brucei: Chromosomes 4 and 8 are partial duplicons. BMC Genomics **8**: 432

Jaquinod M, Villiers F, Kieffer-Jaquinod S, Hugouvieux V, Bruley C, Garin J, Bourguignon J (2007) A proteomics dissection of Arabidopsis thaliana vacuoles isolated from cell culture. Mol. Cell. Proteomics **6**: 394-412

Jia H-F, Chai Y-M, Li C-L, Lu D, Luo J-J, Qin L, Shen Y-Y (2011) Abscisic Acid Plays an Important Role in the Regulation of Strawberry Fruit Ripening. Plant Physiol. **157**: 188-199

Jiang L, Phillips TE, Hamm CA, Drozdowicz YM, Rea PA, Maeshima M, Rogers SW, Rogers JC (2001) The protein storage vacuole. J. Cell Biol. **155**: 991-1002

Johri MM (2008) Hormonal regulation in green plant lineage families. Physiol. Mol. Biol. Plants **14**: 23-38

Kaiser G, Weiler EW, Hartung W (1985) The intracellular distribution of abscisic acid in mesophyll cells : the role of the vacuole. Journal of Plant Physiol. **119**: 237-245

Kang J, Hwang J-U, Lee M, Kim Y-Y, Assmann SM, Martinoia E, Lee Y (2010) PDR-type ABC transporter mediates cellular uptake of the phytohormone abscisic acid. Proc. Natl. Acad. Sci. U.S.A. **107**: 2355-2360

Kang J, Park J, Choi H, Burla B, Kretzschmar T, Lee Y, Martinoia E (2011) Plant ABC Transporters. The Arabidopsis Book 9: e0153

Katinka MD, Duprat S, Cornillot E, Méténier G, Thomarat F, Prensier G, Barbe V, Peyretaillade E, Brottier P, Wincker P, et al (2001) Genome sequence and gene compaction of the eukaryote parasite Encephalitozoon cuniculi. Nature **414**: 450-453

Kavak E, Unlu M, Nister M, Koman A (2010) Meta-analysis of cancer gene expression signatures reveals new cancer genes, SAGE tags and tumor associated regions of co-regulation. Nucleic Acids Res. **38**: 7008-7021

Keitel V, Nies AT, Brom M, Hummel-Eisenbeiss J, Spring H, Keppler D (2003) A common Dubin-Johnson syndrome mutation impairs protein maturation and transport activity of MRP2 (ABCC2). Am. J. Physiol. Gastrointest. Liver Physiol. **284**: G165-G174

Keppler D Multidrug Resistance Proteins (MRPs, ABCCs): Importance for Pathophysiology and Drug Therapy. *In* Drug Transporters, Springer Berlin Heidelberg, 2011, pp 299-323

Khandelwal A, Cho SH, Marella H, Sakata Y, Perroud P-F, Pan A, Quatrano RS (2010) Role of ABA and ABI3 in Desiccation Tolerance. Science **327**: 546-546

Kim SI, Andaya CB, Goyal SS, Tai TH (2008) The rice OsLpa1 gene encodes a novel protein involved in phytic acid metabolism. Theor. Appl. Genet. **117**: 769-779

Kim T-H, Böhmer M, Hu H, Nishimura N, Schroeder JI (2010) Guard cell signal transduction network: advances in understanding abscisic acid, CO2, and Ca2+ signaling. Annu. Rev. Plant. Biol. **61**: 561-591

Kirkness EF, Haas BJ, Sun W, Braig HR, Perotti MA, Clark JM, Lee SH, Robertson HM, Kennedy RC, Elhaik E, et al (2010) Genome sequences of the human body louse and its primary endosymbiont provide insights into the permanent parasitic lifestyle. Proc. Natl. Acad. Sci. U.S.A. **107**: 12168-12173

Klein M, Burla B, Martinoia E (2006) The multidrug resistance-associated protein (MRP/ABCC) subfamily of ATP-binding cassette transporters in plants. FEBS Lett. **580**: 1112-1122

Klein M, Mamnun YM, Eggmann T, Schüller C, Wolfger H, Martinoia E, Kuchler K (2002) The ATP-binding cassette (ABC) transporter Bpt1p mediates vacuolar sequestration of glutathione conjugates in yeast. FEBS Lett. **520**: 63-67

Klein M, Weissenböck G, Dufaud A, Gaillard C, Kreuz K, Martinoia E (1996) Different Energization Mechanisms Drive the Vacuolar Uptake of a Flavonoid Glucoside and a Herbicide Glucoside. J. Biol. Chem. **271**: 29666-29671

Kocabas AM, Crosby J, Ross PJ, Otu HH, Beyhan Z, Can H, Tam W-L, Rosa GJM, Halgren RG, Lim B, et al (2006) The transcriptome of human oocytes. Proc. Natl. Acad. Sci. U.S.A. **103**: 14027-14032

Koike K, Oleschuk CJ, Haimeur A, Olsen SL, Deeley RG, Cole SPC (2002) Multiple Membrane-associated Tryptophan Residues Contribute to the Transport Activity and Substrate Specificity of the Human Multidrug Resistance Protein, MRP1. J. Biol. Chem. **277**: 49495-49503

Kolukisaoglu Ü, Bovet L, Klein M, Eggmann T, Geisler M, Wanke D, Martinoia E, Schulz B (2002) Family business: the multidrug-resistance related protein (MRP) ABC transporter genes in Arabidopsis thaliana. Planta **216**: 107-119

Koshimizu K, Inui M, Fukui H, Mitsui T (1968) Isolation of (+)-Abscisyl-β-D-glucopyranoside from Immature Fruit of Lupinus luteus. Agricultural and Biological Chemistry **32**: 789-791

Kovalchuk A, Driessen A (2010) Phylogenetic analysis of fungal ABC transporters. BMC Genomics **11**: 177

Krohn M, Lange C, Hofrichter J, Scheffler K, Stenzel J, Steffen J, Schumacher T, Brüning T, Plath A-S, Alfen F, et al (2011) Cerebral amyloid-β proteostasis is regulated by the membrane transport protein ABCC1 in mice. J. Clin. Invest. **121**: 3924-3931

Krzywinski MI, Schein JE, Birol I, Connors J, Gascoyne R, Horsman D, Jones SJ, Marra MA (2009) Circos: An information aesthetic for comparative genomics. Genome Res. **19**: 1639-45

Kuromori T, Hirayama T, Kiyosue Y, Takabe H, Mizukado S, Sakurai T, Akiyama K, Kamiya A, Ito T, Shinozaki K (2004) A collection of 11 800 single-copy Ds transposon insertion lines in Arabidopsis. Plant J. **37**: 897-905

Kuromori T, Miyaji T, Yabuuchi H, Shimizu H, Sugimoto E, Kamiya A, Moriyama Y, Shinozaki K (2010) ABC transporter AtABCG25 is involved in abscisic acid transport and responses. Proc. Natl. Acad. Sci. U.S.A. **107**: 2361-2366

Kushiro T, Okamoto M, Nakabayashi K, Yamagishi K, Kitamura S, Asami T, Hirai N, Koshiba T, Kamiya Y, Nambara E (2004) The Arabidopsis cytochrome P450 CYP707A encodes ABA 8[prime]-hydroxylases: key enzymes in ABA catabolism. EMBO J. **23**: 1647-1656

Labbé R, Caveney S, Donly C (2011) Genetic analysis of the xenobiotic resistance-associated ABC gene subfamilies of the Lepidoptera. Insect Mol. Biol. **20**: 243-256

Larkin MA, Blackshields G, Brown NP, Chenna R, McGettigan PA, McWilliam H, Valentin F, Wallace IM, Wilm A, Lopez R, et al (2007) Clustal W and Clustal X version 2.0. Bioinformatics **23**: 2947-2948

Laskowski RA, MacArthur MW, Moss DS, Thornton JM (1993) PROCHECK: a program to check the stereochemical quality of protein structures. J. Appl. Crystallogr. **26**: 283-291

Lazarowski ER, Boucher RC, Harden TK (2000) Constitutive release of ATP and evidence for major contribution of ecto-nucleotide pyrophosphatase and nucleoside diphosphokinase to extracellular nucleotide concentrations. J. Biol. Chem. **275**: 31061-31068

Lee HC (1997) Mechanisms of calcium signaling by cyclic ADP-ribose and NAADP. Physiol. Rev. **77**: 1133-1164

Lee KH, Piao HL, Kim H-Y, Choi SM, Jiang F, Hartung W, Hwang I, Kwak JM, Lee I-J, Hwang I (2006) Activation of Glucosidase via Stress-Induced Polymerization Rapidly Increases Active Pools of Abscisic Acid. Cell **126**: 1109-1120

Lehmann H, Glund K (1986) Abscisic acid metabolism - vacuolar/extravacuolar distribution of metabolites. Planta **168**: 559-562

Leier I, Jedlitschky G, Buchholz U, Cole SP, Deeley RG, Keppler D (1994) The MRP gene encodes an ATP-dependent export pump for leukotriene C4 and structurally related conjugates. J. Biol. Chem. **269**: 27807-27810

Leonhardt N, Marin E, Vavasseur A, Forestier C (1997) Evidence for the existence of a sulfonylurea-receptor-like protein in plants: Modulation of stomatal movements and guard cell potassium channels by sulfonylureas and potassium channel openers. Proc. Natl. Acad. Sci. U.S.A. **94**: 14156-14161

Lespinet O, Wolf YI, Koonin EV, Aravind L (2002) The Role of Lineage-Specific Gene Family Expansion in the Evolution of Eukaryotes. Genome Res. **12**: 1048-1059

Lévesque CA, Brouwer H, Cano L, Hamilton JP, Holt C, Huitema E, Raffaele S, Robideau GP, Thines M, Win J, et al (2010) Genome sequence of the necrotrophic plant pathogen

Pythium ultimum reveals original pathogenicity mechanisms and effector repertoire. Genome Biol. **11**: R73

Lewandowska D, Simpson CG, Clark GP, Jennings NS, Barciszewska-Pacak M, Lin C-F, Makalowski W, Brown JWS, Jarmolowski A (2004) Determinants of Plant U12-Dependent Intron Splicing Efficiency. Plant Cell **16**: 1340-1352

Liang H, Plazonic KR, Chen J, Li W-H, Fernández A (2008) Protein Under-Wrapping Causes Dosage Sensitivity and Decreases Gene Duplicability. PLoS Genet. **4**: e11

Lim E-K, Doucet CJ, Hou B, Jackson RG, Abrams SR, Bowles DJ (2005) Resolution of (+)-abscisic acid using an Arabidopsis glycosyltransferase. Tetrahedron **16**: 143-147

Lin C-F, Mount SM, Jarmołowski A, Makałowski W (2010) Evolutionary dynamics of U12-type spliceosomal introns. BMC Evol. Biol. **10**: 47

Liu S, Zhou S, Tian L, Guo E, Luan Y, Zhang J, Li S (2011) Genome-wide identification and characterization of ATP-binding cassette transporters in the silkworm, Bombyx mori. BMC Genomics **12**: 491

Lomsadze A, Ter-Hovhannisyan V, Chernoff YO, Borodovsky M Gene identification in novel eukaryotic genomes by self-training algorithm. Nucleic Acids Res. **33**: 6494-6506

Lostao MP, Hirayama BA, Loo DDF, Wright EM (1994) Phenylglucosides and the Na+/glucose cotransporter (SGLT1): Analysis of interactions. J. Membarin. Biol. **142**: 161-70.

Loveys BR (1979) The Influence of Light Quality on Levels of Ahscisic Acid in Tomato Plants, and Evidence for a Novel Abscisic Acid Metabolite. Physiol. Plant. **46**: 79-84

Lu Y-P, Li Z-S, Drozdowicz YM, Hörtensteiner S, Martinoia E, Rea PA (1998) AtMRP2, an Arabidopsis ATP Binding Cassette Transporter Able to Transport Glutathione S-Conjugates and Chlorophyll Catabolites: Functional Comparisons with AtMRP1. Plant Cell **10**: 267-282

Luckenbach T, Epel D (2008) ABCB- and ABCC-type transporters confer multixenobiotic resistance and form an environment-tissue barrier in bivalve gills. Am. J. Physiol. Regul. Integr. Comp. Physiol. **294**: R1919-R1929

MacRobbie EAC (2006) Control of Volume and Turgor in Stomatal Guard Cells. J. Membr. Biol. **210**: 131-142

Maere S, De Bodt S, Raes J, Casneuf T, Van Montagu M, Kuiper M, Van de Peer Y (2005) Modeling gene and genome duplications in eukaryotes. Proc. Natl. Acad. Sci. U.S.A. **102**: 5454-5459

Marchler-Bauer A, Lu S, Anderson JB, Chitsaz F, Derbyshire MK, DeWeese-Scott C, Fong JH, Geer LY, Geer RC, Gonzales NR, et al (2011) CDD: a Conserved Domain Database for the functional annotation of proteins. Nucleic Acids Res. **39**: D225-229

Martin A, Saathoff M, Kuhn F, Max H, Terstegen L, Natsch A (2009) A Functional ABCC11 Allele Is Essential in the Biochemical Formation of Human Axillary Odor. J. Invest. Dermatol. **130**: 529-540

Martinoia E, Grill E, Tommasini R, Kreuz K, Amrhein N (1993) ATP-dependent glutathione S-conjugate “export” pump in the vacuolar membrane of plants. Nature **364**: 247-249

Martinoia E, Klein M, Geisler M, Bovet L, Forestier C, Kolukisaoglu U, Müller-Röber B, Schulz B (2002) Multifunctionality of plant ABC transporters--more than just detoxifiers. Planta **214**: 345-355

Martinoia E, Maeshima M, Neuhaus HE (2007) Vacuolar transporters and their essential role in plant metabolism. J. Exp. Bot. **58**: 83-102

Maurel C, Verdoucq L, Luu D-T, Santoni V (2008) Plant Aquaporins: Membrane Channels with Multiple Integrated Functions. Annu. Rev. Plant. Biol. **59**: 595-624

McGlincy NJ, Smith CWJ (2008) Alternative splicing resulting in nonsense-mediated mRNA decay: what is the meaning of nonsense?. Trends Biochem. Sci. **33**: 385-393

Michealis S, Berkower C (1995) Sequence Comparison of Yeast ATP-binding Cassette Proteins. Cold Spring Harbor Symposia on Quantitative Biology **60**: 291-307

Milborrow BV (1978) The Stability of Conjugated Abscisic Acid during Wilting. J. Exp. Bot. **29**: 1059-1066

Miller MA, Pfeiffer W, Schwartz T (2010) Creating the CIPRES Science Gateway for inference of large phylogenetic trees. Gateway Computing Environments Workshop (GCE), IEEE, 2010, pp 1-8

Moreno-Hagelsieb G, Latimer K (2008) Choosing BLAST options for better detection of orthologs as reciprocal best hits. Bioinformatics **24**: 319-324

Morris P, Phuntumart V (2009) Inventory and Comparative Evolution of the ABC Superfamily in the Genomes of Phytophthora ramorum and Phytophthora sojae. J. Mol. Evol. **68**: 563-575

Morrison HG, McArthur AG, Gillin FD, Aley SB, Adam RD, Olsen GJ, Best AA, Cande WZ, Chen F, Cipriano MJ, et al (2007) Genomic Minimalism in the Early Diverging Intestinal Parasite Giardia lamblia. Science **317**: 1921-1926

Nagamune K, Hicks LM, Fux B, Brossier F, Chini EN, Sibley LD (2008) Abscisic acid controls calcium-dependent egress and development in Toxoplasma gondii. Nature **451**: 207-210

Nagy R, Grob H, Weder B, Green P, Klein M, Frelet-Barrand A, Schjoerring JK, Brearley C, Martinoia E (2009) The Arabidopsis ATP-binding Cassette Protein AtMRP5/AtABCC5 Is a High Affinity Inositol Hexakisphosphate Transporter Involved in Guard Cell Signaling and Phytate Storage. J. Biol. Chem. **284**: 33614-33622

Nambara E, Marion-Poll A (2005) Abscisic acid biosynthesis and catabolism. Annu. Rev. Plant. Biol. **56**: 165-185

Naramoto H, Uematsu T, Uchihashi T, Doto R, Matsuura T, Usui Y, Uematsu S, Li X, Takahashi M, Yamaoka M, et al (2007) Multidrug resistance-associated protein 7 expression is involved in cross-resistance to docetaxel in salivary gland adenocarcinoma cell lines. Int. J. Oncol. **30**: 393-401

Neill SJ, Horgan R, Heald JK (1983) Determination of the levels of abscisic acid-glucose ester in plants. Planta **157**: 371-375

Oakeshott JG, Johnson RM, Berenbaum MR, Ranson H, Cristino AS, Claudianos C (2010) Metabolic enzymes associated with xenobiotic and chemosensory responses in Nasonia vitripennis. Insect Mol. Biol. **19**: 147-163

Oguri T, Ozasa H, Uemura T, Bessho Y, Miyazaki M, Maeno K, Maeda H, Sato S, Ueda R (2008) MRP7/ABCC10 expression is a predictive biomarker for the resistance to paclitaxel in non-small cell lung cancer. Mol. Cancer Ther. **7**: 1150-1155

Okamoto M, Kushiro T, Jikumaru Y, Abrams SR, Kamiya Y, Seki M, Nambara E (2011) ABA 9'-hydroxylation is catalyzed by CYP707A in Arabidopsis. Phytochemistry **72**: 717-722

Okamoto M, Tanaka Y, Abrams SR, Kamiya Y, Seki M, Nambara E (2009) High Humidity Induces Abscisic Acid 8'-Hydroxylase in Stomata and Vasculature to Regulate Local and Systemic Abscisic Acid Responses in Arabidopsis. Plant Physiol. **149**: 825-834

Omote H, Hiasa M, Matsumoto T, Otsuka M, Moriyama Y (2006) The MATE proteins as fundamental transporters of metabolic and xenobiotic organic cations. Trends Pharmacol. Sci. **27**: 587-593

Ortiz DF, Pierre MVS, Abdulmessih A, Arias IM (1997) A Yeast ATP-binding Cassette-type Protein Mediating ATP-dependent Bile Acid Transport. J. Biol. Chem. **272**: 15358-15365

Otsuka M, Matsumoto T, Morimoto R, Arioka S, Omote H, Moriyama Y (2005) A human transporter protein that mediates the final excretion step for toxic organic cations. Proc. Natl. Acad. Sci. U.S.A. **102**: 17923-17928

Le Page-Degivry MT, Garello G, Barthe P (1997) Changes in Abscisic Acid Biosynthesis and Catabolism during Dormancy Breaking in Fagus sylvatica Embryo. J. Plant Growth Regul. **16**: 57-61

Palmgren MG (2001) PLANT PLASMA MEMBRANE H+-ATPases: Powerhouses for Nutrient Uptake. Annu. Rev. Plant Physiol. Plant. Mol. Biol. **52**: 817-845

Papp B, Pal C, Hurst LD (2003) Dosage sensitivity and the evolution of gene families in yeast. Nature **424**: 194-197

Parizot B, Laplaze L, Ricaud L, Boucheron-Dubuisson E, Bayle V, Bonke M, De Smet I, Poethig SR, Helariutta Y, Haseloff J, et al (2008) Diarch Symmetry of the Vascular Bundle in Arabidopsis Root Encompasses the Pericycle and Is Reflected in Distich Lateral Root Initiation. Plant Physiol. **146**: 140-148

Park J, Song W-Y, Ko D, Eom Y, Hansen TH, Schiller M, Lee TG, Martinoia E, Lee Y (2011) The phytochelatin transporters AtABCC1 and AtABCC2 mediate tolerance to cadmium and mercury. Plant J **69**: 278-288

Patel AA, McCarthy M, Steitz JA (2002) The splicing of U12-type introns can be a rate-limiting step in gene expression. EMBO J. **21**: 3804-3815

Payen L, Delugin L, Courtois A, Trinquart Y, Guillouzo A, Fardel O (2001) The sulphonylurea glibenclamide inhibits multidrug resistance protein (MRP1) activity in human lung cancer cells. Br. J. Pharmacol. **132**: 778-784

Pei J, Kim B-H, Grishin NV (2008) PROMALS3D: a tool for multiple protein sequence and structure alignments. Nucl. Acids Res. **36**: 2295-2300

Péret B, De Rybel B, Casimiro I, Benková E, Swarup R, Laplaze L, Beeckman T, Bennett MJ (2009) Arabidopsis lateral root development: an emerging story. Trends Plant Sci. **14**: 399-408

Pierce M, Raschke K (1981) Synthesis and metabolism of abscisic acid in detached leaves of Phaseolus vulgaris L. after loss and recovery of turgor. Planta **153**: 156-165

Piotrowska A, Bajguz A (2011) Conjugates of abscisic acid, brassinosteroids, ethylene, gibberellins, and jasmonates. Phytochemistry **72**: 2097-2112

Poulton JE (1990) Cyanogenesis in Plants. Plant Physiol. **94**: 401-405

Priest DM, Jackson RG, Ashford DA, Abrams SR, Bowles DJ (2005) The use of abscisic acid analogues to analyse the substrate selectivity of UGT71B6, a UDP-glycosyltransferase of Arabidopsis thaliana. FEBS Lett. **579**: 4454-4458

Pulkkinen L, Nakano A, Ringpfeil F, Uitto J (2001) Identification of ABCC6 pseudogenes on human chromosome 16p: implications for mutation detection in pseudoxanthoma elasticum. Hum. Genet. **109**: 356-365

Raichaudhuri A, Peng M, Naponelli V, Chen S, Sánchez-Fernández R, Gu H, Gregory JF, Hanson AD, Rea PA (2009) Plant Vacuolar ATP-binding Cassette Transporters That Translocate Folates and Antifolates in Vitro and Contribute to Antifolate Tolerance in Vivo. J. Biol. Chem. **284**: 8449-8460

Ramaen O, Leulliot N, Sizun C, Ulryck N, Pamlard O, Lallemand J-Y, Tilbeurgh H van, Jacquet E (2006) Structure of the human multidrug resistance protein 1 nucleotide binding domain 1 bound to Mg2+/ATP reveals a non-productive catalytic site. J. Mol. Biol. **359**: 940-949

Rea P, Sanchenz-Fernandez R, Chen S, Peng M, Klein M, Geisler M, Martinoia E The plant ABC transporter superfamily: the functions of a few and identities of many. *In* ABC Proteins from Bacteria to Man, Academic Press, 2003, pp 335-355

Rea PA, Li Z-S, Lu Y-P, Drozdowicz YM, Martinoia E (1998) From Vacuolar GS-X Pump to multispecific ABC transporters. Annu. Rev. Plant Physiol. Plant Mol. Biol. **49**: 727-760

del Refugio Ramos M, Jerz G, Villanueva S, López-Dellamary F, Waibel R, Winterhalter P (2004) Two glucosylated abscisic acid derivates from avocado seeds (Persea americana Mill. Lauraceae cv. Hass). Phytochemistry **65**: 955-962

Reich A, Klatsky P, Carson S, Wessel G (2011) The transcriptome of a human polar body accurately reflects its sibling oocyte. J. Biol. Chem. **286**:40743-40749

Rentsch D, Laloi M, Rouhara I, Schmelzer E, Delrot S, Frommer WB (1995) NTR1 encodes a high affinity oligopeptide transporter in Arabidopsis. FEBS Lett. **370**: 264-268

Rentsch D, Martinoia E (1991) Citrate transport into barley mesophyll vacuoles ? comparison with malate-uptake activity. Planta **184**: 532–537

Richards S, Gibbs RA, Weinstock GM, Brown SJ, Denell R, Beeman RW, Gibbs R, Beeman RW, Brown SJ, Bucher G, et al (2008) The genome of the model beetle and pest Tribolium castaneum. Nature **452**: 949-955

Riordan JR, Deuchars K, Kartner N, Alon N, Trent J, Ling V (1985) Amplification of P-glycoprotein genes in multidrug-resistant mammalian cell lines. Nature **316**: 817-819

Rispe C, Kutsukake M, Doublet V, Hudaverdian S, Legeai F, Simon J-C, Tagu D, Fukatsu T (2008) Large Gene Family Expansion and Variable Selective Pressures for Cathepsin B in Aphids. Mol. Biol. Evol. **25**: 5-17

Robertson HM, Wanner KW (2006) The chemoreceptor superfamily in the honey bee, Apis mellifera: Expansion of the odorant, but not gustatory, receptor family. Genome Res. **16**: 1395-1403

Rokas A (2009) The effect of domestication on the fungal proteome. Trends Genet. **25**: 60-63

Rose AB Intron-Mediated Regulation of Gene Expression. *In* Nuclear pre-mRNA Processing in Plants, Springer Berlin Heidelberg, 2008, pp 277-290

Rowe SM, Miller S, Sorscher EJ (2005) Cystic fibrosis. N. Engl. J. Med. **352**: 1992-2001

Roy SW, Gilbert W (2005) Complex early genes. Proc. Natl. Acad. Sci. U.S.A. **102**: 1986-1991

Roy SW, Penny D (2007) Patterns of Intron Loss and Gain in Plants: Intron Loss–Dominated Evolution and Genome-Wide Comparison of O. sativa and A. thaliana. Mol. Biol. Evol. **24**: 171-181

Sauter A, Dietz K-J, Hartung W (2002) A possible stress physiological role of abscisic acid conjugates in root-to-shoot signalling. Plant Cell Environ. **25**: 223-228

Scarfì S, Ferraris C, Fruscione F, Fresia C, Guida L, Bruzzone S, Usai C, Parodi A, Millo E, Salis A, et al (2008) Cyclic ADP-Ribose-Mediated Expansion and Stimulation of Human Mesenchymal Stem Cells by the Plant Hormone Abscisic Acid. Stem Cells **26**: 2855-2864

Schmutz J, Cannon SB, Schlueter J, Ma J, Mitros T, Nelson W, Hyten DL, Song Q, Thelen JJ, Cheng J, et al (2010) Genome sequence of the palaeopolyploid soybean. Nature **463**: 178-183

Seiler C, Harshavardhan VT, Rajesh K, Reddy PS, Strickert M, Rolletschek H, Scholz U, Wobus U, Sreenivasulu N (2011) ABA biosynthesis and degradation contributing to ABA homeostasis during barley seed development under control and terminal drought-stress conditions. J. Exp. Bot. **62**: 2615-2632

Sharkey TD, Raschke K (1980) Effects of Phaseic Acid and Dihydrophaseic Acid on Stomata and the Photosynthetic Apparatus. Plant Physiol. **65**: 291-297

Shi J, Wang H, Schellin K, Li B, Faller M, Stoop JM, Meeley RB, Ertl DS, Ranch JP, Glassman K (2007) Embryo-specific silencing of a transporter reduces phytic acid content of maize and soybean seeds. Nat. Biotech. **25**: 930-937

Slot AJ, Molinski SV, Cole SPC (2011) Mammalian multidrug-resistance proteins (MRPs). Essays Biochem. **50**: 179-207

Song W-Y, Park J, Mendoza-Cózatl DG, Suter-Grotemeyer M, Shim D, Hörtensteiner S, Geisler M, Weder B, Rea PA, Rentsch D, et al (2010) Arsenic tolerance in Arabidopsis is mediated by two ABCC-type phytochelatin transporters. Proc. Natl. Acad. Sci. U.S.A. **107**: 21187-21192

Spanu P, Kämper J (2010) Genomics of biotrophy in fungi and oomycetes — emerging patterns. Curr. Opin. Plant Biol. **13**: 409-414

Stamatakis A (2006) RAxML-VI-HPC: maximum likelihood-based phylogenetic analyses with thousands of taxa and mixed models. Bioinformatics **22**: 2688-2690

Stanke M, Morgenstern B (2005) AUGUSTUS: a web server for gene prediction in eukaryotes that allows user-defined constraints. Nucleic Acids Res. **33**: W465-W467

Sturm A, Cunningham P, Dean M (2009) The ABC transporter gene family of Daphnia pulex. BMC Genomics **10**: 170

Suh SJ, Wang Y-F, Frelet A, Leonhardt N, Klein M, Forestier C, Mueller-Roeber B, Cho MH, Martinoia E, Schroeder JI (2007) The ATP Binding Cassette Transporter AtMRP5 Modulates Anion and Calcium Channel Activities in Arabidopsis Guard Cells. J. Biol. Chem. **282**: 1916-1924

Sundaram P, Echalier B, Han W, Hull D, Timmons L (2006) ATP-binding Cassette Transporters Are Required for Efficient RNA Interference in Caenorhabditis elegans. Mol. Biol. Cell **17**: 3678-3688

Swarbreck D, Wilks C, Lamesch P, Berardini TZ, Garcia-Hernandez M, Foerster H, Li D, Meyer T, Muller R, Ploetz L, et al (2007) The Arabidopsis Information Resource (TAIR): gene structure and function annotation. Nucleic Acids Res. **36**: D1009-D1014

Symmons O, Váradi A, Arányi T (2008) How Segmental Duplications Shape Our Genome: Recent Evolution of ABCC6 and PKD1 Mendelian Disease Genes. Mol. Biol. Evol. **25**: 2601-2613

Szeri F, Iliás A, Pomozi V, Robinow S, Bakos É, Váradi A (2009) The high turnover Drosophila multidrug resistance-associated protein shares the biochemical features of its human orthologues. Biochim. Biophys. Acta **1788**: 402-409

Takayanagi S-I, Kataoka T, Ohara O, Oishi M, Kuo MT, Ishikawa T (2004) Human ATP-binding cassette transporter ABCC10: expression profile and p53-dependent upregulation. J. Exp. Ther. Oncol. **4**: 239-246

Tamura K, Peterson D, Peterson N, Stecher G, Nei M, Kumar S (2011) MEGA5: Molecular Evolutionary Genetics Analysis using Maximum Likelihood, Evolutionary Distance, and Maximum Parsimony Methods. Mol. Biol. Evol. **28**: 2731-279

Tarn W-Y, Steitz JA (1996) A Novel Spliceosome Containing U11, U12, and U5 snRNPs Excises a Minor Class (AT–AC) Intron In Vitro. Cell **84**: 801-811

Taylor IB, Sonneveld T, Bugg TDH, Thompson AJ (2005) Regulation and Manipulation of the Biosynthesis of Abscisic Acid, Including the Supply of Xanthophyll Precursors. J. Plant Growth Regul. **4:** 253-273

Thomas JH (2007) Rapid birth-death evolution specific to xenobiotic cytochrome P450 genes in vertebrates. PLoS Genet. **3**: e67

Tohge T, Ramos MS, Nunes-Nesi A, Mutwil M, Giavalisco P, Steinhauser D, Schellenberg M, Willmitzer L, Persson S, Martinoia E, et al (2011) Toward the storage metabolome: profiling the barley vacuole. Plant Physiol. **157**: 1469-1482

Tommasini R, Evers R, Vogt E, Mornet C, Zaman GJ, Schinkel AH, Borst P, Martinoia E (1996) The human multidrug resistance-associated protein functionally complements the yeast cadmium resistance factor 1. Proc. Natl. Acad. Sci. U.S.A. **93**: 6743-6748

Tommasini R, Vogt E, Schmid J, Fromentau M, Amrhein N, Martinoia E (1997) Differential expression of genes coding for ABC transporters after treatment of Arabidopsis thaliana with xenobiotics. FEBS Lett. **411**: 206-210

Ton J, Flors V, Mauch-Mani B (2009) The multifaceted role of ABA in disease resistance. Trends Plant Sci. **14**: 310-317

Toyoda Y, Sakurai A, Mitani Y, Nakashima M, Yoshiura K-ichiro, Nakagawa H, Sakai Y, Ota I, Lezhava A, Hayashizaki Y, et al (2009) Earwax, osmidrosis, and breast cancer: why does one SNP (538G>A) in the human ABC transporter ABCC11 gene determine earwax type? FASEB J. **23**: 2001-2013

Tusnády GE, Sarkadi B, Simon I, Váradi A (2006) Membrane topology of human ABC proteins. FEBS Lett. **580**: 1017-1022

Tyler BM, Tripathy S, Zhang X, Dehal P, Jiang RHY, Aerts A, Arredondo FD, Baxter L, Bensasson D, Beynon JL, et al (2006) Phytophthora Genome Sequences Uncover Evolutionary Origins and Mechanisms of Pathogenesis. Science **313**: 1261-1266

Vaucheret H, Béclin C, Elmayan T, Feuerbach F, Godon C, Morel J, Mourrain P, Palauqui J, Vernhettes S (1998) Transgene-induced gene silencing in plants. Plant J. **16**: 651-659

Veitia RA (2002) Exploring the etiology of haploinsufficiency. BioEssays **24**: 175-184

Veitia RA, Bottani S, Birchler JA (2008) Cellular reactions to gene dosage imbalance: genomic, transcriptomic and proteomic effects. Trends Genet. **24**: 390-397

Verrier PJ, Bird D, Burla B, Dassa E, Forestier C, Geisler M, Klein M, Kolukisaoglu U, Lee Y, Martinoia E, et al (2008) Plant ABC proteins--a unified nomenclature and updated inventory. Trends Plant Sci. **13**: 151-159

Vilella AJ, Severin J, Ureta-Vidal A, Heng L, Durbin R, Birney E (2009) EnsemblCompara GeneTrees: Complete, duplication-aware phylogenetic trees in vertebrates. Genome Res. **19**: 327-335

Walgren RA, Lin J-T, Kinne RK-H, Walle T (2000) Cellular Uptake of Dietary Flavonoid Quercetin 4'-β-Glucoside by Sodium-Dependent Glucose Transporter SGLT1. J. Pharmacol. Exp. Ther. **294**: 837-843

Wang P, Zhang Z, Gao K, Deng Y, Zhao J, Liu B, L X (2009) Expression and Clinical Significance of ABCC10 in the Patients with Non-small Cell Lung Cancer. Chin. J. Lung. Cancer **12**: 875-878

Wang R, Okamoto M, Xing X, Crawford N (2003) Microarray Analysis of the Nitrate Response in Arabidopsis Roots and Shoots Reveals over 1,000 Rapidly Responding Genes and New Linkages to Glucose, Trehalose-6-Phosphate, Iron, and Sulfate Metabolism. Plant Physiol. **132**: 556-567

Wanke D, Kolukisaoglu Ü (2010) An update on the ABCC transporter family in plants: many genes, many proteins, but how many functions? Plant Biol. **12**: 15-25

Ward JM, Mäser P, Schroeder JI (2009) Plant Ion Channels: Gene Families, Physiology, and Functional Genomics Analyses. Annu. Rev. Physiol. **71**: 59-82

Waterhouse AM, Procter JB, Martin DMA, Clamp M, Barton GJ (2009) Jalview Version 2 - a multiple sequence alignment editor and analysis workbench. Bioinformatics **25**: 1189-1191

Weigel D, Glazebrook J (2006) Transformation of Agrobacterium Using Electroporation. CSH Protoc **2006**: pdb.prot4665

Weiler EW (1980) Radioimmunoassays for the differential and direct analysis of free and conjugated abscisic acid in plant extracts. Planta **148**: 262-272

Willard L, Ranjan A, Zhang H, Monzavi H, Boyko RF, Sykes BD, Wishart DS (2003) VADAR: a web server for quantitative evaluation of protein structure quality. Nucleic Acids Res. **31**: 3316-3319

Wolffram S, Blöck M, Ader P (2002) Quercetin-3-glucoside is transported by the glucose carrier SGLT1 across the brush border membrane of rat small intestine. J. Nutr. **132**: 630-635

Wooden SL, Kalb SR, Cotter RJ, Soloski MJ (2005) Cutting edge: HLA-E binds a peptide derived from the ATP-binding cassette transporter multidrug resistance-associated protein 7 and inhibits NK cell-mediated lysis. J. Immunol. **175**: 1383-1387

Wormit A, Trentmann O, Feifer I, Lohr C, Tjaden J, Meyer S, Schmidt U, Martinoia E, Neuhaus HE (2006) Molecular Identification and Physiological Characterization of a Novel Monosaccharide Transporter from Arabidopsis Involved in Vacuolar Sugar Transport. Plant Cell **18**: 3476-3490

Wu P, Oleschuk CJ, Mao Q, Keller BO, Deeley RG, Cole SPC (2005) Analysis of Human Multidrug Resistance Protein 1 (ABCC1) by Matrix-Assisted Laser Desorption Ionization/Time of Flight Mass Spectrometry: Toward Identification of Leukotriene C4 Binding Sites. Mol. Pharmacol. **68**: 1455-1465

Wuest SE, Vijverberg K, Schmidt A, Weiss M, Gheyselinck J, Lohr M, Wellmer F, Rahnenführer J, von Mering C, Grossniklaus U (2010) Arabidopsis Female Gametophyte Gene Expression Map Reveals Similarities between Plant and Animal Gametes. Curr. Biol. **20**: 506-512

Xu Z-J, Nakajima M, Suzuki Y, Yamaguchi I (2002) Cloning and Characterization of the Abscisic Acid-Specific Glucosyltransferase Gene from Adzuki Bean Seedlings. Plant Physiol. **129**: 1285-1295

Yang R, Cui L, Hou YX, Riordan JR, Chang XB (2003) ATP Binding to the First Nucleotide Binding Domain of Multidrug Resistance-associated Protein Plays a Regulatory Role at Low Nucleotide Concentration, whereas ATP Hydrolysis at the Second Plays a Dominant Role in ATP-dependent Leukotriene C4 Transport. J. Biol. Chem. **278**: 30764-30771

Yoshihisa K, Masafumi H, Nobukazu S, Kazufumi Y (2009) Unusual expression of an Arabidopsis ATP-binding cassette transporter ABCC11. Plant Biotechnol. **26**: 261-265

Zaharia LI, Walker-Simmon MK, Rodríguez CN, Abrams SR (2005) Chemistry of Abscisic Acid, Abscisic Acid Catabolites and Analogs. J Plant Growth Regul. **24**: 274-284

van Zanden JJ, Wortelboer HM, Bijlsma S, Punt A, Usta M, Bladeren PJ van, Rietjens IMCM, Cnubben NHP (2005) Quantitative structure activity relationship studies on the flavonoid mediated inhibition of multidrug resistance proteins 1 and 2. Biochem. Pharmacol. **69**: 699-708

Zeevaart JAD (1980) Changes in the Levels of Abscisic Acid and Its Metabolites in Excised Leaf Blades of Xanthium strumarium during and after Water Stress. Plant Physiol **66**: 672-678

Zeevaart JAD (1983) Metabolism of Abscisic Acid and Its Regulation in Xanthium Leaves during and after Water Stress. Plant Physiol. **71**: 477-481

Zeevaart JAD Chapter 8 Abscisic acid metabolism and its regulation. *In* Biochemistry and Molecular Biology of Plant Hormones, Elsevier, 1999, pp 189-207

Zeevaart JAD, Boyer GL (1984) Accumulation and Transport of Abscisic Acid and Its Metabolites in Ricinus and Xanthium. Plant Physiol. **74**: 934-939

Zeng H, Liu G, Rea PA, Kruh GD (2000) Transport of Amphipathic Anions by Human Multidrug Resistance Protein 3. Cancer Res. **60**: 4779-4784

Zhao H-J, Liu Q-L, Ren X-L, Wu D-X, Shu Q-Y (2008) Gene identification and allele-specific marker development for two allelic low phytic acid mutations in rice (Oryza sativa L.). Mol. Breeding **22**: 603-612

Zhao J, Dixon RA (2009) MATE Transporters Facilitate Vacuolar Uptake of Epicatechin 3'-O-Glucoside for Proanthocyanidin Biosynthesis in Medicago truncatula and Arabidopsis. Plant Cell **21**: 2323-2340

Zhao J, Huhman D, Shadle G, He X-Z, Sumner LW, Tang Y, Dixon RA (2011) MATE2 Mediates Vacuolar Sequestration of Flavonoid Glycosides and Glycoside Malonates in Medicago truncatula. Plant Cell **23**: 1536-1555

Zhao Z, Thomas JH, Chen N, Sheps JA, Baillie DL (2007) Comparative Genomics and Adaptive Selection of the ATP-Binding-Cassette Gene Family in Caenorhabditis Species. Genetics **175**: 1407-1418

Zhu W, Brendel V (2003) Identification, characterization and molecular phylogeny of U12-dependent introns in the Arabidopsis thaliana genome. Nucleic Acids Res. **31**: 4561-4572

Zocchi E, Carpaneto A, Cerrano C, Bavestrello G, Giovine M, Bruzzone S, Guida L, Franco L, Usai C (2001) The temperature-signaling cascade in sponges involves a heat-gated cation channel, abscisic acid, and cyclic ADP-ribose. Proc. Natl. Acad. Sci. U.S.A. **98**: 14859-14864

8. Acknowledgments

This thesis would not have been possible without the kind support, knowledge, advice, and friendship from many people.

I am very grateful to my supervisor, Professor Enrico Martinoia, who allowed me to make my PhD thesis in his lab. His confidence and openness to let me follow my ideas, and his kindness were important aspects of my time in his laboratory. Furthermore, I would like to thank Professor Youngsook Lee from the POSTEC University, Pohang, South Korea, for financial support. I also thank Professor Beat Keller and Professor Kentaro Shimizu for discussions and being members of my thesis committee. I thank Professor Katsuhiro Shiratake, Nagoya University, Japan, very much for providing me with the constructs and valuable information on AtABCC13. Furthermore, I especially want to thank Tobias Kretzschmar for the AtABCC13 constructs and for the many discussions. His work was indispensable for the characterization of this gene. I thank Marianne Suter-Grotemeyer, University of Bern, for teaching me the vacuole isolation method. Many thanks go to Maik Hadorn, Stefan Meyer, Undine Krügel, Santiago Alejandro Martinez, and Karen for looking through this manuscript. Moreover, I would like to thank Samuel Wüst for sharing his data, and Professor Marc Robinson-Rechavi and his group from the University of Lausanne, Markus Klein, Markus Geisler, and Professors Stefan Hörtensteiner and Felix Keller for ideas and discussions.

I am very grateful to the members of the lab, who helped, advised and supported me always and who created a happy and relaxing working atmosphere: Réka Nagy, Barbara Weder, Hanne Grob, Rita Saraiva, Rita Francisco, Undine Krügel. Thanks go also to Vincent Vincenzetti, Maja Schellenberg, and to Daniel Bollier, Reto Schild, Italia Sacco, Daniel Stutz, Rolf Christig and the secretary office for assistances and keeping the lab running. Then I would like to thank all the other friends who helped and supported me, especially Peter Kovermann, Santiago Alejandro Martinez, Anne Endler, Ulrike Schmidt, Miyoung Lee, Alexis De Angeli and HaKam. Moreover, I want to thank my former biology teacher Otto Gyr for the introduction into the microcosm, and I am deeply grateful to Gerhard Zürcher, one of my supervisors and teachers when I was an apprentice many years ago, from whom I learned so much about scientific laboratory work, and who encouraged me to continue study.

My cordial thanks go to Stefan Meyer and Réka Nagy, and to Maik Hadorn, Roman Furrer, and Philippe Saner for their friendship, for their support, discussions, ideas, reviewings, advices, encouragements, and for many funny and relaxing coffee breaks and drinks out throughout all this time. Maik, Roman, Philippe and me studied biology together, spent hours studying together and had countless interesting discussions. It was and is a great time.

I would like to deeply thank my parents, Mor and Far, and my sister Laila for enabling me to study again, for the support in all those years, and for showing me the art and beauty in nature. ☺

9. Curriculum vitae

Name	BURLA
First names	Bo Johannes
Date of birth	06.07.1973
Place of origin	Burg bei Murten, FR

Education

1989 - 1992	Apprenticeship as 'Biology laboratory technician' Hoffmann - La Roche Ltd, Basel, Switzerland
1998 - 2000	Preparation for the university-entrance diploma (Matura), AKAD, Zürich, Switzerland
2000	Eidgenössische Matura, Typus C (Qualification exam for university entrance)
2000 - 2005	Studies of Biology (major subject: plant biology, minor subject: geography) University of Zürich, Switzerland
2005	Diploma thesis Title: 'Characterization of the ABC transporter AtMRP14 in *Arabidopsis thaliana*' Institute of Plant Biology, University of Zürich, Switzerland Supervisor: Prof. Dr. Enrico Martinoia
2006 - 2011	PhD thesis Title: 'Evolutionary analysis of ABCC transporters and characterization of vacuolar transport mechanisms of the glucosylated phytohormone abscisic acid' Institute of Plant Biology, University of Zürich, Switzerland Supervisor: Prof. Dr. Enrico Martinoia

Work and research experience

1992 - 1998	Biology laboratory technician. Hoffmann - La Roche Ltd, Basel, Switzerland
1999 - 2005	Software developer. Part-time (10 – 40%) gli software engineering, Zürich, Switzerland
2006	Research assistant. Artificial Intelligence Lab. Part-time (50%) Institute of Informatics, University of Zürich, Switzerland
2005 - 2006	Research assistant. Department of Molecular Plant Physiology. Part-time (20%). Institute of Plant Biology, University of Zürich, Switzerland
2012 -	Research associate. University Hospital Zürich, Zürich, Switzerland

List of peer-reviewed publications

Klein M, **Burla B**, Martinoia, E. (2006) The multidrug resistance-associated protein (MRP/ABCC) subfamily of ATP-binding cassette transporters in plants. *FEBS Letters* 580: 1112-1122

Lee M, Choi Y, **Burla B**, Kim Y-Y, Jeon B, Maeshima M, Yoo J-Y, Martinoia E, Lee Y (2008) The ABC transporter AtABCB14 is a malate importer and modulates stomatal response to CO_2. *Nature Cell Biology*. 10: 1217-1223

Verrier PJ, Bird D, **Burla B**, Dassa E, Forestier C, Geisler M, Klein M, Kolukisaoglu U, Lee Y, Martinoia E, Murphy A., Rea PA, Samuels L, Schulz B, Spalding EJ, Yazaki K, Theodoulou FL (2008) Plant ABC proteins - a unified nomenclature and updated inventory. *Trends in Plant Science* 13: 151-159

Saner P, Lim R, **Burla B**, Ong RC, Scherer-Lorenzen M, Hector A (2009) Reduced soil respiration in gaps in logged lowland dipterocarp forests. *Forest Ecology and Management* 258: 2007-2012

Hadorn M, **Burla B**, Eggenberger Hotz P (2009) Towards Tailored Communication Networks in Assemblies of Artificial Cells, in: Korb, K., Randall, M., Hendtlass, T. (Eds.), Artificial Life: Borrowing from Biology. Springer Berlin Heidelberg, Berlin, Heidelberg, pp. 126-135

Schelbert S, Aubry S, **Burla B**, Agne B, Kessler F, Krupinska K, Hörtensteiner S (2009) Pheophytin pheophorbide hydrolase (pheophytinase) is involved in chlorophyll breakdown during leaf senescence in Arabidopsis. *The Plant Cell* 21: 767-785

Cho J-I, **Burla B**, Lee D-W, Ryoo N, Hong S-K, Kim H-B, Eom J-S, Choi S-B, Cho M-H, Bhoo SH, Hahn T-R, Neuhaus HE, Martinoia E, Jeon J-S. (2010) Expression analysis and functional characterization of the monosaccharide transporters, OsTMTs, involving vacuolar sugar transport in rice (Oryza sativa). *New Phytologist* 186: 657-668

Kretzschmar T, **Burla B**, Lee Y, Martinoia E, Nagy R (2011) Functions of ABC transporters in plants. *Essays in Biochemistry* 50: 145-160

Meyer S, Scholz-Starke J, De Angeli A, Kovermann P, **Burla B**, Gambale F, Martinoia E (2011) Malate transport by the vacuolar AtALMT6 channel in guard cells is subject to multiple regulation. *Plant Journal* 67: 247-257

Kang J, Park J, Choi H, **Burla B**, Kretzschmar T, Lee Y, Martinoia E (2011) Plant ABC Transporters. *The Arabidopsis Book* 9: e0153